Lifetime risks for lung cancer related to radon exposure

Manuel Sommer

München 2025

Lifetime risks for lung cancer related to radon exposure

Manuel Sommer

Dissertation
an der Fakultät für Mathematik, Informatik und Statistik
der Ludwig–Maximilians–Universität
München

vorgelegt von
Manuel Sommer
aus München

München, den 08. Mai 2025

Erstgutachter: Prof. Dr. Christian Heumann
Zweitgutachter: Prof. Dr. Daniel Wollschläger
Drittgutachter: Prof. Dr. Matthias Schmid
Tag der mündlichen Prüfung: 07. Juli 2025

Eidesstattliche Versicherung

Ich erkläre hiermit an Eides statt, dass ich die vorliegende Dissertation ohne Hilfe Dritter und ohne Benutzung anderer als der angegebenen Hilfsmittel angefertigt habe; die aus fremden Quellen direkt oder indirekt übernommenen Gedanken sind als solche kenntlich gemacht.

München, den 08. Mai 2025

Manuel Sommer

Acknowledgements

First and foremost I want to thank my loving mother for her undoubted support throughout my entire academic journey. She provided the environment for me to be able to pursue an academic education and, in particular, this PhD degree. She is my role model and a spring of knowledge. She considerably shaped my way of thinking and inspired me always to ask questions. Thank you.

Further, I want to thank my girlfriend Adriana for her moral support and willingness to listen to my research-related thoughts, although it is Sunday morning and she did not even have her first coffee yet.

I would like to express my deepest gratitude to my two closest colleagues, Nora and Felix. You two significantly contributed to my education as a scientist in the past three years. Your unwavering support and invaluable insights during our weekly exchanges have been instrumental in deepening my understanding, both in research-related and sometimes non-research-related topics. Overall, a big Thank You to my employer, the German federal office for radiation protection (Bundesamt für Strahlenschutz), and especially to my principal Peter, and the whole department on radiation epidemiology and risk assessment for letting me focus on tasks that were always related to my research question. For any questions at hand, I was fortunate to have had a team of supportive and expert colleagues to consult with at any time. Moreover, my research has greatly benefited from stimulating discussions with international experts at various scientific conferences. I particularly want to extend my gratitude to David B. Richardson, Ladislav Tomášek, and Kaitlin Kelly-Reif for their valuable insights.

I am very grateful to my supervisors, Prof. Dr. Christian Heumann and Prof. Dr. Daniel Wollschläger, for their support, guidance, and expertise on statistical methods and radiation epidemiology, respectively. I would also like to thank Prof. Dr. Matthias Schmid for serving as a reviewer of this dissertation.

Last but not least, I sincerely want to thank my friends for proofreading several of my manuscripts.

Zusammenfassung

Radon ist eine der bedeutendsten Ursachen für Lungenkrebs nach dem Rauchen. In dieser Dissertation wird das Lebenszeitrisiko für den Lungenkrebstod infolge von Radonexposition untersucht – ein zentrales Maß zur Bewertung der Schädlichkeit von Radon für den Menschen. Das Lebenszeitrisiko allgemein ist eine statistische Größe, die die Wahrscheinlichkeit beschreibt, im Laufe des Lebens an einer bestimmten Krankheit zu erkranken oder zu sterben. Lebenszeitrisiken für Lungenkrebs durch Radon nehmen im Strahlenschutz eine zentrale Rolle ein, beispielsweise bei der Radon-Dosiskonversion, und können maßgeblich zur Festlegung gesetzlicher Radongrenzwerte und damit zum Schutz der öffentlichen Gesundheit beitragen. Das Lebenszeitrisiko für Lungenkrebs durch Radon ist eine zusammengesetzte Größe, die mehrere, unabhängig voneinander durchgeführte Analysen zu Mortalitätsraten und zum Radon-Risiko kombiniert. Diese Dissertation adressiert bestehende Defizite bei der Schätzung solcher Lebenszeitrisiken und der damit verbundenen Unsicherheiten, mit besonderem Fokus auf berufliche Radonexposition. Der Schwerpunkt liegt dabei auf der Berechnungsmethodik, der Identifikation einflussreicher Komponenten sowie der Bewertung und Quantifizierung relevanter Unsicherheiten. Die Dissertation basiert auf vier wissenschaftlichen Veröffentlichungen und enthält ergänzende Hintergrundinformationen, um diese in einen breiteren fachlichen Kontext einordnen zu können.

Eine zentrale Komponente bei der Berechnung von Lebenszeitrisiken für Lungenkrebs durch Radon sind die verwendeten Risikomodelle, die die aus Uranbergarbeiter-Kohorten abgeleitete Expositions-Wirkung-Beziehung zwischen Radon und Lungenkrebs abbilden. In Kreuzer et al. (2023) wurden aktualisierte Risikomodelle auf Basis der deutschen Wismut Uranbergarbeiter-Kohortenstudie mit Follow-up bis 2018 entwickelt – der weltweit größten Einzelkohorte von Uranbergarbeitern. Die abgeleiteten Risikomodelle bestätigten und präzisierten die etablierte Beziehung zwischen Radonexposition und einem erhöhten Lungenkrebsrisiko. Diese verbesserten Risikomodelle bilden eine entscheidende Grundlage für genauere Schätzungen von Lebenszeitrisiken für Lungenkrebs durch Radon und tragen damit auch zur internationalen Diskussion über die Radon-Dosiskonversion bei.

Mit Sommer et al. (2025) wurden umfassende Sensitivitätsanalysen durchgeführt, um die Auswirkungen verschiedener Berechnungskomponenten auf das Lebenszeitrisiko für Lungenkrebs durch Radon systematisch zu untersuchen. Zudem wurde eine standardisierte Methodik zur Berechnung dieser Lebenszeitrisiken etabliert. Die Analysen zeigten, dass das verwendete Risikomodell – mit der zugrunde liegenden Kohorte – sowie die angenommenen Mortalitätsraten für Lungenkrebs maßgeblich die Schätzung des Lebenszeitrisikos beeinflussen. Andere Komponenten, wie das gewählte berufliche Radonexposi-

tionsszenario oder das spezifische Lebenszeitrisikomaß, hatten einen vergleichsweise geringen Einfluss. Die Studie unterstreicht somit die Bedeutung einer sorgfältigen Auswahl einflussreicher Berechnungskomponenten und liefert eine praxisorientierte Grundlage für zukünftige Berechnungen von Lebenszeitrisiken im Strahlenschutz. Insbesondere legt diese Arbeit das Fundament für eine gezielte Quantifizierung von statistischen Unsicherheiten im Lebenszeitrisiko.

In Kreuzer et al. (2024) wurden Lebenszeitrisiken für Lungenkrebs unter Verwendung von Risikomodellen berechnet, die aus der Pooled Uranium Miners Analysis (PUMA)-Studie abgeleitet wurden – der weltweit größten gepoolten Studie zu Uranbergarbeitern, die sieben Einzelkohorten aus Kanada, Tschechien, Frankreich, Deutschland und den USA umfasst. Zusätzlich wurden Schätzer für Lebenszeitrisiken auf Basis früherer, teilweise in PUMA integrierter Studien, präsentiert – darunter insbesondere die aktualisierten Risikomodelle der deutschen Wismut-Kohorte (Kreuzer et al., 2023). Der Einsatz eines standardisierten Berechnungsverfahrens ermöglichte einen direkten und methodisch konsistenten Vergleich der Lebenszeitrisiken aus den verschiedenen Studien. Die Analyse zeigt, dass Lebenszeitrisiken ein geeignetes Maß zur Bewertung der Expositions-Risiko-Beziehung zwischen Radon und Lungenkrebs in unterschiedlichen Kohorten darstellen – selbst bei erheblichen Unterschieden in Radonexposition und Modellstruktur. Mit den abgeleiteten Lebenszeitrisiken liefert diese Arbeit eine fundierte, epidemiologisch gestützte Grundlage für die laufende wissenschaftliche Diskussion zur Radon-Dosiskonversion.

In Sommer et al. (2024) wurden Ansätze zur statistischen Modellierung von Unsicherheiten im Lebenszeitrisiko mittels 95%-Unsicherheitsintervallen vorgestellt, basierend auf früheren Erkenntnissen. Am Beispiel der deutschen Wismut-Kohorte zeigte die Analyse, dass Unsicherheiten der Risikomodellparameter maßgeblich zur Gesamtunsicherheit des Lebenszeitrisikos beitragen. Auch Unsicherheiten in den Mortalitätsraten wurden berücksichtigt, deren Einfluss jedoch geringer ist. Für ein Gesamtverständnis der Unsicherheit in Lebenszeitrisiken genügt meist die Quantifizierung der Risikomodellparameter-Unsicherheiten. Zwei methodische Ansätze wurden entwickelt: Ein auf Likelihood-Konzepten basierender Ansatz (Approximate Normality Assumption, ANA) sowie ein Bayes'scher Ansatz. Die resultierenden 95%-Unsicherheitsintervalle stimmen gut mit der in der Literatur beschriebenen Variation von Lebenszeitrisiken aus verschiedenen Studien überein, was die Validität der Ergebnisse unterstreicht. Der ANA-Ansatz erweist sich für anwendungsorientierte Zwecke im Strahlenschutz als zuverlässige Methode zur Quantifizierung von Unsicherheiten. Der flexiblere Bayes'sche Ansatz ermöglicht eine differenziertere Bewertung und Integration von Vorwissen, ist jedoch komplexer und weniger anwendungsfreundlich, was die breitere Anwendbarkeit einschränkt. Diese Arbeit leitete erstmals Unsicherheitsintervalle für das Lebenszeitrisiko von Lungenkrebs durch berufliche Radonexposition ab und schließt damit eine zentrale methodische Lücke. Frühere Studien lieferten lediglich Punktschätzungen ohne direkte Vergleichbarkeit. Die vorgestellte Methode ermöglicht den systematischen Vergleich von Lebenszeitrisiken und trägt wesentlich zur wissenschaftlichen Bewertung, Risikokommunikation und regulatorischen Entscheidungsfindung bei.

Summary

Exposure to radon is one of the most important causes of lung cancer after smoking. This dissertation investigates the lifetime risk of lung cancer death related to radon exposure – a central metric for assessing the health effects of radon. In general, a lifetime risk is a statistical quantity that describes the probability of developing or dying from a specific disease over the course of a lifetime. Lifetime lung cancer risks related to radon play a crucial role in radiation protection, such as in radon dose conversion, and can inform the setting of regulatory limits for radon exposure, thus contributing to public health protection. A lifetime lung cancer risk estimate depends on several calculation components and is a composite quantity combining multiple, independently conducted analyses, particularly on mortality rates and radon risk. This dissertation addresses existing deficits in the estimation of such lifetime risks and corresponding uncertainties, with a special emphasis on occupational radon exposure. The focus is on the development and evaluation of calculation methodologies, the identification of influential calculation components, and the evaluation and quantification of uncertainties in the lifetime risk estimation process. This cumulative dissertation is based on four scientific publications and provides additional context and background to embed the findings in a broader scientific framework.

A key component in the estimation of lifetime lung cancer risk from radon is the risk model employed, which shapes the exposure-risk relationship derived from uranium miners cohort data. In Kreuzer et al. (2023), updated lung cancer risk models were derived from the German Wismut uranium miners cohort with follow-up 2018 – the largest single cohort of uranium miners worldwide. These updated risk models confirmed and refined the well-established association between radon exposure and lung cancer risk. They serve as a key basis for more accurate lifetime risk assessments and are an important contribution to the international discourse on radon dose conversion.

In Sommer et al. (2025), comprehensive sensitivity analyses were conducted to systematically assess the impact of various calculation components on lifetime risk estimates for radon-related lung cancer. Furthermore, a standardized methodology for calculating lifetime risks was developed. The analyses revealed that the choice of risk model – including the underlying cohort – and assumptions about baseline lung cancer mortality rates have the greatest influence on the estimated lifetime risk. Other components, such as the occupational exposure scenario or the specific lifetime risk metric used, were found to have relatively minor effects. This study highlights the importance of carefully selecting key calculation components and provides a practical basis for future lifetime risk estimations in radiation protection. Moreover, it lays the groundwork for a targeted quantification of

statistical uncertainties, as further elaborated in Sommer et al. (2024).

In Kreuzer et al. (2024), lifetime lung cancer risks were calculated based on risk models derived from the Pooled Uranium Miners Analysis (PUMA) study – the largest pooled uranium miners cohort worldwide, comprising seven individual cohorts from Canada, the Czech Republic, France, Germany, and the USA. Additionally, lifetime risk estimates based on risk models from previous studies were presented, some of which were included in PUMA (e.g., updated Wismut models (Kreuzer et al., 2023)). The use of a standardized calculation methodology enabled consistent comparisons of lifetime risk estimates across different risk models. The analyses demonstrate that lifetime risks are a suitable measure for evaluating exposure–response relationships across various cohorts, even when exposure levels and model structures differ considerably. The derived variation of lifetime risk estimates across different risk models provides a robust epidemiological foundation for ongoing scientific discussions on radon dose conversion.

Finally, Sommer et al. (2024) introduced advanced statistical approaches for quantifying uncertainty in lifetime risk using 95% uncertainty intervals building on previous findings (Sommer et al., 2025). Using data from the German Wismut cohort, this analysis illustrates that uncertainties in the risk model parameters account for a major share of the overall quantifiable uncertainty in lifetime risks. Uncertainties in mortality rates were also considered, although their influence is generally smaller in comparison. For a comprehensive understanding of uncertainty in lifetime risks, quantifying risk model parameter uncertainty is usually sufficient. Two methodological approaches were developed for this purpose: one based on maximum likelihood concepts (Approximate Normality Assumption, ANA), and a more flexible Bayesian approach. The resulting 95% uncertainty intervals align well with the variability of lifetime risks observed in the literature from different miner studies, thereby supporting the validity of the methods and results. The ANA approach proves to be a suitable and reliable method for quantifying uncertainties in most cases – particularly for practical applications in radiation protection. The more flexible Bayesian approach allows for a more nuanced assessment and integration of prior knowledge, but it is more complex and less user-friendly, which limits its broader applicability. This work is the first to derive uncertainty intervals for lifetime risk estimates of lung cancer due to occupational radon exposure, thereby addressing a key methodological gap. Previous studies typically reported point estimates without any assessment of comparability. The uncertainty quantification presented here enables systematic comparisons between different lifetime risk estimates – for example, by examining interval overlap – and makes an important contribution to scientific risk evaluation, risk communication, and regulatory decision-making.

Abbreviations and notation

This thesis frequently uses the following abbreviations for international institutions and organizations:

Short form	Long form
IARC	International Agency for Research on Cancer
ICRP	International Commission on Radiological Protection
NRC	National Research Council of the United States
OECD	Organisation for Economic Co-operation and Development
UNSCEAR	United Nations Scientific Committee on the Effects of Atomic Radiation
WHO	World Health Organization

In addition, the following abbreviations are used to denote commonly applied functional forms to calculate excess lifetime risks (so called lifetime risk measures):

Short form	Long form
ELR	Excess lifetime risk
LEAR	Lifetime excess absolute risk
RADS	Radiation attributable decrease of survival
REID	Risk of exposure-induced death

The mathematical symbols listed below represent calculation components and related quantities used in this thesis in the context of lifetime risk estimation:

Symbol	Meaning
$r_0(t)$	Baseline lung cancer mortality rate at age t
$r_E(t)$	Lung cancer mortality rate at age t under radiation exposure
$EAR(t;\Theta)$	Excess absolute risk of dying of lung cancer at age t
$ERR(t;\Theta)$	Excess relative risk of dying of lung cancer at age t
Θ	Generic risk model parameter vector to be estimated
$\hat{\Theta}$	Estimate of parameter Θ
$q_0(t)$	Baseline all-cause mortality rate at age t
$q_E(t)$	All-cause mortality rate at age t under radiation exposure
$S(t)$	Generic survival function at age t
$S(t\|a)$	Generic survival function at age t, conditioned on attaining age a
$S_0(t)$	Survival function at age t in the absence radiation exposure
$S_E(t)$	Survival function at age t under radiation exposure
X	Cohort data
$\mathbb{1}(x)$	Indicator function: $\mathbb{1}(x)$ is 1 if x is true and 0 otherwise

Contents

Part I.

Foundations and context

1. Introduction

This work explores the concept and importance of lifetime risks, with a particular focus on lifetime risks for lung cancer due to radon exposure. The topic is highly relevant to radiation epidemiology and public health. This introductory chapter lays the foundation by motivating the need for improved lifetime risk estimation, clarifying the goals and scientific contributions of the dissertation. Additionally, an overview of the structure of this dissertation is provided.

1.1. Motivation and background

Exposure to the radioactive gas radon and its decay products (radon progeny) is a leading cause of lung cancer worldwide and represents a considerable public health concern (World Health Organization [WHO], 2023). Accurately assessing the health risks associated with radon exposure is essential for developing effective mitigation strategies and public health guidelines.

Radon risk assessments are primarily based on large-scale cohort studies of underground miners, who were exposed to high concentration levels of radon and its radioactive decay products (United Nations Scientific Committee on the Effects of Atomic Radiation [UNSCEAR], 2021a). These studies form the basis for deriving risk models that describe the relationship between radon exposure and lung cancer risk (exposure-risk relationship). These models, while central to risk estimation, are often complex and not easily interpretable.

Lifetime risks are an intuitive and interpretable metric that incorporate risk models and, importantly, facilitates the comparison of model results across miner studies with differing characteristics. They are a statistical quantity and describe the probability of developing (or dying of) a specific disease (here: lung cancer death related to radon exposure) in the course of a lifetime (Thomas et al., 1992; Vaeth & Pierce, 1990).[1] In the context of this dissertation, lifetime lung cancer risks related to radon exposure are a measure of the harm of radon relevant to public health.[2]

[1] The actual calculation of lifetime risks is outlined in Section 3.1.

[2] More detailed information on radon and its health risks is presented in Chapter 2.

In particular, such lifetime risks play a central role in the current international discussion on converting radon exposure, expressed in Becquerel per cubic meter (Bq/m^3) or in the context of miners often in Working Level Months (WLM), into an effective dose in millisievert (mSv), a process known as "radon dose conversion" (Marsh et al., 2021). This relies on a dose conversion coefficient that links radon activity concentration and the resulting dose in the human body. By applying this coefficient, one can estimate the potential health risks associated with radon exposure, contributing to the implementation of appropriate radon mitigation measures (Marsh et al., 2010).[3]

International organizations like the International Commission on Radiological Protection (ICRP) and the United Nations Scientific Committee on the Effects of Atomic Radiation (UNSCEAR) recognize this and awaited the calculation of lifetime lung cancer risks for the German uranium miners cohort study (Wismut cohort), the largest single cohort of uranium miners worldwide (Kreuzer et al., 2009). The Wismut cohort and corresponding lifetime risks contribute to the Pooled Uranium Miners Analysis (PUMA) study, the worldwide largest pooled study of uranium miners conducted to-date (Rage et al., 2020). The Federal Office for Radiation Protection in Germany is responsible for maintaining and regularly updating the Wismut cohort data, from which comprehensive statistical analyses are derived. This vast cohort size provides exceptional statistical power for investigating the health effects related to occupational radon exposure. Further, lifetime risks are employed to derive the "radiation detriment", a concept developed by the ICRP to quantify the burden of in particular radon exposure to the human population (International Commission on Radiological Protection [ICRP], 2022). Note that throughout this dissertation, the term "lifetime risk" specifically refers to the lifetime risk of lung cancer death related to (occupational) radon exposure, unless otherwise stated. In most cases, this specifically includes the commonly used lifetime excess absolute risk (LEAR) and other functional forms for estimating excess lifetime risks, collectively referred to as (excess) lifetime risk measures (see Section 3.1).

Despite the outlined relevance of lifetime risks, previous studies have mostly reported single point estimates for specific combinations of calculation components, without addressing the variability or statistical uncertainty inherent in these estimates. This limits scientific interpretation and comparability: while different studies may report varying lifetime risks, the lack of a clear understanding of the influential calculation components or associated uncertainty intervals, makes it unclear whether such differences are statistically relevant. This absence of uncertainty assessment represents a critical methodological gap.

[3] Further details on these units and on radon dose conversion are provided in Section 2.1 and Section 6.2.1.

1.2. Aim and scientific contribution of the dissertation

This dissertation addresses the above-mentioned gaps by investigating how variability and uncertainties in lifetime lung cancer risk estimates due to radon exposure can be assessed and quantified. The main objectives are:

- To estimate lifetime risks for lung cancer due to occupational radon exposure, using particularly recent data from the German Wismut cohort.
- To systematically evaluate how calculation components and assumptions – such as radon exposure scenarios, risk models, and other inputs – affect lifetime risk estimates (sensitivity analysis).
- To develop and apply novel statistical methods to quantify lifetime risk uncertainties with 95% uncertainty intervals.

The key scientific contribution of this dissertation lies in introducing the first comprehensive quantification of statistical uncertainty in lifetime risk estimates for occupational radon exposure. This marks a considerable advancement as previously mostly point estimates were reported in the literature, limiting comparability and interpretability. As a crucial preparatory step, comprehensive sensitivity analyses were conducted to identify the main drivers of lifetime risk results. These analyses clarified which input components require careful consideration and which have only minor influence. This insight improves transparency and guides future model development and regulatory focus. Building on this, by deriving statistical uncertainty intervals, this dissertation enables formal comparison of lifetime risks across studies – for example, by assessing overlap between intervals. This directly improves the interpretability, comparability, and credibility of lifetime risk estimates in radiation epidemiology and regulatory decisions.

Although focused on occupational radon exposure, the methodological framework and insights gained are also transferable to non-occupational (e.g., residential) radon risk assessments and can inform general lifetime risk calculations in other contexts.

1.3. Structure of the dissertation

This cumulative dissertation, together with the attached scientific publications in the second part, is structured to provide a comprehensive understanding of lifetime risks associated with radon exposure with a particular focus on occupational settings and inherent uncertainties. While the first part of this dissertation provides essential background, context, and methodological explanations, quantitative analyses are presented in the contributing publications (second part).

This introduction, which establishes the research context, is followed by a section explaining the element radon and its associated risks. Thereafter, the basic methodology for

calculating lifetime risks is outlined, followed by a brief literature overview of existing relevant studies in this context.

Each subsequent chapter is dedicated to one of the scientific publications contributing to this cumulative thesis (Table 1.1). The chapters start with a concise overview of the motivation, main findings, and implications of the publication followed by comprehensive background information and additional insights that complement the respective studies.

The first part of the dissertation ends with a conclusive chapter summarizing key findings, discussing study limitations, and suggesting directions for future research in the context of lifetime risks. The second part provides the full text of the relevant publications listed in Table 1.1 with a corresponding declaration of contribution.

	Publication title	cited as
Contribution 1	Updated risk models for lung cancer due to radon exposure in the German Wismut cohort of uranium miners, 1946–2018	(Kreuzer et al., 2023)
Contribution 2	Lifetime risks for lung cancer related to occupational radon exposure: a systematic analysis of estimation components	(Sommer et al., 2025)
Contribution 3	Lifetime excess absolute risk for lung cancer due to exposure to radon: results of the pooled uranium miners cohort study PUMA	(Kreuzer et al., 2024)
Contribution 4	Methods to derive uncertainty intervals for lifetime risks for lung cancer related to occupational radon exposure	(Sommer et al., 2024)

Table 1.1.: Overview of publications contributing to this cumulative dissertation. The order reflects the chronology in which the work was conducted. Note that the publication dates may not align with this order due to the journal peer review and editorial process. Full texts and declarations of contribution are provided in the second part of this dissertation.

2. Radon

While the public is aware of radiation risks from sources like medical treatments and nuclear accidents, other harmful sources, such as radon exposure, are less recognized despite their relevance to public health (Cori et al., 2022; Esan et al., 2020). This thesis focuses on radon and its role in lung cancer risk.

This chapter introduces the element radon, highlighting its relevance to lung cancer risk through its radioactive properties and the risk assessment derived from studies of miners. It includes a brief summary of the history of radon risk assessment and concludes with an interlude on residential radon exposure, as the thesis otherwise primarily focuses on occupational radon exposure.

2.1. Radon exposure and lifetime cancer risk

The chemical element radon is an invisible, odourless, and tasteless radioactive noble gas that naturally occurs as a decay product of uranium. It appears in different isotopes, with Radon-222 being the most common, and is found everywhere, in varying concentrations in soil, rock, and water. Outdoors, radon mixes well with air resulting in low concentrations. However, in indoor environments (homes) it can accumulate to high concentrations, especially in poorly ventilated spaces (WHO, 2023). Continuous exposure to radon and its radioactive decay products, called radon progeny or radon daughters, causes lung cancer, as was shown by several studies (J. B. Little, 2000; National Research Council [NRC], 1999; The International Agency for Research on Cancer [IARC], 1988; UNSCEAR, 2021a). Radon and radon progeny are particularly alpha-particle emitters, damaging sensitive lung tissue when inhaled. Polonium-218 and polonium-214 are major contributors to health effects among radon daughters. By inhaling radon, the decay products, whether attached to aerosol particles or not, tend to deposit on the surface of the respiratory tract. These decay products then undergo a continuous radioactive decay up to stable lead (Figure 2.1). The energetic alpha and associated gamma radiation emitted during decay affect lung cells (Degu Belete & Alemu Anteneh, 2021). After smoking, radon exposure is a leading cause of lung cancer (WHO, 2023).[1] Further, lung cancer is one of the most frequent cancer-related deaths in both men and women (Ferlay et al., 2019), making radon mitigation and risk assessment a critical public health issue (Riudavets et al., 2022).

[1] Smoking itself is recognized as the most important risk factor for lung cancer (Pesch et al., 2012; IARC, 2004).

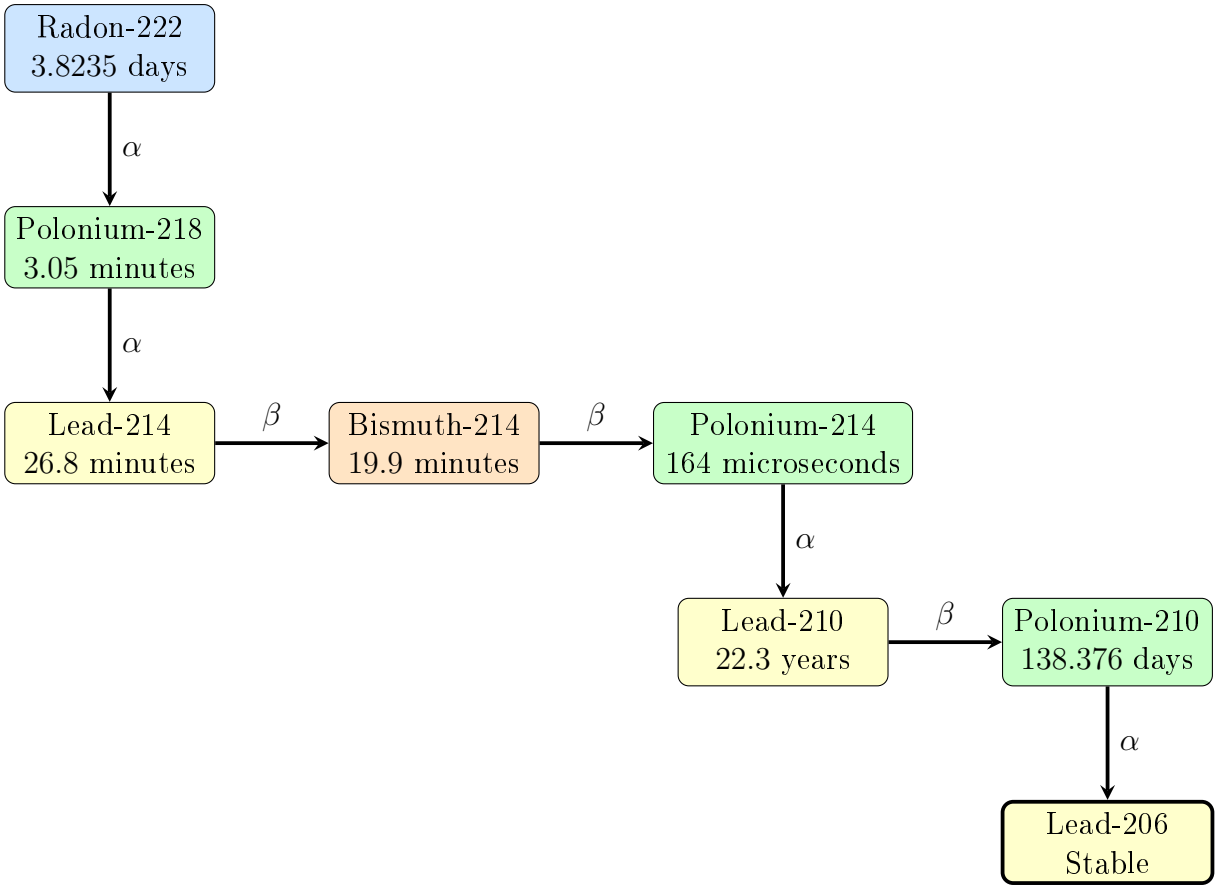

Figure 2.1.: Illustration of the decay chain from Radon-222 to stable Lead-206 with half-life times and arrows corresponding to the type of emitted radiation: alpha radiation is represented by α, and beta radiation by β.

Note that radon exposure corresponds to so-called "High-LET" (Linear Energy Transfer) radiation exposure. In general, the terms "High-LET" and "Low-LET" radiation describe the amount of energy transferred to biological tissue per unit distance travelled. High-LET radiation, such as alpha particles and neutrons, deposits a large amount of energy in a small area. This can result in substantial biological damage, including direct DNA breaks, making it more harmful even at lower doses. In contrast, low-LET radiation, including gamma rays and X-rays, transfers energy more sparsely across a larger area. While low-LET radiation also causes direct biological damage, such as single-strand DNA breaks, it is less efficient at doing so compared to high-LET radiation. Low-LET radiation primarily adverse effects through indirect mechanisms, such as the generation of unstable atoms potentially damaging organs (free radicals) (Grdina, 2022; Pearson, 2021). The differentiation between high-LET and low-LET radiation is important for understanding their different biological consequences and the associated risks.

The risk assessment for radon exposure comes in particular from cohort studies of underground miners typically exposed to elevated levels of radon and radon progeny (and other pollutants), resulting in a significantly higher risk of lung cancer compared to the general population. Such miner studies indicate a well-understood linear relationship between cumulative occupational radon exposure and lung cancer risk. This effect is influenced by factors like attained age, time since exposure, age at exposure, and exposure rate (Kreuzer et al., 2023; NRC, 1999).

However, risk assessment methods, assumptions, and the explicit modelling of exposure–risk relationships for radon and lung cancer (risk models) vary between studies. Lifetime risk calculations allow for the comparison of different risk models from different cohorts and give a quantitative interpretation of the harm of radon. In particular, lifetime risk estimates enable clear risk communication to the public. For lifetime lung cancer risks related to occupational radon exposure, one is mostly concerned with exposure in units of WLM. This unit is typically used in the risk assessment of occupational radon exposure and corresponds to an exposure of 1 Working Level (WL) (1.3×10^5 Mega electron-volt (MeV) potential alpha energy per litre air) over 170 working hours (monthly working time) (Bundesamt für Strahlenschutz [BfS], 2024).

WLM is a historical unit used to quantify radon exposure specifically in the context of mining, accounting for both radon gas and its decay products. The conversion between units of activity concentration as Becquerel per cubic meter (Bq/m^3), specifically how many radon atoms decay per second in a cubic meter of air, and exposure in WLM involves several factors. These include the equilibrium factor between radon and its progeny (typically assumed to be 0.4 in indoor environments), the duration of exposure, and assumptions about the time a person spends in the environment, typically 2,000 hours per year in a workplace or 7,000 hours in a residential setting (e.g., at home). For instance, continued exposure to a radon concentration of 300 Bq/m^3 corresponds to an annual exposure of 0.38 WLM at work and 1.32 WLM at home (ICRP, 1993, Table 3).

Both Bq/m^3 and WLM are units regarding radon exposure. It is important to understand the difference between exposure units, e.g. WLM, and a dose unit as the effective dose in mSv: exposure in WLM describes the exposure to radon and radon decay products and is directly measurable, while effective dose in mSv is a measure of the potential biological effect resulting from that exposure, considering the type and energy of the radiation, the specific tissues or organs exposed, and their sensitivity to radiation (Stabin, 2008, The Effective Dose Concept). The conversion between WLM (or Bq/m^3) and mSv is particularly challenging and remains a subject of ongoing debate ("radon dose conversion"). While various units are introduced here, the primarily focus is on WLM throughout this dissertation.

Corresponding lifetime risk calculations are concerned with low to moderate radon exposure scenarios to represent nowadays realistic exposures, especially in homes. Extreme exposure scenarios with over 1000 WLM cumulative radon exposure as they occurred in the early years of mining, are not of concern anymore (Kreuzer et al., 2009).

2.2. History of radon risk assessment

The history of radon risk assessment is characterized by a series of key events spanning several centuries (George, 2008; Mc Laughlin, 2012). In the 16th century, underground silver miners in the Ore Mountains Germany (Erzgebirge) experienced unusually high mortality from respiratory diseases. Paracelsus described the disease as "Bergsucht" (Paracelsus, 1567). In hindsight, the diagnosis "Bergsucht" must be understood as a generic term for a variety of (fatal) respiratory diseases, including lung cancer among miners (Schüttmann, 1993). In the 19th century an increased incidence of a certain type of "Bergsucht" occurred among miners in Schneeberg, Saxony. Due to the clear geographic origin of this type of "Bergsucht", German physicians developed the term "Schneeberger Lungenkrankheit" (Schneeberg lung disease) (Schüttmann, 1993). By 1879, the disease was identified as lung cancer (Härting & Hesse, 1879), where 75% of the miners in the Schneeberg region died from it since the beginning of the 19th century (Schüttmann, 1993).[2] The discovery of radioactivity (Becquerel, 1896; Curie & Curie, 1898) and the identification of radon (Dorn, 1901) provided a new explanation for the high incidence of lung cancer cases. Radon was identified as a cause of lung cancer during the first half of the 20th century, marking a milestone in understanding the health risks associated with radon exposure and the first epidemiological studies of miners on the health effects of radiation exposure started in the 1960s (Samet, 2020). In 1988, the International Agency for Research on Cancer (IARC) officially classified radon as a human carcinogen, based on studies of underground miners exposed to high levels of radon (IARC, 1988). In 1994, a pooled analysis of 11 underground miner studies provided additional evidence of the link between radon exposure and lung cancer. Building on this, in 1999 the influential BEIR VI (Biological Effects of Ionizing Radiation) report by the U.S. National Research Council (NRC), titled "Health Effects of Exposure to Radon", thoroughly addressed and quantified the health risks associated with radon exposure (NRC, 1999). After that, from 2004 to 2006, pooled studies for indoor radon exposure were conducted including studies from Europe, North America, and China, elaborating on the lung cancer risk related to radon exposure in homes (Darby et al., 2005). In 2019, the global Pooled Uranium Miner Analysis (PUMA) study – the largest pooled cohort study to date – was launched. It involves uranium miner studies from Canada, the USA, the Czech Republic, France, and Germany focusing on lung cancer risk from occupational radon exposure (Kelly-Reif et al., 2023; Rage et al., 2020; Richardson et al., 2022). Among the studies contributing to PUMA is the German Wismut cohort study, the largest single cohort of uranium miners worldwide (Kreuzer et al., 2009). The data from this cohort is the backbone for a substantial part of the analyses presented in this dissertation and contributing publications. A detailed description of the Wismut cohort is provided in Section 4.2.1.

[2] While detailed records of total miner fatalities from lung cancer are not readily available, Härting and Hesse (1879) report that between 1869 and 1877, 150 miners died from the disease, with an average of 650 miners employed.

Ongoing research and analysis have led to a deeper understanding of the health risks associated with radon exposure, ultimately contributing to the development of strategies to mitigate these risks and protect public health. Today, the International Commission on Radiological Protection (ICRP) and the United Nations Scientific Committee on the Effects of Atomic Radiation (UNSCEAR) are two prominent international bodies responsible for assessing the risks associated with radiation exposure and guiding radiation protection. The ICRP provides recommendations and guidance on all aspects of protection against ionizing radiation. UNSCEAR conducts scientific assessments of the health effects of ionizing radiation, including radon, and provides the scientific basis for ICRP's work on radiation protection. Both regularly publish reports. Their research and recommendations help governments and organizations worldwide formulate policies and regulations to protect public health from, in particular, radon-induced lung cancer (ICRP, 2014; UNSCEAR, 2021a).

2.3. Interlude on residential radon exposure

This thesis primarily explores the health effects of radon exposure in occupational settings, with a particular focus on uranium miner cohorts. While the findings are most directly applicable to occupational exposure, they are also relevant to residential radon risk. Although the effects of residential radon exposure are not the main focus of this work, a brief overview of the lung cancer risks associated specifically with residential radon exposure is provided here, given the public relevance of this topic:

While studies of miners provide valuable insights, directly extrapolating these findings to residential radon exposure involves challenges. Occupational and residential radon exposures differ not only in magnitude – residential levels are considerably lower – but also in measurement methods, environmental factors, and confounding variables such as smoking, exposure duration, and ventilation practices (NRC, 1999; Pavia et al., 2003). Additionally, the units of measurement differ: occupational exposure is often expressed in WLM, which accounts for radon decay products and working conditions. The unit was based on the energy that inhaled progeny would deposit in the lung. In old uranium mines, the ventilation was often poor and the limited airflow allowed radon progeny to accumulate to levels close to equilibrium with the radon gas (ICRP, 1993). In contrast, residential exposure is typically measured in Bq/m^3, based on long-term average concentrations of radon gas and progeny in indoor air, usually measured over periods of several months (Darby et al., 2005).

Note that analyses of miners with lower cumulative exposure ($<$100 WLM) have shown consistent patterns of risk, suggesting that the extrapolation to residential exposure scenarios is valid, though the risk per unit exposure may differ (Lane et al., 2019; Lubin et al., 1997). This supports using occupational data to inform residential radon risk assessments, despite challenges in extrapolation and confounding factors.

Due to the mentioned differences, dedicated studies are necessary to assess the risks associated with residential radon exposure. However, these studies face unique challenges. This is, among other reasons, due to the considerably lower levels of radon concentration in homes. Specifically, a case-control study is often preferred over a cohort study, as the latter would need to be excessively large to contain enough lung cancer cases.

Despite these challenges, residential radon studies demonstrate a significant lung cancer risk. The relative risk of lung cancer increases with residential radon concentrations, demonstrating a clear, presumably linear, exposure-risk relationship (Darby et al., 2005). Studies estimate that indoor radon exposure is responsible for 3–20% of all lung cancer deaths worldwide (Kim et al., 2016). In Germany, recent studies indicate that 6.3% of lung cancer cases are attributable to residential radon, which translates to around $2,800$ lung cancer deaths per year (Heinzl et al., 2024). Reducing radon levels in homes under recommended action levels could decrease lung cancer deaths by 2-4% according to earlier research (Lubin et al., 1995). This confirms that residential radon exposure is an important risk factor for lung cancer, highlighting the need for corresponding protective measures.

3. Methods and literature

Here, the basic underlying methodology for lifetime risk calculations performed in this dissertation is outlined. Further, an overview is given of the research landscape concerning lifetime risks, both in general and for lung cancer related to occupational radon exposure, establishing the context for this thesis and contributing publications.

3.1. Basic methodology

3.1.1. Lifetime risk calculation

Typically, one is interested in the excess lifetime risk imposed from radiation exposure compared to the baseline lifetime risk in the absence of exposure. Different functional forms to calculate excess lifetime risks (lifetime risk measures) are employed in the literature for various causes of death and radiation types, including – but not limited to – lung cancer related to radon exposure (M. P. Little et al., 2008; Thomas et al., 1992; Ulanowski et al., 2019; Vaeth & Pierce, 1990). All of them are following a similar approach:

Excess lifetime risks are calculated as the difference between the lifetime risk under exposure $LR_E(a)$ and the baseline lifetime risk $LR_0(a)$ for a certain cause of death. A lifetime risk is calculated as the cumulative sum of age-specific (years) mortality rates weighted by the survival probability to attain each age. A baseline lifetime risk $LR_0(a)$ without exposure is expressed as

$$LR_0(a) = \int_a^\infty r_0(t) S_0(t|a)\, dt, \tag{3.1}$$

where

- a is the attained age or minimum age at risk, typically $a = 0$,
- $r_0(t)$ is the baseline cause-specific mortality rate at age t in absence of exposure,
- $S_0(t|a)$ is the conditioned all-cause survival function in the absence of exposure, defined as $S_0(t|a) = \mathbb{P}(T \geq t | T \geq a) = \frac{\mathbb{P}(T \geq t \,\cap\, T \geq a)}{\mathbb{P}(T \geq a)} = S_0(t)/S_0(a)$ with $T \geq 0$ the unknown random retention time until the event of death and unconditioned all-cause survival function with $S_0(t) = S_0(t|0) = \mathbb{P}(T \geq t)$.

The corresponding lifetime risk under exposure $LR_E(a)$ is written as

$$LR_E(a) = \int_a^\infty r_E(t) S_E(t|a)\, dt, \tag{3.2}$$

where $r_E(t)$ is the cause-specific mortality rate at age t under exposure with corresponding all-cause survival function $S_E(t)$. The final excess lifetime risk estimate is the difference $LR_E(a) - LR_0(a)$.

This general formulation applies to any cause of death (typically cancer) and exposure type. In this work, it is applied specifically to lung cancer risks from (occupational) radon exposure, where the rate $r_E(t)$ is projected as

$$r_E(t) = r_0(t)(1 + ERR(t)), \tag{3.3}$$

where $ERR(t) = \frac{r_E(t) - r_0(t)}{r_0(t)}$ is the excess relative risk of dying of lung cancer at age t. The $ERR(t)$ term is parametrized by a set of M parameters $\Theta = (\theta_1, \ldots, \theta_M)$. To emphasize this dependence, the notation $ERR(t; \Theta)$ will be used in the following, which is equivalent to $ERR(t)$. Note that for other cause of deaths and radiation types, the risk projection $r_E(t) = r_0(t) + EAR(t; \Theta)$ via the excess absolute risk $EAR(t; \Theta) = r_E(t) - r_0(t)$ is often used in the literature (ICRP, 2007). However, in the context of lung cancer related to chronic (occupational) radon exposure, excess relative risk projections are typically used. EAR models are not established in the literature for occupationally radon-exposed miners (UNSCEAR, 2021a).

Further, it is not specifically differentiated between mortality rates (number of deaths in a specific period relative to the population) and mortality risks (probabilities) here. Mortality risks are typically approximated with mortality rates and there are specific methods to obtain risk estimates from corresponding rates (Eisenmenger & Emmerling, 2011; Flaskämper, 1962). However, such methods are beyond the scope of this thesis and we rely on using mortality rates.

Assuming no protective effect of radon exposure, consistent with the Linear-No-Threshold (LNT) model for an exposure-risk relationship (Laurier et al., 2023), it holds $r_E(t) \geq r_0(t)$ and $ERR(t; \Theta) \geq 0$ for all ages t. Note that assuming the LNT model is consistent with the position of major radiation protection authorities, including international bodies like UNSCEAR (2021b) and the ICRP (2007), as well as influential committees like BEIR VII (NRC, 2006).

The modelling of $S_E(t|a)$ and $S_0(t|a)$ varies across studies. However, typically and also here, the survival functions are modelled as

$$S_0(t|a) = \exp\left\{ -\int_a^t q_0(u)\, du \right\}, \tag{3.4}$$

$$S_E(t|a) = \exp\left\{ -\int_a^t q_E(u)\, du \right\}, \tag{3.5}$$

with baseline all-cause mortality rate $q_0(u)$ at age u and corresponding all-cause mortality rate $q_E(u)$ under exposure. The application of survival functions depends on the chosen lifetime risk measure. For example, the commonly used excess lifetime risk measure $LEAR(a)$ ignores radiation effects in the survival function and applies $S_0(t)$ in the calculation of both $LR_E(a)$ and $LR_0(a)$, resulting in

$$LEAR(a) = \int_a^\infty r_E(t) S_0(t|a)\, dt - \int_a^\infty r_0(t) S_0(t|a)\, dt = \int_a^\infty r_0(t) ERR(t;\Theta) S_0(t|a)\, dt. \quad (3.6)$$

Among other minor components, estimates for (excess) lifetime lung cancer risk related to radon depend on three central components:

- Baseline lung cancer and all-cause mortality rates $r_0(t)$, $q_0(t)$ for every age t, respectively,
- Risk model structure and parameter estimates $\hat{\Theta}$ derived from cohort data shaping $ERR(t;\hat{\Theta})$,
- Individual radon exposure scenario with annual exposure levels in units of WLM influencing $ERR(t;\Theta)$ at every age t.

Note that throughout this dissertation the term "risk model" refers to the combination of model structure, i.e. the functional form of the $ERR(t;\Theta)$ term, and cohort data used to estimate the model parameters Θ. This distinction is important, as differences in risk models and corresponding lifetime risks often arise from variations in the underlying cohort data rather than from the specific model structure themselves.[1]

For the calculation of (excess) lifetime lung cancer risks, baseline lung cancer and all-cause mortality rates, $r_0(t)$ and $q_0(t)$, respectively, and corresponding survival functions, are typically derived from population data or obtained from ICRP reference rates (ICRP, 2007). Further, the functional form of the $ERR(t;\Theta)$ term and the components of the parameter vector Θ are chosen based on experience, international practices, expert knowledge, and, most importantly, a sufficiently good fit to the cohort data. The parameters are estimated using statistical methods, such as maximum likelihood estimation, based on regression analysis of data from radiation-exposed populations, such as uranium miners. The radon exposure scenario is either a reference occupational scenario to resemble average working conditions (e.g. 2 WLM from age 18-64 years) or inspired by individual miner exposure histories.

[1] For example in (Kreuzer et al., 2023) Table 2, the variation of lifetime risk estimates is larger across the cohorts than across the model structures.

3.1.2. Risk model parameter derivation

The risk models used in this thesis are derived from cohort data on (uranium) miners occupationally exposed to radon and radon progeny.[2] Here, Poisson regression on the number of lung cancer deaths is applied to a grouped dataset from the underlying miners cohort data to estimate risk model parameters. The corresponding likelihood function $L(\Delta, \Theta|X)$ with risk model parameter vector $\Theta = (\theta_1, \ldots, \theta_M)$ and baseline stratification parameter vector $\Delta = (\delta_1, \ldots, \delta_K)$, given grouped cohort data X, is based on the assumption that the number of lung cancer deaths C_i in group i for $i = 1, \ldots, N$ is Poisson-distributed via

$$C_i \sim Poi\left(PY_i e^{\eta_i(\Delta)}\left(1 + ERR_i\left(\Theta\right)\right)\right), \tag{3.7}$$

with person-years at risk PY_i and excess relative risk $ERR_i\left(\Theta\right)$. The specific shape of $ERR_i\left(\Theta\right)$ depends on the prescribed risk model structure. The baseline risk predictor $\eta_i(\Delta) = \delta_1 + \sum_{k=2}^{K} \delta_k \mathbb{1}_{\{k\}}(x_i)$, where x_i is a categorical variable with K levels, describes the baseline stratification with K levels.

Although the full likelihood model includes both the parameters Δ and Θ, typically only the important maximum likelihood estimates for Θ are shown. This likelihood function and detailed parameter estimation is investigated further in Section 4.2.2.

While the actual computation of lifetime risks involves further complexities, this overview provides a framework for understanding the basic process. All lifetime risk calculations for this thesis were performed with the statistical software *R* (R Core Team, 2023) and the programming environment *RStudio* (Posit team, 2023). To meet the specific needs of this research, we developed and implemented a comprehensive, custom-built *R* solution for these calculations. The fitting of risk model parameters is mostly carried out with the specialized software *Epicure* (Preston et al., 1993) or, when explicitly stated, with another tailored *R* implementation.

3.2. Literature overview on lifetime risks

The following literature overview aims to briefly summarize key advancements in lifetime risk assessments in general and specifically for lung cancer related to radon exposure. Publications directly contributing to this dissertation are not listed here. More detailed assessments of existing research are provided in the introductions of the respective contributing articles.

This thesis focuses on the (excess) lifetime risk of lung cancer death related to radon exposure, primarily based on uranium miner cohort studies. Lifetime risks in general are a widely used metric for quantifying cancer risk from ionizing radiation (NRC, 2006; UNSCEAR, 2021b). They are also applied to other indoor air pollutants, such as benzene

[2] Note that risk models for other types of radiation are for example derived from the atomic bomb survivors Life-Span Study (LSS) (Preston et al., 2007).

(WHO Regional Office for Europe, 2010). However, radon typically results in substantially higher lifetime risks compared to other chemicals considered, emphasizing its importance as a major carcinogenic air pollutant.

Early investigations addressing lifetime risk estimation methods in general was provided by Vaeth and Pierce (1990) and Thomas et al. (1992), who introduced the basic methodology to compute lifetime risks, that remain relevant today. Over time, several lifetime risk measures were introduced and applied, including Excess Lifetime Risk (ELR), Risk of Exposure Induced Death (REID), Lifetime Excess Absolute Risk (LEAR) (Hunter et al., 2015; Kellerer et al., 2001; Thomas et al., 1992), and more recently, the Radiation-Attributed Decrease of Survival (RADS) (Ulanowski et al., 2019).

Kellerer et al. (2001) discussed and evaluated the lifetime risk calculation methodology and identified flaws such as the sensitivity to demographic assumptions, and the lack of standardized computational conventions. A thorough application of lifetime risk assessments to various types of radiation-induced cancer have been presented by M. P. Little et al. (2008, 2020). In the context of radon and dose conversion, a rich body of literature exists, including multiple ICRP publications (ICRP, 1993, 2007, 2010). These assessments often rely on risk models derived from the atomic bomb survivors LSS (Preston et al., 2007).

Specifically for lung cancer related to occupational (chronic) radon exposure, lifetime risk calculations derived from miner studies led to a new proposal for the epidemiological approach for radon dose conversion coefficients (Tomášek, Rogel, Laurier, & Tirmarche, 2008). This was a step forward since miners (chronic exposure) have different exposure characteristics compared to atomic bomb survivors (acute exposure), as in the LSS. Subsequent studies examined model assumptions, particularly smoking behaviour, and conducted sensitivity analyses across different miner cohorts and applied lifetime risk calculations to specific populations (Chen et al., 2017; Hunter et al., 2015; Tomášek, 2020). The analyses underscore the substantial impact of risk model structure, reference population choice, or smoking behaviour on lifetime risk estimates.

The understanding of the exposure-risk relationship for radon and lung cancer improved over the years, specifically by pooling of miner cohorts, leading to refined risk models and corresponding lifetime risk estimates. Notable mentions are the established BEIR VI and recent PUMA risk models (Kelly-Reif et al., 2023; NRC, 1999; Richardson et al., 2022).

While uncertainties in lifetime cancer risk estimates have been well studied for acute radiation exposure (NRC, 2006; UNSCEAR, 2021b; Xue & Shore, 2001), and are quantified through software tools as "RadRAT" (Berrington de Gonzalez et al., 2012) and "CONFIDENCE" (Walsh et al., 2020), comparable evaluations for lung cancer related to occupational (chronic) radon exposure are limited (Pawel & Puskin, 2003; Tomášek, 2020).

4. Updated risk models for lung cancer due to radon exposure in the German Wismut cohort of uranium miners, 1946–2018

4.1. Publication overview

Context and motivation

The underlying publication (Kreuzer et al., 2023) follows the recommendation of UNSCEAR to focus on more contemporary uranium miners for research of lung cancer risk at low radon exposures or exposure rates (UNSCEAR, 2021a). It presents updated and refined risk models derived from the German uranium miners cohort study (Wismut cohort), which shape the exposure–risk relationship for lung cancer due to occupational radon exposure and enable more precise lifetime risk estimates.

Key findings and scientific relevance

The updated Wismut risk models derived with the software *Epicure* confirm and refine the established association between radon exposure and increased lung cancer risk. Specifically the sub-cohort of miners first hired in 1960 or later (1960+ sub-cohort), characterized by low radon exposure and exposure rates with high-quality exposure assessment, provides now, through the extended follow-up to 2018, risk estimates consistent with other international 1960+ sub-cohorts. This all together makes the 1960+ sub-cohort risk model the preferred model to estimate lung cancer risk at low exposure and exposure rate levels.

Risk models are essential for estimating lifetime risks. Employing updated and refined risk models enhances the accuracy of these estimates, which also contributes to the international discussion on radon dose conversion coefficients. This is especially true when using the updated risk models fit on the 1960+ sub-cohort with its high-quality exposure data. The updated methodology, in line with other international results, contributes to the comparability of results between miner studies.

Outlook and future directions

Continued follow-up of the cohort is expected to reduce statistical uncertainty, especially at older ages within the 1960+ sub-cohort. This will provide a robust basis for future radon-related lung cancer risk assessment. More modern risk modelling approaches such as excess hazard models, may offer certain advantages over methods from the established *Epicure* software, see e.g. (Aßenmacher et al., 2019). However, *Epicure* itself remains a highly regarded and widely used tool within the radiation epidemiology community, continues to be maintained, and regularly receives updates.

4.2. Background on material and methods

Here, additional background information on the German uranium miners cohort study and the corresponding Wismut company is presented. Further, the methodology of risk model fitting on miners cohort data is explained in more detail. This chapter emphasizes the importance of employing valuable, robust, and sound radon-related risk assessment models for estimating corresponding lifetime risks.

4.2.1. The German uranium miners cohort study

The German uranium miners cohort study (Wismut cohort) is a cohort study that was started in the 1990s by the German Federal Office for Radiation Protection and comprises almost 59,000 male miners employed at the Wismut AG between 1946 and 1989, with 2.5 million person-years at risk, and 4,329 confirmed lung cancer deaths, with current passive mortality follow-up 1946-2018 (Kreuzer et al., 2023). It is the largest single study of miners occupationally exposed to radon and radon progeny worldwide. In addition, this cohort has a long follow-up period of 42 years on average and a low percentage of loss-to-follow-up with 3% (Kreuzer et al., 2023). The database contains information about different miner-specific endpoints such as (among others) radon exposure in WLM for every calendar year between 1946 and 1989, date of beginning and end of employment at the Wismut company, annual working days, and (if available) cause of death. Every 5 years a passive mortality follow-up on the cohort with updated vital statuses and causes of death for the miners is performed. The information is taken from death certificates and autopsy files. Until now, results from five passive mortality follow-ups from 1946 up until the year 1998, 2003, 2008, 2013, and 2018 were published (Grosche et al., 2006; Kreuzer et al., 2010, 2015, 2018, 2023).

The goal of the Wismut cohort study is to investigate health effects associated with employment in the Wismut company and verification of established estimates of radon-related lung cancer risk with an independent data set. Besides the effect of inhalation of radon and radon progeny, the study investigates the health effects of multiple pathogens like inhalation of uranium dust, fine dust, silica dust, and arsenic dust, and exposure to exter-

nal gamma radiation (Kreuzer et al., 2009). Among other results, this study contributed to exposure-risk relationship insights on lung cancer and other cancers related to radon (Fenske et al., 2025; Kreuzer et al., 2023), lung cancer by silica dust (Sogl et al., 2012), and silicosis by silica dust (Kreuzer et al., 2013).

During the total period of uranium mining by the Wismut company from 1946-1989, three different periods are distinguished: In the period 1946-1954, working conditions were poor with no radiation or work protection, only natural ventilation, and dry drilling for uranium ore. There was no radon measurement and miners were exposed to high concentrations of dust and radiation. From 1955-1970 the working conditions improved with radon measurements, begin of radiation protection measures, several ventilation measures leading to a decrease in radon concentration, and the introduction of wet drilling decreasing the exposure by less swirled-up radon and dust particles in the drilling process. After 1970 international standards for radiation protection and occupational safety were introduced, as well as individual radon measurements. Due to these improved protective measures, the mean radon exposure reduced from 1955 on over the years reaching low exposure levels of international radiation protection standards in the 1970s. The uranium mines were closed with the German reunification in 1990 (Grosche et al., 2006; Kreuzer et al., 2009).

Due to missing exact radon measurements in the early years of mining, the full cohort suffers from high exposure uncertainty in these early years. Radiation exposure assessment was carried out by using a detailed job-exposure matrix (JEM) which includes information on radiation for each calendar year of employment between 1946-1989, each place of work (underground, milling/processing, and surface), and each type of job. For the period from 1946 to 1954 without radon measurements, radon concentrations were derived retrospectively by an expert judgment based on measurements from 1955. Information on the other pathogens as dust and silica is also based on a similar job-exposure matrix (Kreuzer et al., 2009). The 1960+ sub-cohort includes roughly $26,000$ miners and is characterized by low radon exposure of high quality, offering a strong basis for lung cancer risk estimation at low radon exposures and low exposure rates.

In total, more than $400,000$ persons were employed at the Wismut company between 1946 and 1989 with roughly $8,000$ compensations for radiation induced cancer as an occupational disease by the end of 1999 (Schröder et al., 2002).

The corresponding mines were located in Eastern Germany in Saxony and Thuringia in the Ore Mountains (Erzgebirge). Shortly after the Second World War, previously shut down mines were re-opened by order of the Soviet Union to extract uranium, a material needed for the construction of nuclear weapons. For that cause, the corporation Wismut AG was founded with the code name WISMUT[1] to disguise the nuclear intention of the company. The operation was presented as bismuth and cobalt mining to mask uranium extraction. Due to rich uranium deposits in the Ore Mountains, the Wismut AG quickly became the main contributor of uranium in the Soviet Union. Today, the successor company Wismut

[1] Wismut is the German word for the mineral bismuth.

GmbH (headquartered in Chemnitz) is a federal company entrusted with the restoration and renaturation of the legacies of the Wismut mining industry. For further reading, the thorough German source by Hiller and Ducke (1999) is recommended.

4.2.2. Risk model parameter estimation and software

The relationship between lung cancer risk and radon exposure is modelled using a relative risk approach, as previously introduced (Section 3.1). The shape of the excess relative risk term is defined by a preselected risk model structure. These risk model structures are based on experience, international practices, and expert judgment. Studies on miners have established that the relative risk of lung cancer increases approximately linearly with cumulative exposure to radon and radon progeny. Additionally, effect-modifying variables such as attained age, time since exposure, and exposure rate further influence this risk (UNSCEAR, 2021a). Risk models contain (to be estimated) parameters accounting for those effect-modifying variables.

Risk model parameter estimation theory

The risk model parameter estimates $\hat{\Theta} = \left(\hat{\theta}_1, \ldots, \hat{\theta}_M\right)$ stated in the underlying publication are computed with the established software *Epicure* (Preston et al., 1993) using maximum likelihood methods with the theory and notation introduced in Section 3.1.2. A baseline stratification parameter vector $\Delta = (\delta_1, \ldots, \delta_K)$ with $K = 720$ strata is used.[2] The number of risk model parameters M depends on the chosen model and ranges from $M = 1$ to $M = 12$. For reference, the total number of groups N in the grouped dataset depends on the complexity of the assumed categories and ranges approximately from $5,000$ to $500,000$.

The likelihood function $L(\Delta, \Theta|X)$, given grouped cohort data X, with baseline risk predictor $\eta_i = \eta_i(\Delta) = \delta_1 + \sum_{k=2}^{K} \delta_k \mathbb{1}_{\{k\}}(x_i)$ and assuming independent and identically Poisson-distributed observations, is expressed as:

$$L(\Delta, \Theta|X) = \prod_{i=1}^{N} \frac{\left(PY_i e^{\eta_i(\Delta)}(1 + ERR_i(\Theta))\right)^{C_i} e^{-PY_i e^{\eta_i(\Delta)}(1+ERR_i(\Theta))}}{C_i!}, \tag{4.1}$$

[2] 16 categories for age, 15 categories for calendar year, and 3 categories for duration of employment results in $16 \times 15 \times 3 = 720$ different baseline risk predictor estimates η_i.

with log-likelihood

$$\begin{aligned}\ell(\Delta,\Theta|X) = \log L(\Delta,\Theta|X) &= \sum_{i=1}^{N} C_i \left(\log PY_i + \eta_i(\Delta) + \log\left(1 + ERR_i\left(\Theta\right)\right)\right) \\ &- \sum_{i=1}^{N} PY_i e^{\eta_i(\Delta)} \left(1 + ERR_i\left(\Theta\right)\right) - \sum_{i=1}^{N} \log C_i! \\ &\propto \sum_{i=1}^{N} C_i \left(\log PY_i + \eta_i(\Delta) + \log\left(1 + ERR_i\left(\Theta\right)\right)\right) - \sum_{i=1}^{N} PY_i e^{\eta_i(\Delta)} \left(1 + ERR_i\left(\Theta\right)\right).\end{aligned}$$

This log-likelihood $\ell(\Delta,\Theta|X)$ can then be optimized with usual optimization procedures to obtain maximum-likelihood estimates (MLEs) $\hat{\Theta}$ and $\hat{\Delta}$. Note that the classical regularity conditions to ensure an asymptotically normally distributed likelihood function are fulfilled here, compare (Amemiya, 1985, Chapter 4).

The baseline strata vector Δ is typically high-dimensional and simultaneously optimizing for $\hat{\Theta}$ and $\hat{\Delta}$ is computationally expensive. Luckily, one can analytically deduce

$$\frac{\partial}{\partial \delta_1}\ell(\Delta,\Theta|X) = S - e^{\delta_1}\left(T_1 + \sum_{k=2}^{K} T_k e^{\delta_k}\right) \stackrel{!}{=} 0, \tag{4.2}$$

$$\frac{\partial}{\partial \delta_k}\ell(\Delta,\Theta|X) = S_k - T_k e^{\delta_1+\delta_k} \stackrel{!}{=} 0 \text{ for } k = 2,\ldots,K, \tag{4.3}$$

where $S = \sum_{i=1}^{N} C_i$, $S_k = \sum_{i|x_i=k} C_i$ and $T_k = \sum_{i|x_i=k} PY_i\left(1 + ERR_i(\Theta)\right)$. Solving equation (4.3) for δ_k and plugging the result in equation (4.2) solving for δ_1 yields

$$\begin{aligned}\delta_1 &= \log\left(S - \sum_{k=2}^{K} S_k\right) - \log(T_1), \\ \delta_k &= \log(S_k) - \log(T_k) - \delta_1 \text{ for } k = 2,\ldots,K.\end{aligned}$$

With this analytical result, the optimal baseline strata parameters $\Delta = \Delta\left(\Theta\right)$ are a function of the risk model parameter Θ and numerically deriving the MLEs $\hat{\Theta}$ and $\hat{\Delta}$ is reduced to finding $\hat{\Theta}$ because the baseline strata MLEs are obtained by evaluating Δ at the MLE $\hat{\Theta}$, i.e. $\hat{\Delta} = \Delta\left(\hat{\Theta}\right)$.

Besides parameter point estimates, corresponding confidence intervals are of particular interest. To derive these, standard errors of point estimates (i.e., the covariance matrix) are obtained from the inverse of the Fisher information matrix $I\left(\Delta,\Theta\right)$ with

$$I\left(\Delta,\Theta\right) = \begin{bmatrix} P & Q' \\ Q & R \end{bmatrix} \in \mathbb{R}^{(K+M)\times(K+M)},$$

where

$$P = (p_{k,k'})_{k,k'=1,\dots,K} \in \mathbb{R}^{K\times K}, \quad p_{k,k'} = -\frac{\partial^2}{\partial\delta_k\partial\delta_{k'}}\ell(\Delta,\Theta|X),$$
$$Q = (q_{m,k})_{m=1,\dots,M;k=1,\dots,K} \in \mathbb{R}^{M\times K}, \quad q_{m,k} = -\frac{\partial^2}{\partial\theta_m\partial\delta_k}\ell(\Delta,\Theta|X),$$
$$R = (r_{m,m'})_{m,m'=1,\dots,M} \in \mathbb{R}^{M\times M}, \quad r_{m,m'} = -\frac{\partial^2}{\partial\theta_m\partial\theta_{m'}}\ell(\Delta,\Theta|X),$$

and Q' denoting the transposed matrix of Q. The inverse of the Fisher information matrix $I(\Delta,\Theta)$ evaluated at the ML estimate is an estimator for the asymptotic covariance matrix (Rüger, 1998). One is particularly interested in the standard errors for the risk model parameters Θ. The covariance matrix for the important risk model parameters Θ is $(R - QP^{-1}Q')^{-1}$. This results from the inverse of the block matrix $I(\Delta,\Theta)$, see e.g. (Lu & Shiou, 2002). In particular, it is insufficient to derive R^{-1}. Although the baseline strata parameter estimates are not numerically derived, the covariance matrix for Θ must be adjusted for the estimation of Δ.

Classical $(1-\alpha)\cdot 100\%$ confidence intervals for the risk model parameter estimates $\hat{\theta}_m$ for all $m = 1,\dots,M$ are derived via

$$\hat{\theta}_m \pm 1.96 z_{1-\alpha/2} \cdot \left(R - QP^{-1}Q'\right)^{-1}_{mm}, \tag{4.4}$$

where $z_{1-\alpha/2}$ is the standard-normal quantile at $1-\alpha/2$.

This estimation process is similarly explained in (Higueras & Howes, 2018) and contributed to understanding the mechanisms behind the fitting process in *Epicure*. In particular, the notation is adapted here. Note that this likelihood structure is different from a usual generalized linear models (GLM) (Nelder & Wedderburn, 1972) and typical tools for GLMs cannot be applied here. In general, there is no suitable link function unless the ERR model structure is simple (Higueras & Howes, 2018).

Software

Cohort studies in radiation epidemiology involve complex data structures with time-varying variables and non-standard regression models, necessitating the use of specialized software like *Epicure* (Preston et al., 1993). This software facilitates the grouping of datasets and the use of internal Poisson regression to model excess relative risks as explained above.

The risk modelling software *Epicure* is often used in radiation epidemiology instead of *R* (R Core Team, 2023) or similar modern statistical software because *Epicure* was developed in the 1980s explicitly for research questions emerging from radiation epidemiology and corresponding data analysis. The development was motivated by the need for models explaining excess relative risks, which were more suitable in describing exposure-risk relationships and effect modifications compared to Cox proportional hazard models. Further,

Epicure provided solutions to create detailed person-year tables and the explicit modelling of time-dependent variables. *Epicure* quickly became the standard for modelling radiation health effects and found extensive application in various fields including medicine, public health, epidemiology, and economics. With over 1,000 citations in research papers, *Epicure* remains an established tool in epidemiological research and data analysis.[3] With *Epicure* being recognized in the radiation epidemiology community, there was no demand for *R* solutions. The agreement to one software for risk assessment supports the comparability of results within the community. However, from today's perspective, the user experience with *Epicure* is rather dated and in comparison, *R* offers a more intuitive and flexible programming experience.

Epicure consists of a module for the creation of person-year or risk tables (grouped dataset), including time stratification. Further there are specific modules for Poisson regression for rates or counts, Cox regression for survival data, and binomial regression for case-control data. The risk model parameter fitting process for this publication involves the modules for the creation of person-year tables (grouped dataset) and the subsequent Poisson regression as follows:

First, the raw cohort data is transformed, generating and storing time-varying variables such as cumulative exposure or age at median exposure. A grouped dataset is then constructed by defining specific categories (or intervals) for various factors, such as radon exposure, age, and duration of employment. This grouped dataset forms a matrix with N rows for every combination of categories and columns for every category group (exposure, exposure rate, age, calendar year, number of lung cancer cases, etc.). Within each matrix cell, the person-time weighted mean value is calculated. Additionally, the sum of lung cancer deaths and total person-years at risk is stored for each category combination. Lastly, the Poisson regression module is applied to the grouped dataset for various risk model structures $ERR(t;\Theta)$ (equation (3.7)) to obtain parameter estimates $\hat{\Theta}$.

While *Epicure* provides a powerful framework for risk modelling, certain limitations must be acknowledged. The structure and dimension of the grouped dataset, particularly the number of rows N, may be influenced by the chosen risk model specification. For example, models fitted to the 1960+ sub-cohort use fewer exposure rate categories compared to models fitted to the full cohort (compare Table 2 and Table 3 in (Sommer et al., 2025)), resulting in considerably smaller grouped datasets. This also applies to models of varying complexity within the same cohort: simpler models may exclude effect modifiers like age at median exposure or time since exposure, which could lead to discarding seemingly irrelevant categories when constructing the grouped dataset. However, omitting such "empty" categories can influence final estimates. Similarly, the choice of how to define category boundaries can influence results (Richardson & Loomis, 2004). Thus, even with identical underlying raw cohort data, subjective choices in data grouping process prior to model fitting can introduce biases or variability.

[3]This claim is based on information provided by Hirosoft, the developers of Epicure, available at https://hirosoft.com/epicure_short/ (accessed January 17, 2025).

5. Lifetime risks for lung cancer related to occupational radon exposure: a systematic analysis of estimation components

5.1. Publication overview

Context and motivation

Lifetime risks for lung cancer related to occupational radon exposure play a key role in several areas of radiation protection as in the epidemiological approach for radon dose conversion (ICRP, 1993, 2007, 2010) or in the concept of radiation detriment (ICRP, 2022). Typically, such estimates are based on one specific combination of calculation components (Tomášek, Rogel, Laurier, & Tirmarche, 2008), yet the sensitivity of lifetime risks to variations in calculation components has not been thoroughly examined.

Key findings and scientific relevance

The underlying study (Sommer et al., 2025) systematically assessed the influence of various calculation components on lifetime risk estimates, with particular focus on the LEAR per unit of exposure WLM. It employed a custom-built, modular R solution to allow efficient recalculations under varying input assumptions. The analysis identified the choice of risk model with underlying miners cohort and baseline lung cancer mortality rates as major drivers of lifetime risk variation, while showing that the radon exposure scenario – within occupationally relevant bounds – has only a limited effect. In particular, there is no benefit from choosing complex scenarios over the internationally typical scenario of 2 WLM from age 18-64 years to represent an occupational radon exposure scenario.

By emphasizing the importance of carefully selecting high-impact components, this study contributes to a better understanding of the main drivers of lifetime risks. The validation of the typical occupational exposure scenario, along with the practicable LEAR measure, provides a practical framework for calculating lifetime risks, thereby simplifying methodological decisions for researchers and policymakers alike. The discovered strong impact

of risk models and baseline lung cancer rates lays the groundwork for reasonable and focused lifetime risk uncertainty quantification, as further explored in (Sommer et al., 2024) (Chapter 7).

Outlook and future directions

Looking ahead, the substantial influence of baseline lung cancer mortality suggests that future studies should consider country-specific lifetime risk calculations to better reflect regional health contexts. Additionally, the insights gained from this work motivate a more targeted approach to uncertainty assessment in lifetime risk estimation.

5.2. Background on material and methods

Here, additional information related to influential lifetime risk calculation components as the utilized mortality data and risk model cohorts is presented.

5.2.1. Mortality rate data

A lifetime risk estimate for lung cancer related to radon exposure depends (among other components) on all-cause and lung cancer baseline mortality rates and the corresponding choice of mortality data. For sensitivity analyses here, data from the World Health Organization (WHO) Mortality Database (WHO, 2022) were utilized. This database is a comprehensive freely accessible online data repository managed by the WHO. It collects and collates population and mortality data since 1950 from over 100 countries worldwide, enabling analysis and comparison of death rates and causes across different regions and calendar years. It includes information on population size, deaths by cause, sex, age, and year, with the causes of death classified according to the International Classification of Diseases (ICD). This data is transmitted from national civil registration and vital statistics systems. All mortality data is reported annually by WHO member states, maintaining high standards for data quality and reliability to support cross-national comparisons. Despite its extensive coverage, the database faces challenges such as timely data submission and varying completeness of data sets, which can affect the overall data accuracy and usability. This valuable database provides essential data for comparative epidemiological studies and is often utilized by researchers. In addition, the WHO provides various tools that ease the retrieval and analysis of data, supporting the use of the database.

It is important to note that the WHO database does not include data on potential confounders such as smoking behaviour, a significant factor in lung cancer mortality. Given this, additionally information from the Organisation for Economic Co-operation and Development (OECD, 2023) Health Statistics on tobacco consumption (% of the population aged 15+ who are daily smokers) by country and year is integrated to derive the heavy- and

light-smoker population mortality rates. Note that rankings of smoking prevalence might vary depending on the measures and sources of smoking behaviour data used. Another notable comprehensive resource also providing extensive information on global smoking behaviour is *The Tobacco Atlas* (2022).

In parallel, the OECD Health Statistics offers an extensive and comprehensive set of data specifically focused on health and healthcare systems across the OECD member states, as well as some key partners and additional nations. The database covers a wide range of health indicators including life expectancy, hospital beds, health workforce, health risks like tobacco consumption and obesity rates, total health spending, and patient-reported indicators among others. Regularly updated, these statistics are valuable for performing comparative epidemiological analyses.

5.2.2. Risk models and cohorts

This work compares existing and established models for the excess relative risk $ERR(t;\Theta)$ at all ages t across different miner cohorts. Note that excess absolute risk models are not typically applied for modelling lung cancer risks related to occupational radon exposure (UNSCEAR, 2021a).

A distinction is made between categorical and parametric (continuous) risk models. Categorical models are characterized by factors that can change abruptly based on input variables. For example, one factor might apply to the age group 55-59 and a different factor to the age group 60-64 years indicating a sharp change transitioning from age 59 to 60. In such categorical models, distinct factors are used for different categories of input variables. Conversely, parametric (continuous) models do not have abrupt changes in factors. Instead, they employ a continuous relationship by applying a uniform factor to the input variable. For instance, a specific factor might be multiplied by the attained age, ensuring a smooth transition without abrupt changes. Note that, although technically both model types use parameters estimated from cohort data, the radiation epidemiology community has adopted the term "parametric" to specifically refer to continuous models.

Categorical risk models

Jacobi model

To recognize work-related illnesses, employers' liability insurance associations introduced in the 1990s the task of calculating the probability of lung cancer causation due to occupational radiation exposure among previous uranium miners in Eastern Germany at Wismut AG. Therefore, Jacobi (1993) developed a risk model (Jacobi model) to calculate the excess relative risk of lung cancer death with the primary objective to evaluate the probability of causation of lung cancer in these miners (ICRP, 1993, A.3.3 (A23)). The developed model considerably advanced the understanding of radon-induced lung cancer risk in the early 1990s, and was later adopted by the ICRP in their report 65, where it is referred to as the

"GSF model" (ICRP, 1993). This model extends earlier approaches that combined epidemiological and dosimetric methods as in the ICRP publication 50 (ICRP, 1987) and the BEIR IV report (NRC, 1988). Jacobi's work represented a more sophisticated integration of these techniques.

Jacobi's approach incorporated data from six key miner cohorts: uranium miners in Bohemia (former Czechoslovakia), the Colorado Plateau (USA), New Mexico (USA), Ontario (Canada), and Eldorado (Canada), as well as from iron ore miners in Malmberget (Sweden). All mines were followed up between 1948 and 1985. In total, the cohort consists of around 30,000 miners with 600,000 person-years at risk and 912 observed lung cancer deaths. This comprehensive inclusion of diverse cohorts enhanced the model's applicability across different mining contexts and exposure scenarios. The model considered the physical behaviour of radon and radon progeny in the respiratory tract, estimated doses to different parts of the lung and accounted for varying radiosensitivity of lung cell types. This biophysical basis provided a nuanced understanding of the exposure-risk relationship (Jacobi, 1993). In addition to cumulative radon exposure, the Jacobi model incorporates factors for age at exposure and time since exposure.

The ICRP's adoption of the Jacobi model in the ICRP report 65 adjusted the model by a uniform factor of 0.83 to account for risk overestimation and standardized radon risk assessment internationally, providing a framework for setting action levels in homes and workplaces. It enabled the calculation of dose conversion factors and integrated radon protection into the broader system of radiological protection (ICRP, 1993). This adjusted Jacobi model was used to compute initial factors for radon dose conversion factors and continues to be a reference for legal decision-making in Germany up to today (Strahlenschutzverordnung [StrlSchV], 2021).

BEIR VI model

The BEIR VI report is a thorough scientific study conducted by the National Research Council (NRC) of the United States, focusing on the health risks associated with exposure to radon and other sources of ionizing radiation (NRC, 1999). Published in 1999, the report is part of a series of BEIR reports that examine the effects of low-level radiation exposure on human health. It is well-established from previous studies on uranium mining and residential exposure that radon and radon progeny increase the risk of lung cancer (Lubin, 1994; UNSCEAR, 1994). However, due to the uncertainties at lower levels of radon exposure, such as in living rooms and buildings in general, these risks were re-evaluated with the BEIR VI report. For this purpose, information on lung cancer was collected from miners who were mostly exposed to high levels of radon, as risk estimates from studies in homes alone were inadequate. In total, the analysis includes data from 11 different epidemiological studies: miner studies from China, former Czechoslovakia, Colorado (USA), Ontario (Canada), Newfoundland, Sweden, New Mexico (USA), Beaverlodge (Canada), Port Radium (Canada), Radium Hill (Australia), and France. Together, these studies encompass approximately $60,000$ miners, with a total of $900,000$ person-years at risk and

2,674 observed lung cancer deaths. The study recommends two similar categorical models: the exposure-age-concentration and the exposure-age-duration model, both only differ in the consideration of exposure concentration (exposure rate) or exposure duration. Both models incorporate factors for cumulative exposure, time since exposure, and attained age. The final model parameter estimates were derived by fitting the complex model structure to the data of 11 epidemiological studies.

The BEIR VI report and the associated risk models contributed essentially to the understanding of radon-related health risks and had a considerable impact on public health policies and radiation protection standards, such as mitigation strategies implemented by the Environmental Protection Agency (EPA) in the United States (Pawel & Puskin, 2003).

PUMA models

The Pooled Uranium Miners Analysis (PUMA) risk models follow the BEIR VI exposure-age-concentration model structure but parameter estimates are derived by fitting the model structure to the PUMA cohort data (full cohort and 1960+ sub-cohort). The PUMA cohort is the largest cohort of uranium miners worldwide, with the Wismut cohort representing approximately half of all miners in the PUMA cohort (Rage et al., 2020). It encompasses several large and important miner cohorts and reflects the latest advancements in radiation risk modelling. Hence, risk estimates derived from this cohort are highly relevant. More details about the PUMA cohort are found in Section 6.2.2.

Parametric risk models

Joint Czech-French model

This model originates from (Tomášek, Rogel, Tirmarche, et al., 2008) and considers, in addition to the cumulative exposure in WLM, also the effect-modifiers age at median exposure and time since median exposure. The model is based on data observed from Czech and French uranium miner studies until 1995. Both cohorts consist of nearly 5,000 individuals and are characterized by low exposure over a prolonged period. Motivated by a European project, this study aimed at a better understanding of the exposure-risk relationship for radon-related lung cancer at low exposures (Tirmarche et al., 2003). Accurate quantification based on occupational exposure in miners was still required to estimate the risk and factors that modify the dependence on cumulative exposure. Therefore, new analyses based on a cohort of miners with low levels of exposure, low exposure rate, and good quality of exposure estimates were conducted. Similar to the other mentioned models, age at exposure and time since exposure are significant effect modifiers in this study, in addition to cumulative exposure.

Wismut models

The Wismut models from Kreuzer et al. (2018) also aim to determine the risk factors at low exposures and low exposure rates. Here, the large Wismut cohort study with around 60,000 uranium miners, 2.3 million person-years at risk, and 3,942 observed lung cancer deaths was used as a data basis. The Wismut cohort characteristics are explained in detail in Section 4.2.1. Note that the underlying publication employs slightly older risk models from the Wismut cohort follow-up 1946-2013 for lifetime risk sensitivity analyses instead of follow-up 1946-2018. The older models were chosen because they offer greater heterogeneity in the range of selected models. Analogous to the Joint Czech+French cohort model, in addition to cumulative exposure, the effect modifying variables recommended by UNSCEAR (2021b), age at median exposure and time since median are significant factors.

5.2.3. Exposure scenario data

The exposure scenario defines the radon exposure at every age t in units of WLM. Since most effect modifiers in the considered risk models are sensitive to changing (cumulative) exposure, the magnitude of the excess relative risk term $ERR(t;\Theta)$ is notably influenced by the chosen exposure scenario at every age t. Here, exposure scenarios with chronic exposure over several years to represent occupational exposure scenarios were chosen. Note that also (high) acute exposure scenarios at one specific time point are important, especially for detriment calculations (ICRP, 2022). However, they are of lesser relevance in occupational settings and are briefly examined in the supplement of the publication.

The chosen exposure scenarios are the international standard choice of 2 WLM per year from age 18-64 years, compare (Tomášek, Rogel, Laurier, & Tirmarche, 2008). Further with the rich data on miner exposures in the Wismut cohort study, three different exposure scenarios representing very high, high, and low occupational radon exposure were constructed from real exposure data (compare Section 4.2.1). Exposure data are reported in calendar years. To enable age-specific analyses, individual ages at exposure were derived using birthdates of miners.

One major advantage of the constructed Wismut exposure scenarios is the non-homogeneity in exposure across ages in contrast to the homogeneous exposure of 2 WLM from age 18-64 years. This allows analysing age at exposure effect in the LEAR (and other lifetime risk measures) in more detail.

6. Lifetime excess absolute risk for lung cancer due to exposure to radon: results of the pooled uranium miners cohort study PUMA

6.1. Publication overview

Context and motivation

Lung cancer risk from radon exposure remains a key concern in radiation epidemiology. To improve the precision and comparability of risk estimates, the Pooled Uranium Miners Analysis (PUMA) study was initiated to get more precise estimates of the lung cancer risk associated with radon based on standardized statistical analyses of established miner cohorts (Rage et al., 2020). Previous PUMA publications have addressed various aspects of the pooled cohort, including the cohort profile (Rage et al., 2020), standardized mortality ratios among miners (Richardson et al., 2021), and radon-related lung cancer mortality for both the 1960+ sub-cohort (Richardson et al., 2022) and the full cohort (Kelly-Reif et al., 2023).

The underlying study (Kreuzer et al., 2024) builds upon these efforts by determining the LEAR per unit of exposure (LEAR per WLM) using risk models derived from PUMA data, while also incorporating established models from earlier uranium miner studies, including the recently updated Wismut cohort models (Kreuzer et al., 2023). The use of a standardized calculation methodology enhances the comparability of LEAR estimates across cohorts. Further, the quantity LEAR per WLM is employed for the "epidemiological" approach for radon dose conversion coefficients (Section 6.2.1) and there has been ongoing scientific controversy regarding the most appropriate value for this dose conversion coefficient (Harrison, 2021; Laurier et al., 2020; Marsh et al., 2021).

Key findings and scientific relevance

The derived lifetime risks in this study are consistent with previous results based on smaller studies and the derived range of estimates is also compatible with the dosimetric approach for radon dose conversion coefficients (Harrison, 2021). This analysis confirms that lifetime risk are a suitable metric to compare risk models across cohorts, despite substantial differences in exposure levels and risk model structure. Further it demonstrates, across multiple cohorts, that risk models derived from the 1960+ sub-cohort translate to considerably higher excess relative risks and corresponding lifetime risks. Overall this shows that current risk models describing radon-risk mechanisms are well understood and the international expertise on this topic is steadily increasing.

This PUMA paper addressing questions related to radon dose conversion has a considerable impact on the radiation protection community. The identified range of LEAR per WLM estimates provides a clear and evidence-based answer to previously open questions regarding the epidemiological approach for radon dose conversion. As the range aligns well with the dosimetric approach (Harrison, 2021; ICRP, 2017), this study also strengthens the scientific foundation of dose conversion practices. Further, this work complements sensitivity analyses conducted in (Sommer et al., 2025) by systematically comparing multiple heterogeneous risk models derived from different cohorts.

Outlook and future directions

Future work incorporating extended follow-up of individual PUMA studies will allow for further refinement of risk estimates, particularly for the 1960+ sub-cohorts. Alongside steadily improving statistical methods, continued research may enhance the detection of radon-related risks and potentially reveal reliable evidence for health effects beyond lung cancer, including other cancers and non-cancer diseases (Fenske et al., 2025; Henyoh et al., 2024).

6.2. Background on material and methods

Here, the important topic of radon dose conversion and its implications are introduced, followed by an overview of the PUMA cohort.

6.2.1. Radon dose conversion

The following description is based in parts on documents and materials from the German Federal Office for Radiation Protection. Corresponding information can also be found in (Breckow, 2018; Marsh et al., 2021; Schnelzer & Fenske, 2019).

Introduction

Radon dose conversion coefficients are employed to convert radon exposure – calculated as the product of radon activity concentration and exposure time – into a dose quantity, such as effective dose (Stather, 2004). These coefficients reflect the relationship between the activity concentration of radon and its decay products in a given environment and the resulting dose received by an individual over time. They account for the specific radiological properties of radon, and the physiological response of human tissues and organs to radon exposure.

Central authorities in the field of radiation protection like ICRP and UNSCEAR hold divergent views on the optimal use of radon dose conversion coefficients. The question of which factors should be employed in such conversions is a complex and internationally debated topic (Harrison, 2021; Müller et al., 2016). This has several reasons: Firstly, the determination of radon dose coefficients is inherently complex. There are two distinct concepts and calculation methods associated with the "epidemiological" and "dosimetric" approaches, both of which are subject to considerable uncertainty. Additionally, the magnitude of the coefficients has practical implications for radiation protection and public health: for example, by an increase in the radon dose coefficient for both radon in homes and radon in workplaces, the same radon exposures lead to higher effective doses. At workplaces, this means that the requirements of occupational radiation protection have to be met more frequently and the limit values for the effective dose are exceeded more often. Accordingly, the pressure to implement costly measures to reduce the radon activity concentration would increase considerably.

In Germany, radon exposure is regulated under the Strahlenschutzgesetz (StrlSchG, English: Radiation Protection Act). The StrlSchG sets a reference level for the averaged annual radon activity concentration of 300 Bq/m^3 for indoor workplaces and recreation areas. If radon levels exceed this limit, reduction measures must be implemented (StrlSchV, 2021). Should concentrations remain high despite these measures, the effective dose is calculated using the radon dose coefficient to determine further action. The StrlSchG also mandates that occupational radiation protection requirements must be met if the effective dose exceeds 6 mSv per calendar year due to radon exposure.

Approaches to determine dose coefficients

There are two main approaches for converting radon exposure into radon dose: the epidemiological and the dosimetric approach. Both approaches are outlined and compared in this paragraph.

Epidemiological approach

The epidemiological approach is based on the following idea: radon exposure associated with a certain increase in health risk is equated with the effective dose that leads to the

same increase in risk. This makes it possible to derive which radon exposure corresponds to which dose and how these quantities can be converted into each other. The risk estimates are derived from epidemiological studies (Beck, 2017; Marsh et al., 2010).

The approaches to calculate the risk per exposure unit and per dose unit differ considerably. Firstly, completely different risk measures are calculated: The lifetime excess absolute risk is calculated per exposure unit (LEAR per WLM), while the so-called "detriment" is calculated per dose unit, in which loss of quality of life, relative loss of lifetime and heritable effects are also taken into account. While the LEAR per exposure unit only considers the risk of lung cancer, the detriment per dose unit includes 13 other types of cancer in addition to lung cancer. Furthermore, the study populations based on which the risks were determined also differ: the LEAR per exposure unit is calculated based on miner studies (only men, heavy work), whereas the detriment per dose unit is essentially determined based on the atomic bomb survivors Life Span Study in Japan (general population) (Preston et al., 2007). The exposure situations therefore differ notably: the miners were exposed to chronic, internal exposure (i.e. within the body) to high-LET radiation for many years. The radiation energy was mainly absorbed by the lungs. The atomic bombings, on the other hand, exposed people to acute, external low-LET radiation. The radiation energy affected not only the lungs but the entire body. In addition, the risk models show clear differences. Overall, the epidemiological approach is based on many assumptions and parameters, and the resulting conversion factors are associated with great uncertainties.

Dosimetric approach

The dosimetric approach is concerned with the calculation of radiation doses within the human body (Hofmann & Winkler-Heil, 2011; Porstendörfer & Reineking, 1999). Biokinetic models track the duration of radionuclides from a certain exposure remaining within specific body regions. For example, the "Human Respiratory Tract Model" is utilized for radon and its progeny in lung tissues (ICRP, 1994). These models also estimate the number of nuclear transformations that release energy in different body regions. Dosimetric models then employ radiation transport programs, typically based on Monte Carlo methods, to determine the average absorbed dose by the organs, accounting for various types of radiation (alpha, beta, gamma) (ICRP, 2016). The sum of the absorbed doses for an organ weighted with radiation weighting factors yields the organ equivalent dose. Finally, the effective dose is calculated as the sum of these organ equivalent doses, weighted by tissue weighting factors (D. R. Fisher & Fahey, 2017; McCollough & Schueler, 2000). In general, effective doses derived with the dosimetric approach are model-based estimates subject to large uncertainties. This is because many essential variables are unknown and assumptions have to be made, compare e.g. (Makumbi et al., 2024). Consequently, the dose is dependent to a considerable extent on the often insufficiently known initial assumptions (e.g., the size and solubility of the inhaled particles). Furthermore, many of the metabolic and physiological processes involved can only be described approximately.

Comparison of both approaches

Both approaches are associated with large uncertainties that are challenging to compare. Still, the epidemiological and dosimetric approaches provide estimates of radon dose coefficients that are of approximately the same order of magnitude, although the two approaches are independent of each other and are based on completely different assumptions (Marsh et al., 2021; Stather, 2004). The epidemiological approach is supported by the fact that risk estimates per exposure unit and per dose unit are based on extensive and reliable epidemiological studies. It is reasonable to conclude that both risk estimates are well-founded in their own right. Nevertheless, the idea of equating the two risk estimates is questionable due to the discrepancies in methodology and data sources. The results of the comparison are also highly dependent on the choice of risk models derived from miner studies, including effect-modifying variables and the assumptions for the exposure scenario and population structure. One argument in favour of the dosimetric approach is that it is already used for all other radionuclides, thus ensuring a uniform approach.

Contribution of this study to dose conversion

This study calculated the lifetime risks related to radon exposure as part of the PUMA project and made a considerable contribution to determining and validating these lifetime risks across multiple international cohort studies. It serves as the basis for the epidemiological approach to dose conversion, demonstrating results that are consistent with those obtained using the dosimetric approach in (ICRP, 2017). Further, the currently applied dose conversion coefficients e.g. in Germany – 4 mSv/WLM for homes and public settings, and 5 mSv/WLM for workplaces (StrlSchV, 2021) – fall at the lower end of the derived range of coefficients. Consequently, the ICRP proposes higher conversion coefficients (dosimetric approach), which is supported by results from this study (epidemiological approach).

6.2.2. PUMA cohort description

PUMA is a cohort mortality study that represents the largest study of uranium miners conducted to date, encompassing 119,709 miners, including open pit miners, underground miners, and surface workers, totalling 4.3 million person-years at risk, and 7,754 reported lung cancer deaths (Kreuzer et al., 2024). The miners, mostly men, were hired between 1942 and 1996 and followed up between 1946 and 2013. The study size is achieved by pooling eight cohorts of uranium miners from Canada, Europe, and the United States. In particular, it advances upon the established pooled study from the BEIR VI report from the late 1990s (NRC, 1999). PUMA consolidates data from several of the largest epidemiological cohort studies of uranium miners worldwide (Rage et al., 2020).

The PUMA study found a strong positive association between cumulative radon exposure and lung cancer across all cohorts, with lung cancer accounting for approximately half of all cancer-related deaths. Lung cancer mortality was consistently elevated relative to national

or regional reference rates, with the magnitude varying for different radon exposure levels (Rage et al., 2020). However, associations between radon exposure and cancers other than lung cancer remain inconclusive, likely due to the much lower absorbed doses to other organs compared to the lungs, making any excess risk small (Fenske et al., 2025). Large studies like PUMA are needed to detect such associations, but results across cohorts for cancers such as larynx, brain, kidney, stomach, and leukaemia, as well as non-cancer diseases like circulatory system diseases, remain mixed.

The PUMA study's main advantages include its exceptionally large sample size, the largest of its kind, long-term follow-up, high-quality quantitative exposure data, particularly for more recent miners, and the ability to assess radon-related risks across a wide range of exposure conditions. This allows for more precise analyses of lung cancer and other health outcomes. Additionally, the study addresses confounding factors like diesel and arsenic exposure.

However, the study's reliance on mortality data instead of incidence data and historical exposure misclassification, especially in older cohorts, pose limitations. Further, the potential heterogeneity between included cohorts (e.g., differences in exposure levels and mining practices), may introduce biases.

In summary, the PUMA studies provide an extensive database that includes thousands of miners and years of follow-up, enabling the precise estimation of cancer risks associated with different levels and durations of radon exposure. By pooling data from multiple studies across countries, PUMA offers a broader and more accurate assessment of radon-related health risks compared to smaller, individual studies.

7. Methods to derive uncertainty intervals for lifetime risks for lung cancer related to occupational radon exposure

7.1. Publication overview

Context and motivation

Lifetime lung cancer risk estimates related to occupational radon exposure can influence regulatory decisions on radon mitigation strategies to protect the public from excessive exposure (compare to detriment (Breckow & Emami, 2016) or dose conversion in Section 6.2.1). However, uncertainties associated with these estimates are hardly quantified in the literature (Pawel & Puskin, 2003; Tomášek, 2020), despite their relevance for informed decision-making and effective risk communication. The underlying study (Sommer et al., 2024) aims to fill this gap by systematically deriving and discussing reliable uncertainty intervals for lifetime risk estimates in particular based on risk models from Kreuzer et al. (2023), using the German Wismut uranium miners cohort as a practical example. In general, uncertainty intervals convey how precise or reliable single estimates are, contributing to scientific integrity. Here, it contributes to a more complete understanding of the risks associated with radon exposure.

Key findings and scientific relevance

This work showed that risk model parameter sampling uncertainty describes an adequate representation of overall lifetime risk uncertainty and introduced two methods to derive corresponding uncertainty intervals. The proposed Approximate Normality Assumption (ANA) approach proves to be both practical and suitable for radiation protection purposes. In addition, an alternative Bayesian approach was explored offering greater flexibility and a more intuitive interpretation of uncertainty. However, this approach requires considerable computational resources and relies on subjective prior assumptions (Ferson, 2005). While uncertainties in baseline mortality rates are also relevant, they play a comparatively less critical role here. The derived uncertainty intervals correspond well to the range of lifetime

risk estimates from miner studies in the literature, thus lifetime risk variability derived by both methods are mutually confirmed (Kreuzer et al., 2024).

Given its practicality and transparency, the ANA approach remains the preferred choice to derive uncertainty intervals for most applications in radiation protection. Nonetheless, the Bayesian approach may offer substantial advantages by providing a flexible framework to integrate results and combine knowledge from distinct miner cohorts, provided that the choice of priors is well-justified.

Overall, the introduced methods expand the methodological toolbox for uncertainty assessment by providing the first comprehensive quantification of statistical uncertainty in lifetime risk estimates related to occupational radon exposure. These uncertainty intervals enable formal comparisons between different lifetime risk estimates, especially across miner studies, for example by examining interval overlap, thereby enhancing the interpretability and credibility of such estimates in radiation protection and regulatory decision-making.

Outlook and future directions

Despite promising methodological developments, certain areas remain to be explored. The applied risk models are specific to the Wismut cohort, and results may differ for other miner cohorts with varying characteristics. More consistent data grouping and model fitting practices across miner studies could improve comparability and reduce ambiguity in risk estimates (Richardson & Loomis, 2004). Improved reporting standards and accessible *R* packages for model development and uncertainty analysis, as proposed by Higueras and Howes (2018) and Lee et al. (2022), could enhance reproducibility and methodological clarity. Longer follow-up, especially of the 1960+ Wismut sub-cohort, offers potential to reduce uncertainties and strengthen evidence, as this sub-cohort benefits from more accurate exposure data compared to the earlier years of mining (Kreuzer et al., 2009). Future work may explicitly explore country-specific mortality uncertainties, account for smoking behaviour once reliable models are developed (Rage et al., 2020; Zhang et al., 2020), and explore other flexible survival modelling techniques such as Cox proportional hazard or Accelerated-Failure-Time (AFT) models (Aßenmacher et al., 2019). To support informed decision-making, uncertainty quantification should accompany point estimates, as it provides a more complete understanding of lifetime risk estimates.

7.2. Perspective on lifetime risk uncertainties

This section provides an overview of uncertainty in statistics and epidemiology, including types of uncertainties and methods for their assessment. It also examines specific uncertainties in estimating lifetime risks for lung cancer due to radon exposure, detailing statistical inference and specific uncertainties in calculating these risks.

7.2.1. Fundamental concepts

What are uncertainties in epidemiology and statistics

In the field of pure mathematics, for example, a strictly predefined set of assumptions can be undoubtedly proven to imply a result. A correct mathematical proof is free of uncertainty because, by definition, there is complete knowledge about the assumptions and the behaviour of mathematical objects. In contrast, epidemiological investigations are subject to the inherent complexity of biological systems and variability among individuals.[1] Gathered data (observations, measurements) may deviate from the true underlying value, and proposed relationships may fail to reflect the true causal mechanisms (Rothman et al., 2008).

The difference between an estimate of a quantity and its true (but unknown) value is referred to as the "error", which itself cannot be directly observed or quantified (UNSCEAR, 2015, II A. Statistical concepts of uncertainty). The derivation of probability distributions for such errors is called "uncertainty analysis" or "uncertainty assessment", while expressing uncertainty in numbers (e.g. through uncertainty intervals) belongs to "uncertainty quantification".

Most statistical analyses begin with data (i.e. observations, measurements) extracted from dynamic, complex, and often incomplete systems. This introduces multiple sources of error and uncertainty. Especially in epidemiology, data is often limited due to feasibility constraints, ethical considerations, or historical context. Modelling assumptions – such as those regarding smoking behaviour or exposure patterns – are often simplifications. As a result, statistical models may not fully capture the complexity of the underlying processes. This limits their explanatory power and complicates both interpretation and inference: understanding relationships between observed variables and drawing conclusions about potential causes is inherently uncertain. A central challenge lies in appropriately characterizing and accounting for these uncertainties in both models and their interpretation (Bonita et al., 2007; Clayton & Hills, 1993).

Establishing causal effects in epidemiology and statistical analyses is particularly difficult.[2] The broader problem of inferring causation from observational data has been widely studied (Hernán, 2004; Pearl & Mackenzie, 2019; Rothman & Greenland, 2005; Spirtes et al., 2001).

Occurrence of different types of uncertainties

Recognizing uncertainties is crucial for accurately interpreting the findings of scientific studies, while accounting for uncertainties improves the reliability of the results. On the

[1] For example, Clayton and Hills (1993) refers to epidemiological models as "stochastic" in contrast to "deterministic" models that describe predictable phenomena.

[2] The often cited "Bradford Hill Criteria" (Fedak et al., 2015; Hill, 1965) comprises nine principles to aid in establishing evidence for a causal effect in epidemiological research.

level of statistical analysis, one is confronted with the limitation of data, data measurement error (for continuous data) and data misclassification (for categorical variables) (Gustafson, 2003), uncertainty in statistical estimates that results from drawing a sample from the entire population (sampling uncertainty), and uncertainty in choosing and deriving a suitable model structure (model uncertainty). On an individual level, cognitive biases affect statistical reasoning, decision-making, and therewith risk communication. For example, the tendency to rather publish significant than non-significant results (publication bias) (Rosenthal, 1979; Rothstein et al., 2005), or the proneness to favour information that confirms their pre-existing beliefs while disregarding or downplaying information that contradicts them (confirmation bias) (Nickerson, 1998). Such tendencies are prone to "p-hacking", the manipulation of statistical analyses and data to achieve statistically significant results (p-values), often by conducting multiple tests or selectively reporting findings (Head et al., 2015). Further, especially in the field of public health and epidemiology, the goal is often risk mitigation and risk education (e.g. smoking and lung cancer (Pesch et al., 2012; IARC, 2004)). However, the interpretation of risk in the target group is not always rational (Kahneman, 2012; Slovic et al., 2004).

Overall, quantifying uncertainties may involve assessing the extent of missing knowledge in the data, sampling variation, limitations in capturing the true underlying mechanisms (model uncertainty), and decisions made during the estimation process, many of which are invisible to the target group, and cognitive biases in general.

Quantifying cognitive biases is hardly possible due to the inherent variability of human reasoning processes (Bierema et al., 2021; Enke & Graeber, 2023). Quantifying missing knowledge in the data and sampling uncertainty is achievable to some extent. Other sources of uncertainty are challenging to quantify (Thomas et al., 1992). However, knowing of their existence improves statistical reasoning. This overview shows that practically every step from data generation (measurement), statistical analysis, presentation and interpretation of results is prone to errors and biases.

Methods for uncertainty assessment

Here, an overview of common techniques to assess uncertainty in statistical analysis and radiation epidemiology are presented. Those include methods to assess parameter uncertainty, measurement errors and attempts to set up universal frameworks for statistical analysis.

The two most commonly used methods for statistical inference are the frequentist inference and the Bayesian inference (Held & Bové, 2021). Both rely on a statistical model (e.g. the likelihood function) and unknown parameters to be fit to the data at hand. Here, statistical inference is understood as the process of using observations y of a sample Y to draw conclusions about the distribution of Y itself. Such inference relies heavily on underlying distributional assumptions (Rüger, 1998). Both frequentist and Bayesian inference come with a natural quantification of parameter estimate uncertainty with confidence intervals

(frequentist) and credible intervals (Bayesian). More details on frequentist and Bayesian inference and methods are provided in Section 7.3.1.

Specifically, measurement errors in the data, especially in epidemiology, are typically accounted for with methods called "Simulated Extrapolation (SIMEX)" and "Calibrated Regression" (Keogh et al., 2020; Wallace, 2020). For SIMEX, additional measurement errors are added to the data in a controlled manner by simulation. Estimates are computed from this manipulated data, establishing a trend between the estimates and the variance of the added errors. Final SIMEX estimates are obtained by extrapolating this trend back to the case of no measurement error (Cook & Stefanski, 1994; Hardin et al., 2003). For regression calibration, the basic idea is to substitute the unobserved true exposure with a predicted value from a calibration function with takes into account the observed data and other covariates. Then, standard inference is applied to this predicted value. Finally, standard errors are calculated, accounting for the prior substitution (Carroll et al., 2006; Fuller, 1987; Spiegelman et al., 1997). In particular, the literature differentiates between different types of measurement errors and provides corresponding error correction methods (Keogh & White, 2014).

For situations with more complex and numerous sources of uncertainty, modern "Hierarchical Bayesian" methods are employed (Ellenbach et al., 2022; Khazaei et al., 2023). A hierarchical model allows for the distinction of various levels of information and the incorporation of multiple complex sub-models connected by conditional independence assumptions.

Finally, Monte Carlo simulations are a powerful, flexible, and practical method able to account for various uncertainties (Robert & Casella, 2005). Monte Carlo techniques propose probability distributions on model components and use repeated sampling from these distributions (with the help of computers), to allow inference about the underlying model.

There are numerous statistical methods to tackle given research questions in epidemiology. This induces further variability since different methods imply different decisions during the analysis process. This impacts the results of statistical analysis on epidemiological data but also affects the beforehand generation of epidemiological data (e.g. the construction of cohorts). The resulting non-replicability of many research findings undermines scientific trustworthiness and is an important issue. To increase replicability, there are attempts to set up universal frameworks for observational studies (von Elm et al., 2007) and corresponding statistical analyses (Hoffmann et al., 2021; Kümpel & Hoffmann, 2022).

7.2.2. Special case: Lifetime risks for lung cancer related to radon exposure

Transitioning from the broader context of epidemiology and statistics, the following section elaborates on uncertainties for the specific metric of lifetime risk for lung cancer related to radon exposure.

Particularities in lifetime risks: statistical inference

A direct application of frequentist (e.g. maximum likelihood) or Bayesian inference to lifetime risk measures like the LEAR is not feasible, as it requires a likelihood function based on observations. However, such a likelihood does not exist for lifetime risks. Estimating the lifetime risk of lung cancer related to radon exposure directly would require a cohort in which each lung cancer death could be assigned with certainty to a specific radon exposure. This is hardly possible due to general challenges in causal inference in epidemiology (Rothman & Greenland, 2005) and the biological complexity of radon-induced lung cancer (Truta-Popa et al., 2011). Hence, lifetime risks like the LEAR cannot be interpreted as directly estimable parameters, and classical Bayesian or frequentist methods are not directly applicable.

Instead, lifetime risk estimates are composite quantities, derived from the combination of various results obtained through separate analyses. For instance, the baseline lung cancer mortality rates $r_0(t)$ and the survival function $S(t)$ are estimated from population data (e.g., the WHO mortality database (WHO, 2022)), independently of the excess relative risk term $ERR(t;\Theta)$, which is based on data from miner cohorts.

To assess overall lifetime risk uncertainty, the uncertainties associated with each component of the lifetime risk calculation are examined. These components are typically derived from robust statistical methods, such as maximum likelihood. The uncertainty in lifetime risks is construed as a function of the uncertainties associated with its components.

Uncertainties when calculating lifetime risks

As outlined by Thomas et al. (1992), lifetime risk calculations are subject to three principal types of uncertainties:

- sampling uncertainty when deriving parameter estimates
- model uncertainty
- uncertainties that cannot be formally specified with probability distributions: errors in the source data (data preprocessing, measurement errors); validity of assumptions; etc.

While sampling uncertainty can be formally addressed using statistical methods, model uncertainty and other non-specifiable uncertainties are more difficult to quantify (Hoffmann et al., 2021; NRC, 1999).[3]

To provide a more comprehensive context for the quantification of uncertainties, the following overview presents key sources of errors, uncertainties, and decision points that can

[3] A notable mention to reduce model uncertainty is "Multi-model inference" (Burnham & Anderson, 2002; Kaiser et al., 2012). This approach involves assessing risk by considering multiple plausible models depending on their descriptive capabilities.

influence lifetime risk estimation in the context of radon-induced lung cancer. This list is inspired from the discussions in (NRC, 1999, pp. 100–104):

- Modelling and estimation of the risk model $ERR(t;\Theta)$ derived from miners cohort data, influenced by
  - Uncertainty about the true exposure of miners (Küchenhoff et al., 2018; Pawel & Puskin, 2003)
  - Model uncertainty concerning the functional structure of $ERR(t;\Theta)$
  - Sampling uncertainty for the parameter estimate $\hat{\Theta}$
  - Latency time L between age at exposure and age at actual risk amplification (Richardson et al., 2011)
  - Data grouping processes necessary for applying Poisson regression on cohort data (Richardson & Loomis, 2004)
  - Internal baseline risk stratification
  - Accounting for non-lung cancer effects potentially associated with radon exposure (Fenske et al., 2025; Mozzoni et al., 2021)
  - Risk transfer from the cohort population to the general population
  - Accounting for confounders (e.g., smoking behaviour)
- Modelling and estimation of the baseline lung cancer and all-cause mortality rates $r_0(t), q_0(t)$
  - Estimation of the survival function $S(t)$
  - Potential errors in the underlying mortality data used for estimation
- Choice of lifetime risk measure (LEAR is one of four measures discussed in the literature (Thomas et al., 1992; Ulanowski et al., 2019))
- Definition of baseline lifetime risks LR_0 under the assumption of zero radon exposure, although such conditions do not occur naturally
- Choice of the radon exposure scenario
- Discretization of the lifetime risk measure from a theoretical integral to a calculable sum, constrained by data availability
- Correlation between calculation components and across attained ages

It should be noted that while this compilation is extensive, many of the listed elements are either difficult to quantify or have only a minor influence on the overall lifetime risk estimates within the plausible range of values, as addressed in (Sommer et al., 2025).

In the context of occupational radon exposure, literature addressing uncertainties for lifetime lung cancer risks is sparse (Pawel & Puskin, 2003; Tomášek, 2020). In contrast, uncertainties for other radiation exposures have been extensively analysed in the literature, especially for the atomic bomb survivors (M. P. Little et al., 2008; Pierce et al., 1990; Xue & Shore, 2001) with classical likelihood- (using regression calibration) and Bayesian techniques (Darby et al., 2006). In the end, uncertainty not only arises in risk quantification itself, but also in the interpretation and communication of risks by decision-makers and the public (Hoti et al., 2020).

7.3. Background on material and methods

This section elaborates on the statistical inference framework used in the underlying publication to deduce uncertainty intervals accounting for risk model parameter uncertainty. This is followed by an explanation of the algorithms employed in the context of Bayesian inference and a brief discussion on the selection of prior distributions.

As risk model parameter uncertainty was identified as the primary contributor to overall lifetime risk uncertainty, this chapter focuses on providing further details and background information on this component. Mortality rate uncertainty and other contributors are sufficiently addressed in the underlying publication and its supplement.

Approach for uncertainty assessment in this study

The primary objective of the underlying publication is to derive reliable lifetime risk uncertainty intervals using a practical methodology that emphasizes radiation protection, minimizes subjectivity, and avoids unnecessary complexity. Consequently, influential factors such as risk model parameters and mortality rates, as identified in (Sommer et al., 2025) are prioritized, while components with negligible influence are not overemphasized.

Since lifetime risks are a composite measure and not a statistical parameter, approaches such as SIMEX or calibrated regression are not applicable here. Further, it is important to note that uncertainties in the cohort data underlying the risk model – such as those arising from measurement error, disease misclassification, confounders, or data grouping – are inherited by the LEAR. Such uncertainties are not the primary focus of this study, as they have been addressed elsewhere (Ellenbach et al., 2022; Küchenhoff et al., 2018).

In the underlying publication, suitable probability distributions were assigned to the influential calculation components for lifetime risk calculations. These were based either on the asymptotic normal distribution of maximum likelihood estimates for risk model parameters or derived from the large-scale WHO mortality database for mortality rates (WHO, 2022). Monte Carlo simulations were then employed to independently sample values from these distributions and compute corresponding lifetime risk estimates. This process yields a distribution of lifetime risks from which empirical uncertainty intervals are derived.

This approach not only captures the composite nature of lifetime risks such as the LEAR but also enables a transparent and flexible modelling of uncertainty contributions from individual calculation components. Additional sensitivity analyses are presented in the supplement of the publication to evaluate the credibility of the uncertainty assessment. These include the effects of choosing different probability distributions, varying the underlying datasets, and testing various modelling assumptions.

As a side note, the delta method for uncertainty assessment, which has been used in other studies (see e.g. (Hoef, 2012; Xue & Shore, 2001)), is avoided here, as it introduces notable subjectivity through the need to specify predefined variances.

7.3.1. Frameworks for statistical inference

This section introduces the idea behind frequentist and Bayesian inference, two fundamental yet distinct approaches for statistical inference and uncertainty quantification. The differences between these approaches reach deep into the foundation of probability, resulting in different schools of thought. Frequentists understand the probability of an event as its relative frequency over time, whereas Bayesians see probability as a measure of "degree of belief" (de Elía & Laprise, 2005).

In the underlying publication, both frameworks are applied to derive probability distributions for risk model parameters, given their dominant role in overall lifetime risk uncertainty. The frequentist framework is employed in the Approximate Normality Assumption (ANA) approach which is derived from maximum likelihood methods, while the Bayesian framework is used in the corresponding Bayesian approach.

By drawing samples from the resulting parameter distributions and computing corresponding lifetime risk estimates, a distribution of lifetime risks is generated (Monte Carlo simulation).

Frequentist inference

Frequentist inference, also known as classical inference, is a statistical framework that relies on the frequency or proportion of data to estimate parameters. The underlying interpretation, first systematically outlined by Richard von Mises in 1919 (Lehmann, 2008), views probability as the relative frequency of events in an infinite number of repeated trials or samples (Von Mises, 1928; Young & Smith, 2005). The frequentist approach operates under the assumption that the data being analysed is a random sample from a larger population.

The principles of statistical inference, foundational to modern statistical analysis, were further systematically formalized by R. A. Fisher (1925), where he developed key concepts like maximum likelihood estimation (point estimation), hypothesis testing, significance levels, and p-values based on sample data.

In point estimation, a single value, known as the estimator $\hat{\theta}$, is used to approximate an unknown population parameter θ. The estimator is a function of the sample data. Since sample data are random variables (drawn from the population), the estimator $\hat{\theta}$ is also a random variable. Its distribution depends on the sampling distribution of the data (Hespanhol et al., 2019). Interval estimation, on the other hand, involves constructing confidence intervals, that provide a range of values such that if the sampling process is repeated many times and a confidence interval is computed for each sample, a certain proportion (e.g., 95%) of those intervals would contain the true parameter θ. In confidence intervals, "confidence" refers to the randomness of the interval itself. Figure 7.1 shows a visualization of frequentist confidence intervals. The frequentist perspective treats the unknown parameter as fixed, without a probability distribution, while the confidence interval bounds are considered random due to their dependence on random samples (Bland & Altman, 1998). For the frequentist hypothesis testing, the probability of observing data as extreme as (or more extreme than) the collected data, given the null hypothesis is true, is calculated. This result, known as the p-value, indicates how likely the observed data would be under the assumption of the null hypothesis (Fornacon-Wood et al., 2022).

Frequentist inference does not incorporate prior beliefs or information about parameters before observing the data. Instead, it relies solely on the observed data, ensuring objectivity and replicability (Rüger, 1998). This approach is widely used in various scientific disciplines offering well-established methodologies. However, this approach requires careful interpretation: a low p-value indicates that the observed data is unlikely under the null hypothesis, but it does not measure the probability that the null hypothesis itself is true or false.

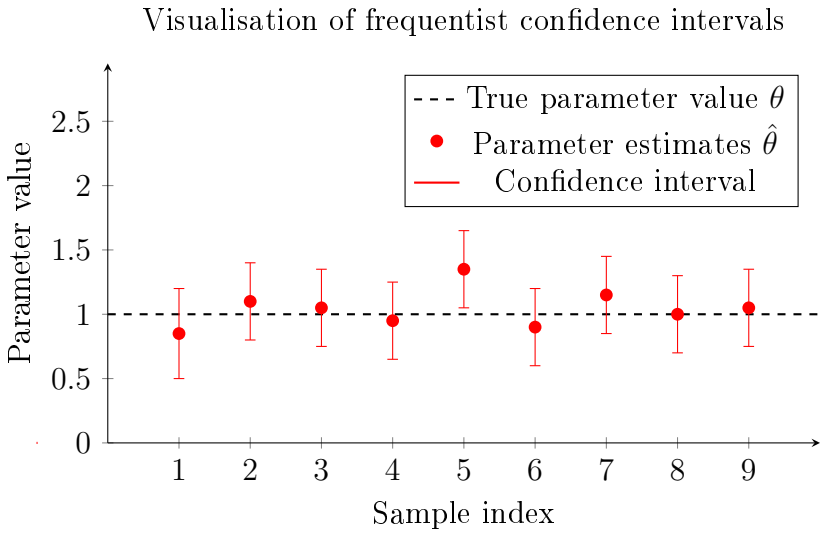

Figure 7.1.: Frequentist confidence intervals: Each interval is computed from a different sample, with most intervals covering the true parameter value. The red dots indicate parameter estimates from different samples.

Bayesian inference

Bayesian inference offers a distinct framework for statistical analysis, grounded in the principles of Bayes' theorem. This approach integrates prior knowledge or beliefs about parameters along with observed data to update the probability of observing the parameters. Bayesian inference treats probabilities as a measure of belief or certainty about an event, rather than long-term frequencies.

This approach is rooted in the work of Thomas Bayes, who introduced the idea of updating probabilities based on new evidence in his posthumous essay "An Essay towards solving a Problem in the Doctrine of Chances" (1763). The framework was later formalized and extensively developed by Pierre-Simon Laplace in the early 19^{th} century, establishing the basis of modern Bayesian methods (Bayes, 1763; Laplace, 1812).

At the heart of Bayesian inference lies Bayes' theorem, which describes how to update the probability of a hypothesis based on new evidence. The theorem is mathematically expressed as:

$$P(\theta \mid \text{data}) = \frac{P(\text{data} \mid \theta)P(\theta)}{P(\text{data})},$$

where $P(\theta \mid \text{data})$ is the posterior probability of the parameter θ given the observed data, $P(\text{data} \mid \theta)$ is the likelihood of the data given θ, $P(\theta)$ is the prior probability of θ, and $P(\text{data})$ is the marginal likelihood of the data (Held & Bové, 2021).

The prior distribution $P(\theta)$ captures any pre-existing knowledge or beliefs about the parameter before observing the data. The likelihood function $P(\text{data} \mid \theta)$ reflects the probability of the observed data given the parameter, based on a chosen statistical model. The posterior distribution $P(\theta \mid \text{data})$ combines these elements to provide an updated probability distribution for the parameter, incorporating both the prior information and the observed data.

One of the key advantages of Bayesian inference is its flexibility in incorporating prior knowledge, which can be particularly valuable in situations with limited data or where expert knowledge is available. Additionally, Bayesian methods provide a coherent framework for sequential updating, allowing for continuous refinement of parameter estimates as new data becomes available.

Bayesian inference also offers a natural way to handle uncertainty. Instead of deriving confidence intervals separately after calculating single-point estimates as in the frequentist approach, Bayesian methods generate a full posterior distribution for the parameters, providing a more comprehensive picture of uncertainty. Point estimates along with credible intervals are derived from this posterior distribution, carrying all information. Credible intervals indicate the range within the parameter is likely to lie with a certain probability, typically 95%. In contrast to frequentist confidence intervals, interval bounds from Bayesian credible intervals are fixed and the unknown parameter itself is a random variable. A visualization of Bayesian credible intervals is depicted in Figure 7.2.

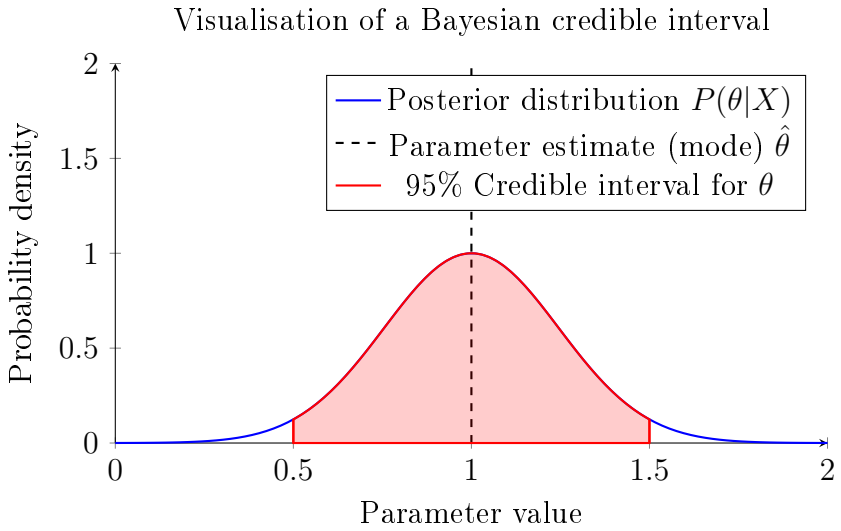

Figure 7.2.: Bayesian credible interval: The exemplary credible interval $[0.5, 1.5]$ shows where the parameter value θ falls with 95% probability given the data X and some prior distribution $P(\theta)$. Correspondingly, the shaded red area covers 95% of the distribution $P(\theta|X)$.

Despite its many advantages, Bayesian inference requires the specification of prior distributions, which can introduce subjectivity. Moreover, the computational complexity of Bayesian methods, particularly for high-dimensional models, can be challenging. However, advances in computational techniques, such as Markov Chain Monte Carlo (MCMC) methods, have substantially expanded the feasibility and application of Bayesian approaches in modern statistical analysis (Robert & Casella, 2005).

7.3.2. Sampling techniques and prior selection in Bayesian inference

Here two important sampling techniques are introduced, that are used in the underlying study to obtain samples Θ from the risk model parameter posterior distribution $P(\Theta|X)$. To maintain generality, the algorithms are described using a generic variable y and target distribution $p(y)$. This section is inspired by (Robert & Casella, 2005). Challenges that come with choosing a prior distribution and corresponding ideas are briefly elaborated on.

Rejection sampling algorithm

The rejection sampling algorithm (Algorithm 1 with illustration in Figure 7.3), also called acceptance-rejection method, is a Monte Carlo simulation technique to obtain samples from a certain target probability distribution $p(y)$ that is difficult to sample from directly. It works by employing a simpler distribution $q(y)$, called the proposal distribution, which is easier to sample from. A sample from the proposal $q(y)$ is drawn and either accepted as a representative for a sample from the target $p(y)$ or rejected. The rejection sampling algorithm requires knowing the target distribution density at every point y up to a multiplicative constant. Further, the proposal distribution $q(y)$ must dominate $p(y)$ such that there exists a constant M, where

$$p(y) \leq Mq(y), \quad \text{for all } y.$$

The efficiency of rejection sampling depends on the value of M and how closely the proposal distribution $q(y)$ matches the shape of the target distribution. The unconditional sample acceptance probability is $1/M$ (Martino et al., 2018). Note that this method is based on a fundamental idea called the *Fundamental Theorem of Simulation* (Robert & Casella, 2005, Theorem 2.15): simulating a random variable $Y \sim f(y)$ is equivalent to simulating the pair

$$(Y, U) \sim \mathcal{U}\{(y, u) : 0 < u < f(y)\},$$

where $U \sim \mathcal{U}[0, 1]$ is a uniform distributed random variable. So the simulation of $Y \sim f(y)$ is reduced to generating uniform variables on the constrained set $\{(y, u) : 0 < u < f(y)\}$.

While rejection sampling is a straightforward and intuitive method, it has its drawbacks. Besides its efficiency depending on the proposal distribution $q(y)$ and the constant M, sampling becomes exponentially more difficult in high-dimensional spaces (see "curse of dimensionality" (Bellman, 1957)). For such situations, alternative sampling methods like the Metropolis-Hastings algorithm utilizing MCMC techniques may be more suitable.

Algorithm 1 Rejection sampling algorithm

1: **Define target distribution** $p(y)$, possibly not normalized.
2: **Choose proposal distribution** $q(y)$ such that $p(y) \leq Mq(y)$ for some constant $M > 0$.
3: **repeat**
4: Sample y^* from $q(y)$.
5: Generate uniform distributed $u \sim \mathcal{U}[0, 1]$.
6: **if** $u \leq \frac{p(y^*)}{Mq(y^*)}$ **then**
7: Accept y^*.
8: **else**
9: Reject y^*.
10: **end if**
11: **until** desired number of samples obtained
12: **if** $p(y)$ not normalized **then**
13: Normalize accepted samples if needed by dividing by the normalizing constant.
14: **end if**

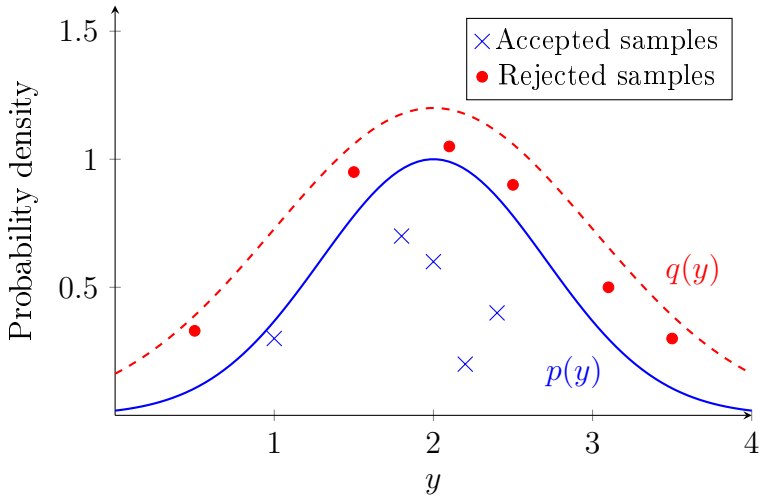

Figure 7.3.: Illustration of rejection sampling. The target distribution $p(y)$ (solid blue curve) is approximated using the proposal distribution $q(y)$ (dashed red curve). Accepted samples are shown with blue crosses, and rejected samples are indicated with red dots.

For the analyses in the underlying publication, the rejection sampling method performed well for the simple linear risk model with a uniform proposal distribution but was not applicable for the more complex risk models with higher dimensional parameter vectors.

Metropolis-Hastings algorithm

The Metropolis-Hastings algorithm (Algorithm 2 with illustration in Figure 7.4) generalizes the basic Metropolis algorithm, which adapts a random walk with an acceptance/rejection rule to converge to a specific target distribution (Gelman et al., 2013). Therewith, it allows obtaining random samples from probability distributions where direct sampling is difficult.

The algorithm is part of the broader family of MCMC methods (Karras et al., 2022). These methods construct a Markov chain $(y_t)_{t\geq 0}$ whose stationary distribution is the desired target distribution $p(y)$. The initial state y_0 for the Markov chain $(y_t)_{t\geq 0}$ can be a random guess or drawn from a distribution related to $p(y)$. The movement of the Markov chain and the success of the Metropolis-Hastings algorithm depends on the choice of the proposal distribution $q(y^*|y_t)$. Candidate samples from the proposal $q(y^*|y_t)$ are accepted as target distribution samples with a certain probability, depending on the state of the Markov chain. The algorithm balances between exploring high-probability regions and allowing occasional jumps to less probable regions, which helps avoid being trapped in local modes of the distribution. Once the chain has reached its stationary distribution, samples drawn from the chain can be considered as approximate samples from the target distribution $p(y)$.

Note that the stationarity and the Markov chain property (i.e. "memorylessness") are key to the algorithm's behaviour. Further, a poorly chosen proposal can result in very slow convergence to the stationary distribution. Since the early samples of the Markov chain may not adequately represent the target distribution, a certain fraction of these initial samples are typically discarded to account for a so-called "burn-in period" (Gelman et al., 2013).

The Metropolis-Hastings algorithm is a widely used and flexible MCMC method because it can be applied to almost any distribution. It is especially useful in high-dimensional problems and Bayesian inference. In particular, unlike for rejection sampling, the algorithm does not require the target distribution to be bounded by a scaled version of the proposal distribution. For more theory on Markov chains see Durrett (2016) with advanced applications in Levin and Peres (2017).

Algorithm 2 Metropolis-Hastings sampling algorithm

1: **Define target distribution**: Specify the target distribution $p(y)$, possibly not normalized.
2: **Choose proposal distribution**: Select a proposal distribution $q(y^*|y_t)$ that is easy to sample from, which proposes new states y^* based on the current state y_t.
3: **Initialize Markov chain**: Choose an initial state y_0 for the Markov chain $(y_t)_{t\geq 0}$.
4: **repeat**
5: **Generate candidate point**: Sample a candidate y^* from $q(y^*|y_t)$.
6: **Calculate acceptance probability**:

$$\alpha = \min\left(1, \frac{p(y^*)q(y_t|y^*)}{p(y_t)q(y^*|y_t)}\right)$$

7: **Generate uniform random number**: Draw $u \sim \mathcal{U}[0,1]$.
8: **if** $u \leq \alpha$ **then**
9: Accept y^* by setting $y_{t+1} = y^*$.
10: **else**
11: Reject y^* and keep $y_{t+1} = y_t$.
12: **end if**
13: **until** the desired number of samples is obtained
14: **Burn-in period (optional)**: Discard initial samples to ensure the chain has reached its stationary distribution.

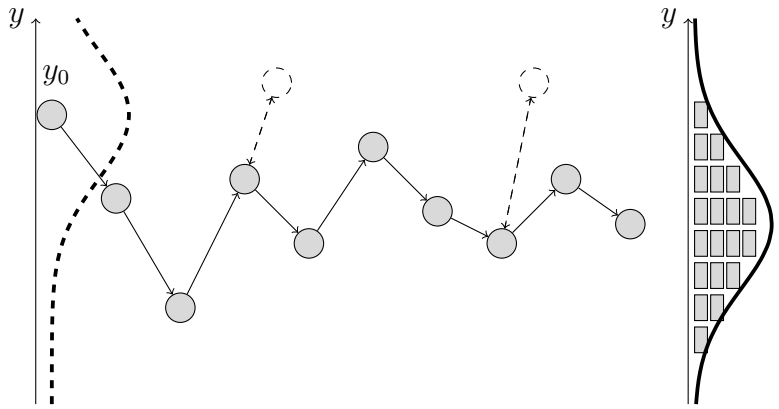

Proposal distribution $q(y^*|y_t)$ Target distribution $p(y)$

Figure 7.4.: Illustration of the Metropolis-Hastings algorithm. On the left, the proposal distribution $q(y^*|y_0)$ with Markov chain starting value y_0 is shown (dashed curve). The Markov chain path is illustrated with accepted points forming a chain and rejected samples in dashed circles. On the right, the target distribution $p(y)$ is shown (solid curve), with histogram of accepted samples, showing converges towards the target distribution.

In the underlying publication, the Metropolis-Hastings algorithm was applied to sample from the Bayesian marginal posterior distribution $P(\Theta|X)$ for the risk model parameter vector Θ, given cohort data X (equation (7.4) below). Inspired by the approach from Higueras and Howes (2018), $P(\Theta|X)$ was analytically deduced from the full posterior $P(\Omega|X) \propto P(\Omega)L(\Omega|X)$ with parameter vector $\Omega = (\Theta, \Delta)$ incorporating baseline strata parameters $\Delta = (\delta_1, \delta_2, \ldots, \delta_K)$. Assuming independence between the baseline strata and the risk model parameters, and specifically adopting non-informative priors for the strata parameters δ_k for all $k = 1, \ldots, K$, the full posterior $P(\Omega|X)$ with prior $P(\Omega) = P(\Theta)\prod_{k=1}^{K} P(\delta_k) \propto P(\Theta)$ and likelihood $L(\Omega|X)$ reads

$$P(\Omega|X) \propto P(\Omega)L(\Omega|X) \tag{7.1}$$

$$\propto P(\Theta)\exp\left(S\delta_1 - e^{\delta_1}\sum_{i=1}^{n} PY_i e^{\sum_{k=2}^{K}\delta_k \mathbb{1}_{\{k\}}(x_i)}\left(1 + ERR_i\left(\Theta\right)\right)\right) \tag{7.2}$$

$$\cdot \prod_{i=1}^{n}\left(PY_i e^{\sum_{k=2}^{K}\delta_k \mathbb{1}_{\{k\}}(x_i)}\left(1 + ERR_i\left(\Theta\right)\right)\right)^{C_i}, \tag{7.3}$$

with lung cancer cases C_i, person-years at risk PY_i and excess relative risk $ERR_i\left(\Theta\right)$ and $S = \sum_{i=1}^{n} C_i$. The likelihood structure is based on the assumption that the number of lung cancer deaths follows a Poisson distribution, as detailed in Section 3.1.2 and 4.2.2. The corresponding marginal posterior $P\left(\Theta|X\right)$ for the important risk model parameters Θ is

$$P\left(\Theta|X\right) = \frac{P\left(\Theta\right)\left[\prod_{i=1}^{n}\left(1 + ERR_i\left(\Theta\right)\right)^{C_i}\right]\left[\sum_{i|x_i=1} PY_i\left(1 + ERR_i\left(\Theta\right)\right)\right]^{-S_1}}{M_0\prod_{k=2}^{K}\left[\sum_{i|x_i=k} PY_i\left(1 + ERR_i\left(\Theta\right)\right)\right]^{S_k}}, \tag{7.4}$$

with lung cancer cases in strata k, $S_k = \sum_{i|x_i=k} C_i$ for $k = 1, \ldots, K$, and normalizing constant M_0.

Choosing prior distributions

The Bayesian framework enables incorporating prior beliefs and updating them based on observed data (Stauffer, 2007). A central challenge is selecting suitable prior distributions, which can strongly influence the posterior distribution and subsequent analyses (Bustamante et al., 2023). Appropriate priors can substantially improve the accuracy and reliability of estimates, especially when prior knowledge – whether from previous analyses or expert opinion – is available (Tian et al., 2023; Wilson & Fronczyk, 2017).

Prior selection is often subjective, shaped by the analyst's background and assumptions (Canfield & Teed, 1977). When prior knowledge is limited, uninformative or vague priors can be used. Flat priors carrying no information such as uniform distributions are common, though they are not invariant under reparametrization.

As an alternative, "Jeffrey's prior", based on the Fisher information, is non-informative and robust to parameter transformation (Kass & Wasserman, 1996; Stauffer, 2007). Improper priors (i.e. priors that do not integrate to a finite number), may be employed in certain cases, but care must be taken to ensure that the resulting posterior distribution is proper (Bernardo, 2005; Kass & Wasserman, 1996). Another pragmatic approach avoiding external information is the empirical Bayes method, where prior parameters are estimated from the observed data (Robert, 2007).

In some cases, conjugate priors – those from the same distributional family as the likelihood – are chosen as they allow deriving a closed-form expression of the posterior distribution and hence, easy sampling (Raiffa & Schlaifer, 1961).

Informative priors are used when reliable prior knowledge exists, typically taken from expert judgement, previous studies, or both. This approach corresponds to the "subjective Bayesian approach" (Goldstein, 2006) and may incorporate personal beliefs and opinions. This idea, while powerful, can introduce biases: experts, despite their domain knowledge, are susceptible to cognitive biases (Kahneman & Klein, 2009). Such tendencies, as the availability heuristic[4], can lead to systematic errors in judgment and decision-making (Kahneman, 2012; Tversky & Kahneman, 1974). For further discussions on choosing prior distributions see (Gelman et al., 2013; Kass & Wasserman, 1996; Stauffer, 2007).

In the underlying publication, prior distributions for the risk model parameters Θ were selected based on two goals: (a) to obtain posterior distributions $P(\Theta|X)$ that are minimally influenced by prior assumptions (e.g., uniform priors), and (b) to assess the Bayesian framework's ability to integrate results from distinct cohort studies. In the latter case (b), informative prior distributions were chosen such that their modes aligned with parameter estimates from other cohorts. The distribution choice, e.g. the gamma distribution as a prior for the β parameter that substantially shapes the exposure-risk relationship between radon and lung cancer, can be interpreted as expert judgement. Gamma distributions are appropriate to model (excess) risks and rates (Devianto et al., 2023; Havulinna, 2011), and they guarantee non-negative samples consistent with the assumption that no protective effect[5] is expected for radon exposure (Shore et al., 2018).

Overall, in the context of Bayesian risk model assessment, effectively integrating true prior knowledge based on external cohorts is a major challenge. Cohorts and corresponding risk models often differ substantially in design, population, and model structure, making it difficult to treat their results as prior knowledge in the classical Bayesian sense. Consequently, rather than attempting to encode prior knowledge, the Bayesian framework serves as a useful tool to combine results from heterogeneous cohorts, as done in the underlying publication. The choice of prior distribution and its parameters serves to calibrate the degree of integration between cohorts, together with the corresponding likelihood function.

[4]The tendency to judge the probability of events based on how easily examples come to mind.
[5]Sometimes called "radiation hormesis", compare (Macklis & Beresford, 1991).

8. Summary and final thoughts

8.1. Summary

This cumulative dissertation, comprising four published scientific articles, has collectively contributed to a comprehensive examination and refinement of lifetime risk assessment for lung cancer related to radon exposure. The work involved deriving and applying advanced risk models, establishing unified methodologies, and conducting an extensive uncertainty assessment. This assessment included sensitivity analyses, broad comparisons across international miner studies, and rigorous statistical quantification of uncertainties. Overall, this thesis enhances the interpretability, comparability, and credibility of lifetime risk assessments and thereby contributes to more informed risk communication and decision-making in radiation protection and public health.

- The work presented in Kreuzer et al. (2023) provided updated risk models derived from the German Wismut uranium miners cohort, the largest single cohort of uranium miners. The derived risk models confirmed and further sharpened the understanding of the radon-risk relationship. Acknowledging that risk models are a crucial and highly influential component of lifetime risk calculations makes this publication the foundation for sound lifetime risk estimates and corresponding uncertainty or variability assessments, as addressed in the subsequent publications.
- In Sommer et al. (2025), sensitivity analyses of various components of lifetime risk calculations clarified that risk models and baseline lung cancer mortality rates are highly influential compared to other components. The development of a unified calculation methodology allows for consistent calculations of lifetime risks, thereby improving comparability across different miner studies. The identification of the main lifetime risk drivers provides a practical basis for future lifetime risk estimations in radiation protection and targeted uncertainty quantification.
- The work in Kreuzer et al. (2024) offers a comprehensive overview and comparison of lifetime risk estimates across various international miner studies, utilizing the unified calculation methodology from Sommer et al. (2025). This comparison enhances the understanding of lifetime risk variability and confirms that lifetime risks are a suitable metric for evaluating exposure–risk relationships for radon and lung cancer across cohorts with varying exposures and model structures. The observed variation in lifetime risk estimates across risk models provides a solid epidemiological basis for current discussions on radon dose conversion.

- Ultimately, in Sommer et al. (2024), lifetime risk uncertainties are discussed and quantified with 95% uncertainty intervals using advanced statistical methods. The derived uncertainty intervals correspond well to the range of excess lifetime risks across miner studies in the literature (see (Kreuzer et al., 2024)), thus mutually confirming uncertainties derived by both approaches. This work expands on ideas from Sommer et al. (2025), and is the first to derive such intervals for lifetime risk estimates of lung cancer due to occupational radon exposure. Previous studies typically reported point estimates only, limiting comparability and interpretability. The uncertainty quantification presented here enables systematic comparisons across studies and makes an important contribution to scientific risk evaluation, risk communication, and regulatory decision-making.

8.2. Outlook and future research

This work has contributed to a deeper understanding of lifetime lung cancer risks associated with radon exposure, particularly in occupational settings. Building upon this, future research may benefit from incorporating more detailed population datasets, particularly regarding smoking behaviour – a key factor in lung cancer risk – and its interaction with radon exposure, once such datasets and corresponding risk models become more widely available. Lifetime risk assessments are subject to limitations from the underlying risk models, particularly when adjusting for smoking-related radon risk. Future studies utilizing updated follow-up data from miner cohorts will naturally improve the precision and reliability of miner risk models and corresponding lifetime risk estimates.

Another natural extension of this work lies in the targeted application of the developed methodologies to residential radon exposure scenarios, including the use of risk models derived from residential radon studies. Many of the presented methods and insights are equally relevant tor residential exposure and already enhance the understanding of associated lifetime risks. This broader application would further strengthen the practical relevance of radon risk assessments for public health and regulatory decisions.

Overall, continued progress in data collection, model development, and analytical techniques are expected to further strengthen the quality of radon risk assessments, particularly regarding its interaction with smoking, and extend their applicability to residential and other non-occupational settings. The methods and insights presented in this thesis provide a strong foundation for such developments and support future efforts to better quantify and communicate radon-related health risks.

Bibliography

Amemiya, T. (1985). *Advanced econometrics*. Harvard University Press.

Aßenmacher, M., Kaiser, J. C., Zaballa, I., Gasparrini, A., & Küchenhoff, H. (2019). Exposure-lag-response associations between lung cancer mortality and radon exposure in German uranium miners. *Radiation and Environmental Biophysics*, *58*(3), 321–336. https://doi.org/10.1007/s00411-019-00800-6

Bayes, T. (1763). An essay towards solving a problem in the doctrine of chances [Communicated by Mr. Price in a letter to John Canton]. *Philosophical Transactions of the Royal Society of London*, *53*, 370–418. https://doi.org/10.1098/rstl.1763.0053

Beck, T. R. (2017). The conversion of exposures due to radon into the effective dose: The epidemiological approach. *Radiation and Environmental Biophysics*, *56*(4), 353–364.

Becquerel, H. (1896). On the rays emitted by phosphorescence. *Comptes Rendus de l'Académie des Sciences*, *122*, 420–421.

Bellman, R. E. (1957). *Dynamic programming*. Princeton University Press.

Bernardo, J. M. (2005). Reference analysis. In *Handbook of statistics* (pp. 17–90). Elsevier.

Berrington de Gonzalez, A., Iulian Apostoaei, A., Veiga, L. H. S., Rajaraman, P., Thomas, B. A., Owen Hoffman, F., Gilbert, E., & Land, C. (2012). RadRAT: A radiation risk assessment tool for lifetime cancer risk projection. *Journal of Radiological Protection*, *32*(3), 205–222. https://doi.org/10.1088/0952-4746/32/3/205

Bierema, A., Hoskinson, A.-M., Moscarella, R., Lyford, A., Haudek, K., Merrill, J., & Urban-Lurain, M. (2021). Quantifying cognitive bias in educational researchers. *International Journal of Research & Method in Education*, *44*(4), 395–413. https://doi.org/10.1080/1743727X.2020.1804541

Bland, J. M., & Altman, D. G. (1998). Bayesians and frequentists. *BMJ (Clinical Research Ed.)*, *317*(7166), 1151–1160. https://doi.org/10.1136/bmj.317.7166.1151

Bonita, R., Beaglehole, R., Kjellstrom, T., & World Health Organization. (2007). *Basic epidemiology* (2nd ed.). World Health Organization.

Breckow, J. (2018). Radon-Dosiskoeffizienten: Wie soll man eine Radon-Konzentration in eine Dosis umrechnen? [Raon dose coefficients: how should one convert a radon concentration into a dose?] *StrahlenschutzPRAXIS*, *3*, 75–78. https://www.fs-ev.org/fileadmin/user_upload/05_SSP/Hefte-Komplett/ssp_3_2018_komplett.pdf

Breckow, J., & Emami, S. (2016). Untersuchung und Bewertung des Detrimentbegriffs im Strahlenschutz [Examination and evaluation of the concept of detriment in radiation protection] [Online; accessed 2024-06-12]. https://www.bmuv.de/fileadmin/

Daten_BMU/Pools/Forschungsdatenbank/fkz_3615_s_72264_detrimentbegriff_untersuchung_bf.pdf

Bundesamt für Strahlenschutz. (2024). Definition of unit Working Level Month (WLM) [Online; accessed 2024-01-03]. https://www.bfs.de/SharedDocs/Glossareintraege/EN/W/wlm.html

Burnham, K. P., & Anderson, D. R. (2002). *Model selection and multimodel inference* (K. P. Burnham & D. R. Anderson, Eds.; 2nd ed.). Springer.

Bustamante, R. O., Iturriaga, A., Flores-Alvarado, S., García, R. A., & Goncalves, E. (2023). On the use of prior distributions in Bayesian inference applied to Ecology: An ecological example using binomial proportions in exotic plants, Central Chile. *Revista Chilena de Historia Natural*, *96*(1). https://doi.org/10.1186/s40693-023-00118-0

Canfield, R. V., & Teed, J. C. (1977). Selecting the prior distribution in Bayesian estimation. *IEEE Transactions on Reliability*, *R-26*(4), 283–285. https://doi.org/10.1109/TR.1977.5220158

Carroll, R. J., Ruppert, D., Stefanski, L. A., & Crainiceanu, C. M. (2006). *Measurement error in nonlinear models: A modern perspective* (2nd ed.). Chapman; Hall/CRC.

Chen, J., Murith, C., Palacios, M., Wang, C., & Liu, S. (2017). A discussion on different approaches for assessing lifetime risks of Radon-induced lung cancer. *Radiation Protection Dosimetry*, *176*(3), 226–234. https://doi.org/10.1093/rpd/ncw385

Clayton, D., & Hills, M. (1993). *Statistical models in epidemiology*. Oxford University Press.

Cook, J. R., & Stefanski, L. A. (1994). Simulation-extrapolation estimation in parametric measurement error models. *Journal of the American Statistical Association*, *89*(428), 1314. https://doi.org/10.2307/2290994

Cori, L., Curzio, O., Donzelli, G., Bustaffa, E., & Bianchi, F. (2022). A systematic review of radon risk perception, awareness, and knowledge: Risk communication options. *Sustainability*, *14*(17), 10505. https://doi.org/10.3390/su141710505

Curie, P., & Curie, M. (1898). On a new radioactive substance contained in pitchblende. *Comptes Rendus de l'Académie des Sciences*, *127*, 175–178.

Darby, S., Hill, D., Auvinen, A., Barros-Dios, J., Baysson, H., Bochicchio, F., Deo, H., Falk, R., Forastiere, F., Hakama, M., Heid, I., Kreienbrock, L., Kreuzer, M., Lagarde, F., Mäkeläinen, I., Muirhead, C., Oberaigner, W., Pershagen, G., Ruano-Ravina, A., & Doll, R. (2005). Radon in homes and risk of lung cancer: Collaborative analysis of individual data from 13 European case-control studies. *BMJ (Clinical Research Ed.)*, *330*, 223. https://doi.org/10.1136/bmj.38308.477650.63

Darby, S., Hill, D., Deo, H., Auvinen, A., Barros-Dios, J. M., Baysson, H., Bochicchio, F., Falk, R., Farchi, S., Figueiras, A., Hakama, M., Heid, I., Hunter, N., Kreienbrock, L., Kreuzer, M., Lagarde, F., Mäkeläinen, I., Muirhead, C., Oberaigner, W., ... Doll, R. (2006). Residential radon and lung cancer–detailed results of a collaborative analysis of individual data on 7148 persons with lung cancer and 14,208 persons without lung cancer from 13 epidemiologic studies in Europe. *Scandinavian Journal of Work, Environment & Health*, *32 Suppl 1*, 1–83.

de Elía, R., & Laprise, R. (2005). Diversity in interpretations of probability: Implications for weather forecasting. *Monthly Weather Review*, *133*(5), 1129–1143. https://doi.org/10.1175/MWR2913.1

Degu Belete, G., & Alemu Anteneh, Y. (2021). General overview of radon studies in health hazard perspectives. *Journal of Oncology*, *2021*, 6659795. https://doi.org/10.1155/2021/6659795

Devianto, D., Maiyastri, Wahyuni, E., & Febrianti, I. K. (2023). The Gamma-Poisson conjugate hierarchical model on the mortality rate of dengue fever cases in Indonesia. *Communications in Mathematical Biology and Neuroscience*, *2023*, 127. https://doi.org/10.28919/cmbn/8256

Dorn, E. (1901). Über die von radioaktiven Substanzen ausgesandte Emanation [On the Emanation Emitted by Radioactive Substances]. *Abhandlungen der Naturforschenden Gesellschaft zu Halle*, *23*, 1–15. https://publikationen.ub.uni-frankfurt.de/opus4/frontdoor/deliver/index/docId/17242/file/E001458681_a.pdf

Durrett, R. (2016). *Essentials of stochastic processes* (3rd ed.). Springer International Publishing.

Eisenmenger, M., & Emmerling, D. (2011). Amtliche Sterbetafeln und Entwicklung der Sterblichkeit [Official life tables and the development of mortality]. In *Wirtschaft und Statistik* (pp. 219–238, Vol. 3). Statistisches Bundesamt.

Ellenbach, N., Rehms, R., & Hoffmann, S. (2022). *Ermittlung der Unsicherheiten der Strahlenexpositionsabschätzung in der Wismut-Kohorte - Teil II - Vorhaben 3618S12223 [Determination of uncertainties of radiation exposure assessment in the Wismut cohort part II - Project 3618S12223]* (tech. rep. No. BfS-RESFOR-138/18). Bundesamt für Strahlenschutz. https://doris.bfs.de/jspui/handle/urn:nbn:de:0221-2018080615802

Enke, B., & Graeber, T. (2023). Cognitive Uncertainty. *The Quarterly Journal of Economics*, *138*(4), 2021–2067. https://doi.org/10.1093/qje/qjad025

Esan, D. T., Obed, R. I., Afolabi, O. T., Sridhar, M. K., Olubodun, B. B., & Ramos, C. (2020). Radon risk perception and barriers for residential radon testing in Southwestern Nigeria. *Public Health in Practice*, *1*(100036), 100036. https://doi.org/10.1016/j.puhip.2020.100036

Fedak, K. M., Bernal, A., Capshaw, Z. A., & Gross, S. (2015). Applying the Bradford Hill criteria in the 21st century: How data integration has changed causal inference in molecular epidemiology. *Emerging Themes in Epidemiology*, *12*(1), 14. https://doi.org/10.1186/s12982-015-0037-4

Fenske, N., Deffner, V., Schnelzer, M., & Kreuzer, M. (2025). Does radon cause diseases other than lung cancer? Findings on mortality within the German uranium miners cohort study, 1946–2018 [Advance online publication]. *Occupational and Environmental Medicine*. https://doi.org/10.1136/oemed-2024-109923

Ferlay, J., Colombet, M., Soerjomataram, I., Mathers, C., Parkin, D. M., Piñeros, M., Znaor, A., & Bray, F. (2019). Estimating the global cancer incidence and mortality in 2018: GLOBOCAN sources and methods. *International Journal of Cancer*, *144*(8), 1941–1953. https://doi.org/10.1002/ijc.31937

Ferson, S. (2005). Bayesian methods in risk assessment [Online; accessed 2024-10-10]. https://www.researchgate.net/publication/228805839_Bayesian_Methods_in_Risk_Assessment

Fisher, D. R., & Fahey, F. H. (2017). Appropriate use of effective dose in radiation protection and risk assessment. *Health Physics*, *113*(2), 102–109. https://doi.org/10.1097/HP.0000000000000674

Fisher, R. A. (1925). *Statistical methods for research workers*. Oliver; Boyd.

Flaskämper, P. (1962). *Bevölkerungsstatistik*. Meiner.

Fornacon-Wood, I., Mistry, H., Johnson-Hart, C., Faivre-Finn, C., O'Connor, J. P. B., & Price, G. J. (2022). Understanding the differences between Bayesian and frequentist statistics. *International Journal of Radiation Oncology – Biology – Physics*, *112*(5), 1076–1082. https://doi.org/10.1016/j.ijrobp.2021.12.011

Fuller, W. A. (1987). *Measurement error models* (W. A. Fuller, Ed.). Wiley.

Gelman, A., Carlin, J. B., Stern, H. S., Dunson, D. B., Vehtari, A., & Rubin, D. B. (2013). *Bayesian data analysis* (3rd ed.). Chapman & Hall/CRC.

George, A. C. (2008). World History Of Radon Research And Measurement From The Early 1900's To Today. *AIP Conference Proceedings*, *1034*(1), 20–33. https://doi.org/10.1063/1.2991210

Goldstein, M. (2006). Subjective Bayesian Analysis: Principles and Practice. *Bayesian Analysis*, *1*(3), 403–420. https://doi.org/10.1214/06-BA116

Grdina, D. J. (2022). Ionizing radiation. In *Holland-frei cancer medicine* (pp. 1–9). John Wiley & Sons, Ltd. https://doi.org/10.1002/9781119000822.hfcm025.pub2

Grosche, B., Kreuzer, M., Kreisheimer, M., Schnelzer, M., & Tschense, A. (2006). Lung cancer risk among German male uranium miners: A cohort study, 1946-1998. *British Journal of Cancer*, *95*(9), 1280–1287. https://doi.org/10.1038/sj.bjc.6603403

Gustafson, P. (2003). *Measurement error and misclassification in statistics and epidemiology*. Chapman; Hall.

Hardin, J. W., Schmiediche, H., & Carroll, R. J. (2003). The simulation extrapolation method for fitting generalized linear models with additive measurement error. *The Stata Journal*, *3*(4), 373–385. https://doi.org/10.1177/1536867X0400300407

Harrison, J. D. (2021). Lung cancer risk and effective dose coefficients for radon: UNSCEAR review and ICRP conclusions. *Journal of Radiological Protection*, *41*(2), 433–441. https://doi.org/10.1088/1361-6498/abf547

Härting, F. H., & Hesse, W. (1879). *Der Lungenkrebs, die Bergkrankheit in den Schneeberger Gruben* [Lung cancer, the miners' disease in the Schneeberg mines]. https://www.industrydocuments.ucsf.edu/tobacco/docs/#id=nqlk0090

Havulinna, A. (2011). *Bayesian spatial and temporal epidemiology of non-communicable diseases and mortality* (Publication No. 138) [Doctoral thesis]. Aalto University.

Head, M. L., Holman, L., Lanfear, R., Kahn, A. T., & Jennions, M. D. (2015). The extent and consequences of p-hacking in science. *PLoS Biology*, *13*(3), e1002106. https://doi.org/10.1371/journal.pbio.1002106

Heinzl, F., Schnelzer, M., & Scholz-Kreisel, P. (2024). Lung cancer mortality attributable to residential radon in germany. *Radiation and Environmental Biophysics*, *63*(4), 505–517. https://doi.org/10.3205/24gmds527

Held, L., & Bové, D. S. (2021). *Likelihood and Bayesian inference* (2nd ed.). Springer.

Henyoh, A. M. S., Laurent, O., Mandin, C., & Clero, E. (2024). Radon exposure and potential health effects other than lung cancer: A systematic review and meta-analysis. *Frontiers in Public Health*, *12*, 1439355. https://doi.org/10.3389/fpubh.2024.1439355

Hernán, M. A. (2004). A definition of causal effect for epidemiological research. *Journal of Epidemiology and Community Health*, *58*(4), 265–271. https://doi.org/10.1136/jech.2002.006361

Hespanhol, L., Vallio, C. S., Costa, L. M., & Saragiotto, B. T. (2019). Understanding and interpreting confidence and credible intervals around effect estimates. *Brazilian Journal of Physical Therapy*, *23*(4), 290–301. https://doi.org/10.1016/j.bjpt.2018.12.006

Higueras, M., & Howes, A. (2018). Poisson excess relative risk models: New implementations and software. *SORT (Statistics and Operations Research Transactions)*, *42*, 237–252. https://doi.org/10.2436/20.8080.02.76

Hill, A. B. (1965). The Environment and Disease: Association or Causation? *Journal of the Royal Society of Medicine*, *58*(5), 295–300. https://doi.org/10.1177/003591576505800503

Hiller, A., & Ducke, G. (1999). *Chronik der Wismut [Chronicle of Wismut]*. Wismut GmbH.

Hoef, J. M. V. (2012). Who Invented the Delta Method? *The American Statistician*, *66*(2), 124–127. https://doi.org/10.1080/00031305.2012.687494

Hoffmann, S., Schönbrodt, F., Elsas, R., Wilson, R., Strasser, U., & Boulesteix, A.-L. (2021). The multiplicity of analysis strategies jeopardizes replicability: Lessons learned across disciplines. *Royal Society Open Science*, *8*(4), 201925. https://doi.org/10.1098/rsos.201925

Hofmann, W., & Winkler-Heil, R. (2011). Radon lung dosimetry models. *Radiation Protection Dosimetry*, *145*(2-3), 206–212. https://doi.org/10.1093/rpd/ncr059

Hoti, F., Perko, T., Thijssen, P., & Renn, O. (2020). Radiation risks and uncertainties: A scoping review to support communication and informed decision-making. *Journal of Radiological Protection*, *40*(2), 612. https://doi.org/10.1088/1361-6498/ab885f

Hunter, N., Muirhead, C. R., Bochicchio, F., & Haylock, R. G. E. (2015). Calculation of lifetime lung cancer risks associated with radon exposure, based on various models and exposure scenarios. *Journal of Radiological Protection*, *35*(3), 539–555. https://doi.org/10.1088/0952-4746/35/3/539

International Commission on Radiological Protection. (1987). Lung cancer risk from exposures to radon daughters. *ICRP Publication 50, Annals of the ICRP*.

International Commission on Radiological Protection. (1993). Protection against radon-222 at home and at work. *ICRP Publication 65, Annals of the ICRP*.

International Commission on Radiological Protection. (1994). Human respiratory tract model for radiological protection. *ICRP Publication 66, Annals of the ICRP*.

International Commission on Radiological Protection. (2007). The 2007 recommendations of the international commission on radiological protection. *ICRP Publication 103, Annals of the ICRP*.

International Commission on Radiological Protection. (2010). Lung cancer risk from radon and progeny and statement on radon. *ICRP Publication 115, Annals of the ICRP*.

International Commission on Radiological Protection. (2014). Radiological protection against radon exposure. *ICRP Publication 126, Annals of the ICRP*.

International Commission on Radiological Protection. (2016). The ICRP computational framework for internal dose assessment for reference adults: Specific absorbed fractions. *ICRP Publication 133, Annals of the ICRP*.

International Commission on Radiological Protection. (2017). Occupational intakes of radionuclides: Part 3. *ICRP Publication 137, Annals of the ICRP*.

International Commission on Radiological Protection. (2022). Radiation detriment calculation methodology. *ICRP Publication 152, Annals of the ICRP*.

Jacobi, W. (1993). *Verursachungs-Wahrscheinlichkeit von Lungenkrebs durch die berufliche Strahlenexposition von Uran-Bergarbeitern der Wismut-AG: gutachterliche Stellungnahme im Auftrage der Berufsgenossenschaften* [Probability of causation of lung cancer due to occupational radiation exposure of uranium miners at Wismut AG: Expert opinion commissioned by the trade associations]. GSF.

Kahneman, D. (2012). *Thinking, fast and slow*. Penguin Books.

Kahneman, D., & Klein, G. (2009). Conditions for intuitive expertise: A failure to disagree. *American Psychologist*, *64*(6), 515–526. https://doi.org/10.1037/a0016755

Kaiser, J. C., Jacob, P., Meckbach, R., & Cullings, H. M. (2012). Breast cancer risk in atomic bomb survivors from multi-model inference with incidence data 1958-1998. *Radiation and Environmental Biophysics*, *51*(1), 1–14. https://doi.org/10.1007/s00411-011-0387-4

Karras, C., Karras, A., Avlonitis, M., & Sioutas, S. (2022). An overview of MCMC methods: From theory to applications. In I. Maglogiannis, L. Iliadis, J. Macintyre, & P. Cortez (Eds.), *Artificial Intelligence Applications and Innovations. AIAI 2022 IFIP WG 12.5 International Workshops* (pp. 319–332). Springer International Publishing. https://doi.org/10.1007/978-3-031-08341-9_26

Kass, R., & Wasserman, L. (1996). The Selection of Prior Distributions by Formal Rules. *Journal of the American Statistical Association*, *91*, 1343–1370. https://doi.org/10.1080/01621459.1996.10477003

Kellerer, A. M., Nekolla, E. A., & Walsh, L. (2001). On the conversion of solid cancer excess relative risk into lifetime attributable risk. *Radiation and Environmental Biophysics*, *40*, 249–57. https://doi.org/10.1007/s004110100106

Kelly-Reif, K., Bertke, S. J., Rage, E., Demers, P. A., Fenske, N., Deffner, V., Kreuzer, M., Samet, J., Schubauer-Berigan, M. K., Tomášek, L., Zablotska, L. B., Wiggins, C., Laurier, D., & Richardson, D. B. (2023). Radon and lung cancer in the pooled uranium miners analysis (PUMA): Highly exposed early miners and all miners. *Occupational and Environmental Medicine*, *80*(7), 385–391. https://doi.org/10.1136/oemed-2022-108532

Keogh, R. H., Shaw, P. A., Gustafson, P., Carroll, R. J., Deffner, V., Dodd, K. W., Küchenhoff, H., Tooze, J. A., Wallace, M. P., Kipnis, V., & Freedman, L. S. (2020). STRATOS guidance document on measurement error and misclassification of variables in observational epidemiology: Part 1 - basic theory and simple methods of adjustment. *Statistics in Medicine*, *39*(16), 2197–2231. https://doi.org/10.1002/sim.8532

Keogh, R. H., & White, I. R. (2014). A toolkit for measurement error correction, with a focus on nutritional epidemiology. *Statistics in Medicine*, *33*(12), 2137–2155. https://doi.org/10.1002/sim.6095

Khazaei, Y., Küchenhoff, H., Hoffmann, S., Syliqi, D., & Rehms, R. (2023). Using a Bayesian hierarchical approach to study the association between non-pharmaceutical interventions and the spread of Covid-19 in Germany. *Scientific Reports*, *13*(1), 18900. https://doi.org/10.1038/s41598-023-45950-2

Kim, S.-H., Hwang, W. J., Cho, J.-S., & Kang, D. R. (2016). Attributable risk of lung cancer deaths due to indoor radon exposure. *Annals of Occupational and Environmental Medicine*, *28*(1), 8. https://doi.org/10.1186/s40557-016-0093-4

Kreuzer, M., Deffner, V., Sommer, M., & Fenske, N. (2023). Updated risk models for lung cancer due to radon exposure in the German Wismut cohort of uranium miners, 1946–2018. *Radiation and Environmental Biophysics*, *62*(4), 415–425. https://doi.org/10.1007/s00411-023-01043-2

Kreuzer, M., Dufey, F., Laurier, D., Nowak, D., Marsh, J. W., Schnelzer, M., Sogl, M., & Walsh, L. (2015). Mortality from internal and external radiation exposure in a cohort of male German uranium millers, 1946-2008. *International Archives of Occupational and Environmental Health*, *88*(4), 431–441. https://doi.org/10.1007/s00420-014-0973-2

Kreuzer, M., Grosche, B., Schnelzer, M., Tschense, A., Dufey, F., & Walsh, L. (2010). Radon and risk of death from cancer and cardiovascular diseases in the German uranium miners cohort study: Follow-up 1946-2003. *Radiation and Environmental Biophysics*, *49*(2), 177–185. https://doi.org/10.1007/s00411-009-0249-5

Kreuzer, M., Sobotzki, C., Schnelzer, M., & Fenske, N. (2018). Factors modifying the radon-related lung cancer risk at low exposures and exposure rates among German uranium miners. *Radiation Research*, *189*(2), 165. https://doi.org/10.1667/rr14889.1

Kreuzer, M., Sogl, M., Brüske, I., Möhner, M., Nowak, D., Schnelzer, M., & Walsh, L. (2013). Silica dust, radon and death from non-malignant respiratory diseases in German uranium miners. *Occupational and Environmental Medicine*, *70*(12), 869–875. https://doi.org/10.1136/oemed-2013-101582

Kreuzer, M., Sommer, M., Deffner, V., Bertke, S., Demers, P. A., Kelly-Reif, K., Laurier, D., Rage, E., Richardson, D. B., Samet, J. M., Schubauer-Berigan, M. K., Tomášek, L., Wiggins, C., Zablotska, L. B., & Fenske, N. (2024). Lifetime excess absolute risk for lung cancer due to exposure to radon: Results of the pooled uranium miners cohort study PUMA. *Radiation and Environmental Biophysics*, *63*(1), 7–16. https://doi.org/10.1007/s00411-023-01049-w

Kreuzer, M., Schnelzer, M., Tschense, A., Walsh, L., & Grosche, B. (2009). Cohort profile: The German uranium miners cohort study (WISMUT cohort), 1946–2003. *International Journal of Epidemiology*, *39*(4), 980–987. https://doi.org/10.1093/ije/dyp216

Küchenhoff, H., Deffner, V., Aßenmacher, M., Neppl, H., Kaiser, C., & Güthlin, D. (2018). *Ermittlung der Unsicherheiten der Strahlenexpositionsabschätzung in der Wismut-Kohorte - Teil I - Vorhaben 3616S12223 [Determination of uncertainties of radiation exposure assessment in the Wismut cohort part I Project 3616S12223]* (tech. rep. No. BfS-RESFOR-138/18). Bundesamt für Strahlenschutz. http://nbn-resolving.de/urn:nbn:de:0221-2018080615802

Kümpel, H., & Hoffmann, S. (2022). A formal framework for generalized reporting methods in parametric settings. https://arxiv.org/abs/2211.02621

Lane, R. S. D., Tomášek, L., Zablotska, L. B., Rage, E., Momoli, F., & Little, J. (2019). Low radon exposures and lung cancer risk: Joint analysis of the Czech, French, and Beaverlodge cohorts of uranium miners. *International Archives of Occupational and Environmental Health*, *92*(5), 747–762. https://doi.org/10.1007/s00420-019-01411-w

Laplace, P.-S. (1812). *Théorie analytique des probabilités* [Analytical theory of probabilities]. Courcier.

Laurier, D., Marsh, J. W., Rage, E., & Tomášek, L. (2020). Miner studies and radiological protection against radon. *Annals of the ICRP*, *49*(1_suppl), 57–67. https://doi.org/10.1177/0146645320931984

Laurier, D., Billarand, Y., Klokov, D., & Leuraud, K. (2023). The scientific basis for the use of the linear no-threshold (LNT) model at low doses and dose rates in radiological protection. *Journal of Radiological Protection*, *43*(2). https://doi.org/10.1088/1361-6498/acdfd7

Lee, J., Kim, Y. M., Park, Y., Jang, E., Yoo, J., Seo, S., Cha, E. S., & Lee, W. J. (2022). LARisk: An R package for lifetime attributable risk from radiation exposure. *medRxiv*. https://doi.org/10.1101/2022.02.21.22271307

Lehmann, E. L. (2008). Foundations I: The Frequentist Approach. In *Reminiscences of a Statistician: The Company I Kept* (pp. 160–177). Springer New York. https://doi.org/10.1007/978-0-387-71597-1_10

Levin, D. A., & Peres, Y. (2017). *Markov chains and mixing times* (2nd ed.). American Mathematical Society.

Little, J. B. (2000). Radiation carcinogenesis. *Carcinogenesis*, *21*(3), 397–404. https://doi.org/10.1093/carcin/21.3.397

Little, M. P., Hoel, D. G., Molitor, J., Boice, J. D., Wakeford, R., & Muirhead, C. R. (2008). New models for evaluation of radiation-induced lifetime cancer risk and its uncertainty employed in the UNSCEAR 2006 report. *Radiation Research*, *169*(6), 660–676. https://doi.org/10.1667/rr1091.1

Little, M. P., Pawel, D., Misumi, M., Hamada, N., Cullings, H. M., Wakeford, R., & Ozasa, K. (2020). Lifetime mortality risk from cancer and circulatory disease predicted from the japanese atomic bomb survivor life span study data taking account of dose

measurement error. *Radiation Research*, *194*(3), 259–276. https://doi.org/10.1667/RR15571.1

Lu, T.-T., & Shiou, S.-H. (2002). Inverses of 2 × 2 block matrices. *Computers & Mathematics with Applications*, *43*(1-2), 119–129. https://doi.org/10.1016/S0898-1221(01)00278-4

Lubin, J. H., Boice, J. D., Jr, Edling, C., Hornung, R. W., Howe, G. R., Kunz, E., Kusiak, R. A., Morrison, H. I., Radford, E. P., & Samet, J. M. (1995). Lung cancer in radon-exposed miners and estimation of risk from indoor exposure. *Journal of the National Cancer Institute*, *87*(11), 817–827. https://doi.org/10.1093/jnci/87.11.817

Lubin, J. H., Tomášek, L., Edling, C., Hornung, R. W., Howe, G., Kunz, E., Kusiak, R. A., Morrison, H. I., Radford, E. P., Samet, J. M., Tirmarche, M., Woodward, A., & Yao, S. X. (1997). Estimating lung cancer mortality from residential radon using data for low exposures of miners. *Radiation Research*, *147*(2), 126–134. https://doi.org/10.2307/3579412

Lubin, J. H. (1994). *Radon and lung cancer risk: A joint analysis of 11 underground miners studies*. U.S Department of Health; Human Services.

Macklis, R., & Beresford, B. (1991). Radiation hormesis. *Journal of Nuclear Medicine: official publication, Society of Nuclear Medicine*, *32*, 350–359.

Makumbi, T., Breustedt, B., & Raskob, W. (2024). Parameter uncertainty analysis of the equivalent lung dose coefficient for the intake of radon in mines: A review. *Journal of Environmental Radioactivity*, *276*, 107446. https://doi.org/https://doi.org/10.1016/j.jenvrad.2024.107446

Marsh, J. W., Harrison, J. D., Laurier, D., Blanchardon, E., Paquet, F., & Tirmarche, M. (2010). Dose conversion factors for radon: Recent developments. *Health Physics*, *99*(4), 511–516. https://doi.org/10.1097/HP.0b013e3181d6bc19

Marsh, J. W., Tomášek, L., Laurier, D., & Harrison, J. D. (2021). Effective dose coefficients for radon and progeny: A review of ICRP and UNSCEAR values. *Radiation Protection Dosimetry*, *195*(1), 1–20. https://doi.org/10.1093/rpd/ncab106

Martino, L., Luengo, D., & Míguez, J. (2018). *Independent Random Sampling Methods* (1st ed.). Springer International Publishing.

Mc Laughlin, J. (2012). An historical overview of radon and its progeny: Applications and health effects. *Radiation Protection Dosimetry*, *152*(1-3), 2–8. https://doi.org/10.1093/rpd/ncs189

McCollough, C. H., & Schueler, B. A. (2000). Calculation of effective dose. *Medical Physics*, *27*(5), 828–837. https://doi.org/https://doi.org/10.1118/1.598948

Mozzoni, P., Pinelli, S., Corradi, M., Ranzieri, S., Cavallo, D., & Poli, D. (2021). Environmental/occupational exposure to radon and non-pulmonary neoplasm risk: A review of epidemiologic evidence. *International Journal of Environmental Research and Public Health*, *18*(19), 10466. https://doi.org/10.3390/ijerph181910466

Müller, W.-U., Giussani, A., Rühm, W., Lecomte, J.-F., Harrison, J., Kreuzer, M., Sobotzki, C., & Breckow, J. (2016). Current knowledge on radon risk: Implications for practical radiation protection? radon workshop, 1/2 December 2015, Bonn, BMUB (Bundesministerium für Umwelt, Naturschutz, Bau und Reaktorsicherheit; Federal Min-

istry for the Environment, Nature Conservation, Building and Nuclear Safety). *Radiation and Environmental Biophysics*, *55*(3), 267–280. https://doi.org/10.1007/s00411-016-0657-2

National Research Council. (1988). *Health Risks of Radon and Other Internally Deposited Alpha-Emitters: BEIR IV*. National Academies Press.

National Research Council. (1999). *Health Effects of Exposure to Radon: BEIR VI*. The National Academies Press. https://doi.org/10.17226/5499

National Research Council. (2006). *Health Risks from Exposure to Low Levels of Ionizing Radiation: BEIR VII Phase 2*. The National Academies Press. https://doi.org/10.17226/11340

Nelder, J. A., & Wedderburn, R. W. M. (1972). Generalized linear models. *Journal of the Royal Statistical Society. Series A (General)*, *135*(3), 370–384. https://doi.org/10.2307/2344614

Nickerson, R. (1998). Confirmation bias: A ubiquitous phenomenon in many guises. *Review of General Psychology*, *2*, 175–220. https://doi.org/10.1037/1089-2680.2.2.175

Organisation for Economic Co-operation and Development. (2023). OECD Health Statistics [Online; accessed 2023-03-02]. https://stats.oecd.org/

Paracelsus, T. (1567). *Von der Bergsucht oder Bergkranckheiten drey Bücher, inn dreyzehen Tractat verfast unnd beschriben worden* [On mountain sickness or mountain diseases: Three books, composed and described in thirteen tracts]. Meyer Verlag (Bayrische Staatsbibliothek).

Pavia, M., Bianco, A., Pileggi, C., & Angelillo, I. F. (2003). Meta-analysis of residential exposure to radon gas and lung cancer. *Bulletin of the World Health Organisation*, *81*(10), 732–738. https://doi.org/10.1590/S0042-96862003001000008

Pawel, D. J., & Puskin, J. S. (2003). *EPA Assessment of Risks from Radon in Homes*. U.S. Environmental Protection Agency.

Pearl, J., & Mackenzie, D. (2019). *The Book of Why*. Penguin Books.

Pearson, D. D. (2021). *An analysis of alpha particle radiation exposure from the population level to the biological consequences* [Doctoral thesis]. University of Calgary.

Pesch, B., Kendzia, B., Gustavsson, P., Jöckel, K.-H., Johnen, G., Pohlabeln, H., Olsson, A., Ahrens, W., Gross, I. M., Brüske, I., Wichmann, H.-E., Merletti, F., Richiardi, L., Simonato, L., Fortes, C., Siemiatycki, J., Parent, M.-E., Consonni, D., Landi, M. T., ... Brüning, T. (2012). Cigarette smoking and lung cancer-relative risk estimates for the major histological types from a pooled analysis of case-control studies. *International Journal of Cancer*, *131*(5), 1210–1219. https://doi.org/10.1002/ijc.27339

Pierce, D. A., Stram, D. O., & Vaeth, M. (1990). Allowing for random errors in radiation dose estimates for the atomic bomb survivor data. *Radiation Research*, *123 (3)*, 275–284. https://doi.org/10.2307/3577733

Porstendörfer, J., & Reineking, A. (1999). Radon: Characteristics in air and dose conversion factors. *Health Physics*, *76*(3), 300–305. https://doi.org/10.1097/00004032-199903000-00011

Posit team. (2023). *Rstudio: Integrated development environment for R*. Posit Software, PBC. Boston, MA.

Preston, D. L., Lubin, J. H., Pierce, D. A., & McConney, M. (1993). *Epicure users guide*. Hirosoft International Corporation. Seattle, WA. https://hirosoft.com

Preston, D. L., Ron, E., Tokuoka, S., Funamoto, S., Nishi, N., Soda, M., Mabuchi, K., & Kodama, K. (2007). Solid cancer incidence in atomic bomb survivors: 1958-1998. *Radiation Research*, *168*(1), 1–64. https://doi.org/10.1667/RR0763.1

R Core Team. (2023). *R: A language and environment for statistical computing*. R Foundation for Statistical Computing. Vienna, Austria.

Rage, E., Richardson, D. B., Demers, P. A., Do, M., Fenske, N., Kreuzer, M., Samet, J., Wiggins, C., Schubauer-Berigan, M. K., Kelly-Reif, K., Tomášek, L., Zablotska, L. B., & Laurier, D. (2020). PUMA - pooled uranium miners analysis: Cohort profile. *Occupational and Environmental Medicine*, *77*(3), 194–200. https://doi.org/10.1136/oemed-2019-105981

Raiffa, H., & Schlaifer, R. (1961). *Applied statistical decision theory*. Harvard Business School Press.

Richardson, D. B., & Loomis, D. (2004). The impact of exposure categorisation for grouped analyses of cohort data. *Occupational and Environmental Medicine*, *61*(11), 930–935. https://doi.org/10.1136/oem.2004.014159

Richardson, D. B., Rage, E., Demers, P. A., Do, M. T., DeBono, N., Fenske, N., Deffner, V., Kreuzer, M., Samet, J., Wiggins, C., Schubauer-Berigan, M. K., Kelly-Reif, K., Tomášek, L., Zablotska, L. B., & Laurier, D. (2021). Mortality among uranium miners in North America and Europe: The pooled uranium miners analysis (PUMA). *International Journal of Epidemiology*, *50*(2), 633–643. https://doi.org/10.1093/ije/dyaa195

Richardson, D. B., Cole, S. R., Chu, H., & Langholz, B. (2011). Lagging exposure information in cumulative exposure-response analyses. *American Journal of Epidemiology*, *174*(12), 1416–1422. https://doi.org/10.1093/aje/kwr260

Richardson, D. B., Rage, E., Demers, P. A., Do, M. T., Fenske, N., Deffner, V., Kreuzer, M., Samet, J., Bertke, S. J., Kelly-Reif, K., Schubauer-Berigan, M. K., Tomášek, L., Zablotska, L. B., Wiggins, C., & Laurier, D. (2022). Lung cancer and radon: Pooled analysis of uranium miners hired in 1960 or later. *Environmental Health Perspectives*, *130*(5), 57010. https://doi.org/10.1289/EHP10669

Riudavets, M., Garcia de Herreros, M., Besse, B., & Mezquita, L. (2022). Radon and lung cancer: Current trends and future perspectives. *Cancers*, *14*(13), 3142. https://doi.org/10.3390/cancers14133142

Robert, C. (2007). *The Bayesian choice* (2nd ed.). Springer.

Robert, C., & Casella, G. (2005). *Monte carlo statistical methods* (2nd ed.). Springer.

Rosenthal, R. (1979). The file drawer problem and tolerance for null results. *Psychological Bulletin*, *86*, 638–641. https://doi.org/10.1037/0033-2909.86.3.638

Rothman, K. J., Greenland, S., & Lash, T. L. (2008). *Modern Epidemiology* (3rd ed.). Lippincott Williams & Wilkins.

Rothman, K. J., & Greenland, S. (2005). Causation and causal inference in Epidemiology. *American Journal of Public Health, 95 Suppl 1*(S1), S144–50. https://doi.org/10.2105/AJPH.2004.059204

Rothstein, H., Sutton, A. J., & Borenstein, M. (Eds.). (2005). *Publication bias in meta-analysis*. Wiley-Blackwell.

Rüger, B. (1998). *Test- und Schätztheorie [Test and estimation theory]*. Walter de Gruyter.

Samet, J. M. (2020). Carcinogenesis and lung cancer: 70 years of progress and more to come. *Carcinogenesis*, *41*(10), 1309–1317. https://doi.org/10.1093/carcin/bgaa094

Schnelzer, M., & Fenske, N. (2019). Die Wismut-Studie und der Radon-Dosiskoeffizient [The Wismut study and the radon dose coefficient]. *StrahlenschutzPRAXIS*, *1*, 59–63. https://www.fs-ev.org/fileadmin/user_upload/05_SSP/Hefte-Komplett/ssp_1_2019_komplettes_Heft.pdf

Schröder, C., Friedrich, K., Butz, M., Koppisch, D., & Otten, H. (2002). Uranium mining in Germany: incidence of occupational diseases 1946-1999. *International Archives of Occupational and Environmental Health*, *75*(4), 235–242. https://doi.org/10.1007/s00420-001-0295-z

Schüttmann, W. (1993). Schneeberg lung disease and uranium mining in the Saxon Ore Mountains (Erzgebirge). *American Journal of Industrial Medicine*, *23*(2), 355–368. https://doi.org/10.1002/ajim.4700230212

Shore, R. E., Beck, H. L., Boice, J. D., Caffrey, E. A., Davis, S., Grogan, H. A., Mettler, F. A., Preston, R. J., Till, J. E., Wakeford, R., Walsh, L., & Dauer, L. T. (2018). Implications of recent epidemiologic studies for the linear nonthreshold model and radiation protection. *Journal of Radiological Protection*, *38*(3), 1217–1233. https://doi.org/10.1088/1361-6498/aad348

Slovic, P., Finucane, M. L., Peters, E., & MacGregor, D. G. (2004). Risk as analysis and risk as feelings: Some thoughts about affect, reason, risk, and rationality. *Risk Analysis*, *24*(2), 311–322. https://doi.org/https://doi.org/10.1111/j.0272-4332.2004.00433.x

Sogl, M., Taeger, D., Pallapies, D., Brüning, T., Dufey, F., Schnelzer, M., Straif, K., Walsh, L., & Kreuzer, M. (2012). Quantitative relationship between silica exposure and lung cancer mortality in German uranium miners, 1946-2003. *British Journal of Cancer*, *107*(7), 1188–1194. https://doi.org/10.1038/bjc.2012.374

Sommer, M., Fenske, N., Heumannn, C., Scholz-Kreisel, P., & Heinzl, F. (2024). Methods to derive uncertainty intervals for lifetime risks for lung cancer related to occupational radon exposure. https://arxiv.org/abs/2412.06054

Sommer, M., Heinzl, F., Scholz-Kreisel, P., Wollschläger, D., Heumannn, C., & Fenske, N. (2025). Lifetime risks for lung cancer due to occupational radon exposure: A systematic analysis of estimation components. *Radiation Research*, *203*(3), 175–187. https://doi.org/10.1667/RADE-24-00060.1

Spiegelman, D., McDermott, A., & Rosner, B. (1997). Regression calibration method for correcting measurement-error bias in nutritional epidemiology. *The American Journal of Clinical Nutrition*, *65*(4), 1179S–1186S. https://doi.org/10.1093/ajcn/65.4.1179S

Spirtes, P., Glymour, C., & Scheines, R. (2001). *Causation, prediction, and search* (F. Bach, Ed.; 2nd ed.). Bradford Books.

Stabin, M. G. (2008). *Fundamentals of Nuclear Medicine Dosimetry*. Springer.

Stather, J. W. (2004). Dosimetric and epidemiological approaches to assessing radon doses–can the differences be reconciled? *Radiation Protection Dosimetry*, *112*(4), 487–492. https://doi.org/10.1093/rpd/nch103

Stauffer, H. B. (2007). *Contemporary Bayesian and Frequentist Statistical Research Methods for Natural Resource Scientists*. Wiley-Blackwell.

Strahlenschutzverordnung. (2021). StrlSchV: Strahlenschutzverordnung vom 29. November 2018 (BGBl. I S. 2034, 2036; 2021 I S. 5261), die zuletzt durch Artikel 1 der Verordnung vom 8. Oktober 2021 (BGBl. I S. 4645) geändert worden ist [Radiation Protection Ordinance of November 29, 2018 (BGBl. I p. 2034, 2036; 2021 I p. 5261), as last amended by Article 1 of the Ordinance of October 8, 2021 (BGBl. I p. 4645)].

The International Agency for Research on Cancer. (1988). Radon. In *IARC monographs on the identification of carcinogenic hazards to humans* (pp. 173–259). Oxford University Press.

The International Agency for Research on Cancer. (2004). Tobacco smoke and involuntary smoking. *IARC Monographs on the Identification of Carcinogenic Hazards to Humans*, *83*, 1–1438.

The Tobacco Atlas (7th ed.) [Online; accessed 2024-07-01]. (2022). Vital Strategies; Tobacconomics at the University of Illinois at Chicago. https://tobaccoatlas.org/

Thomas, D., Darby, S., Fagnani, F., Hubert, P., Vaeth, M., & Weiss, K. (1992). Definition and estimation of lifetime detriment from radiation exposures. *Health Physics*, *63*(3), 259–272. https://doi.org/10.1097/00004032-199209000-00001

Tian, Q., Lewis-Beck, C., Niemi, J. B., & Meeker, W. Q. (2023). Specifying prior distributions in reliability applications. *Applied Stochastic Models in Business and Industry*. https://doi.org/10.1002/asmb.2752

Tirmarche, M., Laurier, D., Bergot, D., Billon, S., Brueske-Hohlfeld, I., Collier, C., Grosche, B., Bijwaard, H., Hammer, G., & Wichmann, H. E. (2003). *Quantification of lung cancer risk after low radon exposure and low exposure rate: Synthesis from epidemiological and experimental data. Final scientific report, February 2000–July 2003* (Contract No. FIGH-CT1999-00013). European Commission. Brussels.

Tomášek, L., Rogel, A., Laurier, D., & Tirmarche, M. (2008). Dose conversion of radon exposure according to new epidemiological findings. *Radiation Protection Dosimetry*, *130*(1), 98–100. https://doi.org/10.1093/rpd/ncn117

Tomášek, L., Rogel, A., Tirmarche, M., Mitton, N., & Laurier, D. (2008). Lung cancer in French and Czech uranium miners: Radon-associated risk at low exposure rates and modifying effects of time since exposure and age at exposure. *Radiation Research*, *169*(2), 125–137. https://doi.org/10.1667/rr0848.1

Tomášek, L. (2020). Lung cancer lifetime risks in cohort studies of uranium miners. *Radiation Protection Dosimetry*, *191*(2), 171–175. https://doi.org/10.1093/rpd/ncaa143

Truta-Popa, L. A., Hofmann, W., Fakir, H., & Cosma, C. (2011). The effect of non-targeted cellular mechanisms on lung cancer risk for chronic, low level radon exposures.

International Journal of Radiation Biology, *87*(9), 944–953. https://doi.org/10.3109/09553002.2011.584936

Tversky, A., & Kahneman, D. (1974). Judgment under uncertainty: Heuristics and biases. *Science*, *185*(4157), 1124–1131. https://doi.org/10.1126/science.185.4157.1124

Ulanowski, A., Kaiser, J. C., Schneider, U., & Walsh, L. (2019). On prognostic estimates of radiation risk in medicine and radiation protection. *Radiation and Environmental Biophysics*, *58*(3), 305–319. https://doi.org/10.1007/s00411-019-00794-1

United Nations Scientific Committee on the Effects of Atomic Radiation. (1994). *Sources and effects of ionizing radiation: UNSCEAR 1994 report to the general assembly, with scientific annexes*. United Nations.

United Nations Scientific Committee on the Effects of Atomic Radiation. (2015). *UNSCEAR 2012 Report, Annex B, Uncertainties in risk estimates for radiation-induced cancer*. United Nations.

United Nations Scientific Committee on the Effects of Atomic Radiation. (2021a). *UNSCEAR 2019 Report, Annex B, Lung cancer from exposure to radon*. United Nations.

United Nations Scientific Committee on the Effects of Atomic Radiation. (2021b). *UNSCEAR 2019 Report: Sources, effects and risks of ionizing radiation*. United Nations.

Vaeth, M., & Pierce, D. A. (1990). Calculating excess lifetime risk in relative risk models. *Environmental Health Perspectives*, *87*, 83–94. https://doi.org/10.1289/ehp.908783

Von Mises, R. (1928). *Wahrscheinlichkeit Statistik und Wahrheit [Probability, Statistics and Truth]*. Springer.

von Elm, E., Altman, D. G., Egger, M., Pocock, S. J., Gøtzsche, P. C., Vandenbroucke, J. P., & STROBE Initiative. (2007). Strengthening the reporting of observational studies in epidemiology (STROBE) statement: Guidelines for reporting observational studies. *BMJ (Clinical Research Ed.)*, *335*(7624), 806–808. https://doi.org/10.1136/bmj.39335.541782.AD

Wallace, M. (2020). Analysis in an imperfect world. *Significance (Oxford, England)*, *17*(1), 14–19. https://doi.org/10.1111/j.1740-9713.2020.01353.x

Walsh, L., Ulanowski, A., Kaiser, J., Woda, C., & Raskob, W. (2020). A new European cancer risk assessment tool for application after nuclear accidents. *Radioprotection*, *55*, S95–S99. https://doi.org/10.1051/radiopro/2020018

WHO Regional Office for Europe. (2010). *WHO guidelines for indoor air quality: Selected pollutants*. https://www.who.int/publications/i/item/9789289002134

Wilson, A. G., & Fronczyk, K. M. (2017). Bayesian reliability: Combining information. *Quality Engineering*, *29*(1), 119–129. https://doi.org/10.1080/08982112.2016.1211889

World Health Organization. (2022). WHO Mortality Database [Online; accessed 2022-02-05]. https://www.who.int/data/data-collection-tools/who-mortality-database

World Health Organization. (2023). Statement on radon [Online; accessed 2023-12-01]. https://www.who.int/news-room/fact-sheets/detail/radon-and-health

Xue, X., & Shore, R. E. (2001). Assessing excess lifetime risk for disease after radiation exposure. *Health Physics*, *80*(5), 462–469. https://doi.org/10.1097/00004032-200105000-00006

Young, G. A., & Smith, R. L. (2005). *Essentials of Statistical Inference*. Cambridge University Press.

Zhang, W., Laurier, D., Cléro, E., Hamada, N., Preston, D., Vaillant, L., & Ban, N. (2020). Sensitivity analysis of parameters and methodological choices used in calculation of radiation detriment for solid cancer. *International Journal of Radiation Biology*, *96*(5), 596–605. https://doi.org/10.1080/09553002.2020.1708499

Part II.

Contributing publications

I, Manuel Sommer, declare that I have made substantial contributions to the publications presented in this dissertation. For each publication listed, a detailed description of my specific contributions is provided, followed by the corresponding publication itself. The order in which the publications are presented in the following reflects the chronology in which the work was conducted. Note that the publication dates of the articles may not align with this order due to the review and editing process.

9. Updated risk models for lung cancer due to radon exposure in the German Wismut cohort of uranium miners, 1946–2018

Contributing publication

Kreuzer, M., Deffner, V., Sommer, M., & Fenske, N. (2023). Updated risk models for lung cancer due to radon exposure in the German Wismut cohort of uranium miners, 1946–2018. *Radiation and Environmental Biophysics*, 62(4), 415–425. https://doi.org/10.1007/s00411-023-01043-2

Declaration of contributions

Michaela Kreuzer and Nora Fenske wrote the main manuscript. I, Manuel Sommer, carried out and contributed the following work for the publication:

- **Statistical analysis**
  - Development and estimation of lung cancer risk models with the statistical software *Epicure* under the supervision of Nora Fenske, including sensitivity analyses
  - Conception and implementation of lifetime risk calculation in statistical software *R*
  - Preparation of figures and tables
- **Writing**
  - Writing and description of methodology for lifetime risk calculations in section "LEAR calculations"
  - Review of the manuscript (together with all other authors)

Radiation and Environmental Biophysics (2023) 62:415–425
https://doi.org/10.1007/s00411-023-01043-2

RESEARCH

Updated risk models for lung cancer due to radon exposure in the German Wismut cohort of uranium miners, 1946–2018

M. Kreuzer[1] · V. Deffner[1] · M. Sommer[1] · N. Fenske[1]

Received: 16 August 2023 / Accepted: 18 August 2023 / Published online: 11 September 2023

Abstract
UNSCEAR recently recommended that future research on the lung cancer risk at low radon exposures or exposure rates should focus on more contemporary uranium miners. For this purpose, risk models in the German Wismut cohort of uranium miners were updated extending the follow-up period by 5 years to 1946–2018. The full cohort ($n = 58{,}972$) and specifically the 1960 + sub-cohort of miners first hired in 1960 or later ($n = 26{,}764$) were analyzed. The 1960 + sub-cohort is characterized by low protracted radon exposure of high quality of measurements. Internal Poisson regression was used to estimate the excess relative risk (ERR) for lung cancer per cumulative radon exposure in Working Level Months (WLM). Applying the BEIR VI exposure-age-concentration model, the ERR/100 WLM was 2.50 (95% confidence interval (CI) 0.81; 4.18) and 6.92 (95% CI < 0; 16.59) among miners with attained age < 55 years, time since exposure 5–14 years, and annual exposure rates < 0.5 WL in the full ($n = 4329$ lung cancer deaths) and in the 1960 + sub-cohort ($n = 663$ lung cancer deaths), respectively. Both ERR/WLM decreased with older attained ages, increasing time since exposure, and higher exposure rates. Findings of the 1960 + sub-cohort are in line with those from large pooled studies, and ERR/WLM are about two times higher than in the full Wismut cohort. Notably, 20–30 years after closure of the Wismut mines in 1990, the estimated fraction of lung cancer deaths attributable to occupational radon exposure is still 26% in the full Wismut cohort and 19% in the 1960 + sub-cohort, respectively. This demonstrates the need for radiation protection against radon.

Keywords Radon · Lung cancer · Epidemiology · Cohort · Risk

Introduction

The United Nations Scientific Committee on the Effects of Atomic Radiation (UNSCEAR) has recently reviewed the radon-related lung cancer risk in epidemiological studies (UNSCEAR 2020). They concluded that in miners studies the relationship between cumulative exposure to radon and relative risk of lung cancer is approximately linear and that the linear increase is additionally modified by time since exposure, attained age and exposure rate. The preferred risk model is thus a model including these three modifiers. The lifetime excess absolute risk (LEAR) of lung cancer per WLM was calculated for several cohort studies of miners based on the BEIR VI exposure-age-concentration model, using a mixed male/female population and exposure scenario of 2 WLM from age 18 to 64 years (UNSCEAR 2020). The resulting LEARs ranged from 2.4 (Wismut cohort) to 7.5 (Eldorado cohort) $\times 10^{-4}$ per WLM, and represent an important database for the epidemiological approach for radon dose conversion. The variability of LEARs across the studies offers different possibilities of dose conversion, which led to some controversial discussions in the International Commission on Radiological Protection (ICRP) (Harrison et al. 2020, 2021; Laurier et al. 2020; Marsh et al. 2021). The LEARs from epidemiological studies depend—among other factors—to a large extent on the risk model derived from the different studies of miners. In order to improve risk models, UNSCEAR (2020) recommended that future research on the lung cancer risk at low radon exposure or exposure rates should focus on time periods with the best available exposure assessment to reduce measurement error and should consider age- and time-related effect modifiers, exposure rate and, if possible, potential confounders.

For this purpose, the 1960 + sub-cohort of German uranium miners (Wismut miners) was updated; this sub-cohort

✉ M. Kreuzer
mkreuzer@bfs.de

[1] Federal Office for Radiation Protection, Ingolstaedter Landstr. 1, 85764 Neuherberg, Germany

includes only miners hired in 1960 or later with protracted exposure to low radon concentrations, which has been assessed based on radon measurements. In previous risk analyses this sub-cohort (Kreuzer et al. 2015, 2018) was characterized by a relatively young age, which hampered a valid estimation of effect modifiers at older ages or longer times since exposure. Due to the extended mortality follow-up by 5 years to the end of 2018, the proportion of deceased individuals in this sub-cohort increased from 19.3% to 25.1%, and the number of lung cancer deaths from 495 to 663. The larger number of deaths, longer time since exposure and older attained age together with the availability of data on important confounders (e.g. smoking, occupational exposure to silica dust and external gamma radiation) allow to further improve risk models at low exposures and exposure rates. Two types of risk models were estimated for the 1960 + sub-cohort and for comparison with previous results also for the full cohort: (1) parametric models including time since median exposure and age at median exposure as continuous variables and exposure rate as categorical variable (Tomasek et al. 2008; Kreuzer et al. 2018), (2) the categorical BEIR VI exposure-age-concentration model as used in the pooled study of the 11 miners cohorts (NRC 1999), UNSCEAR (2009, 2020) and the new PUMA study (Pooled Uranium Miners Analysis) (Richardson et al. 2022; Kelly-Reif et al. 2023). For both types of models, the relative risk was predicted for the exposure scenario of 2 WLM at age 18 to 64 over attained age up to 94 years as in other publications (Tirmarche 2010; UNSCEAR 2020) and the corresponding LEARs were calculated. In addition, differences in risk estimates between the full cohort and the 1960 + sub-cohort were discussed.

Methods

Study population

The German cohort of uranium miners has been described previously (Kreuzer et al. 2010, 2018). The full cohort includes 58,972 men employed for at least 180 days in the Wismut company in former Eastern Germany in the operation period from 1946 to 1990, the 1960 + sub-cohort includes 26,764 men hired for the first time in 1960 or later. Mortality follow-up has been extended by 5 years to the end of 2018 (i.e., 31/12/2018). Vital status was provided by local registration offices. Causes of death were obtained from death certificates and autopsy files from the Wismut pathology archive. In addition to new follow-up data, 359 previously missing causes of death from 1955 to 2013 were successfully traced through extensive searches in archival documents, many of them from the 1960s. In the present analyses, the cohort entry date was defined as the date of first employment plus 180 days (inclusion criterion), and the exit date was defined as the earliest date of death, loss to follow-up, or end of follow-up.

The early period of mining (1946–1955) at the Wismut company was characterized by high radon exposures due to lack of radiation protection measures and lack of radon measurements. In 1955, ambient air measurements of radon gas started in the different mines and from 1955 to 1958 the radon concentrations sharply decreased due to introduction of ventilation measures in the mines (Appendix Fig. 1). Annual cumulative exposure to radon progeny in Working Level Months (WLM: concentration of short-lived radon progeny per litre of air that gives rise to 1.3×10^5 MeV of alpha-particle energy after complete decay for 1 month (170 h) = 3.5 mJ h m^{-3}) was retrospectively assessed for each miner via a comprehensive job-exposure matrix (JEM). For each mining facility, workplace (underground, open pit, milling or surface) and calendar year the exposure to radon progeny in WLM was determined by an expert group for scientific purposes (HVBG 2005). The JEM was based on ambient measurements, if available, or, for years without measurements (particularly for the early mining period from 1946 to 1954), on expert ratings considering the first available ambient measurements of radon gas in later years, uranium deposit and delivery, ventilation and mine architecture over time.

Information on smoking habits were extracted from the Wismut health archives, mainly based on data from the regular medical check-ups which had been introduced in 1970. In these documents, the current smoking habits were given in predefined categories for each year. This only allows the definition of three rough smoking categories for risk analyses in the 1960 + sub-cohort: "non-smoker" (in all years "non-smoker"), "moderate/heavy smoker" (if in any year the classification "more than 5 years of smoking or more than 10 cigarettes smoked per day" was indicated) and "light smoker" (for all other specifications such as "occasional smoker", "less than 5 years or less than 10 cigarettes smoked per day", "cigar/pipe smoked"). In order to be comparable to previous risk analyses (Kreuzer et al. 2015, 2018) and due to the small number of lung cancer deaths among non-smokers, the categories non-smoker and light smoker were combined. Data on smoking were available for 56% of the 1960 + sub-cohort.

Statistical modelling

Typical statistical methodology was applied to model radon-related lung cancer risks by internal Poisson regression (NRC 1999; Kreuzer et al. 2018; Richardson et al. 2022; Tomasek et al. 2008; Walsh et al. 2010), and two different model types were fitted: parametric models with continuous age- and time-related effect-modifying variables and the

BEIR VI exposure-age-concentration model. For this purpose, individual data was first converted into grouped datasets to tabulate person-years at risk and lung cancer deaths in categories. Two grouped datasets were created, one for each model type. The following basic cross-classifications were used in both datasets: age a in 16 categories (0–14, 15–19, 20–24, …, 85 + years), calendar year in 15 categories (1946–1949, 1950–1954, …, 2005–2009, 2010–2014, 2015–2018), duration of employment d in three categories (0– < 5, 5– < 15, ≥ 15 years) calculated in a time-varying way, and start of employment in two categories (1946–1959, 1960–1989) to allow separate modelling of the 1960 + subcohort. Further categorization was model-specific and is described below.

For both model types, lung cancer mortality rates were assumed to follow an excess relative risk (ERR) model with the general structure:

$$r(a, y, d, w, ...) = r_0(a, y, d) \times [1 + ERR(w, ...)]$$

Here, the mortality rate $r(a,y,d,w,\ldots)$ depends on attained age a, calendar year y, cumulative 5 year lagged exposure to radon progeny w, and potential further variables (indicated by "…"). It is expressed as the internal baseline mortality rate $r_0\,(a,y,d)$ stratified by age, calendar year and duration of employment, multiplied by an excess relative risk term $ERR(w,\ldots)$. Note that technically an excess relative *rate* is modelled here, which is called excess relative *risk* in the following for simplification purposes. This term varied according to complexity and type of considered models. 95% Wald-type confidence intervals were calculated for the model parameters. All models were fitted for both, the full cohort and the 1960 + sub-cohort. Grouping of the datasets and statistical modelling was performed with the Epicure software.

Parametric models

In the first type of models, age- and time-related effect modification was modelled based on continuous variables. The grouped dataset was additionally cross-classified by cumulative 5 year lagged exposure to radon progeny w in nine categories (0, > 0– < 10, 10– < 50, 50– < 100, 100– < 200, 200– < 500, 500– < 1,000, 1,000– < 1,500, ≥ 1,500 WLM), exposure rate er in six categories (0– < 0.5, 0.5– < 1, 1– < 2, 2– < 4, 4– < 10, ≥ 10 WL), age at median exposure e in nine categories (0–19, 20–24, …, 55 + years), and time since median exposure t in 10 categories (0– < 5, 5– < 10, 10– < 15, …, ≥ 45 years) as in Kreuzer et al. (2018). Age at median exposure and time since median exposure referred to the point in time when one-half of the exposure cumulated up to a given date was reached and thus varied over time. Exposure rate was calculated as the total cumulative exposure (with a lag) divided by the total individual duration of exposure in months up to a given date, and thus represented a time-varying "average" exposure rate. In each cell of the grouped dataset, person-time weighted mean values of cumulative exposure, age at and time since median exposure were calculated and used as continuous variables in the parametric models.

Parametric models of different complexity were fitted:

$$ERR(w) = \beta\, w \qquad \text{(Model 1)}$$

$$ERR(w, e, t) = \beta\, w \times \exp\left[\alpha\,(e - 30) + \varepsilon\,(t - 20)\right] \qquad \text{(Model 2)}$$

$$ERR(w,\, er,\, e,\, t) = \sum\nolimits_{j=1}^{6} \beta_j\, er_j\, w \times \exp\left[\alpha\,(e - 30) + \varepsilon(t - 20)\right] \qquad \text{(Model 3)}$$

In all models, β quantifies the excess relative risk per unit of cumulative exposure to radon progeny w (and is in the following abbreviated with ERR/WLM or, in case of other scaling, with ERR/100 WLM). Model 1 denotes the "simple" linear ERR model. Model 2 contains exponential modifying effects for age at median exposure e (centered at 30 years) and time since median exposure t (centered at 20 years), with choice of centering values for comparability with previous results. Model 3 additionally contains exposure-rate specific estimates β_j for cumulative exposure split based on six categories of exposure rate, these were defined by binary variables er_j for $j = 1,\ldots,6$. The models were selected and compared based on their deviances and likelihood ratio tests, as for example described in Richardson et al. (2022).

BEIR VI exposure-age-concentration model

The BEIR VI exposure-age-concentration model is based on categorical effect-modifying variables. For this model type, the grouped dataset contained cumulative 5 year lagged exposure to radon progeny split into four variables w_{5-14}, w_{15-24}, w_{25-34} and w_{35+}, each with nine categories (0, > 0– < 10, 10– < 50, 50– < 100, 100– < 200, 200– < 500, 500– < 1000, 1000– < 1500, ≥ 1500 WLM), reflecting cumulative exposures received 5–14, 15–24, 25–34 and 35 and more years prior to a considered date, respectively. Exposure rate er was calculated in a similar way as described above, and classified in six categories (0– < 0.5, 0.5– < 1, 1– < 3, 3– < 5, 5– < 15, ≥ 15 WL) as in the pooled BEIR VI study (NRC 1999).

The following model was fitted:

$$ERR(w,\, a,\, er) = \beta\,(\theta_1\, w_{5-14} + \theta_2\, w_{15-24} + \theta_3\, w_{25-34} + \theta_4\, w_{35+})\, \phi_{\text{age}}\, \gamma_{\text{rate}} \qquad \text{(Model 4)}$$

where β represents the ERR/WLM in the reference category, since $\theta_1 = 1$ by definition. Parameters θ_2, θ_3 and θ_4 quantify

effect modification by time since exposure. The parameters ϕ_{age} and γ_{rate} denote effect-modifying factors based on the representation of categorical variables with multiple binary variables and describe effects of categories of attained age (< 55, 55–64, 65–74 and 75 + years) and of exposure rates, respectively.

LEAR calculations

The lifetime excess absolute risk (LEAR) is the difference in lifetime risks for an individual from an exposed population LR_E compared with an individual from an unexposed population LR_0 and is here approximated by

$$LEAR = LR_E - LR_0 \approx \sum_{a=a_{min}}^{a_{max}} r_E(a) S\left(a|a_{min}\right) - \sum_{a=a_{min}}^{a_{max}} r_0(a) S\left(a|a_{min}\right)$$

where $S\left(a|a_{min}\right) = \exp(-\sum_{u=a_{min}}^{a-1} q_0(u))$ is the probability to survive until age a given survival to age a_{min} with all-cause mortality rates $q_0(a)$ at age a. $r_0(a)$ is the baseline lung cancer mortality rate at age a in absence of exposure. Likewise, $r_E(a)$ corresponds to the lung cancer mortality rate at age a under exposure.

For the calculation of LEARs, attained age a_{min} is set to 0 to account for the full lifetime of an individual. The baseline lung cancer mortality rates $r_0(a)$ and all-cause mortality rates $q_0(a)$ are taken from the ICRP Euro-American-Asian mixed population (ICRP 2007) with $a_{max} = 94$. The exposure scenario is 2 WLM from age 18 to 64 with a lag of $L = 5$ years between age at exposure and age at actual risk amplification as used in Tomasek et al (2008). The terms for $ERR(\cdot)$ were chosen as described above. Note that the total LEAR can be obtained by multiplying the value for the LEAR per WLM with 94. All LEAR calculations were performed with the statistical software R (R Core Team 2022).

Interaction of radon and smoking

As in previous analyses (Kreuzer et al. 2018; UNSCEAR 2020; Leuraud et al. 2011), the following geometric mixture model (GMM) was fitted:

$$r(a, y, d, w, s) = r_0(a, y, d) \times [(1 + \beta w) \exp(\gamma s)]^{\lambda} \times [\beta w + \exp(\gamma s)]^{1-\lambda}$$

where γ describes the parameter associated with smoking category s. Depending on the choice of the mixing parameter λ, this model incorporates an additive ($\lambda = 0$) and a multiplicative model ($\lambda = 1$), as well as supra-additive/sub-multiplicative models ($0 < \lambda < 1$) and supra-multiplicative models ($\lambda > 1$). Here, models for a grid of values $0 \le \lambda \le 1.5$ were compared based on the model deviances.

Sensitivity analyses

Sensitivity analyses in the models of the full cohort and the 1960 + sub-cohort considered (1) restriction to duration of employment for at least 5 years and (2) exclusion of open pit miners and millers. Potential confounding in the 1960 + sub-cohort was investigated by adjustment for cumulative exposure to external gamma radiation in mSv in an additive way and for smoking in a multiplicative way (Kreuzer et al. 2018). For sensitivity analyses, grouped datasets contained additional cross-classifications for workplace (four categories), 5 year lagged cumulative exposure to gamma radiation (eight categories) and smoking (three categories, as described above).

Results

Table 1 provides a description of the cohorts. The mean duration of follow-up was 41.7 years and 39.6 years and corresponding person-years at risk 2,461,269 and 1,058,712 in the full cohort and 1960 + sub-cohort, respectively. While in the full cohort 57% of all cohort members were deceased by end of follow-up, this proportion was 25% in the 1960 + sub-cohort. The number of lung cancer deaths in the full cohort is appreciably higher than in the 1960 + sub-cohort (4329 versus 663). Notable is the more than fifteen times higher mean cumulative radon exposure in the full cohort compared to the 1960 + sub-cohort (280 WLM versus 17 WLM). This is mainly due to the extremely high average annual radon exposures in the years of operation before 1960 as illustrated in Appendix Fig. 1.

In Table 2, risk estimates based on parametric models (models 1–3) are given. Using a simple linear model, the ERR/100 WLM is 0.18 (95% CI 0.16; 0.21) in the full cohort and 1.34 (95% CI 0.75; 1.93) in the 1960 + sub-cohort, respectively. There is no overlap in both confidence intervals, indicating heterogeneity. The same holds true when model 2 was applied that takes additionally the two modifiers age at and time since median exposure into account. Model 2 provides a statistically significantly better fit than the simple linear model in both cohorts and is thus preferred. The ERR/WLM decreased with increasing age at median exposure and time since median exposure. Additional consideration of exposure rate in six categories in model 3 provides the best fit in the full cohort and is the finally preferred model for the full cohort, while no improvement of fit was found in the 1960 + sub-cohort, indicating that model 2 is the finally preferred model for the 1960 + sub-cohort. The inclusion of exposure rate has a strong influence on the lung cancer risk due to radon in the full cohort, showing a clear decrease in the ERR/100 WLM with increasing exposure rate, the so-called "inverse exposure-rate effect". Although

Table 1 Description of the full Wismut cohort and the 1960 + sub-cohort of miners first hired in 1960 or later, 1946–2018

Variable	Full cohort	1960 + sub-cohort
Persons, *n*	58,972	26,764
Person-years at risk	2,461,269	1,058,712
Mean duration of employment in years	13.4	10.1
Mean age at death in years	68	58
Mean age at end of follow-up	67	61
Mean duration of follow-up in years	41.7	39.6
Vital status, *n (%)*		
Alive at end of follow-up	23,330 (39.6)	19,457 (72.7)
Deceased	33,794 (57.3)	6719 (25.1)
Lost to follow-up	1848 (3.1)	588 (2.2)
Availability of cause of death, *n (%)*	32,411 (95.9)	6534 (97.2)
Lung cancer deaths, *n*	4329	663
Radon exposed miners, *n (%)*	50,759 (86.1)	22,571 (84.3)
Mean (Max) cumulative exposure in WLM	280 (3224)	17 (334)
Mean (Max) exposure rate[a] in WL	2.95 (26.66)	0.23 (4.65)

WLM working level months

[a]Time-varying average exposure rate, calculated as the total cumulative exposure (without lag) divided by the total individual duration of exposure in months up to a given date

Table 2 Radon-related lung cancer risk estimates according to parametric models applied to the Wismut full cohort and 1960 + sub-cohort

	Parameter	Full cohort	1960 + sub-cohort
Lung cancer deaths		4329	663
Person-years at risk		2,461,269	1,058,712
Model 1			
ERR/100 WLM (95% CI)	β	0.18 (0.16; 0.21)	1.34 (0.75; 1.93)
LEAR per WLM ($\times 10^4$)		**0.82**	**6.09**
Model 2			
ERR/100 WLM[a] (95% CI)	β	0.53 (0.40; 0.66)	4.66 (1.71; 7.62)
Age at median exposure	exp(10α)	0.64 (0.54; 0.76)	0.74 (0.44; 1.26)
Time since median exposure	exp(10ε)	0.53 (0.46; 0.61)	0.47 (0.30; 0.73)
p-value (Model 2 vs. 1)		< 0.001	< 0.001
LEAR per WLM ($\times 10^4$)		**0.79**	**7.13**
Model 3			
ERR/100 WLM (95% CI)			
< 0.5 WL	β_1	2.83 (1.57; 4.09)	5.38 (1.76; 8.99)
0.5–1 WL	β_2	1.58 (0.91; 2.25)	4.66 (1.08; 8.23)
1–2 WL	β_3	1.13 (0.74; 1.52)	2.87 (< 0; 6.02)
2–4 WL	β_4	0.90 (0.63; 1.16)	–
4–10 WL	β_5	0.75 (0.55; 0.96)	–
10 + WL	β_6	0.48 (0.33; 0.63)	–
Age at median exposure	exp(10α)	0.60 (0.51; 0.72)	0.70 (0.41; 1.21)
Time since median exposure	exp(10ε)	0.48 (0.41; 0.55)	0.47 (0.30; 0.74)
p-value (Model 3 vs. 2)		< 0.001	0.417
LEAR per WLM ($\times 10^4$)		**3.62**	**7.83**

Values of LEAR per WLM ($\times 10^4$) (bold)

ERR excess relative risk, *CI* confidence interval, *WLM* working level months, *WL* working level

p-value of likelihood ratio test between two nested models

LEAR lifetime excess absolute risk (exposure of 2 WLM from age 18 to 64 years, maximum age 94 and ICRP Euro-American-Asian mixed population)

Baseline stratified by attained age, calendar year and duration of employment

[a]ERR/100 WLM for age at median exposure of 30 years and time since median exposure of 20 years

not statistically significant, this effect was also indicated in the 1960 + sub-cohort. The use of model 3 reduces heterogeneity between full cohort and 1960 + sub-cohort. The ERR/100 WLM at < 0.5 WL, centred at age at median exposure 30 years and time since median exposure 20 years is 2.83 (95% CI 1.57; 4.09) in the full cohort and 5.38 (95% CI 1.76; 8.99) in the 1960 + sub-cohort; both confidence intervals overlap, but the risk estimates differ by a factor of two. The LEARs per WLM for the finally preferred models are 3.62×10^{-4} (model 3) versus 7.13×10^{-4} (model 2) for the full and the 1960 + sub-cohort, respectively. The corresponding risk predictions for the exposure scenario of 2 WLM per year from age 18 to 64 years are given in Fig. 1.

Table 3 shows the results of the risk analyses using the BEIR VI exposure-age-concentration model (model 4). The ERR/100 WLM at 5–14 years since exposure, < 55 years of attained age and < 0.5 WL exposure rate was 2.50 (95% CI 0.81; 4.18) in the full cohort compared to 6.92 (95% CI < 0; 16.59) in the 1960 + sub-cohort. The ERR/100 WLM decreased with increasing time since exposure, attained age and exposure rate in both cohorts. However, in the full cohort more than 25 years after exposure and more than 65 years of attained age no further decrease in risk was observed. This is also illustrated in Fig. 1. In the 1960 + sub-cohort, the confidence intervals of parameter estimates were very wide and did not indicate statistical significance. The estimated LEAR per WLM was about two times higher in the 1960 + sub-cohort compared to the full cohort with 6.10×10^{-4} and 3.13×10^{-4}, respectively.

Table 4 provides information on the estimated fraction of lung cancer deaths attributable to occupational radon among exposed miners by category of cumulative radon exposure,

Table 3 Radon-related lung cancer risk according to BEIR VI exposure-age-concentration model (model 4) applied to the Wismut full cohort and 1960 + sub-cohort

	Full cohort	1960 + sub-cohort
Lung cancer deaths	4329	663
Person-years at risk	2,461,269	1,058,712
ERR/100 WLM (95% CI)	2.50 (0.81; 4.18)	6.92 (< 0; 16.59)
Time since exposure (years)		
5–14	1.0	1.0
15–24	0.96 (0.47; 1.46)	0.95 (< 0; 2.40)
25–34	0.64 (0.30; 0.97)	0.36 (< 0; 0.92)
35 +	0.61 (0.27; 0.94)	
Attained age (years)		
< 55	1.0	1.0
55–64	0.44 (0.27; 0.70)	0.83 (0.24; 2.84)
65–74	0.33 (0.20; 0.55)	0.34 (0.08; 1.52)
75 +	0.34 (0.19; 0.60)	0.09 (0.01; 5.89)
Exposure rate (WL)		
< 0.5	1.0	1.0
0.5–1.0	0.60 (0.36; 0.99)	0.90 (0.50; 1.64)
1.0–3.0	0.40 (0.26; 0.61)	0.57 (0.20; 1.62)
3.0–5.0	0.34 (0.22; 0.53)	–
5.0–15	0.28 (0.18; 0.44)	–
15 +	0.15 (0.08; 0.26)	–
LEAR per WLM ($\times 10^4$)	**3.13**	**6.10**

Baseline stratified by attained age, calendar year and duration of employment

Values of LEAR per WLM ($\times 10^4$) (bold)

ERR excess relative risk, *CI* confidence interval, *WLM* working level months, *WL* working level, LEAR lifetime excess absolute risk (exposure of 2 WLM from age 18 to 64 years, maximum age 94 and ICRP Euro-American-Asian mixed population)

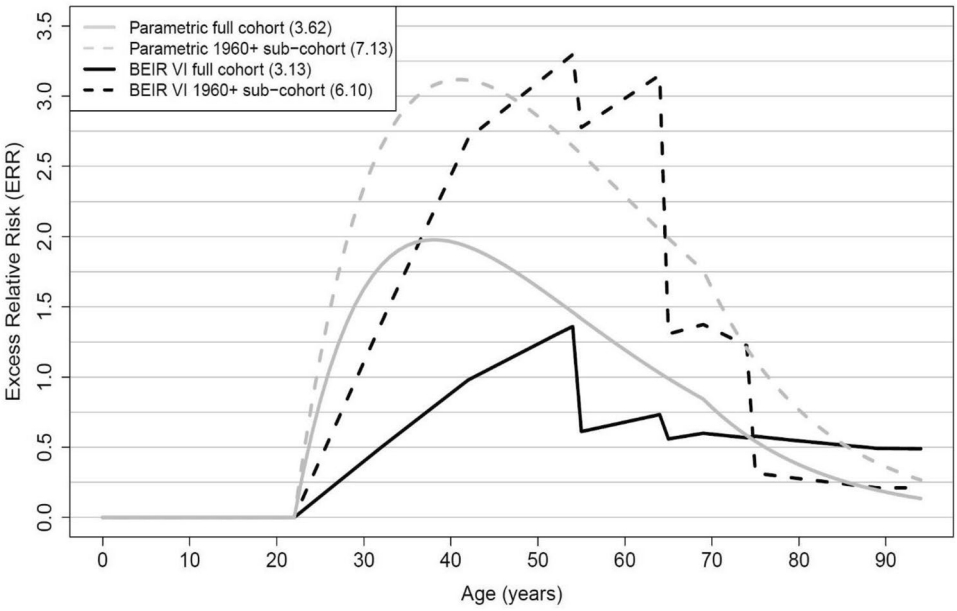

Fig. 1 Excess relative risk predicted for different models in the full cohort and the 1960 + sub-cohort for the exposure scenario of 2 WLM from age 18 to 64 up to age 94 assuming a 5 year lag with corresponding total LEAR in brackets in figure legend (parametric full cohort: model 3, parametric 1960 + sub-cohort: model 2, BEIR VI full cohort and 1960 + sub-cohort: model 4, exposure-age-concentration model)

calendar year of death and attained age based on the BEIR VI model. In the full cohort, a total of 47% of all lung cancer deaths are estimated to be attributable to occupational radon exposure, i.e. 1853 out of 3956 lung cancer deaths could have been avoided without this exposure. In the 1960 + sub-cohort the attributable fraction is 31%. The attributable fraction increases with increasing cumulative radon exposure; for example, in the exposure category 1500 WLM or more 91% of the observed lung cancer deaths are estimated to be attributable to occupational radon. There is a clear decrease of attributable lung cancer deaths with increasing calendar year of death and increasing age in both, the full cohort and the 1960 + sub-cohort, reflecting the decrease in risk with increasing time since exposure and attained age. Importantly, 1 in 4 lung cancer deaths in the full cohort (26%) are still estimated to be attributable to occupational radon exposure and 1 in 5 lung cancer deaths of miners first hired in 1960 or later (19%) (see Appendix Fig. 2).

Some information on smoking is available for 56% of the 1960 + sub-cohort. Among those with known smoking status, 42% were non-/light smokers and 58% moderate/heavy smokers, the corresponding numbers among lung cancer deaths were 10% ($n = 33$), and 90% ($n = 297$), respectively. In a separate analysis among both groups, with the simple linear model, the ERR/100 WLM was 1.77 (95% CI < 0; 5.04) and 1.06 (95% CI 0.28; 1.85) among non-/light and moderate/heavy smokers, respectively. The slightly higher ERR/100 WLM for non/-light smokers compared to moderate/heavy smokers indicates a sub-multiplicative interaction of radon and smoking. The nature of this interaction was investigated in more detail by fitting GMM models for different values of the mixing parameter λ that determines the type of interaction as in Kreuzer et al. (2018). The minimum deviance was achieved for $\lambda = 0.6$, indicating a sub-multiplicative interaction (Fig. 2).

Table 4 Estimated excess lung cancer deaths due to radon exposure according to the BEIR VI exposure-age-concentration model (model 4) applied to the full cohort and 1960 + sub-cohort

Lung cancer deaths	Full cohort			1960 + sub-cohort		
	Excess n[b]	Observed n	Attributable fraction	Excess n[b]	Observed n	Attributable fraction
0 WLM	0	373	–	0	112	–
> 0 WLM[a]	1853	3956	46.8	171	551	31.0
Cum. radon exp. (WLM)						
> 0–10	12	442	2.7	15	179	8.4
10–50	63	442	14.3	75	230	32.6
50–100	59	242	24.4	51	98	52.0
100–500	387	912	42.4	30	44	68.2
500–1000	602	964	62.4	–	–	–
1000–1500	430	623	69.0	–	–	–
1500 +	300	331	90.6	–	–	–
Calendar year of death						
< 1960	8	15	53.3	–	–	–
1960–1970	145	197	73.6	–	–	–
1970–1980	378	577	65.5	5	8	62.5
1980–1990	453	816	55.5	17	29	58.6
1990–2000	432	949	45.5	36	71	50.7
2000–2010	290	838	34.6	65	191	34.0
2010–2018	146	564	25.9	48	252	19.0
Attained age (years)						
< 45	72	113	63.7	14	27	51.9
45–55	309	461	67.0	34	80	42.5
55–65	566	1166	48.5	79	218	24.8
65–75	566	1391	40.7	40	183	21.9
75 +	339	825	41.1	3	43	7.0

WLM working level months

[a]5 year lagged

[b]Small deviations in totals possible due to rounding

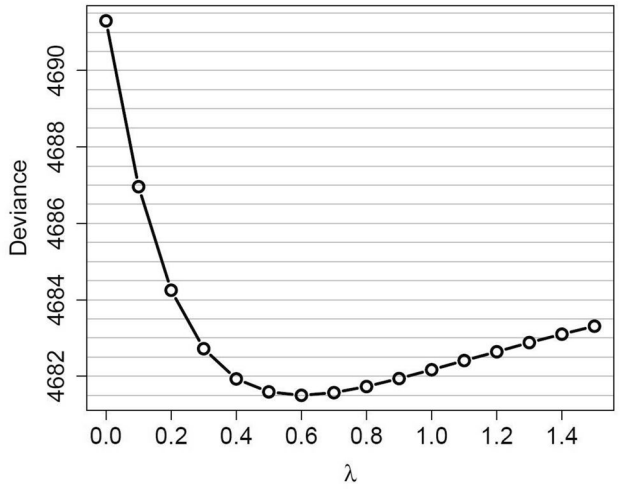

Fig. 2 Deviance obtained when modelling the interaction of radon exposure and smoking related to lung cancer mortality depending on mixing parameter λ, based on geometric mixture models (GMM)

Discussion

The updated findings of the Wismut cohort of uranium miners confirmed the previously observed linear relationship between the relative lung cancer risk and cumulative exposure to radon progeny, which was modified by time since exposure, attained age and exposure rate in the full cohort (Kreuzer et al. 2018). The ERR/WLM decreased with increasing time since exposure, attained age and exposure rate, both for parametric and BEIR VI-type models. For the first time, a statistically significant effect modification of the ERR/WLM by attained age and time since exposure was found in the 1960 + sub-cohort. Notably the ERR/WLM and corresponding LEAR per WLM were about two times higher in the 1960 + sub-cohort compared to the full cohort in models including effect modifiers. For example, when the BEIR VI exposure-age-concentration model was applied, the ERR/100 WLM among miners with attained age < 55 years, time since exposure 5–14 years, and annual exposure rates < 0.5 WL was 2.50 (95% CI 0.81; 4.18) compared to 6.92 (95% CI < 0; 16.59) in the full cohort and in the 1960 + sub-cohort, respectively. The same was true for the parametric model (model 3). Here, the ERR/100 WLM was 2.83 (95% CI 1.57; 4.09) compared to 5.38 (95% CI 1.76; 8.99), respectively, for exposure rates below 0.5 WL, 30 years of age at median exposure and 20 years of time since median exposure.

Comparison with previous Wismut findings

Previous estimates of lung cancer risk in the Wismut cohort had been slightly lower compared to those of the current analyses for both the full cohort and the 1960 + sub-cohort (Kreuzer et al. 2015, 2018). One of the reasons for this is that previously no baseline stratification for duration of employment was applied. Consistent with findings in the PUMA analyses (Kelly-Reif et al. 2023; Richardson et al. 2022) this stratification was added in the current analyses and led also here to an increase in risk estimates. For example, for the BEIR VI model in the full cohort, the reference ERR/100 WLM with and without additional stratification was 2.50 versus 1.62 and the corresponding LEAR per WLM 3.13×10^{-4} versus 2.08×10^{-4}, respectively (see Appendix Table 1). This effect was also present in the 1960 + sub-cohort, here the ERR/100 WLM in the simple linear model was 1.34 (95% CI 0.75; 1.93) versus 0.94 (95% CI 0.51; 1.37) with and without stratification for duration of employment (Appendix Table 2), and the LEAR per WLM in the finally preferred parametric model 2 (including two modifiers) 7.13×10^{-4} and 4.12×10^{-4}, respectively. An explanation for the strong effect of stratification by duration of employment could be the healthy worker survivor effect (Keil et al. 2015), which means that healthy workers are more likely to work for a long time underground and thus accumulate high radon exposures compared to those who have health problems and change their workplace, e.g. from underground to surface or elsewhere. This could artificially lead to lower risks among long-term workers compared to short-term workers. The Wismut cohort is characterized by a wide range of employment durations, around 25% of the cohort members worked for more than 20 years and 13% for more than 30 years in the company.

Due to the young age of the 1960 + sub-cohort, no statistically significant effect modification of the ERR/WLM by attained age or time since exposure has been found previously (Kreuzer et al. 2015, 2018). Such an effect modification was demonstrated in the large PUMA 1960 + sub-cohort (Richardson et al. 2022), and now also in the current extended follow-up until 2018 in the Wismut 1960 + sub-cohort. However, even in the current follow-up there are only 43 lung cancer deaths among radon exposed miners with an age above 75 years (see Table 4), therefore risk estimates for longer times since exposure and higher attained ages involve uncertainties. There is some evidence that exposure rate might be an additional modifier in the 1960 + sub-cohort, although the model including this factor was not statistically significantly better than the model without this factor (Table 2, model 3 vs. model 2).

Differences in risk between full Wismut cohort and 1960 + sub-cohort

There are two to three times higher risk estimates at low exposures and exposure rates in the 1960 + sub-cohort compared to the full cohort, which require further clarification.

Several reasons may account for this. Firstly, uncertainties in the assessment of radon exposure in the early years may have led to an underestimation of the true risk in the full cohort. The job-exposure matrix was based on expert rating rather than measurements in the early years of mining in the Wismut company, thus bias due to exposure measurement error is of concern. In some uranium miners cohort studies risk estimates were higher when focussing on miners in more recent years compared to earlier years (Tomasek et al. 2008; UNSCEAR 2020; Lane et al. 2019). This fact has sometimes been attributed to lower quality of exposure assessment and a potentially higher impact of measurement error on the risk estimation in the early years. Currently, a research project (Küchenhoff et al. 2018; Ellenbach et al. 2023) is running to investigate sources, magnitude and potential effects of exposure measurement error in the Wismut cohort. Similar investigations have been performed in the Colorado Plateau (Stram et al. 1999), Ontario (Navaranjan et al. 2019) or French (Hoffmann et al. 2017) cohort of uranium miners.

Secondly, the mortality follow-up was rather incomplete in the early years. For example, the proportion of loss to follow-up was 10% versus 2% for those with end of employment before 1960 or later, respectively; this was mainly because the persons could no more be identified by the registration offices under the last known address from the 1950s. The proportion of missing causes of death before 1970 was 44% compared with 3.5% later; the main reason was that copies of death certificates from before 1970 were often no more available. For the early years in the full cohort, the incomplete mortality follow-up concerned particularly miners with young age at death and short time of follow-up—the factors associated with the highest risk. Thirdly, in the early mining years, exposures to both silica dust and radon were extremely high, therefore the risk of lung cancer may be underestimated in the full cohort due to the competing risk of dying from silicosis (e.g. a total of 1,067 miners died from silicosis as underlying cause of death in the full cohort, in contrast to only 11 silicosis deaths in the 1960 + sub-cohort).

Another reason for differences in risk estimates between the full and 1960 + sub-cohort could be overestimation of risk in the 1960 + sub-cohort. Time since exposure turned out to be a strong modifier in most studies of miners, showing that the ERR/WLM is highest 5–15 years after exposure and decreases with increasing time since exposure (NRC 1999; UNSCEAR 2009, 2020). In the 1960 + sub-cohort, the duration of follow-up is shorter than for miners hired prior to 1960. In addition, average age is appreciably younger (Table 1). Consequently, the decrease in risk with increasing time since exposure and attained age cannot be completely described by the data of the 1960 + sub-cohort. This is illustrated in the 1960 + sub-cohort when risk estimates from the BEIR VI model are compared for end of follow-up by 2013 and 2018. In analyses with end of follow-up in 2013 an increase in risk is observed in age category 75 + years (Appendix Table 3), which is also seen in risk predictions in Appendix Fig. 4. These findings indicate that the higher LEAR per WLM of 9.22×10^{-4} in analyses based on data with end of follow-up in 2013 compared to 6.10×10^{-4} with end of follow-up in 2018 (Appendix Table 3), resulted from a lack of decrease in risk after 75 years of age.

Comparison with PUMA findings

The PUMA study includes seven uranium cohorts of miners from Europe and North America, among them the Wismut cohort with mortality follow-up by end of 2013 excluding millers (Rage et al. 2020; Richardson et al. 2021). Two papers on the lung cancer risk by radon have been published by now, one on the full cohort (Kelly-Reif et al. 2023) and one on the 1960 + sub-cohort (Richardson et al. 2022). In the full PUMA cohort, a reference ERR/100 WLM of 4.68 (95% CI 2.88; 6.96) was observed for the BEIR VI exposure-age-concentration model (Kelly-Reif et al. 2023). However, a statistically significant heterogeneity between cohorts was present, which was in part attributable to the comparably lower risk in the full Wismut cohort, which forms about half of the PUMA cohort. The PUMA 1960 + sub-cohort did not show such heterogeneity between study cohorts, here the corresponding reference ERR/100 WLM was 6.98 (95% CI 1.97; 16.15) (Richardson et al. 2022), which is consistent to the estimates of the updated Wismut 1960 + sub-cohort of 6.92 (95% CI < 0, 16.59), of the pooled 11 miners study of 7.68 (NRC 1999) and others (Lane et al. 2010, 2019). Lifetime risk calculations for lung cancer and radon within PUMA are planned by the PUMA consortium in a separate paper.

Interaction of radon and smoking

The present analysis indicated a sub-multiplicative interaction of radon and smoking in the 1960 + sub-cohort via GMM modelling. This finding is supported by the results of a simple linear model separately for both smoking groups, here the ERR/100 WLM in non-/light smokers was slightly higher compared to moderate/heavy smokers (1.77 versus 1.06). Previous analyses based on the last Wismut follow-up (Kreuzer et al. 2018) also found higher ERR/100 WLM among non-/light smokers compared to moderate/heavy smokers (2.0 versus 1.2), however at that time GMM modelling indicated rather a multiplicative to supra-multiplicative interaction. Statistical uncertainty due to a small number of lung cancer deaths among non-/light smokers ($n = 33$) is still of concern. Further follow-up may bring more insights into the interaction of radon and smoking. A sub-multiplicative interaction is compatible with the findings from most other miner studies, while in residential radon studies, no obvious

deviation from a multiplicative interaction has been consistently observed (UNSCEAR 2020).

Strengths and weaknesses of the study

The Wismut cohort is unique due to its large size, long follow-up period from 1946 to 2018, wide range of exposures and availability of individual data not only on radon exposure, but also on silica dust, long-lived radionuclides and external gamma radiation as well as in the 1960 + sub-cohort in part on rough data on smoking. Detailed investigation of potential confounding of the radon-related lung cancer risk by these factors have been performed previously in the full cohort (Walsh et al. 2010) and in a nested case–control study on lung cancer with smoking data (Schnelzer et al. 2010). Overall, none of the above-mentioned variables led to major confounding, except for silica dust, here a 25% decrease in lung cancer risk estimates was observed after including silica dust in the risk model (Walsh et al. 2010). In the 1960 + sub-cohort, confounding could be even more relevant due to the lower occupational radon exposure and thus smaller radon-related lung cancer risk. As shown in Appendix Table 2 additional adjustment for smoking and external gamma radiation in model 2 resulted in slight decreases in the risk estimates and thus no major confounding. The mean cumulative occupational silica dust exposure was 1.0 mg/m^3-years in the 1960 + sub-cohort in contrast to 6 mg/m^3-years in the full cohort or even 12 mg/m^3-years among miners first hired between 1946 and 1954, and is thus far below the threshold of 10 mg/m^3, above which a silica dust related lung cancer risk was observed in the full Wismut cohort (Sogl et al. 2012).

The Wismut study includes next to underground and surface workers also millers and open pit miners, which differ by working conditions and are characterised by very low radon exposures. Exclusion of millers and open pit miners did not lead to a major change in risk, as shown in the sensitivity analysis presented in Appendix Table 1. Short-term workers (< 5 years of duration of employment) may differ in risk from long-term workers, as reflected by the healthy worker survivor effect. In addition to baseline stratification by duration of employment, excluding this group in sensitivity analyses showed virtually no change in risk (Appendix Tables 1 and 2). Exposure measurement error in the early years is an issue, as noted above, and the potential influence on risk is currently investigated.

Conclusion

The updated Wismut cohort study shows an increased lung cancer risk by radon for former miners even 20 to 30 years after the mines were closed and occupational radon exposures ended. The estimated lifetime excess absolute risk (LEAR per WLM) to die from lung cancer per unit of cumulative radon exposure in WLM varies between 3 and 7×10^{-4} depending on model and (sub-) cohort, i.e. among 100 people with a cumulative occupational radon exposure of 100 WLM between 3 and 7 additional (excess) lung cancer deaths would occur due to this exposure during lifetime. The 1960 + sub-cohort is characterized by low protracted radon exposure of high quality and provides now, through the extension of follow-up to end of 2018, a good basis for the estimation of lung cancer risks at low radon exposures and low exposure rates. Risk estimates from the 1960 + sub-cohort are consistent with those from 1960 + sub-cohorts of large pooled studies. The Wismut 1960 + sub-cohort is thus preferred to the full Wismut cohort in order to estimate lung cancer risks at low protracted exposure rates for more contemporary miners, although the statistical power is lower than in the full cohort. Further follow-up of the Wismut 1960 + sub-cohort and pooled analyses of updated individual cohorts of PUMA will increase precision, particularly for attained ages above 75 years and longer times since exposure, this will lead to a better understanding of the lung cancer risk at low radon exposures and exposure rates.

Supplementary Information The online version contains supplementary material available at https://doi.org/10.1007/s00411-023-01043-2.

Author contributions M.K. and N.F. wrote the main manuscript and M.S. did the statistical analyses and prepared the figures. All authors reviewed the manuscript.

Funding Open Access funding enabled and organized by Projekt DEAL.

Data availability Access to the data can be obtained after a positive evaluation of the proposal by the Steering Committee on the German Uranium Mining Studies of the German Radiation Protection Commission (SSK) and the German Federal Office for Radiation Protection (BfS). The procedure of opening of the Wismut data to external researchers is described here: https://www.bfs.de/EN/bfs/science-research/projects/wismut/wismut-cohort-proposals.html.

Declarations

Competing interests The authors have no relevant financial or non-financial interests to disclose.

References

Ellenbach N, Rehms R, Hoffmann S (2023) Ermittlung der Unsicherheiten der Strahlenexpositionsabschätzung in der Wismut-Kohorte—Teil II / Determination of uncertainties of radiation exposure assessment in the Wismut cohort Part II in Ressortforschungsberichte zum Strahlenschutz. Bundesamt für Strahlenschutz/Federal Office for Radiation Protection, Germany

Harrison JD (2021) Lung cancer risk and effective dose coefficients for radon: UNSCEAR review and ICRP conclusions. J Radiol Prot. https://doi.org/10.1088/1361-6498/abf547

Harrison JD, Marsh JW (2020) ICRP recommendations on radon. Ann ICRP 49:68–76

Hoffmann S, Rage E, Laurier D, Laroche P, Guihenneuc C, Ancelet S (2017) Accounting for Berkson and Classical measurement error in radon exposure using a Bayesian structural approach in the analysis of lung cancer mortality in the French cohort of uranium miners. Radiat Res 187(2):196–209

HVBG, BBG (2005) Belastung durch ionisierende Strahlung, Staub und Arsen im Uranerzbergbau der ehemaligen DDR (Version 08/2005). Gera Bergbau BG (BBG), St. Augustin: Hauptverband der gewerblichen Berufsgenossenschaften (HVBG).

ICRP (2007) The 2007 recommendations of the International Commission on Radiological Protection. ICRP publication 103. Ann ICRP 37:2–4

Keil AP, Richardson DB, Troester MA (2015) Healthy worker survivor bias in the Colorado Plateau uranium miners cohort. Am J Epidemiol 181(10):762–770

Kelly-Reif K, Bertke S, Rage E, Demers PA, Fenske N, Deffner V, Kreuzer M, Samet JM, Schubauer-Berigan MK, Tomasek L, Zablotska LB, Wiggins C, Laurier D, Richardson DB (2023) Radon and lung cancer in the Pooled Uranium Miners Analysis (PUMA): highly-exposed early miners and all miners. Occup Environ Med 80:385–391

Kreuzer M, Schnelzer M, Tschense A, Walsh L, Grosche B (2010) Cohort profile: the German uranium miners cohort study (WISMUT cohort), 1946–2003. Int J Epidemiol 39:980–987

Kreuzer M, Fenske N, Schnelzer M, Walsh L (2015) Lung cancer risk at low radon exposure rates in German uranium miners. Br J Cancer 113:1367–1369

Kreuzer M, Sobotzki C, Schnelzer M, Fenske N (2018) Factors modifying the radon-related lung cancer risk at low exposures and exposure rates among German uranium miners. Radiat Res 189:165–176

Küchenhoff H, Deffner V, Aßenmacher M, Neppl H, Kaiser C, Güthlin D (2018) Ermittlung der Unsicherheiten der Strahlenexpositionsabschätzung in der Wismut-Kohorte—Teil I / Determination of uncertainties of radiation exposure assessment in the Wismut cohort part I in Ressortforschungsberichte zum Strahlenschutz. Bundesamt für Strahlenschutz/Federal Office for Radiation Protection, Germany

Lane RS, Frost SE, Howe GR, Zablotska LB (2010) Mortality (1950–1999) and cancer incidence (1969–1999) in the cohort of Eldorado uranium workers. Radiat Res 174:773–785

Lane RS, Tomášek L, Zablotska LB, Rage E, Momoli F, Little J (2019) Low radon exposures and lung cancer risk: joint analysis of the Czech, French, and Beaverlodge cohorts of uranium miners. Int Arch Occup Environ Health 92:747–762

Laurier D, Marsh JW, Rage E, Tomasek L (2020) Miner studies and radiological protection against radon. Ann ICRP 49:57–67

Leuraud K, Schnelzer M, Tomasek L, Hunter N, Tirmarche M, Grosche B, Kreuzer M, Laurier D (2011) Radon, smoking and lung cancer risk: results of a joint analysis of three European case-control studies among uranium miners. Radiat Res 176(3):375–387

Marsh JW, Tomasek L, Laurier D, Harrison JD (2021) Effective dose coefficients for radon and progeny: a review of ICRP and UNSCEAR values. Radiat Prot Dosimetry 195:1–20

Navaranjan G, Chambers D, Thompson PA, Do M, Berriault C, Villeneuve PJ, Demers PA (2019) Uncertainties associated with assessing Ontario uranium miners' exposure to radon daughters. J Radiol Prot 39(1):136–149

NRC (1999) Health effects of exposure to radon - BEIR VI report (Committee on Health Risks of Exposure to Radon, Board on Radiation Effects Research). National Academy Press, Washington

R Core Team (2022) R: a language and environment for statistical computing. R Foundation for Statistical Computing, Vienna

Rage E, Richardson DB, Demers PA, Do M, Fenske N, Kreuzer M, Samet J, Wiggins C, Schubauer-Berigan MK, Kelly-Reif K, Tomasek L, Zablotska LB, Laurier D (2020) PUMA—pooled uranium miners analysis: cohort profile. Occup Environ Med 77(3):194–200

Richardson DB, Rage E, Demers PA, Do MT, DeBono N, Fenske N, Deffner V, Kreuzer M, Samet J, Wiggins C, Schubauer-Berigan MK, Kelly-Reif K, Tomasek L, Zablotska LB, Laurier D (2021) Mortality among uranium miners in North America and Europe: the Pooled Uranium Miners Analysis (PUMA). Int J Epidemiol 50:633–643

Richardson DB, Rage E, Demers PA, Do MT, Fenske N, Deffner V, Kreuzer M, Samet J, Bertke SJ, Kelly-Reif K, Schubauer-Berigan MK, Tomasek L, Zablotska LB, Wiggins C, Laurier D (2022) Lung cancer and radon: pooled analysis of uranium miners hired in 1960 or later. Environ Health Perspect 130:57010

Schnelzer M, Hammer GP, Kreuzer M, Tschense A, Grosche B (2010) Accounting for smoking in the radon-related lung cancer risk among German uranium miners: results of a nested case-control study. Health Phys 98(1):20–28

Sogl M, Taeger D, Pallapies D, Brüning T, Dufey F, Schnelzer M, Straif K, Walsh L, Kreuzer M (2012) Quantitative relationship between silica exposure and lung cancer mortality in German uranium miners, 1946–2003. Br J Cancer 07:1188–1194

Stram DO, Langholz B, Huberman M, Thomas DC (1999) Correcting for exposure measurement error in a reanalysis of lung cancer mortality for the Colorado Plateau Uranium Miners cohort. Health Phys 77(3):265–275

Tirmarche M, Harrison JD, Laurier D, Paquet F, Blanchardon E, Marsh JW (2010) ICRP publication 115. Lung cancer risk from radon and progeny and statement on radon. Ann ICRP 40:1–64

Tomasek L, Rogel A, Tirmarche M, Mitton N, Laurier D (2008) Lung cancer in French and Czech uranium miners: radon-associated risk at low exposures and modifying effects of time since exposure and age at exposure. Radiat Res 169:125–137

UNSCEAR (2009) Effects of ionizing radiation. United Nations Scientific Committee on the Effects of Atomic Radiation. UNSCEAR 2006 Report Volume II, annex E. Sources-to-effects assessment for radon in homes and workplaces. United Nations, New York

UNSCEAR (2020) UNSCEAR 2019 Report, Annex B, Lung cancer from exposure to radon. Report of the United Nations Scientific Committee on the Effects of Atomic Radiation. United Nations, New York

Walsh L, Tschense A, Schnelzer M, Dufey F, Grosche B, Kreuzer M (2010) The influence of radon exposures on lung cancer mortality in German uranium miners, 1946–2003. Radiat Res 173:79–90

10. Lifetime risks for lung cancer due to occupational radon exposure: a systematic analysis of estimation components

Contributing publication

Sommer, M., Heinzl, F., Scholz-Kreisel, P., Wollschläger, D., Heumannn, C., & Fenske, N. (2025). Lifetime risks for lung cancer due to occupational radon exposure: A systematic analysis of estimation components. *Radiation Research* 203(3), 175-187. https://doi.org/10.1667/RADE-24-00060.1

Declaration of contributions

I, Manuel Sommer, wrote the main manuscript and carried out and contributed the following work for the publication:

- **Statistical analysis**
  - Data collection and preparation (WHO mortality database)
  - Statistical analysis from concept to execution in *R*, accompanied by discussions on methodology with Nora Fenske, Felix Heinzl, and Christian Heumann
  - Conception and preparation of figures and tables
- **Writing**
  - Conception and writing of the manuscript
  - Literature screening with support from Nora Fenske, Felix Heinzl, and Peter Scholz-Kreisel
  - Review of manuscript (together with all other authors)

RADIATION RESEARCH **203**, 175–187 (2025)
0033-7587/25 $15.00

DOI: 10.1667/RADE-24-00060.1

Lifetime Risks for Lung Cancer due to Occupational Radon Exposure: A Systematic Analysis of Estimation Components

M. Sommer,[a,1] F. Heinzl,[a] P. Scholz-Kreisel,[a] D. Wollschläger,[b] C. Heumann,[c] N. Fenske[a]

[a] Federal Office for Radiation Protection, Ingolstädter Landstrasse 1, 85764 Neuherberg, Germany; [b] Institute of Medical Biostatistics, Epidemiology and Informatics University Medical Center Mainz, Langenbeckstrasse 1, 55131 Mainz, Germany; [c] Department of Statistics, LMU Munich, Ludwigstrasse 33, 80539 Munich, Germany

Sommer M, Heinzl F, Scholz-Kreisel P, Wollschläger D, Heumann C, Fenske N. Lifetime Risks for Lung Cancer due to Occupational Radon Exposure: A Systematic Analysis of Estimation Components. Radiat Res. 203, 175–187 (2025).

Lifetime risk estimates play a key role in many areas of radiation research. Here, the focus is on the lifetime excess absolute risk (LEAR) for dying from lung cancer due to occupational radon exposure based on uranium miners cohort studies. The major components in estimating LEAR were systematically varied to investigate the variability and uncertainties of results. Major components of the LEAR calculation are baseline mortality rates for lung cancer and all causes of death, risk model and exposure scenario. Sex-averaged mortality rates were chosen from a mixed Euro-American-Asian population, in addition to mortality rates to represent heavy and light smokers. Seven radon-related lung cancer risk models derived from different uranium miners cohorts were compared. As exposure scenarios, occupational exposure of two working level months (WLM) from age 18–64 years was considered, and three scenarios from the German uranium miners cohort. Further components were modified in sensitivity analyses. The LEAR was compared to other lifetime risk measures. With a range from less than 0.6×10^{-4} to over 8.0×10^{-4}, LEAR per WLM estimates were influenced heavily by the choice of risk models. Notably, mortality rates, particularly lung cancer mortality rates, had a strong impact on LEAR per WLM across all models. The LEAR per WLM exhibited only low variation to changes in exposure scenarios for all risk models, except for the BEIR VI model fitted on the pooled 11 miners study. All assessed lifetime risk measures displayed a monotonically increasing relationship between exposure and lifetime risk at low to moderate exposures, with minor differences between ELR, REID, and LEAR (all per WLM). RADS yields the largest lifetime risk estimates in most situations. There is substantial variation in LEAR per WLM estimates depending on the choice of underlying calculation components. Reference populations and mortality rates should be selected with care depending on the application of lifetime risk calculations. The explicit choice of the lifetime risk measure was found to be negligible. These findings should be taken into consideration when using lifetime risk measures for radiation protection policy purposes.

[1] Corresponding author: M. Sommer, Federal Office for Radiation Protection, Ingolstädter Landstrasse 1, 85764 Neuherberg, Germany; email: MSommer@bfs.de.

INTRODUCTION

Lifetime risk measures reflect the probability of developing (or dying from) a specific disease of interest over a lifetime. Lifetime risk measures are highly relevant for different areas of radiation research to quantify the lifetime excess risk due to radiation exposure. For example, they are part of the detriment calculation (*1*) with the calculation of nominal risks or the epidemiological approach for radon dose conversion (*2–4*). Here, lung cancer related to occupational radon exposure will be considered. The calculation of (excess) lifetime risks is typically based on one specific combination of calculation components, and in the final estimate, no uncertainties are reflected. The objective of this analysis was to vary the components of the lifetime risk calculation systematically to assess their impacts on the lifetime risk estimate. Therefore, this exploratory analysis contributes to quantifying uncertainties and sensitivities in the lifetime risk of lung cancer related to radon exposure.

Radon exposure is one of the most important causes of lung cancer aside from smoking (*5*). This was demonstrated in uranium miners and residential radon studies (*6–8*). Uranium miners studies have shown a linear relationship between occupational radon exposure and excess lung cancer mortality risk which is modified by age, time since exposure and exposure rate. The risk models are complex and differ between studies. Risk model parameter estimates between cohorts are therefore difficult or even impossible to compare. Lifetime risk measures provide a possibility for comparison and interpretation. Hence, such measures can also contribute to clearer and more comprehensible risk communication.

Different measures for excess lifetime risks include lifetime excess absolute risk (LEAR), risk of exposure-induced death (REID) and excess lifetime risk (ELR) (*9*, *10*). Tomasek et al. (*11*) calculated the LEAR of dying from lung cancer due to radon exposure for different risk models, among them an updated risk projection model for the pooled Czech and

French cohort of uranium miners. These updated lifetime risk calculations were considered in the epidemiological approach for radon dose conversion by ICRP (*4*). ICRP eventually recommended new factors for radon dose conversion (*1*). Even if the ICRP now recommends the dosimetric approach, the epidemiological approach using the LEAR is still relevant for comparison purposes (*4*, *12*).

Understanding the importance and consequences of necessary choices when implementing lifetime risk calculations requires elaborating on the sensitivity of the lifetime risk concept and its underlying calculation components. For example, Hunter et al. (*13*) performed a thorough sensitivity analysis on the REID for U.S. mortality rates focusing on effects of risk models from studies of occupational and residential radon exposure and differences in sex and smoking behavior. Chen et al. (*14*) conducted a sensitivity analysis for indoor radon for the Canadian population. A comparison of LEAR, ELR and REID for a linear risk model can be found in Kellerer et al. (*9*). Ulanowski et al. (*15*) introduced radiation-attributed decrease of survival (RADS) as another lifetime risk measure aimed to be less sensitive to the choice of background rates. Besides sensitivity analyses, uncertainties in lifetime risks have been investigated and quantified only rarely (*16*, *17*). Existing literature on sensitivity analysis of lifetime risks often focuses on a subset of components and selected lifetime risk measures. This highlights a research gap for structured sensitivity analyses incorporating all calculation components and a likewise structured comparison between lifetime risk measures, especially for lung cancer related to radon.

We contribute to this by systematically varying (excess) lifetime risk calculation components and quantifying their impact on the corresponding lifetime risk measure. In particular, we consider different risk models, and multiple heterogeneous exposure scenarios and construct different sex-averaged reference populations to account for a variety of situations and individuals, specifically for lung cancer related to occupational radon exposure. Focusing on the LEAR, we also compare results to ELR, REID and RADS. Further methodological issues are considered and discussed.

METHODS

Lifetime Risk Definition

There are various definitions for excess lifetime risks (*10*, *15*). All considered definitions emerge from the difference between risk under exposure and the baseline risk without exposure. Here we focus on the lifetime excess absolute risk (LEAR), sometimes also referred to as lifetime attributable risk (LAR), e.g. (*9*). The LEAR is defined as

$$LEAR_E(a) = LR_E(a) - LR_0(a) = \int_a^\infty (r_E(t) - r_0(t))S(t|a)\ dt = \int_a^\infty r_0(t)ERR(t)S(t\,|\,a)\ dt \quad (1)$$

with lifetime risk of dying from a specific disease of interest (here: lung cancer) under exposure $LR_E(a) = \int_a^\infty r_E(t)S(t|a)\ dt$, baseline lifetime risk $LR_0(a) = \int_a^\infty r_E(t)S(t|a)\ dt$, minimum age at risk a, baseline lung cancer mortality rates $r_0(t)$ and lung cancer mortality rates under exposure $r_E(t)$ at age t. $S(t\,|\,a)$ is the conditional survival function with $S(t\,|\,a) := P(T \geq t\,|\,T \geq a)$ and $T \geq 0$ the unknown random retention time until death. $S(t\,|\,a)$ describes the probability to survive until age t given the survival to age a. We set $S(t) := S(t\,|\,0) = P(T \geq t)$ and model the survival function as $S(t) = e^{-\int_0^t q_0(u)du}$ with baseline mortality rates for all causes of death $q_0(t)$. $ERR(t)$ denotes the excess relative risk at age t. In Eq. (1), the following risk projection model is assumed:

$$r_E(t) = r_0(t)(1 + ERR(t)). \quad (2)$$

Established risk models for lung cancer from radon exposure follow such an ERR structure (*8*, *18*). The $ERR(t)$ depends not only on age t but on further variables such as cumulative lagged exposure to radon progeny, time since exposure or exposure rate. The exact composition and complexity of the $ERR(t)$ depends on the specific risk model.

Lifetime Risk Calculation and Choice of Components

In the computation of LEAR, we distinguish between major and minor components. Minor components are defined with limited freedom of choice or possess minimal influence on the resulting LEAR. Major components, on the other hand, necessitate further decision-making because they are less constrained, and their choice is consequential.

The $LEAR_E(a)$ relies on three major components: mortality rates, risk models, and exposure scenarios. The first component encompasses mortality rates for lung cancer $r_0(t)$ and all-cause mortality rates $q_0(t)$, at each age t. The relative risk projection model shapes $ERR(t)$ at each age. The exposure scenario involves yearly exposure to radon progeny in working level months (WLM) and has an impact on $ERR(t)$ for every age t. Minor components include minimum age at risk a, maximum age a_{max}, minimum latency time L between exposure and risk amplification, and the chosen approximation approach for the survival function $S(t)$.

The LEAR is subsequently estimated and calculated through the following approximation:

$$LEAR_E(a) \approx \sum_{t=a}^{a_{max}} r_0(t)ERR(t)\widetilde{S}(t\,|\,a), \quad (3)$$

where the approximation $\widetilde{S}(t\,|\,a) = e^{-\sum_{u=a}^{t-1} q_0(u)}$ is utilized for the survival function $S(t\,|\,a)$. This approximation is based on the Nelson-Aalen estimator of the cumulative hazard rate (*19*).

The minimum age at risk a was set to $a = 0$ to account for the full lifetime of an individual. The maximum age a_{max} was set to $a_{max} = 94$ for comparability to previous studies (*20*). For readability, we write $LEAR = LEAR_E(0)$. For the latency period L between exposure to radon progeny and death from lung cancer, the cumulative exposures were lagged by $L = 5$ years since all considered risk projection models also assume $L = 5$. LEAR estimates were computed and compared for different combinations of major calculation components: three sex-averaged reference populations, seven risk models and four exposure scenarios, resulting in $3 \times 7 \times 4 = 84$ distinct LEAR estimates. Besides the total LEAR, the LEAR per WLM (LEAR/WLM) is considered, defined as the LEAR divided by total cumulative exposure accrued over the entire exposure scenario in WLM. All statistical or numerical analyses were conducted with the statistical software R (*21*).

Mortality Rates

The following sex-averaged mortality rates were chosen: ICRP reference rates reflecting a mixed Euro-American-Asian population derived from population data from the years 1993–1997 (*3*, *22*); rates from Greece 2018, the Netherlands 2018 and Norway 2016 based on population data provided by the WHO Mortality Database (*23*) reflecting a heavy smoker reference population; and rates from Costa Rica 2019, USA 2019 and Sweden 2016 reflecting a light smoker population. The country selection was based on smoking behavior following the OECD Health Statistics (*24*) on tobacco consumption (percentage of the population aged 15+ who are daily smokers) from the year 2000 to account for a latency of around 20 years between smoking and the

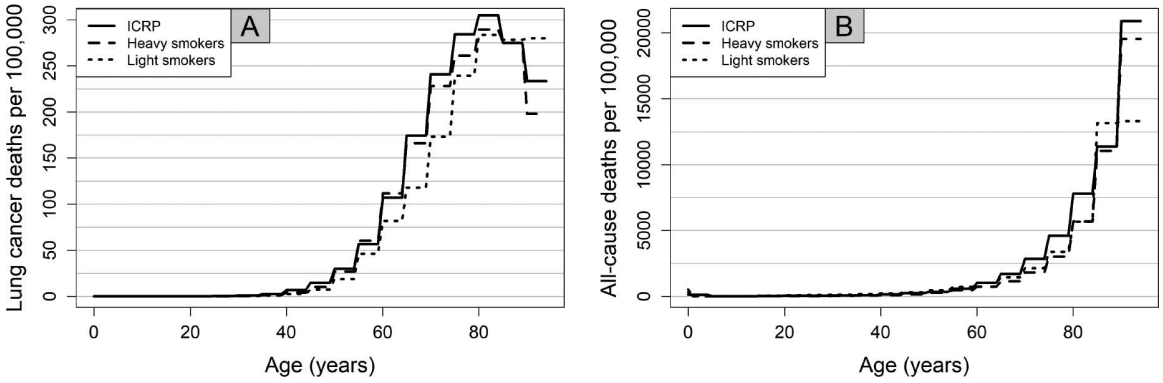

FIG. 1. Lung cancer deaths (panel A) and all-cause deaths (panel B) per 100,000 persons by age in the sex-averaged ICRP reference population (*3*) and in the constructed reference populations for heavy and light smokers.

development of lung cancer. This latency time was chosen based on several studies (*25–27*). The three countries with the highest percentage of daily smokers aged 15 and older (32–35%) were chosen to represent the heavy smoker population, while the three countries with the lowest percentage of daily smokers (12–19%) were chosen to represent the light smoker population. Further, the countries were chosen with the objective to employ complete and recent data.

The rates of heavy and light smokers were constructed by aggregating death cases d_i and population sizes n_i from different countries and sexes, where $i = 1, \ldots, N$ indexes both the country and sex for every age:

$$m = \frac{\sum_{i=1}^{N} d_i}{\sum_{i=1}^{N} n_i}. \tag{4}$$

If d corresponds to lung cancer deaths at age t, this yields the baseline rate $m = r_0(t)$, and if d denotes all-cause death counts at age t, $m = q_0(t)$. The full derivation of Eq. (4) is shown in the Supplementary Materials, Section A (https://doi.org/10.1667/RADE-24-00060.1.S1).[2]

Figure 1 shows the difference in lung cancer deaths (panel A) and all-cause deaths (panel B) per 100,000 persons for all three sex-averaged reference populations (exact numerical values in the Supplementary Table S1; https://doi.org/10.1667/RADE-24-00060.1.S1). Population data is given in 5-year age intervals. Light smoker and heavy smoker populations are similar in all-cause deaths per 100,000, with visible differences only at ages 85+. The ICRP reference population shows considerably more all-cause deaths per 100,000 compared to the smoker populations until age 85. There are notably more lung cancer deaths per 100,000 for heavy smokers than for light smokers (as expected). However, at ages 85+ heavy smoker lung cancer deaths per 100,000 decreased whereas for light smokers, they stayed approximately constant. The ICRP reference population yields relatively many lung cancer deaths, comparable to the heavy smoker population.

Unless explicitly stated otherwise, all lifetime risk estimates are calculated with mean mortality rates for males and females (sex-averaged mortality rates). Lifetime risks with male-specific mortality rates are analyzed in Supplementary Materials, Section B (https://doi.org/10.1667/RADE-24-00060.1.S1).

Risk Models and Cohorts

The LEAR calculation is based on a risk projection model and data from a cohort study, on which the risk model was fitted. Established risk models for lung cancer due to radon exposure in uranium miners cohort studies are based on the general structure in Eq. (2) and are fitted with internal (or sometimes also external) Poisson regression on grouped data. The preferred risk model contains a linear relationship between cumulative occupational radon exposure in WLM and excess relative risk of lung cancer, which is additionally modified by time since exposure, attained age or age at exposure, and in some cases also exposure rate (*8*). Recently, more focus has been given to more recent periods with low-radon exposures or exposure rates ("sub-cohorts 1960+") (*28–30*).

Here, the considered risk models are the categorical BEIR VI exposure-age-concentration model fitted on the pooled 11 miners cohort (BEIR VI model) (*6*) as well as on the Pooled Uranium Miners Analysis (PUMA) cohort (PUMA model) (*18*, *28*), the adjusted Jacobi model fitted on six cohort studies (*2*, *31*), and parametric risk models fitted on the German Wismut cohort (*7*) as well as on the Joint Czech and French miners cohort (*32*).

These models were selected for the following reasons. The initial factors for radon dose conversion were computed using the Jacobi model (*2*). The Joint Czech and French risk model, along with the BEIR VI model fitted to the pooled 11 miners cohort, contributed to a novel radon dose conversion proposal by ICRP (*4*). The German Wismut cohort is the world's largest single cohort of uranium miners. Notably, this extensive cohort was not included for the BEIR VI risk model (as the cohort was only established later). Suitable parametric models are used for both the Wismut 1960+ sub-cohort and full cohort, containing a continuous exposure rate effect for the full cohort that contrasts with the categorical exposure rate considerations in the BEIR VI and PUMA models. Note that we deliberately included Wismut models from the follow-up period 1946–2013 (*7*) rather than from the latest follow-up 1946–2018 (*29*) to ensure a broader variety of risk model structures for sensitivity analyses. While the more recent models offer slightly more precise estimates, such as by additionally stratifying the baseline by duration of employment, they are structurally similar to the other models compared here and do not contribute to the diversity of our model selection. The PUMA study is the largest uranium miners cohort worldwide, encompassing twice as many uranium miners and roughly three times as many lung cancer deaths (*33*) as the pooled 11 miners cohort (*6*). In particular, it includes the German Wismut cohort.

The generic categorical BEIR VI exposure-age-concentration model at age t reads

$$ERR(t) = \beta(W_{5-14}(t) + \theta_{15-24} W_{15-24}(t) + \theta_{25+} W_{25+}(t))\phi_{age}\gamma_z, \tag{5}$$

where W_{5-14}, W_{15-24}, W_{25+} is the cumulative radon exposure in the windows 5–14, 15–24 or 25+ years before age t with corresponding parameters θ_{15-24}, θ_{25+} and ϕ_{age} and γ_z are factors for attained age and exposure rate, respectively. We refer to Eq. (5) as the "BEIR VI" model when fitted to the pooled 11 miners cohort, and as "PUMA full" or "PUMA sub" when fitted to the full PUMA cohort or to the 1960+ sub-cohort, respectively, the latter comprising miners hired in 1960 or later. Note that in PUMA models the exposure rate factor γ_z

[2] Editor's note. The online version of this article (DOI: https://doi.org/10.1667/RADE-24-00060.1) contains supplementary information that is available to all authorized users.

TABLE 1
Overview of all Considered Risk Models and Associated Cohort Data

Model name	Reference	Cohort	Equation	Miners	PYR*	Lung cancer deaths
BEIR VI	NRC 1999 (*6*)	Pooled cohort of 11 studies	(*5*)	67,897	1,155,453	2,799
PUMA full	Kelly-Reif et al. 2023 (*18*)	PUMA cohort	(*5*)	119,709	4,125,533	7754
PUMA sub	Richardson et al. 2022 (*28*)	PUMA 1960+ sub-cohort	(*5*)	57,873	1,887,092	1217
(Adjusted) Jacobi	Jacobi 1993 (*31*)	Pooled cohort of 6 studies	(*6*)	28,702	584,072	912
Joint CZ+F	Tomasek et al. 2008 (*32*)	Pooled Czech and French cohort	(*7*)	10,100	248,782	574
Wismut full	Kreuzer et al. 2018 (*7*)	German uranium miners cohort	(*8*)	58,974	2,332,008	3,942
Wismut sub	Kreuzer et al. 2018 (*7*)	German uranium miners 1960+ sub-cohort	(*7*)	26,765	956,776	495

* PYR, person-years at risk.

accounts for the annual exposure rate, whereas in the classical BEIR VI model γ_z corresponds to the cumulative exposure rate.

The adjusted Jacobi model is the classical Jacobi model in (*31*) adjusted by the factor 0.83 to account for overestimation (*2*). It reads with time since exposure TE, age at exposure $AE = t - TE$, and cumulative exposure $W(t)$ in WLM at age t in years,

$$ERR(t) = 0.83 \sum_{TE \le t} \alpha(AE)\theta(TE)W(AE), \tag{6}$$

with AE-specific parameters $\alpha(AE)$ and TE-specific parameters $\theta(TE)$. Note that although this model is based on six cohorts, the modifying effect structure of time since exposure and age at exposure was estimated solely from the Czech cohort. The parameter estimates in $\alpha(AE)$ are adjusted to match the meta-estimate for ERR per WLM derived from all six cohorts (*31*).

The generic parametric risk models for ERR at age t read,

$$ERR(t) = \beta W(t)\exp\{\alpha(AME(t) - 30) + \varepsilon(TME(t) - 20)\}, \tag{7}$$

$$ERR(t) = \beta W(t)\exp\{\alpha(AME(t) - 30) + \varepsilon(TME(t) - 20) + \psi(ER(t) - 3)\} \tag{8}$$

with cumulative exposure $W(t)$ in WLM and continuous effect modifiers age at median exposure $AME(t)$ in years, time since median exposure $TME(t)$ in years and cumulative exposure rate $ER(t)$ in WL with corresponding parameters β, α, ε and ψ. We consider Eq. (7) fitted on two different cohorts, namely the joint Czech and French and the German uranium miners sub-cohort with miners hired in 1960 or later (Wismut 1960+ sub-cohort). Equation (7) fitted on the joint Czech and French cohort is referred to as the "Joint CZ+F" risk model. We call Eq. (7) fitted on the Wismut 1960+ sub-cohort with follow-up 2013 "Wismut sub", whereas Eq. (8) was fitted to the full German uranium miners cohort and is referred to as 'Wismut full". The parameter estimates differ between cohorts and only Wismut full incorporates an exposure rate effect with $\psi \neq 0$.

All considered risk models include unknown parameters (indicated by Greek letters) which are estimated using Maximum-Likelihood methods based on miners cohort data. In total, we consider four categorical risk models (BEIR VI, PUMA full, PUMA sub, adjusted Jacobi) and three parametric continuous risk models (Joint CZ+F, Wismut full, Wismut sub) (Table 1). Here, the terms "categorical" and "parametric/continuous" refer to the categorical or continuous nature of the effect-modifying variables. Among all seven considered models, three categorical models (BEIR VI, PUMA full, PUMA sub) and one parametric model (Wismut full), account for an exposure rate effect. The explicit parameter estimates for all risk models can be found in Supplementary Materials, Section C (https://doi.org/10.1667/RADE-24-00060.1.S1) or the corresponding references. For the actual calculation of lifetime risk estimates, parameter estimates are plugged into the corresponding risk model structure.

Exposure Scenario

As exposure scenarios, we consider the internationally well-accepted default choice for LEAR calculation with occupational exposure of 2 WLM from age 18–64 (94 WLM total cumulative exposure over lifetime (WLM/life), moderate exposure) as used in (*11*). Furthermore, we use three scenarios calculated from mean exposures during employment of miners from the Wismut cohort depending on the period of begin of employment (1946–1954: 1,750 WLM/life, "very high exposure"; 1955–1970: 352 WLM/life, "high exposure"; and 1971–1989: 54 WLM/life, "low exposure"). The mean exposure was determined by averaging the annual exposures of miners (with WLM > 0) by age. The constructed exposure scenarios differ considerably in shape and yearly exposure (Fig. 2).

Comparison of Lifetime Risk Measures

Three additional lifetime risk measures were calculated: The risk of exposure-induced death REID [first introduced in (*34*) and employed in (*13*, *35*)], the excess lifetime risk ELR (*36*) and the radiation attributable decrease of survival RADS (*15*). The central difference of the additionally considered lifetime risk measures compared to the LEAR is the explicit accounting for radon exposure in the survival function. The LEAR approach assumes that radon exposure affects only the explicit lung cancer risk but not the survival function. Survival under exposure shall be denoted by $S_E(t \mid a)$ and baseline survival by $S_0(t \mid a) = S(t \mid a)$, emphasizing that $S_0(t \mid a)$ does not depend on exposure. It holds,

$$REID_E(a) = \int_a^\infty r_E(t)S_E(t|a)\ dt - \int_a^\infty r_0(t)S_E(t|a)\ dt$$

$$= \int_a^\infty r_0(t)ERR(t)S_E(t|a)\ dt,$$

$$ELR_E(a) = \int_a^\infty r_E(t)S_E(t|a)dt - \int_a^\infty r_0(t)S_0(t|a)dt,$$

$$RADS_E(a) = \lim_{t\to\infty} \frac{S_0(t|a) - S_E(t \mid a)}{S_0(t \mid a)} = 1 - \lim_{t\to\infty} \frac{S_E(t|a)}{S_0(t|a)}.$$

As for the LEAR, we investigate $a = 0$ and write $REID = REID_E(0)$, $ELR = ELR_E(0)$ and $RADS = RADS_E(0)$. To calculate these additional lifetime risk measures, assumptions on the survival function affected by exposure are necessary. Analogously to $S_0(t) = e^{-\int_0^t q_0(u)\ du}$ we set $S_E(t) = e^{-\int_0^t q_E(u)\ du}$ where $q_E(u)$ describes the all-cause mortality rate at age u affected by exposure. For computation of $S_E(t)$ we employ the approximation $\widetilde{S}_E(t) = e^{-\sum_{u=0}^{t-1} q_E(u)}$ and assume that radon exposure only influences the risk for lung

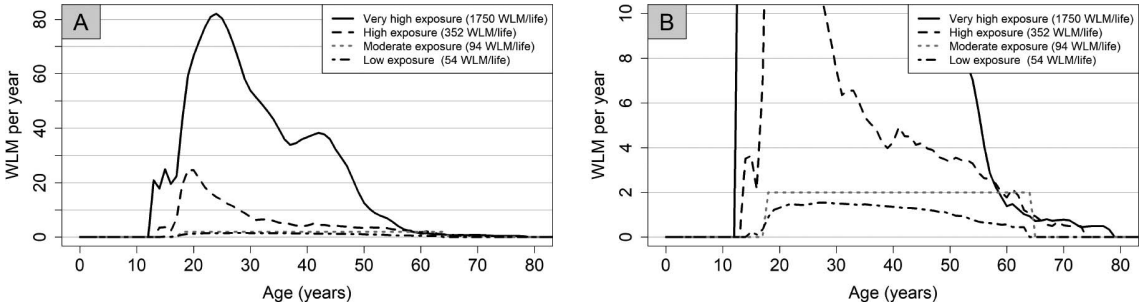

FIG. 2. Exposure to radon progeny in WLM per year by age for the four considered exposure scenarios with total cumulative exposure in parentheses (panel A). Panel B differs in the scale of the y-axis only and gives a more focused view on lower exposures per year.

cancer mortality. Therewith, $q_E(u)$ differs from $q_0(u)$ by an increased lung cancer mortality rate. Hence, $q_E(u) = q_0(u) + r_0(u)ERR(u)$ and

$$\widetilde{S}_E(t) = \widetilde{S}_0(t)e^{-\sum_{u=0}^{t-1} r_0(u)ERR(u)}.$$

Employing the same approximation as for the LEAR, the final approximated formulas for all considered lifetime risk measures are

$$LEAR \approx \sum_{t\geq 0} r_0(t)ERR(t)\widetilde{S}_0(t),$$

$$REID \approx \sum_{t\geq 0} r_0(t)ERR(t)\widetilde{S}_E(t),$$

$$ELR \approx \sum_{t\geq 0} r_0(t)(1+ERR(t))\widetilde{S}_E(t) - \sum_{t\geq 0} r_0(t)\widetilde{S}_0(t),$$

$$RADS \approx 1 - e^{-\sum_{t\geq 0} r_0(t)ERR(t)}.$$

RESULTS

All possible variations of considered mortality rates, risk models and exposure scenarios result in $3 \times 7 \times 4 = 84$ different LEAR and LEAR per WLM estimates (Table 2 and Fig. 3). Note that LEAR estimates are obtained from LEAR per WLM estimates by multiplying the LEAR per WLM by the scenario-specific cumulative exposure in WLM. The LEAR estimates themselves vary heavily from 0.45% to 151.27% and increase monotonically with exposure (as would be expected). Notably, LEAR estimates exceeding 100% are observed for the PUMA sub-risk model and the very high-exposure scenario for all three reference populations. Although absolute risks (i.e., probabilities) are typically bounded by 100%, the LEAR methodology allows for unbounded values, reflecting substantial risk increases under extreme exposure scenarios (see discussion). The LEAR per WLM spans from 0.58×10^{-4} to 8.80×10^{-4}. Roughly, this implies that among 100 individuals with a cumulative occupational radon exposure of 100 WLM, there would be an additional 0.58 to 8.80 (excess) lung cancer deaths attributed to this exposure over their lifetime.

Effects of Reference Populations

The LEAR per WLM estimates for the population of heavy smokers closely align with those of the ICRP reference population, whereas light smokers consistently yield lower estimates. The heavy smoker population (baseline lifetime risk of 5.27%), exhibits higher LEAR per WLM estimates than light smokers (baseline lifetime risk of

TABLE 2
Results for LEAR per WLM $\times 10^4$ Estimates for All Considered Exposure Scenarios, Reference Populations and Risk Models

Exposure scenario	Population	BEIR VI	PUMA full	PUMA sub	Adj. Jacobi	Joint CZ+F	Wismut full	Wismut sub
Very high	Heavy smokers	2.13	4.82	8.64	2.75	4.64	0.81	3.75
	ICRP	2.10	4.47	8.06	2.61	4.67	0.80	3.56
	Light smokers	1.54	3.70	6.50	2.07	3.36	**0.58**	2.81
High	Heavy smokers	3.70	5.08	**8.80**	2.75	4.33	0.87	3.45
	ICRP	3.57	4.80	8.36	2.60	4.36	0.87	3.28
	Light smokers	2.73	3.89	6.60	2.09	3.14	0.63	2.59
Moderate	Heavy smokers	6.15	5.38	7.98	3.41	4.68	1.17	4.50
	ICRP	5.97	5.74	7.50	3.20	4.58	1.13	4.21
	Light smokers	4.42	4.39	6.02	2.56	3.41	0.85	3.40
Low	Heavy smokers	6.25	5.55	8.51	3.19	4.80	1.14	4.28
	ICRP	6.12	5.24	8.04	3.01	4.74	1.12	4.03
	Light smokers	4.50	4.23	6.40	2.39	3.48	0.83	3.22

Note. Minimum and maximum values are bolded.

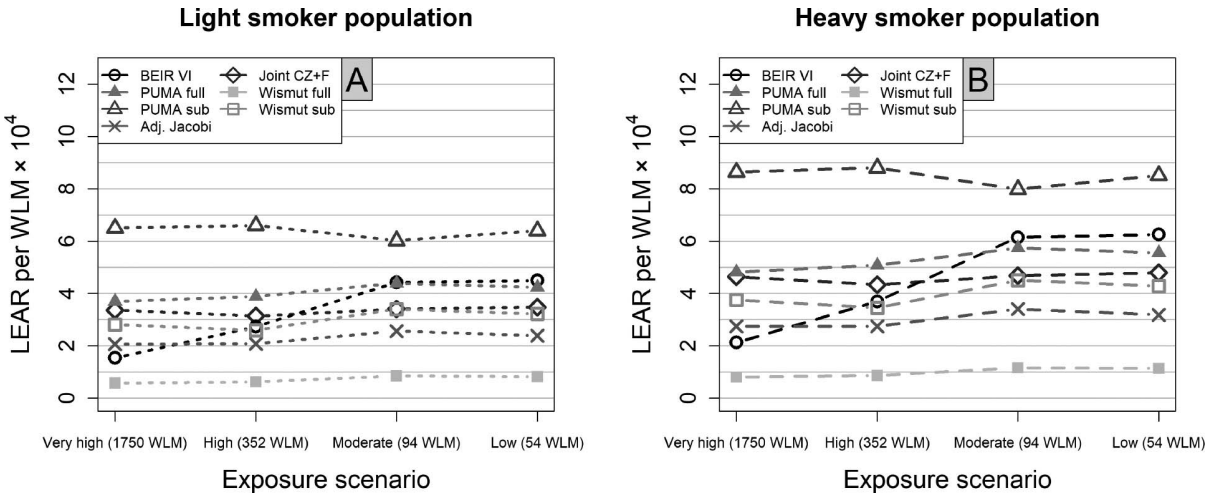

FIG. 3. LEAR per WLM $\times$ 10^4 for the four considered exposure scenarios and all considered risk models. Results of different smoker populations in different plots (panel A: light smokers, panel B: heavy smokers). A plot for the ICRP population is omitted here as it closely mirrors the heavy smokers panel.

4.12%). For comparison, the baseline lifetime risk of the ICRP reference population is 4.83%. The differences between reference populations can be explained when the factors $r_0(t)$ and $S(t)$ are interpreted as weighting factors $r_0(t)S(t)$ for the $ERR(t)$ in the LEAR calculation [Eq. (3)] since these weights completely depend on mortality rates (Fig. 4). The weights $r_0(t)S(t)$ are notably lower for light smokers than for heavy smokers and ICRP reference at all ages except for ages 80+. This characteristic roughly translates to the age-specific contributions $r_0(t)S(t)ERR(t)$ to the final LEAR estimate. Thus, the population of light smokers produces lower LEAR per WLM estimates because lung cancer rates are lower among light smokers, whereas the results for the ICRP reference population and the heavy smoker population are almost similar. Using male-specific compared to sex-averaged mortality rates results in higher lifetime risk estimates across all reference populations, risk models, exposure scenarios, and lifetime risk measures (Supplementary Materials, Section B; https://doi.org/10.1667/RADE-24-00060.1.S1).

Effects of Risk Models and Exposure Scenarios

Despite large differences in the four considered exposure scenarios, the resulting respective LEAR per WLM is notably constant (reading Fig. 3 horizontally). Only estimates with BEIR VI deviate considerably and exhibit an increasing trend with decreasing exposure. Notably, this does not apply to PUMA models, although they have a very similar model structure. Generally, the risk models influence LEAR estimates essentially (Fig. 5). There are large differences in age-at-exposure effects and the magnitude and shape of $ERR(t)$, depending on the chosen risk model. All risk models peak at different ages at exposure. The Joint CZ+F and Wismut sub model exhibit distinct $ERR(t)$ patterns, despite originating from an identical risk model structure [Eq. (7)]. This affects the age-specific contribution $r_0(t)ERR(t)S(t)$ to the LEAR (Fig. 5B). Multiplying the $ERR(t)$ (Fig. 5A) with $r_0(t)S(t)$ at every age t yields the curves from Fig. 5B. Integrating these curves over all ages t yields the LEAR estimate for each risk model.

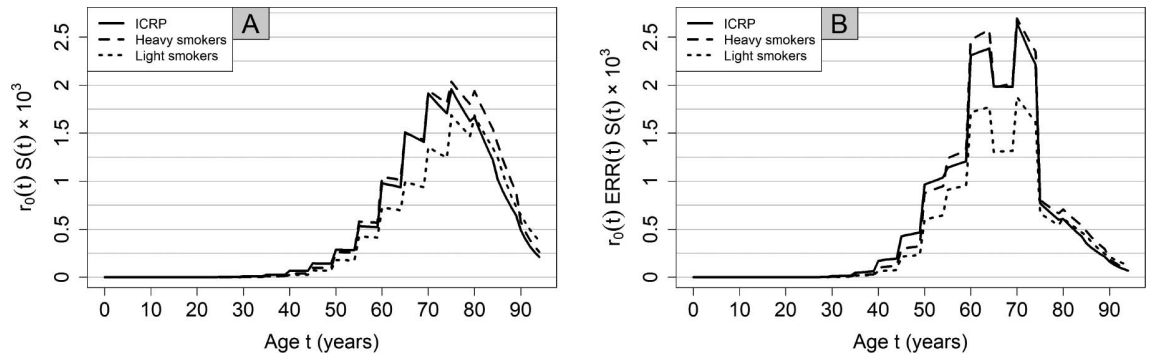

FIG. 4. Illustration of the influence of the three reference populations on LEAR calculation. Panel A: Product of baseline lung cancer mortality rates $r_0(t)$ and survival $S(t)$ $\times$ 10^3; panel B: age-specific contribution to the $LEAR$, $r_0(t)ERR(t)S(t)$ $\times$ 10^3, both for every age t with the BEIR VI risk model and the moderate exposure scenario of 2 WLM from age 18–64 years.

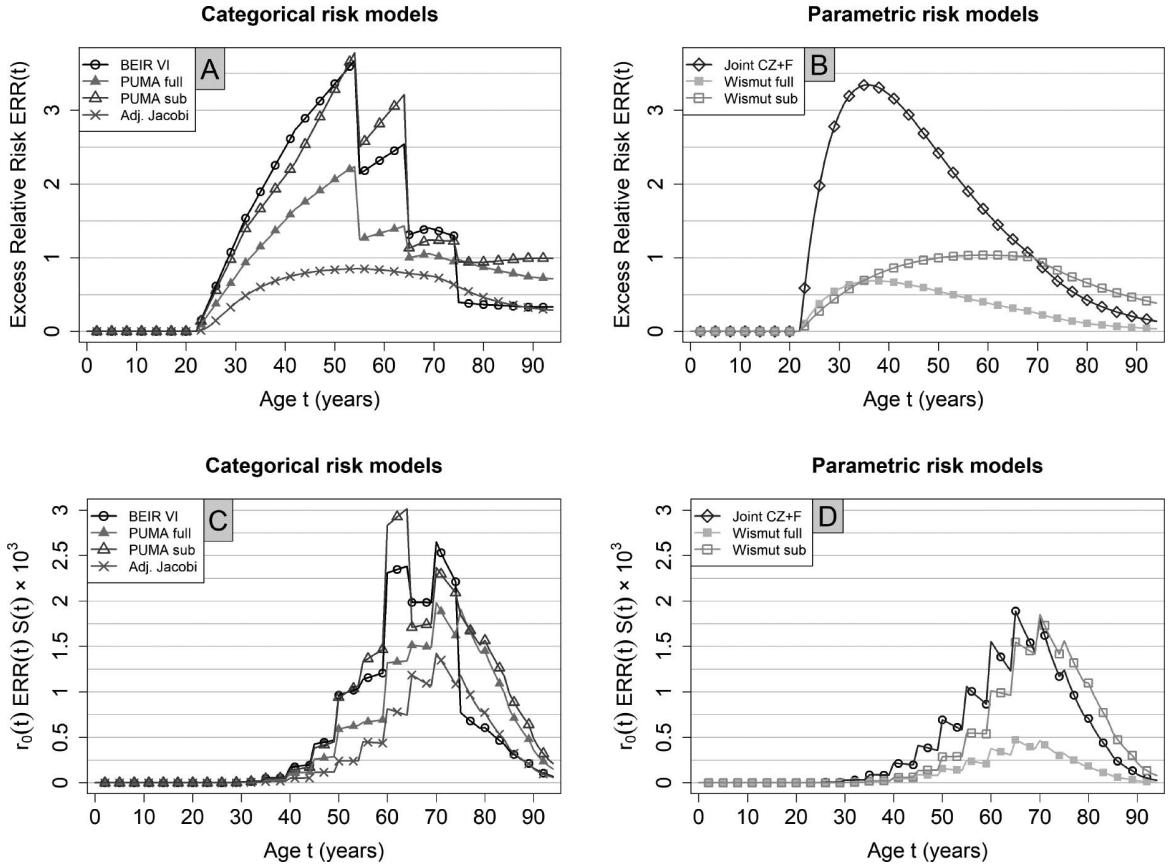

FIG. 5. Excess relative risks of different risk models (panel A: categorical models, panel B: parametric models) and their age-specific contribution to the *LEAR*, $r_0(t)ERR(t)S(t) \times 10^3$ (panels C and D, respectively) for the moderate exposure scenario of 2 WLM from 18–64 years and the ICRP reference population. For readability, data points are displayed only for every third age.

In the Supplementary Materials, Section D (https://doi.org/10.1667/RADE-24-00060.1.S1), further sensitivity analysis on the effects of varying annual exposure and differences between single acute and protracted homogeneous exposure across age are shown for all lifetime risk measures and risk models. Results show stable or slightly declining lifetime risk estimates per WLM for varying annual exposure for all risk models, except for the BEIR VI risk model. Comparing acute exposure at different ages to protracted homogeneous exposure across age reveals substantial differences in lifetime risk estimates especially influenced by the consideration of exposure rate in risk models. Depending on age at acute exposure, the excess lifetime risks (per WLM) differ roughly by a factor of two for all risk models and all lifetime risk measures.

Comparison of Lifetime Risk Measures

Excess lifetime risks were calculated for three additional lifetime risk measures for all combinations of reference populations, risk models and exposure scenarios (Fig. 6 and Table 3 for moderate exposure). There are only slight differences in results for ELR, REID and LEAR, except for very high exposures. RADS estimates are larger than results for the other three measures. We observe the monotonicity ELR $\leq$ REID $\leq$ LEAR $\leq$ RADS (per WLM) for all combinations except for the very high-exposure scenario. At this very high exposure, the monotonicity between lifetime risk measures is ELR $\leq$ REID $\leq$ RADS $\leq$ LEAR (per WLM) for all reference populations and risk models.

DISCUSSION

Lifetime risk estimates depend on several calculation components and assumptions, each being potentially the source of variability and uncertainty. The extensive variation in the calculated LEAR and LEAR per WLM across different reference populations, risk models and exposure scenarios highlight the complexity of assessing the health risks associated with radon exposure. In case of the LEAR for lung cancer related to occupational radon exposure, the observed LEAR per WLM estimates range from 0.58×10^{-4} to 8.80×10^{-4}, underscoring the considerable impact of the calculation components. We identified mortality rates and risk models as the most influential components. LEAR per WLM exhibits only low variation across different exposure scenarios for all risk models except for the BEIR VI model.

Tomasek et al. (*11*) contributed to understanding the variability of LEAR estimates by comparing effects of

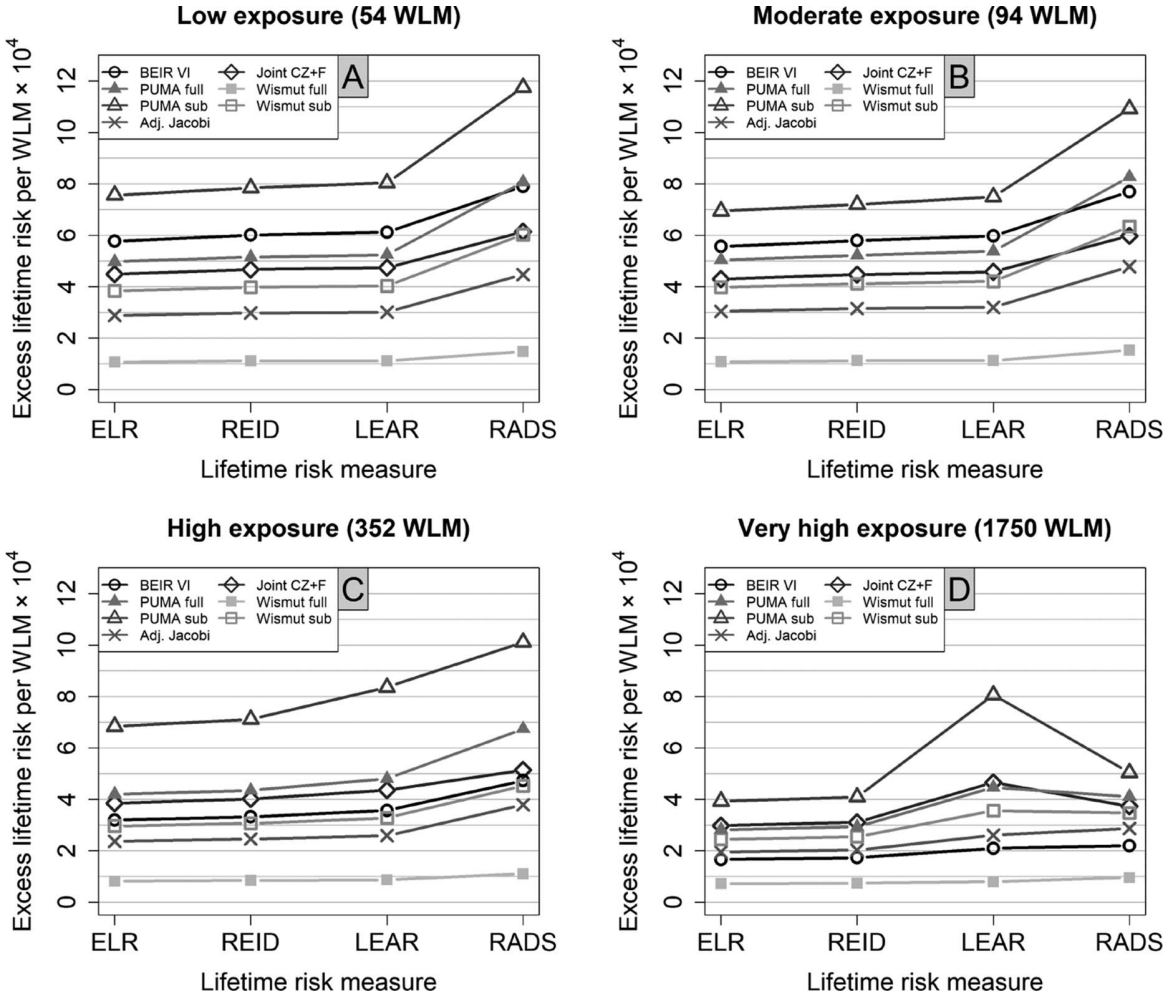

FIG. 6. Excess lifetime risk estimates per WLM $\times$ 10^4 for different lifetime risk measures and the four considered exposure scenarios (panels A–D) were calculated with the ICRP reference population.

different risk models from uranium miners studies and their impact on the radon dose conversion factor. For the REID, Hunter et al. (*13*) performed a sensitivity analysis by additionally accounting for differences in exposure, sex and smoking behavior in the risk model for a U.S. population. The lifetime risk measures LEAR, ELR and REID for occupational exposure were compared for a simple linear risk model in Kellerer et al. (2001) showing clear differences

TABLE 3

Results for Excess Lifetime Risks per WLM $\times$ 10^4 for Different Lifetime Risk Measures, Reference Populations and Risk Models for the Moderate Exposure Scenario of 2 WLM from Age 18–64 Years

Lifetime risk measure	Population	BEIR VI	PUMA full	PUMA sub	Adj. Jacobi	Joint CZ+F	Wismut full	Wismut sub
RADS	Heavy smokers	7.34	7.84	10.43	4.54	5.66	1.45	6.04
	ICRP	7.69	8.27	**10.92**	4.78	5.98	1.53	6.34
	Light smokers	5.99	7.03	9.23	3.96	4.64	**1.19**	5.30
LEAR	Heavy smokers	6.15	5.74	**7.98**	3.41	4.68	1.17	4.50
	ICRP	5.97	5.38	7.50	3.20	4.58	1.13	4.21
	Light smokers	4.42	4.39	6.02	2.56	3.41	**0.85**	3.40
REID	Heavy smokers	5.96	5.57	**7.66**	3.35	4.57	1.16	4.40
	ICRP	5.79	5.22	7.20	3.15	4.47	1.13	4.11
	Light smokers	4.32	4.28	5.82	2.52	3.35	**0.85**	3.34
ELR	Heavy smokers	5.72	5.38	**7.37**	3.23	4.39	1.11	4.24
	ICRP	5.56	5.04	6.94	3.04	4.30	1.08	3.98
	Light smokers	4.17	4.15	5.63	2.45	3.23	**0.82**	3.23

Note. Minimum and maximum values are bolded for every lifetime risk measure.

only at higher exposures (*9*). In the analysis at hand, for the first time variability in the lifetime risk estimates were investigated by directly comparing four lifetime risk measures ELR, REID, LEAR and RADS for different reference populations, risk models and heterogeneous occupational exposure scenarios from real data (German uranium miners cohort).

Effect of Mortality Rates and Reference Populations

Smoking is the greatest risk factor for lung cancer (*37*, *38*) and the interaction effect of smoking and radon on lung cancer is not yet fully understood (*8*). We investigated whether strong differences in the smoking behavior of reference populations are reflected in the corresponding LEAR estimates by constructing a sex-averaged light and heavy smoker reference population. For comparison, the widely accepted ICRP sex-averaged reference population from (*3*) was also considered. In the Supplementary Materials (Section B; https://doi.org/10.1667/RADE-24-00060.1.S1), lifetime risk sensitivities with male-specific mortality rates are additionally investigated.

This analysis clearly showed that employing a smoking reference population results in elevated LEAR per WLM estimates. This confirms the results published in the literature (*39*) that smoking behavior in a reference population influences lifetime risk estimates heavily. This can be explained by acknowledging that smoking amplifies baseline lung cancer risk $r_0(\cdot)$, which enters the LEAR calculation linearly. In particular, the risk models used are not adjusted for smoking, resulting in the implicit assumption of a multiplicative interaction between smoking and radon on the lung cancer risk here, in line with the findings (*8*, *40*). However, other epidemiological studies suggest a sub-multiplicative (*6*, *7*, *30*, *41*) or additive interaction (*42*). While we retain the multiplicative model due to the heterogeneous nature of smoking adjustments in the existing literature and compatibility issues with our heavy- and light-smoker reference rates, exploring lifetime risk estimates with smoking-adjusted risk models could offer interesting insights.

In that manner, if a LEAR for a smoker is of interest, it may be reasonable to compute smoking-specific LEAR estimates with mortality rates from smoker populations and risk models fitted on suitable cohorts of smoking persons with comparable smoking behavior. Especially between countries heavy differences in lung cancer mortality rates may occur not only due to smoking behavior, but also because of variable health care and medical standards (*43*, *44*). Likewise, if a LEAR for a specific country and sex is of interest, country- and sex-specific lifetime risk estimates with corresponding sex-specific mortality rates should be calculated, as similarly recommended for detriment calculations (*45*). Additional analyses (Supplementary Materials, Section B; https://doi.org/10.1667/RADE-24-00060.1.S1) showed an overall increased lifetime risk when calculated with male-specific baseline mortality rates, with lifetime risk variability closely aligning with results obtained using sex-averaged rates. It is expected that lifetime risks calculated with female-specific mortality rates would be lower correspondingly. However, calculating lifetime risks with female-specific rates and risk models derived from male uranium miners amplifies the risk transfer issue, which is why we excluded female-specific analyses in this study.

This analysis further revealed that the ICRP reference population results in remarkably similar LEAR estimates as when using the heavy smoker population and produces generally high LEAR and LEAR per WLM estimates, too. The same result was observed for male-specific reference populations (Supplementary Materials, Section B; https://doi.org/10.1667/RADE-24-00060.1.S1). This indicates that ICRP reference rates rather represent smokers than non-smokers. In particular, LEAR estimates with the ICRP reference population overestimate absolute risks for non-smokers and underestimate (but to a lesser extent) risks for smokers, compare (*2*). However, smoking behavior has evolved over the years and the smoking population rates in this analysis are derived from population data from more recent years (2016–2019) compared to the ICRP reference rates (1993–1997). This may contribute to explaining the results obtained for the ICRP population. Hence results incorporating ICRP rates must be interpreted with care.

Effect of Risk Models

Varying risk models lead to a large variability in LEAR estimates. This becomes clear when interpreting the LEAR as a weighted average of the ERR(·) term (which depends on risk models) with weights $r_0(\cdot)S(\cdot)$. Even risk models with identical ERR(·) term structures (Joint CZ+F and Wismut sub) inherit different parameter estimates and result in distinct LEAR estimates. The BEIR VI model imposes high variation of the LEAR per WLM for different exposure scenarios due to its strong inverse exposure rate effect. The PUMA models use fewer categories for exposure rate and annual exposure rate instead of cumulative mean exposure rate compared to the BEIR VI model. This explains the lower variability of results from PUMA models for different exposure scenarios despite the structural model similarity to BEIR VI. Although Wismut full also incorporates an inverse exposure rate effect, the impact on LEAR per WLM is considerably weaker because of the continuous nature of the model. In considered risk models without exposure rate effect modifiers, the ERR(t) (and therefore the LEAR) increases linearly when the exposure is increased. This results in remarkably stable LEAR per WLM estimates (Fig. 3).

The Wismut full risk model results in remarkably small lifetime risk estimates, particularly compared to the PUMA full model. This is a direct consequence of the fact that parameter estimates of Wismut full are also comparatively small. Compared to other cohorts in PUMA, the Wismut full cohort is characterized by longer duration of employment combined with rather high-cumulative radon exposure at low-exposure rates [(*20*) see table 1]. These structural differences might result in the substantial

differences between parameter and lifetime risk estimates from PUMA full and Wismut full risk models, despite the fact that the Wismut cohort makes up over half of the PUMA study data (2.3 out of 4.1 million person-years at risk) (*33*). In models from the 1960+ sub-cohorts (Wismut sub, PUMA sub), differences between parameter and lifetime risk estimates are less pronounced, which supports that uncertainties in exposure assessment in the early years of the Wismut cohort might also play an important role.

Exposure assessment in the early years of uranium mining relied on expert ratings rather than on direct measurements, increasing the potential for measurement error (*20*). Inconsistencies in exposure assessment across different periods can lead to differences in risk estimates. Improved exposure assessment quality, such as in the 1960+ sub-cohorts of PUMA and Wismut, reduces measurement error and yields more accurate risk estimates at low exposures and exposure rates. Ongoing research explores the effects of measurement error in the early years within the Wismut cohort (*46*, *47*). Measurement errors are one of many possible explanations for the differences in risk estimates at low exposures and exposure rates between the full and the 1960 + sub-cohort (*29*).

Note that the inverse exposure-rate effect, also known as the protraction enhancement effect, plays a critical role in the observed LEAR variability. This effect describes a decrease in (excess) relative risk for higher exposure rates and was demonstrated in many miners studies (*6*, *8*). However, this effect diminished when the analyses were limited to miners with low levels of cumulative exposure in WLM or those employed in more recent times (*30*, *32*), but it was shown to be statistically significant for the first time at such exposure levels in the PUMA 1960+ sub-cohort (*28*).

Generally, variations in LEAR and LEAR per WLM depending on the choice of risk model emerge from differences in underlying cohorts, risk model structures and assumptions for the fitting process of risk model and cohort. Especially decisions in the necessary data grouping process prior to applying Poisson regression on cohort data are highly susceptible to influencing risk model estimates (*48*). Also, the design of baseline stratification, e.g. with the statistical software Epicure (*49*), influences risk model parameter estimates and corresponding lifetime risk estimates (*50*). In categorical risk models, ERR(t) curves might exhibit abrupt changes at specific ages, times since exposure, and exposure rates as given by the model. This raises concerns about the discontinuity of these models. On the other hand, parametric risk models, which also incorporate effect modifiers, provide a smoother and more intuitive transition over age. Therefore, it seems more reasonable and plausible to use parametric risk models (or generally models with a continuous structure), such as those fitted on a representative cohort (cf. (*28*)), for calculating LEAR estimates. Especially for the BEIR VI model, there were attempts to use a smooth version of this categorical risk model by employing spline functions, see e.g. (*51*).

While our analyses focus on established excess relative risk (ERR) models, we acknowledge that lifetime risk estimates incorporating excess absolute risk (EAR) results for lung cancer related to occupational radon exposure are available, as in the electronic attachment of (*8*). The EAR approach offers an alternative perspective on lifetime risk assessment, although comprehensive application across all our studied cohorts is technically constrained. Future research may explore further EAR models, where possible, potentially enriching the interpretation of radon-related risks.

Effect of Exposure Scenario

In the early years of uranium mining at Wismut after 1945, miners were exposed to high levels of radon and its progeny, and had very different exposure situations than miners later. Due to improved measures for occupational safety like air ventilation, the mean exposure at the Wismut reduced constantly from 1955 and reached levels of international radiation protection standards in the 1970s (*52*). The large size of the Wismut cohort study enabled us to construct realistic occupational exposure scenarios with heterogeneous exposure rates over age (low, high, and very high exposure) additional to the default choice of 2 WLM from age 18–64 years (moderate exposure). In particular, the exposure scenario reflecting begin of employment in 1946–1954 (very high exposure) shows very high exposures at early ages due to missing protective measures in the mines. Likewise, but to a considerably lesser extent, this holds for the exposure scenario with begin of employment 1955–1970 (high exposure). On the other hand, the scenarios for begin of employment 1970–1989 (low exposure) and the ICRP default (moderate exposure) show homogeneous exposure over age without clear peaks.

Despite substantial differences in exposure scenarios, the LEAR per WLM remains relatively constant for all risk models except for BEIR VI with a threefold increase from highest to lowest exposure scenario.

The LEAR per WLM tends to slightly increase (except for the PUMA sub-model) for the two exposure scenarios with moderate and low cumulative exposure compared to the other two exposure scenarios. Regarding risk models without an exposure rate effect modifier (Adj. Jacobi, Wismut sub and Joint CZ+F), this is because of the more homogeneous exposure in age in these two scenarios – in contrast to the other two scenarios with high and very high-cumulative exposure where the majority of exposure is at earlier ages. At these earlier ages, LEAR and LEAR per WLM are less affected by exposure (see Fig. 4). However, the effect is small. On the other hand, risk models with an exposure rate modifier (BEIR VI, Wismut full, PUMA full and PUMA sub) are additionally affected by variable cumulative exposure. LEAR estimates with the BEIR VI model are heavily affected by this categorical-inverse-exposure rate effect as mentioned before. PUMA sub behaves differently because of its unique feature of an increasing factor for time since exposure 25–34 years

ago Supplementary Materials, Section C; https://doi.org/10.1667/RADE-24-00060.1.S1). This parameter estimate is likely an artifact stemming from the reduced statistical power of the PUMA sub-cohort compared to the PUMA full cohort.

Note that stable LEAR per WLM estimates translate to a roughly linear relationship between LEAR and exposure, e.g. a doubling in yearly exposure roughly doubles the LEAR as well. The LEAR measure is technically unbounded and may result in unreasonable large values for extreme exposure scenarios. LEAR estimates exceeding 100% are to be interpreted cautiously.

Combining risk models derived from low-exposure cohorts with extreme exposures may not seem reasonable at first glance. Risk models without an exposure rate effect modifier tend to be suitable only for low-exposure scenarios (*7*, *53*). However, the goal of this sensitivity analysis was to particularly investigate and combine extreme cases for a better understanding of LEAR drivers.

In summary, the stability of LEAR per WLM for changing exposure scenarios implies no benefit from employing complex over simple exposure scenarios when calculating lifetime risks for realistic exposures. This confirms the default exposure scenario of 2 WLM from age 18–64 years for a working population as a suitable and reasonable choice.

Effect of Lifetime Risk Measures

Comparisons between the different lifetime risk measures ELR, REID, LEAR and RADS, provide valuable insights. The monotonicity observed for all combinations of major components except for the very high-exposure scenario, i.e. ELR $\leq$ REID $\leq$ LEAR $\leq$ RADS (per WLM), underscores the relationship between these measures.

All four measures preserve mostly the behavior as seen for the LEAR regarding risk model and reference population effects. RADS is the only measure where estimates with ICRP mortality rates are higher than estimates with the heavy smoker reference population. This is because RADS estimates are independent of all-cause mortality rates in contrast to ELR, REID and LEAR.

The three measures ELR, REID and RADS (per WLM) are more severely affected by the very high-exposure scenario than the LEAR because these measures account for excess risk in the survival function.

This can be observed by comparing LEAR to, for example, RADS (per WLM) across varying exposure scenarios, moving from lower to higher levels (Fig. 6). For the very high-exposure scenario, LEAR per WLM stands out as it is barely affected by exposure. RADS per WLM decreases considerably for higher levels of exposure. This confirms the stability of LEAR per WLM in capturing the exposure-response relationship for varying exposure scenarios.

The observed relation ELR $\leq$ REID $\leq$ LEAR (per WLM) can be mathematically proven to hold for all combinations of calculation components. Assuming a harmful effect of radon exposure, it holds $r_E(t) \geq r_0(t)$ and $S_E(t|a) \leq S_0(t \mid a)$ for all $t, a \geq 0$. Evidence shown in Supplementary Materials, Section E (https://doi.org/10.1667/RADE-24-00060.1.S1),

$$ELR(a) \leq REID(a) \leq LEAR(a) \ (per\ WLM),$$

$$REID(a) \leq RADS(a) \ (per\ WLM).$$

For moderate excess absolute risks, it even holds ELR $\leq$ REID $\leq$ LEAR $\leq$ RADS (per WLM). At higher exposures the indefinite growth of LEAR exceeds RADS, breaking the inequality.

A critical aspect in estimating ELR, REID, and RADS is the modeling choice of $S_E(t)$. Since there is currently no reliable evidence that radon can cause diseases other than lung cancer (*54*, *55*), we assume that radon exposure affects solely the lung cancer risk, i.e. $q_E(u) = q_0(u) + r_0(u)ERR(u)$ for all ages u.

LEAR exhibits linear growth for increase in lung cancer mortality rates r_0 or yearly exposure whereas the other three measures grow sublinear due to the additional exponential term in the survival function. This mathematical elegance makes the LEAR particularly appealing (Supplementary Materials, Section D; https://doi.org/10.1667/RADE-24-00060.1.S1). Further, for low lung cancer mortality rates r_0 or yearly exposure, values for LEAR, REID and ELR (per WLM) are similar, while RADS values deviate. The similarity of REID, ELR and LEAR is also observed in detriment calculations (*45*).

We conclude that LEAR and REID are the most practicable lifetime risk measures, in accordance with previous findings (*9*, *10*). Both quantities behave very similar for low to moderate exposures and the LEAR is easier to compute since it avoids the ambiguous radiation-affected survival $S_E(t)$. The ELR has a convenient statistical interpretation but is not linear in increase in lung cancer mortality rates r_0 or yearly exposure and may even turn negative. We recommend sticking with the LEAR approach for its broad applicability across most exposure scenarios encountered today. However, for notably higher exposures, the linearity of LEAR and its indefinite growth is unrealistic, and we recommend employing the REID for such situations. RADS serves well as a comparative tool between risk models, by being less influenced by external baseline mortality rates compared to the other lifetime risk measures (*15*).

Calculation Components with Minor Influence

Prior analyses showed that latency time L, minimum age at risk a, the choice of approximation formula for the survival curve $S(t)$ and maximum age a_{max} have negligible impact on lifetime risk estimates similar to results of sensitivity analyses on radiation detriment (*45*). However, in our lifetime risk calculations for lung cancer related to radon exposure the choices of the lag time $L = 5$ and minimum age at risk $a = 0$ are predetermined by the risk model and to not discard early years of life, respectively.

Strengths and Limitations

For the first time in a sensitivity analysis on excess lifetime risks for lung cancer related to radon, new reference

populations mirroring smoking behavior were constructed from WHO data. Further, realistic exposure scenarios derived from the Wismut cohort study were employed in the calculation. This provides a more accurate representation of the actual conditions and radon concentrations that individuals experience in their working environments, and enhances the reliability of risk assessments.

Since no confidence intervals are presented, it is difficult to evaluate whether the presented lifetime risk estimates are statistically compatible. Further, variations in risk models emerge from differences in the underlying cohort and model structure. Smoking is not accounted for in the risk models and thus, any effects of smoking behavior come from amplified baseline lung cancer risks r_0. In that manner, also the risk transfer from miners cohorts to reference populations stays ambiguous [multiplicative risk transfer (*56*)].

Likewise, it is not accounted for sex-specific risks or further individual characteristics. Data for radon effects on females are sparse. Based on the published literature (*57*) we assumed the same *ERR* for females and males.

Future Perspectives

The results on the large impact of reference lung cancer mortality rates on the LEAR encourage to calculate country-specific lifetime risk estimates in future work. Moreover, quantitative estimates for the underlying uncertainty of lifetime risk estimates will sharpen the understanding of variability in lifetime risk estimates.

CONCLUSION

In the calculation of lifetime risk measures, the choice of lifetime risk measure itself and the specific exposure scenario is considerably less important than the used reference population and risk model. The current study confirms the LEAR as a suitable lifetime risk measure for low and moderate exposures and adds evidence that the LEAR is substantially affected by mortality rate changes, especially for lung cancer mortality rates. Thus, reference populations and mortality rates should be selected with care depending on the application of lifetime risk calculations. Further, the internationally typical moderate exposure scenario of 2 WLM from age 18–64 years to represent a working population is further confirmed as a suitable choice. These findings should be considered when using and interpreting lifetime risk measures for radiation protection policy purposes.

SUPPLEMENTARY MATERIALS

Section A: Mortality rates and mixing of populations.
Section B: Lifetime risks for male-specific mortality rates.
Section C: Risk models.
C1: BEIR VI exposure-age-concentration risk model.
C2: PUMA exposure-age-concentration risk model.
C3 Adjusted Jacobi risk model.
C4: Parametric risk models.
Section D: Comparison of lifetime risk measures and additional analyses.
Section E: Mathematical proofs from main paper statements.

Received: February 12, 2024; accepted: January 17, 2025; published online: January 30, 2025

REFERENCES

1. ICRP, 2022. Radiation detriment calculation methodology. ICRP Publication 152. Ann. ICRP 51(3).
2. ICRP, 1993. Protection Against Radon-222 at Home and at Work. ICRP Publication 65. Ann. ICRP 23(2).
3. ICRP, 2007. The 2007 Recommendations of the International Commission on Radiological Protection. ICRP Publication 103. Ann. ICRP 37 (2–4).
4. ICRP, 2010. Lung Cancer Risk from Radon and Progeny and Statement on Radon. ICRP Publication 115, Ann. ICRP 40(1).
5. WHO Statement on Radon. https://www.who.int/news-room/fact-sheets/detail/radon-and-health (12/01 2023, date last accessed).
6. National Research Council (US). Health Effects of Exposure to Radon: BEIR VI. Washington: The National Academies Press; 1999.
7. Kreuzer M, Sobotzki C, Schnelzer M, et al. Factors Modifying the Radon-Related Lung Cancer Risk at Low Exposures and Exposure Rates among German Uranium Miners. Radiat Res. 2018; 189:165.
8. United Nations Scientific Committee on the Effects of Atomic Radiation (UNSCEAR). Annex B: Lung cancer from exposure to radon. Sources, Effects and Risks of Ionizing Radiation: UNSCEAR 2019 Report to the General Assembly, with Scientific Annexes. New York: United Nations; 2021.
9. Kellerer AM, Nekolla EA, Walsh L. On the conversion of solid cancer excess relative risk into lifetime attributable risk. Radiat Environ Biophys. 2001; 40(4):249–57.
10. Thomas D, Darby S, Fagnani F, et al. Definition and Estimation of Lifetime Detriment From Radiation Exposures. Health Phys. 1992; 63:259–72.
11. Tomasek L, Rogel A, Laurier D, et al. Dose conversion of radon exposure according to new epidemiological findings. Radiat Prot Dosim. 2008; 130:98–100.
12. Marsh JW, Harrison JD, Laurier D, et al. Dose conversion factors for radon: recent developments. Health Phys. 2010; 99(4):511–6.
13. Hunter N, Muirhead CR, Bochicchio F, et al. Calculation of lifetime lung cancer risks associated with radon exposure, based on various models and exposure scenarios. Journal of Radiological Protection. 2015; 35:539–55.
14. Chen J, Murith C, Palacios M, et al. A discussion on different approaches for assessing lifetime risks of radon-induced lung cancer. Radiation Protection Dosimetry. 2017; 176:226–34.
15. Ulanowski A, Kaiser JC, Schneider U, et al. On prognostic estimates of radiation risk in medicine and radiation protection. Radiat Environ Biophys. 2019; 58:305–19.
16. Berrington de Gonzalez A, Iulian Apostoaei A, Veiga LHS, et al. RadRAT: a radiation risk assessment tool for lifetime cancer risk projection. J Radiol Prot. 2012; 32(3):205–22.
17. Tomasek L. Lung cancer lifetime risks in cohort studies of uranium miners. Radiat Prot Dosim. 2020; 191:171–5.
18. Kelly-Reif K, Bertke SJ, Rage E, et al. Radon and lung cancer in the pooled uranium miners analysis (PUMA): highly exposed early miners and all miners. Occup Environ Med. 2023; 80(7): 385–91.
19. Nelson W. Theory and applications of hazard plotting for censored failure data. Technometrics. 1972; 14:945–66.

20. Kreuzer M, Sommer M, Deffner V, et al. Lifetime excess absolute risk for lung cancer due to exposure to radon: results of the pooled uranium miners cohort study PUMA. Radiat Environ Biophys. 2024.
21. R Development Core Team. R: A Language and Environment for Statistical Computing. Vienna, Austria: R Foundation for Statistical Computing; 2024.
22. Cancer incidence in five continents. edited by Parkin DM, Whelan SL, Ferlay J, Teppo L, Thomas DB. Vol VIII. IARC Sci Publ. 2002(155):1–781.
23. World Health Organisation. WHO Mortality Database. https://www.who.int/data/data-collection-tools/who-mortality-database (5 February 2022 2022, date last accessed).
24. OECD Health Statistics. https://stats.oecd.org/ (03/02 2023, date last accessed).
25. Lipfert FW, Wyzga RE. Longitudinal relationships between lung cancer mortality rates, smoking, and ambient air quality: a comprehensive review and analysis. Crit Rev Toxicol. 2019; 49:790–818.
26. Islami F, Torre LA, Jemal A. Global trends of lung cancer mortality and smoking prevalence. Transl Lung Cancer Res. 2015; 4.
27. Heloma A, Nurminen M, Reijula K, et al. Smoking prevalence, smoking-related lung diseases, and national tobacco control legislation. Chest. 2004; 126(6):1825–31.
28. Richardson DB, Rage E, Demers PA, et al. Lung cancer and radon: Pooled analysis of uranium miners hired in 1960 or later. Environ Health Perspect. 2022; 130(5):57010.
29. Kreuzer M, Deffner V, Sommer M, et al. Updated risk models for lung cancer due to radon exposure in the German Wismut cohort of uranium miners, 1946–2018. Radiat Environ Biophys. 2023; 62(4):415–25.
30. Laurier D, Marsh JW, Rage E, et al. Miner studies and radiological protection against radon. Ann ICRP. 2020; 49(1_suppl):57–67.
31. Jacobi W. Verursachungs-Wahrscheinlichkeit von Lungenkrebs durch die berufliche Strahlenexposition von Uran-Bergarbeitern der Wismut-AG: gutachterliche Stellungnahme im Auftrage der Berufsgenossenschaften: GSF; 1993.
32. Tomasek L, Rogel A, Tirmarche M, et al. Lung cancer in French and Czech uranium miners: Radon-associated risk at low exposure rates and modifying effects of time since exposure and age at exposure. Radiat Res. 2008; 169:125–37.
33. Rage E, Richardson DB, Demers PA, et al. PUMA - pooled uranium miners analysis: cohort profile. Occup Environ Med. 2020; 77(3):194–200.
34. United Nations Scientific Committee on the Effects of Atomic Radiation (UNSCEAR). Sources and Effects of Ionizing Radiation: UNSCEAR 1994 Report to the General Assembly, with Scientific Annexes. New York: United Nations; 1994.
35. Little MP, Hoel DG, Molitor J, et al. New Models for Evaluation of Radiation-Induced Lifetime Cancer Risk and its Uncertainty Employed in the UNSCEAR 2006 Report. Radiation Research. 2008; 169:660–76.
36. Vaeth M, Pierce DA. Calculating excess lifetime risk in relative risk models. Environ Health Perspect. 1990; 87:83–94.
37. The International Agency for Research on Cancer. Tobacco smoke and involuntary smoking. Lyon: World Health Organisation; 2004.
38. Pesch B, Kendzia B, Gustavsson P, et al. Cigarette smoking and lung cancer-relative risk estimates for the major histological types from a pooled analysis of case-control studies. Int J Cancer. 2012; 131:1210–9.
39. Bruder C, Bulliard J-L, Germann S, et al. Estimating lifetime and 10-year risk of lung cancer. Preventive Medicine Reports. 2018; 11:125–30.
40. Kurkela O, Nevalainen J, Pätsi SM, et al. Lung cancer incidence attributable to residential radon exposure in Finland. Radiation and Environmental Biophysics. 2023; 62(1):35–49.
41. Leuraud K, Schnelzer M, Tomasek L, et al. Radon, smoking and lung cancer risk: results of a joint analysis of three European case-control studies among uranium miners. Radiat Res. 2011; 176(3):375–87.
42. Tomasek L. Lung cancer risk from occupational and environmental radon and role of smoking in two Czech nested case-control studies. Int J Environ Res Public Health. 2013; 10(3):963–79.
43. Lathan CS. Lung cancer care: the impact of facilities and area measures. Translational Lung Cancer Research. 2015; 4:385–91.
44. Nwagbara UI, Ginindza TG, Hlongwana KW. Health systems influence on the pathways of care for lung cancer in low- and middle-income countries: a scoping review. Globalization and Health. 2020; 16:23.
45. Zhang W, Laurier D, Cléro E, et al. Sensitivity analysis of parameters and methodological choices used in calculation of radiation detriment for solid cancer. Int J Radiat Biol. 2020; 96:596–605.
46. Küchenhoff H, Deffner V, Aßenmacher M, Neppl H, Kaiser C, Güthlin D. Ermittlung der Unsicherheiten der Strahlenexpositionsabschätzung in der Wismut-Kohorte—Teil I/Determination of uncertainties of radiation exposure assessment in the Wismut cohort part I. Germany: Bundesamt für Strahlenschutz/Federal Office for Radiation Protection; 2018. (Ressortforschungsberichte zum Strahlenschutz).
47. Ellenbach N, Rehms R, Hoffmann S. Ermittlung der Unsicherheiten der Strahlenexpositionsabschätzung in der Wismut-Kohorte—Teil II/Determination of uncertainties of radiation exposure assessment in the Wismut cohort Part II. Germany: Bundesamt für Strahlenschutz/Federal Office for Radiation Protection; 2023. (Ressortforschungsberichte zum Strahlenschutz).
48. Richardson DB, Loomis D. The impact of exposure categorisation for grouped analyses of cohort data. Occup Environ Med. 2004; 61:930–5.
49. Preston DL, Lubin JH, Pierce DA, et al. Epicure Users Guide. Seattle, Washington: Hirosoft International Corporation; 1993.
50. Golden AP, Cohen SS, Chen H, et al. Evaluation of statistical modeling approaches for epidemiologic studies of low-dose radiation health effects. International Journal of Radiation Biology. 2019; 98:572–9.
51. Chiu N, Brattin WJ. EPA Assessment of Risks from Radon in Homes. Washington: U.S. Environmental Protection Agency; 2003.
52. Kreuzer M, Schnelzer M, Tschense A, et al. Cohort Profile: The German uranium miners cohort study (WISMUT cohort), 1946–2003. Int J Epidemiol. 2009; 39:980–7.
53. Lubin JH, Boice JD, Edling C, et al. Radon-exposed underground miners and inverse dose-rate (protraction enhancement) effects. Health Physics. 1995; 69:494–500.
54. Darby SC, Whitley E, Howe GR, et al. Radon and cancers other than lung cancer in underground miners: a collaborative analysis of 11 studies. Journal of the National Cancer Institute. 1995; 87: 378–84.
55. United Nations Scientific Committee on the Effects of Atomic Radiation (UNSCEAR). Annex E: Sources-to-effects assessment for radon in homes and workplaces. Effects of Ionizing Radiation: UNSCEAR 2006 Report to the General Assembly with Scientific Annexes. New York: United Nations; 2009.
56. Ulanowski A, Shemiakina E, Güthlin D, et al. ProZES: the methodology and software tool for assessment of assigned share of radiation in probability of cancer occurrence. Radiat Environ Biophys. 2020; 59:601–29.
57. Darby S, Hill D, Auvinen A, et al. Radon in homes and risk of lung cancer: Collaborative analysis of individual data from 13 European case-control studies. BMJ 2005; 330:223.

11. Lifetime excess absolute risk for lung cancer due to exposure to radon: results of the pooled uranium miners cohort study PUMA

Contributing publication

Kreuzer, M., Sommer, M., Deffner, V., Bertke, S., Demers, P. A., Kelly-Reif, K., Laurier, D., Rage, E., Richardson, D. B., Samet, J. M., Schubauer-Berigan, M. K., Tomasek, L., Wiggins, C., Zablotska, L. B., & Fenske, N. (2024). Lifetime excess absolute risk for lung cancer due to exposure to radon: Results of the pooled uranium miners cohort study PUMA. *Radiation and Environmental Biophysics*, 63(1), 7–16. https://doi.org/10.1007/s00411-023-01049-w

Declaration of contributions

Michaela Kreuzer wrote the main manuscript. All authors assisted in revising the paper. I, Manuel Sommer, carried out and contributed the following work for the publication:

- **Statistical analysis**
  - Leading the methodological discussion for lifetime risk calculations
  - Conception and implementation of lifetime risk calculations in statistical software *R*
  - Preparation of figures and tables
- **Writing**
  - Writing the section "Methods"
  - Review of manuscript (together with all other authors)

Radiation and Environmental Biophysics (2024) 63:7–16
https://doi.org/10.1007/s00411-023-01049-w

RESEARCH

Lifetime excess absolute risk for lung cancer due to exposure to radon: results of the pooled uranium miners cohort study PUMA

M. Kreuzer[1] · M. Sommer[1] · V. Deffner[1] · S. Bertke[2] · P. A. Demers[3] · K. Kelly-Reif[2] · D. Laurier[4] · E. Rage[4] · D. B. Richardson[5] · J. M. Samet[6] · M. K. Schubauer-Berigan[7] · L. Tomasek[8] · C. Wiggins[9,10] · L. B. Zablotska[11] · N. Fenske[1]

Received: 24 August 2023 / Accepted: 9 November 2023 / Published online: 3 January 2024

Abstract

The Pooled Uranium Miners Analysis (PUMA) study is the largest uranium miners cohort with 119,709 miners, 4.3 million person-years at risk and 7754 lung cancer deaths. Excess relative rate (ERR) estimates for lung cancer mortality per unit of cumulative exposure to radon progeny in working level months (WLM) based on the PUMA study have been reported. The ERR/WLM was modified by attained age, time since exposure or age at exposure, and exposure rate. This pattern was found for the full PUMA cohort and the 1960 + sub-cohort, i.e., miners hired in 1960 or later with chronic low radon exposures and exposure rates. The aim of the present paper is to calculate the lifetime excess absolute risk (LEAR) of lung cancer mortality per WLM using the PUMA risk models, as well as risk models derived in previously published smaller uranium miner studies, some of which are included in PUMA. The same methods were applied for all risk models, i.e., relative risk projection up to <95 years of age, an exposure scenario of 2 WLM per year from age 18–64 years, and baseline mortality rates representing a mixed Euro-American-Asian population. Depending upon the choice of model, the estimated LEAR per WLM are 5.38×10^{-4} or 5.57×10^{-4} in the full PUMA cohort and 7.50×10^{-4} or 7.66×10^{-4} in the PUMA 1960 + sub-cohort, respectively. The LEAR per WLM estimates derived from risk models reported for previously published uranium miners studies range from 2.5×10^{-4} to 9.2×10^{-4}. PUMA strengthens knowledge on the radon-related lung cancer LEAR, a useful way to translate models for policy purposes.

Keywords Uranium miners · Cohort study · Lung cancer · Radon · Mortality · Lifetime risk

✉ M. Kreuzer
mkreuzer@bfs.de

1 Federal Office for Radiation Protection (BfS), Munich (Neuherberg), Germany

2 National Institute for Occupational Safety and Health, Cincinnati, OH, USA

3 Occupational Cancer Research Centre, Toronto, Canada

4 Institute for Radiological Protection and Nuclear Safety (IRSN), Fontenay-aux-Roses, France

5 University of California, Irvine, CA, USA

6 Colorado School of Public Health, Aurora, CO, USA

7 International Agency for Research on Cancer, Lyon, France

8 National Radiation Protection Institute, Prague, Czech Republic

9 University of New Mexico, Albuquerque, NM, USA

10 New Mexico Tumor Registry, Albuquerque, NM, USA

11 University of California, San Francisco, CA, USA

Introduction

Radon is an established lung carcinogen and an important occupational and environmental cause of lung cancer (UNSCEAR 2020). This was demonstrated in residential radon studies in the general population and in studies of uranium and other radon-exposed underground miners. Cohorts of uranium miners continue to form an important basis for radiation protection standards for radon progeny. They consistently show that the excess relative rate (ERR) of lung cancer mortality increases linearly with increasing cumulative exposure to radon progeny (in the following abbreviated to "radon") in WLM and that the ERR/WLM is modified by attained age, time since exposure or age at exposure, and exposure rate (NRC 1999, UNSCEAR 2020). The calculation of the lifetime excess absolute risk (LEAR) allows the comparison of estimates of the ERR/WLM obtained from different studies with different characteristics while using

the same exposure scenario and baseline mortality rates. Such estimates are also useful for policy considerations. The LEAR of lung cancer related to exposure to radon for example has been used in the past as the basis for the dose conversion convention for radon (ICRP 1993, 2010). This method has been used to convert measured radon activity concentrations into an effective dose in mSv, which is important to check the compliance with occupational radiation limits given in mSv. In this "epidemiological" approach of dose conversion, the LEAR of lung cancer per unit of exposure to radon progeny is divided by the detriment (representing the harm) per unit of effective dose (ICRP 2010). Determining the most appropriate value of this dose conversion coefficient has been the subject of much controversy in recent years (Harrison et al. 2020, 2021; Laurier et al. 2020; Marsh et al. 2021).

While previously an LEAR of 2.8×10^{-4} per WLM was assumed based on risk models derived from a meta-analysis of 7 miners cohort studies (ICRP 1993), this value was revised to 5×10^{-4} per WLM by the International Commission on Radiological Protection (ICRP) in 2010 (ICRP 2010) based on new risk models from a pooled analysis of 11 miners studies (BEIR VI study) (NRC 1999) and a pooled Czech/French study (Tomasek et al. 2008a). Both LEAR calculations used a mixed male/female Euro-American-Asian population for baseline rates of lung cancer mortality (ICRP 2007) and assumed an exposure scenario of 2 WLM per year between age 18 and 64 years. In 2020, the United Nations Scientific Committee on the Effects of Atomic Radiation (UNSCEAR) reviewed epidemiological studies and calculated the LEAR per WLM for death from lung cancer in a similar manner using data from four miners studies (UNSCEAR 2020; Tomasek 2020), among them for the first time the large German Wismut cohort (Kreuzer et al. 2018). The LEAR ranged from 2.4 (Wismut cohort) to 7.5 (Eldorado cohort) $\times 10^{-4}$ per WLM. Heterogeneity in radiation risk estimates between studies may explain differences in the LEAR and could be due to several factors: differences in the range of cumulative exposure and exposure rate, concomitant exposures to other lung cancer carcinogens, duration of follow-up and employment, methods of mortality follow-up, composition of the study population, existence and control for potential confounders, measurement error, loss to follow-up and competing risks for mortality, statistical power, and also statistical methods.

A major step forward was therefore the worldwide pooling of uranium miners studies, the Pooled Uranium Miners Analysis (PUMA) study (Rage et al. 2020; Richardson et al. 2021), which aims to get more precise estimates of the lung cancer risk associated with radon based on standardized statistical analyses of existing cohorts. PUMA includes twice as many uranium miners and about three times as many lung cancer deaths (Rage et al. 2020) as the pooled BEIR VI study (NRC 1999). The majority of included studies have an updated mortality follow-up and all studies follow a common study protocol and statistical methods. Recently, two papers on radon-lung cancer mortality associations among men in PUMA have been published, addressing: (1) the 1960 + sub-cohort of miners hired in 1960 or later (Richardson et al. 2022) with chronic low radon exposures and exposure rates mostly based on measurements, and (2) the full PUMA cohort (Kelly-Reif et al. 2023) including very high radon exposures from the early years of mining and low radon exposures in the later years.

The aim of the present paper is to calculate the LEAR per WLM for death from lung cancer using the new risk models based on the pooled data of the PUMA study and the risk models of previously published uranium miners studies, including the recently updated German Wismut cohort (Kreuzer et al. 2023), while using the same methods for all analyses. To be comparable to previous LEAR calculations as in UNSCEAR (2020) and ICRP (2010), the exposure scenario was defined as 2 WLM per year from age 18–64 years, and baseline mortality rates of the ICRP mixed Euro-American-Asian population (ICRP 2007) were chosen.

Methods

PUMA data

The PUMA study includes seven cohorts from Canada, the Czech Republic, France, Germany, and USA, which have been previously described in detail (Rage et al. 2020; Richardson et al. 2022; Kelly-Reif et al. 2023). The ERR/WLM was estimated in analyses of men included in PUMA based on the BEIR VI exposure–age–concentration model (NRC 1999, UNSCEAR 2020) and an alternative risk model (i.e., the BEIR VI model, but with age at exposure instead of time since exposure). The corresponding statistical methods and findings have been published for the full cohort (Kelly-Reif et al. 2023) and the PUMA 1960 + sub-cohort of miners hired in 1960 or later (Richardson et al. 2022). Main characteristics of both cohorts are described briefly in Table 1.

Statistical methods

Lifetime risks reflect the probability of developing or dying from a specific disease of interest (here: lung cancer mortality) in the course of a lifetime. The lifetime excess absolute risk (LEAR) is defined as the difference between the lifetime risk LR_E for an individual with exposure E (here: exposure to occupational radon) and the lifetime risk LR_0 for an individual without exposure

Table 1 Characteristics of the PUMA full cohort and PUMA 1960 + sub-cohort of miners hired in 1960 or later

	Period of follow-up	Number of miners	Number of lung cancer deaths	Mean duration of employment (years)	Mean cumulative radon exposure (WLM)*	Mean annual exposure rate (WL)*
Full cohort (Rage et al. 2020, Tables 1 and 2)						
Eldorado (Canada)	1950–1999	13,574	517	2	122	8.3
Ontario (Canada)	1954–2007	28,546	1246	5	31	0.9
Czech (Czech Rep.)	1952–2014	9978	1176	8	73	0.8
France (France)	1946–2007	5086	213	17	37	0.8
Colorado (USA)	1960–2005	4137	612	4	579	11.7
New Mexico (USA)	1957–2012	3469	231	9	90	9.6
Wismut (Germany)	1946–2013	54,919	3759	14	304	1.9
PUMA total		119,709	7754	10	191	2.9
PUMA without Wismut		64,790	3995	6	98	3.7
1960 + sub-cohort[#] (Richardson et al. 2022, Tables 1 and 2)						
Eldorado (Canada)	1960–1999	6593	91	2	7	0.2
Ontario (Canada)	1960–2007	15,810	299	6	6	0.4
Czech (Czech Rep.)	1960–2014	5532	228	6	7	0.2
France (France)	1960–2007	2159	19	17	12	0.1
Colorado (USA)	1960–2005	175	16	2	193	7.5
New Mexico (USA)	1960–2012	2537	94	9	39	4.7
Wismut (Germany)	1960–2013	25,067	470	10	18	0.3
PUMA total		57,873	1217	8	13	0.5
PUMA without Wismut		32,806	747	6	10	0.7

More detailed information can be found in Rage et al. (2020) and Richardson et al. (2022)

WLM Working level months; *WL* Working level

*Non-exposed miners (i.e., with WLM = 0) were excluded from calculation of mean values

[#]miners hired in 1960 or later

$$\begin{aligned}\mathrm{LEAR} &= \mathrm{LR}_E - \mathrm{LR}_0 \\ &= \int_0^\infty r_E(a)S(a)da - \int_0^\infty r_0(a)S(a)da,\end{aligned}$$

with survival function $S(a) = e^{-\int_0^a q_0(u)du}$ describing the probability to survive until age a, and baseline mortality rates for all causes of death $q_0(a)$ and for lung cancer $r_0(a)$ at age a in absence of exposure. The lung cancer mortality rate $r_E(a)$ at age a under exposure is assumed to follow the typical general model structure $r_E(a) = r_0(a)(1 + \mathrm{ERR}(a))$ with excess relative risk term $\mathrm{ERR}(a)$. Based on this assumption, the LEAR can be approximated and finally technically calculated by

$$\begin{aligned}\mathrm{LEAR} &\approx \sum_{a=0}^{a_{\max}} r_E(a)\tilde{S}(a) - \sum_{a=0}^{a_{\max}} r_0(a)\tilde{S}(a) \\ &= \sum_{a=0}^{a_{\max}} r_0(a)\mathrm{ERR}(a)\tilde{S}(a),\end{aligned}$$

where $\tilde{S}(a) = e^{-\sum_{u=0}^{a-1} q_0(u)}$ approximates the survival function $S(a)$. The $\mathrm{ERR}(a)$ depends on an exposure pattern and a specific risk model, e.g., with a structure as in the BEIR VI exposure–age–concentration model, and a lag time. The final summary result is reported as the LEAR per WLM, obtained by dividing the calculated LEAR by the cumulative exposure accrued over the entire exposure scenario (here: 94 WLM). For example, an LEAR for lung cancer mortality per WLM of 5×10^{-4} means that among 100 people with a cumulative occupational radon exposure of 100 WLM five additional (excess) lung cancer deaths would occur due to this exposure during lifetime.

Lag time

A lag is assumed between exposure to radon and any observed change in the lung cancer mortality rate. In the risk models employed here, the lag is either directly described by the model structure (e.g., BEIR VI exposure–age–concentration model with $\mathrm{ERR}(a) = 0$ for $\mathrm{TSE}(a) < 5$) or by the data grouping process prior to any model fit as for the parametric risk models with continuous effect modifying variables (e.g., for the Czech/French cohort, Tomasek et al. 2008b). In that analysis, a miner's exposure is lagged a priori by $L = 5$ years. A lag assumption may be incorporated in the LEAR calculation by calculating $\mathrm{ERR}(a)$ at age a only with information about radon exposure until age $a - L$. However, doing so would violate the important equation $a = \mathrm{AME}(a) + \mathrm{TSME}(a)$, with AME being the time-varying age at median exposure and TSME the time since median exposure. This is technically solved by considering $\mathrm{AME}(a - L)$ and $\mathrm{TSME}(a - L) + L$ in the calculation of $\mathrm{ERR}(a)$.

LEAR calculations

For the calculation of LEAR, the maximum age was set to $a_{\max} = 94$, i.e., the LEAR was calculated up to age < 95 years. The baseline lung cancer mortality rates $r_0(a)$ and all-cause mortality rates $q_0(a)$ were taken from the ICRP mixed Euro-American-Asian population (ICRP 2007) to be comparable with previous publications (UNSCEAR 2020, Tomasek et al. 2008b). According to UNSCEAR (2020) and other LEAR calculations (ICRP 2010, Tomasek et al. 2008b), the exposure scenario was defined as 2 WLM per year from age 18 to 64 years with a lag of $L = 5$ years.

To compare LEAR estimates for mortality from lung cancer of the PUMA study with those from previous studies, the LEAR per WLM for all published risk models of uranium miners studies that include time- and age-related effect modifiers have been re-estimated, while using the same exposure scenario, baseline rates, and survival function. For this reason, some estimates may slightly differ from previously published LEAR values. The coefficients describing the relative risk model were the values as reported in the original papers, and are described in Tables 2 and 3 for the PUMA study and in Supplementary Tables 1–3 for other studies. The LEAR for the complete exposure scenario (i.e., 2 WLM per year from age 18 to 64 years, resulting in a cumulative exposure of 94 WLM) can be obtained by multiplying the value for the LEAR per WLM with 94. All LEAR calculations were performed with the statistical software R (R Core Team 2022).

Results

Table 2 shows the radon-related lung cancer risk in the full PUMA cohort and in the PUMA 1960 + sub-cohort based on the BEIR VI exposure–age–concentration model with categorical effect modifiers time since exposure, attained age, and annual exposure rate. The ERR/100 WLM at attained age < 55 years, 5–14 years since exposure, and exposure rate < 0.5 WL was 4.68 (95% CI: 2.88, 6.96) and 6.98 (95% CI: 1.97, 16.15) in the full cohort (Kelly-Reif et al. 2023) and 1960 + sub-cohort (Richardson et al. 2022), respectively. The estimated ERR/100 WLM decreased with increasing attained age, radon exposure rate and time since exposure, the latter decrease, however, is only present in the full cohort and not the 1960 + sub-cohort. The estimated LEAR per WLM is slightly higher in the 1960 + sub-cohort compared with the full cohort (7.50×10^{-4} vs 5.38×10^{-4}, respectively). This is also illustrated in Fig. 1 (upper part) where the $\mathrm{ERR}(a)$ is plotted as a function of attained age, a, under the exposure scenario of interest (i.e., 2 WLM per year from age 18 to 64 years). Notably, using the model coefficients derived for the 1960 + sub-cohort, the ERR/100 WLM increases slightly after age 75 years, which is mainly due to the value of the parameter estimate for the effect modifier time since exposure. The estimated value of the coefficient for this modifier was highest for the category 5–14 years after exposure (reference category 1.0), decreased for the category 15–24 years after exposure to 0.64, and increased again for the category 25 years or more after exposure to 0.89. The bottom part of Fig. 1 shows the corresponding age-specific contribution to LEAR, $r_0(a)\mathrm{ERR}(a)\tilde{S}(a)$ for each age a. Within the full PUMA cohort, the largest LEAR contribution is observed at ages 70–75 years, which is 5–10 years after the maximum cumulative exposure is reached. From age 75 years onwards, there is a strong decrease in the age-specific contribution to the LEAR which reflects the decreasing baseline lung cancer mortality rates $r_0(a)$, the decrease in $\mathrm{ERR}(a)$ with increasing time since exposure, and the decreasing fraction of the cohort who remains at risk of lung cancer (Supplementary Fig. 1). For the PUMA 1960 + sub-cohort, a similar pattern is observed; however, the peak in the contribution to LEAR is between 60 and 65 years, thus 10 years earlier than in the full PUMA cohort.

Table 3 presents the LEAR per WLM based on an alternative risk model for the PUMA study with categorical effect modifiers age at exposure, attained age, and exposure rate (i.e., the BEIR VI model, but with age at exposure instead of time since exposure). The ERR/WLM decreases with increasing attained age and increases with increasing age at exposure in both cohorts. The corresponding LEAR per WLM is 7.66×10^{-4} in the 1960 + sub-cohort and

Table 2 Lifetime excess absolute risk (LEAR) estimates obtained using a model with effect modifiers defined by categories of time since exposure, attained age, and annual exposure rate (BEIR VI exposure–age–concentration model) in the full PUMA cohort and the PUMA 1960 + sub-cohort

	PUMA full cohort Kelly-Reif et al. (2023)		PUMA 1960 + sub-cohort Richardson et al. (2022)	
	Lung cancer deaths (*n*)	Estimate (95% CI)	Lung cancer deaths (*n*)	Estimate (95% CI)
ERR/100 WLM	7754	4.68 (2.88, 6.96)	1217	6.98 (1.97, 16.15)
Time since exposure (years)				
5–14		1.0		1.0
15–24		0.77 (0.56, 1.05)		0.64 (0.17, 2.43)
25–34		0.54 (0.38, 0.76)		0.89 (0.34, 3.01)
35 +		0.39 (0.26, 0.58)		–
Attained age (years)				
< 55	1380	1.0	302	1.0
55–64	2568	0.55 (0.38, 0.82)	490	0.64 (0.25, 1.68)
65–74	2640	0.38 (0.25, 0.57)	351	0.22 (0.06, 0.67)
75 +	1166	0.40 (0.24, 0.66)	74	0.17 (n.d., 0.85)
Annual exposure rate (WL)				
< 0.5		1.0		1.0
0.5–1.0		0.60 (0.31, 1.08)		1.00 (0.38, 2.36)
1.0–5.0		0.42 (0.31, 0.64)		0.29 (0.11, 0.68)
5.0 +		0.17 (0.12, 0.25)		–
LEAR per WLM ($\times 10^4$)		5.38		7.50

ERR Excess relative rate; *CI* Confidence interval; *LEAR* Lifetime excess absolute risk; *PUMA* Pooled uranium miners analysis; *WLM* Working level months, *WL* Working level; *n.d.* Lower bound not determined

Table 3 Lifetime excess absolute risk (LEAR) estimates obtained using a model with effect modifiers defined by categories of age at exposure, attained age, and annual exposure rate in the full PUMA cohort and the PUMA 1960 + sub-cohort

	PUMA full cohort Kelly-Reif et al. (2023)		PUMA 1960 + sub-cohort Richardson et al. (2022)	
	Lung cancer deaths (*n*)	Estimate (95% CI)	Lung cancer deaths (*n*)	Estimate (95% CI)
ERR/100 WLM	7754	6.47 (3.39, 10.06)	1217	8.38 (3.30, 18.99)
Age at exposure (years)				
50 +		1.0		1.0*
35–49		0.83 (0.54, 1.39)		1.0*
< 35		0.55 (0.36, 0.92)		0.59 (0.30, 1.20)
Attained age (years)				
< 55	1380	1.0	302	1.0
55–64	2568	0.40 (0.28, 0.59)	490	0.55 (0.24, 1.30)
65–74	2640	0.21 (0.15, 0.31)	351	0.20 (0.06, 0.53)
75 +	1166	0.19 (0.12, 0.29)	74	0.14 (n.d., 0.64)
Annual exposure rate (WL)				
< 0.5		1.0		1.0
0.5–1.0		0.57 (0.29, 1.00)		1.23 (0.49, 2.77)
1.0–5.0		0.39 (0.28, 0.58)		0.33 (0.13, 0.75)
5.0 +		0.15 (0.11, 0.22)		-
LEAR per WLM ($\times 10^4$)		5.57		7.66

ERR Excess relative rate; *CI* Confidence interval; *LEAR* Lifetime excess absolute risk; *PUMA* Pooled uranium miners analysis; *WLM* Working level months, *WL* Working level; *n.d.* Lower bound not determined

*Reference category is ≥ 35 years (i.e., categories 50 + and 35–49 years are combined)

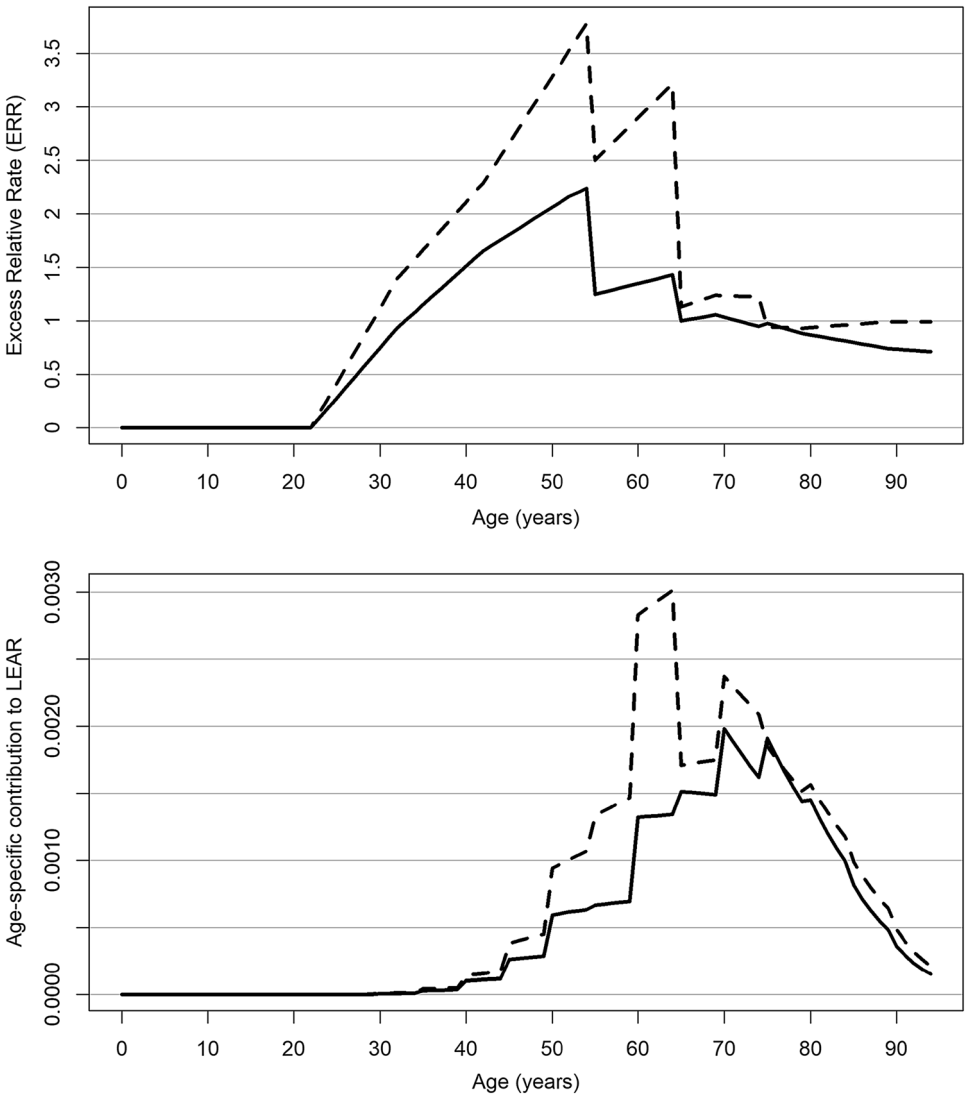

Fig. 1 LEAR components by attained age (Upper part: ERR(a), Bottom part: age-specific contribution to LEAR, $r_0(a)\mathrm{ERR}(a)\tilde{S}(a)$) predicted in the full PUMA cohort (Kelly-Reif et al. 2023, solid line) and the PUMA 1960 + sub-cohort (Richardson et al. 2022, dashed line) for the exposure scenario of 2 working level months (WLM) per year from age 18 to 64 up to age < 95 years, assuming a 5-year lag for the BEIR VI exposure–age–concentration model, and using baseline mortality rates derived from the ICRP mixed Euro-American-Asian population (ICRP 2007)

5.57×10^{-4} in the full cohort, respectively, and thus comparable to that based on the BEIR VI exposure–age–concentration model. Again, the estimated LEAR is higher in the 1960 + sub-cohort compared to the full cohort. Supplementary Fig. 2 (upper part) shows that the ERR(a) is highest at younger attained ages, however no further decrease in ERR(a) is observed after age 65 years in the full cohort or after age 75 years in the 1960 + sub-cohort. Supplementary Fig. 2 (bottom part) provides a similar pattern as for the BEIR VI model. Again, in the full PUMA cohort, there is an increase in the age-specific contribution to LEAR up to age 70–75 years and then a strong decrease. This corresponding peak in the 1960 + sub-cohort is again at ages 60–65 years.

To compare the LEAR per WLM of the PUMA study with those estimated in the previous studies, the LEAR per WLM for all published risk models of uranium miners studies that include time- and age-related effect modifiers have been re-estimated. Table 4 provides an overview of these studies, their characteristics, and related LEAR per WLM. The very first published study providing a relative risk model was a meta-analysis of 7 cohorts, the so-called "Jacobi study" (ICRP 1993; Chmelevsky et al. 1994) with a re-estimated LEAR per WLM of 3.20×10^{-4} based on 1047 lung cancer deaths and 31,486 miners. The cohort included a wide range of exposures and exposure rates; however, risk models did not account for exposure rate. This may have introduced an underestimation of true risk at low exposures due to ignoring the well-established inverse exposure-rate effect (NRC 1999, UNSCEAR 2020). In 1999, the results of the pooled analyses of the 11 miners cohort study were published (NRC 1999), including more than twice the number of miners ($n = 67{,}897$) and three times more lung cancer deaths ($n = 2787$) than the Jacobi study. In addition, as a new model, the BEIR VI exposure–age–concentration model was developed and applied (NRC 1999). For this risk model, the

Table 4 Lifetime excess absolute risk (LEAR) estimates obtained using previously published risk models of uranium miners cohort studies that include time- and age-related effect modifiers

Study	Publication	# Miners	# Lung cancer deaths	Person-years at risk (Mio)	Mean WLM	Mean duration of follow-up	Mean duration of employment	Model	LEAR per WLM ($\times 10^4$)
Meta estimate from 7 miners cohorts	ICRP (1993)	31,486	1047	0.6	120	n.a	n.a	Cat. Model (TSE, AA)	3.20
Full cohorts, full range of exposures, three modifiers TSE or AE, AA, and ER									
Pooled 11 miners cohort	NRC (1999)	67,897	2787	1.2	164	18	6	BEIR VI (TSE, AA, ER)	5.97
Eldorado	Lane et al. (2010)	16,236	618	0.5	117	31	2	BEIR VI (TSE, AA, ER)	8.20
Wismut (FU 2013)	Kreuzer et al. (2018)	58,974	3942	2.3	280	40	13	BEIR VI (TSE, AA, ER)	2.50
Czech cohort	UNSCEAR (2020)	9978	1141	0.3	73	31	8	BEIR VI (TSE, AA, ER)	4.22
Wismut (FU 2018)	Kreuzer et al. (2023)	58,972	4329	2.5	280	42	13	BEIR VI (TSE, AA, ER)	3.13
PUMA	Kelly-Reif et al. (2023)	119,709	7754	4.3	191	36	10	BEIR VI (TSE, AA, ER)	5.38
PUMA	Kelly-Reif et al. (2023)	119,709	7754	4.3	191	36	10	Cat. Model (AE, AA, ER)	5.57
PUMA without Wismut	Kelly-Reif et al. (2023)	64,790	3995	2.2	98	33	6	BEIR VI (TSE, AA, ER)	8.78
Cohorts restricted to more recent periods with chronic low exposures or exposure rates, three modifiers TSE or AE, AA, and ER									
Cz + Fr (measured)*	Tomasek et al. (2008a)	10,100	547	0.2	47	n.a	n.a	Cont. Model (TSME, AME)	4.58
Cz + Fr + Eldorado (< 100 WLM)	Lane et al. (2019)	n.a	408	0.4	36	n.a	n.a	BEIR VI (TSE, AA, ER)	4.56
Wismut 1960 + (FU 2013)	Kreuzer et al. (2023)	26,764	495	1.0	17	36	10	BEIR VI (TSE, AA, ER)	9.22
Wismut 1960 + (FU 2018)	Kreuzer et al. (2023)	26,764	663	1.1	17	40	10	BEIR VI (TSE, AA, ER)	6.10
PUMA 1960 +	Richardson et al. (2022)	57,873	1217	1.9	13	33	8	BEIR VI (TSE, AA, ER)	7.50
PUMA 1960 +	Richardson et al. (2022)	57,873	1217	1.9	13	33	8	Cat. Model (AE, AA, ER)	7.66

LEAR calculation based on: Exposure scenario: 2 WLM per year from age 18 to 64 years, Baseline mortality rate: mixed Euro-American-Asian population (ICRP 2007), Lifetime risk calculated up to age < 95 years, Projection model: relative risk model

TSE Time since exposure; *AA* Attained age; *AE* Age at exposure; *ER* Exposure rate; *TSME* Time since median exposure; *AME* Age at median exposure; *LEAR* Lifetime excess absolute risk; *WLM* Working level months; *BEIR VI*: BEIR VI exposure–age–concentration model (NRC 1999); *n.a.* Not available

*Continuous variables for the effect modifiers time since median exposure (TSME) and age at median exposure (AME) restricted to person-years at risk with "measured" (annual estimates based on current ambient measurements or personal dosimeters) instead of "estimated" (retrospectively estimated or extrapolated) radon concentrations

estimated LEAR per WLM was 5.97×10^{-4} and thus two times higher compared to the Jacobi study.

The BEIR VI pooled analysis did not include the newly established large German Wismut cohort (Grosche et al. 2006). The full Wismut cohort comprises 58,974 workers and 3942 lung cancer deaths at end of follow-up in 2013 (Kreuzer et al. 2018) and resulted in an LEAR per WLM of 2.50×10^{-4}. With the extended mortality follow-up to end of 2018 and additional baseline stratification by duration of employment like in the PUMA cohort, the LEAR per WLM increased to 3.13×10^{-4} (Kreuzer et al. 2023). Two smaller individual studies, the Czech (UNSCEAR 2020) and Eldorado (Lane et al. 2010) cohorts, showed LEAR estimates per WLM of 4.22×10^{-4} and 8.20×10^{-4}, respectively. The PUMA full cohort is currently the largest study with 119,709 miners and 7754 lung cancer deaths and integrates most of the updated studies included in BEIR VI and the Wismut cohort. The estimated LEAR per WLM of 5.38×10^{-4} or 5.57×10^{-4} (depending on choice of model) is consistent with that of the BEIR VI study and two times higher than that for the full Wismut cohort.

Table 4 additionally provides information on cohorts restricted to chronic low exposures and exposure rates. The estimated LEAR per WLM was around 4.6×10^{-4} for two smaller studies, the pooled analyses of full Czech and French cohorts with restriction of person-years at risk to measured radon exposure (Tomasek et al. 2008a) and of the Czech, French and Eldorado sub-cohorts with restriction to more recent years and exposures less than 100 WLM (Lane et al. 2019). The LEAR in the Wismut 1960 + sub-cohort with end of follow-up 2013 and 2018 (Kreuzer et al. 2023) were 9.22×10^{-4} and 6.10×10^{-4}, respectively. Among these low exposure/exposure-rate studies, the PUMA 1960 + sub-cohort is by far the largest study (57,873 miners and 1217 lung cancer deaths) and involves the lowest average radon exposure (13 WLM), the corresponding LEAR was around 7.50×10^{-4}. Compared to the respective full cohorts, the LEAR of the 1960 + sub-cohorts of the PUMA and the Wismut study were somewhat higher.

Discussion

PUMA provides the largest and most informative database to date to estimate the risk of death from lung cancer due to cumulative radon exposure in studies of uranium miners. The LEAR per WLM is estimated to lie between 5.38×10^{-4} and 7.66×10^{-4} depending on the choice of model and the use of the full cohort or the 1960 + sub-cohort with a focus on more recent periods of chronic low exposure. While the choice of model within a given cohort has a nearly negligible effect on the resulting LEAR, the consideration of either the full cohort or 1960 + sub-cohort makes a difference, with somewhat higher LEAR results for the latter cohort. In contrast to the PUMA full cohort, in the 1960 + sub-cohort the estimated parameters of the relative risk model have less heterogeneity between studies, but wider confidence intervals.

Comparison of results from full and 1960 + sub-cohorts

In the full PUMA cohort, heterogeneity in risk estimates between studies has been reported by Kelly-Reif et al. (2023), which was in part attributed to the Wismut study, which forms half of the data of PUMA (2.2 out of 4.3 million person-years at risk). The PUMA full cohort excluding the Wismut study would result in an LEAR per WLM of 8.78×10^{-4}. This restricted cohort differs from the PUMA Wismut cohort in some characteristics, e.g., appreciably lower exposures and shorter duration of employment (see also Table 1). For example, within the full PUMA study, 82% of the person-years at risk accrued from radon exposures above 250 WLM and about 70% of all person-times at risk with duration of employment more than 10 years are from the Wismut cohort (Kelly-Reif et al. 2023 Suppl. Table 1), respectively. It is unclear whether this difference has some influence on the risk estimates. The overview on LEAR estimates from published uranium miners studies in Table 4 shows that the findings of the full Wismut cohort are at the lower end of the range of all calculated LEAR. Possible reasons for this observed lower estimated risk like competing risk of silicosis, measurement error in exposure assessment, or possibly incomplete follow-up in the very early years (1946–1960) were addressed in detail in Kreuzer et al. (2023).

In contrast to the analyses based on full cohorts (Kelly-Reif et al. 2023), PUMA analyses of the 1960 + sub-cohorts did not provide any evidence of heterogeneity in risk estimates between studies (Richardson et al. 2022). The 1960 + sub-cohorts allow direct estimation of health effects of chronic exposure to low radon concentrations at low exposure rates which is of interest for radiation protection today. It also allows to exclude miners with extreme levels of exposure (estimated effective doses for some miners employed in the early years could reach several hundreds or thousands of mSv per year) (Laurier 2020). In addition, no complex modeling of exposure rate is necessary as compared to the full cohort; in several of the component studies, exposure rates were one or two orders of magnitude higher in the early years compared to 1960 or later. Furthermore, exposure assessment in these later years was often based on measurements rather than on expert rating. A higher quality of exposure assessment decreases measurement error and thus the potential for underestimation of risk. However, the 1960 + sub-cohorts involve lower statistical power due to smaller size, high uncertainty in parameter estimates, shorter

duration of follow-up, and younger age compared to the full cohorts. The observed increase in ERR at older ages in the PUMA 1960 + sub-cohort (Fig. 1 upper part) and particularly in the Wismut 1960 + sub-cohort with end of follow-up 2013 (Kreuzer et al. 2023, Supplementary Fig. 3) seems implausibly high. In these young 1960 + sub-cohorts, lung cancer deaths are still rare at ages over 75 years and at more than 35 years since exposure (see Tables 2 and 3). Consequently, it is likely that the decrease in ERR/WLM with increasing time since exposure and attained age cannot be completely described by the data of 1960 + sub-cohorts. For example, in the Wismut 1960 + sub-cohort, the extension of end of follow-up from 2013 to 2018 led to a decrease of LEAR per WLM from 9.22 to 6.10×10^{-4} (Kreuzer et al. 2023 Suppl. Table 3). Thus, further follow-up of individual PUMA studies will allow refining risk estimates derived from 1960 + cohorts in the future.

Strengths and limitations

The current calculations of the LEAR for lung cancer due to radon from various uranium miners studies offer several strengths. First, similar methods have been used, and thus, LEAR values based on different studies and relative risk models are directly comparable. Second, for the first time, LEAR was calculated based on the worldwide largest and most informative study PUMA. More than 4.3 million person-years at risk and nearly 8000 lung cancer deaths with a long duration of follow-up form the basis for PUMA (Rage et al. 2020; Richardson et al. 2021, 2022; Kelly-Reif et al. 2023). This large database allows—in contrast to many individual studies—for detailed consideration of relevant effect modifiers age, time since exposure and exposure rate in the risk model, a recommendation that was recently reinforced by UNSCEAR (2020). Third, the LEAR were determined for cohorts restricted to low exposures and exposure rates including all three effect modifiers in the risk models.

A limitation of the current LEAR analyses is that many factors with potential influence on the LEAR have not yet been evaluated. This concerns (1) the use of different and more suitable baseline mortality rates as well as evaluation of effects of the increasing survival trend for lung cancer, (2) consideration of smoking (interaction of smoking with radon, change of smoking patterns over time), (3) application of other scenarios from occupational or residential radon exposure, (4) consideration of annual instead of average exposure rates in risk models (Tomasek 2020), (5) use of different risk projection models (relative/additive/mixed), and (6) evaluation of uncertainties associated with LEAR estimates (e.g., confidence intervals). A general limitation of all the uranium miners studies considered in this paper is that they include only men and that only mortality and no incidence data for lung cancer are available.

Conclusion

PUMA clearly strengthens evidence on the shape of the exposure–response relationship between radon exposure and lung cancer mortality in uranium miners and thus the estimation of the LEAR. The range of currently available LEAR values for lung cancer at low exposures and exposure rates derived from different models and previous publications based on smaller studies is 2.5 to 9.2×10^{-4} per WLM, with the current PUMA findings (5.4 up to 7.7×10^{-4} per WLM) being in the upper half of this range. Continued mortality follow-up of the studies included in PUMA, particularly of the 1960 + sub-cohorts, is expected to provide additional insights and is therefore strongly recommended.

Supplementary Information The online version contains supplementary material available at https://doi.org/10.1007/s00411-023-01049-w.

Acknowledgements Some contents of Table 1 and 2 are reproduced from [Rage et al. OEM 77(3):194–200, 2020] and some contents of Table 2 and 3 from [Kelly-Reif et al. OEM 80:385–391, 2023], both with permission from BMJ Publishing Group Ltd.

Author contributions MK wrote the main manuscript, MS made the statistical analyses and prepared the figures. All authors reviewed the manuscript.

Funding Open Access funding enabled and organized by Projekt DEAL. This work was supported, in part, by the Centers for Disease Control and Prevention (CDC, R03 OH010946). The construction of the French cohort was partially supported by the Institute for Radiological Protection and Nuclear Safety (IRSN). IRSN thanks ORANO for its cooperation in the elaboration of the French cohort. For the U.S. contribution, funding was provided by the National Institute for Occupational Safety and Health. L.B.Z.'s work was funded and supported by the CDC in association with the National Institute for Occupational Safety and Health (NIOSH; R21OH011452). For the Czech cohort, funding was provided by the National Radiation Protection Institute (SURO; MV-25972-2/OBV). Work on the Ontario cohort was funded by the Canadian Nuclear Safety Commission, the Ontario Ministry of Labor, and the Canadian Cancer Society.

Declarations

Conflict of interest The authors have no relevant financial or non-financial interests to disclose.

Ethical approval This study does not require ethical approval as it is methodological work.

Disclaimer The findings and conclusions of this report are those of the authors and do not necessarily represent the decisions, policy, or views of the International Agency for Research on Cancer/World Health Organization or the National Institute for Occupational Safety and Health, Centers for Disease Control.

References

Chmelevsky D, Barclay D, Kellerer AM, Tomasek L, Kunz E, Placek V (1994) Probability of causation for lung cancer after exposure to radon progeny: a comparison of models and data. Health Phys 67:15–23

Grosche B, Kreuzer M, Kreisheimer M, Schnelzer M, Tschense A (2006) Lung cancer risk among German male uranium miners: a cohort study, 1946–1998. Br J Cancer 95:1280–1287

Harrison JD, Marsh JW (2020) ICRP recommendations on radon. Ann ICRP 49(1_suppl):68–76

Harrison JD (2021) Lung cancer risk and effective dose coefficients for radon: UNSCEAR review and ICRP conclusions. J Radiol Prot 41:433–441

ICRP (2007) The 2007 recommendations of the international commission on radiological protection. ICRP publication 103. Ann ICRP 37:2–4

ICRP (1993) Protection against Radon-222 at home and at work. ICRP Publication 65. Ann ICRP 23(2):413

ICRP (2010) Lung cancer at risk from radon and progeny & statement on radon. ICRP Publication 115. Ann ICRP 40(1):1

Kelly-Reif K, Bertke S, Rage E, Demers PA, Fenske N, Deffner V, Kreuzer M, Samet JM, Schubauer-Berigan MK, Tomasek L, Zablotska LB, Wiggins C, Laurier D, Richardson DB (2023) Radon and lung cancer in the pooled uranium miners analysis (PUMA): highly-exposed early miners and all miners. Occup Environ Med 80:385–391

Kreuzer M, Sobotzki C, Schnelzer M, Fenske N (2018) Factors modifying the radon-related lung cancer risk at low exposures and exposure rates among German uranium miners. Radiat Res 189:165–176

Kreuzer M, Deffner V, Sommer M, Fenske N (2023) Updated risk models for lung cancer due to radon exposure in the German uranium miners cohort, 1946–2018. Radiat Environ Biophys 62:415–425

Lane RS, Frost SE, Howe GR, Zablotska LB (2010) Mortality (1950–1999) and cancer incidence (1969–1999) in the cohort of Eldorado uranium workers. Radiat Res 174:773–785

Lane RS, Tomasek L, Zablotska LB, Rage E, Momoli F, Little J (2019) Low radon exposures and lung cancer risk: joint analysis of the Czech, French, and Beaverlodge cohorts of uranium miners. Int Arch Occup Environ Health 92:747–762

Laurier D, Marsh JW, Rage E, Tomasek L (2020) Miner studies and radiological protection against radon. Ann ICRP 49(1_suppl):57–67

Marsh JW, Tomasek L, Laurier D, Harrison JD (2021) Effective dose coefficients for radon and progeny: a review of ICRP and UNSCEAR values. Radiat Prot Dosim 195:1–20

NRC, National Research Council (1999) Committee on health risks of exposure to Radon. Board on radiation effects research. Health effects of exposure to radon. BEIR VI Report. National Academy Press, Washington

R Core Team (2022) R: a language and environment for statistical computing. R Foundation for Statistical Computing, Vienna, Austria. URL https://www.R-project.org/

Rage E, Richardson DB, Demers PA, Do M, Fenske N, Kreuzer M, Samet J, Wiggins C, Schubauer-Berigan MK, Kelly-Reif K, Tomasek L, Zablotska LB, Laurier D (2020) PUMA—pooled uranium miners analysis: cohort profile. Occup Environ Med 77(3):194–200

Richardson DB, Rage E, Demers PA, Do MT, DeBono N, Fenske N, Deffner V, Kreuzer M, Samet J, Wiggins C, Schubauer-Berigan MK, Kelly-Reif K, Tomasek L, Zablotska LB, Laurier D (2021) Mortality among uranium miners in North America and Europe: the Pooled Uranium Miners Analysis (PUMA). Int J Epidemiol 50:633–643

Richardson DB, Rage E, Demers PA, Do MT, Fenske N, Deffner V, Kreuzer M, Samet J, Bertke SJ, Kelly-Reif K, Schubauer-Berigan MK, Tomasek L, Zablotska LB, Wiggins C, Laurier D (2022) Lung cancer and radon: pooled analysis of uranium miners hired in 1960 or later. Environ Health Perspect 130:57010

Tomasek L, Rogel A, Tirmarche M, Mitton N, Laurier D (2008a) Lung cancer in French and Czech uranium miners: Radon-associated risk at low exposure rates and modifying effects of time since exposure and age at exposure. Radiat Res 169:125–137

Tomasek L, Rogel A, Laurier D, Tirmarche M (2008b) Dose conversion of radon exposure according to new epidemiological findings. Radiat Prot Dosim 130:98–100

Tomasek L (2020) Lung cancer lifetime risks in cohort studies of uranium miners. Radiat Prot Dosim 191:171–175

UNSCEAR (2020) Lung cancer from exposure to radon. UNSCEAR 2019 Report, Annex B, New York.

12. Methods to derive uncertainty intervals for lifetime risks for lung cancer related to occupational radon exposure

Contributing publication

Sommer, M., Fenske, N., Heumann, C., Scholz-Kreisel, P., & Heinzl, F. (2024). Methods to derive uncertainty intervals for lifetime risks for lung cancer related to occupational radon exposure. arXiv preprint arXiv:2412.06054. https://arxiv.org/abs/2412.06054

Declaration of contributions

I, Manuel Sommer, wrote the main manuscript and carried out and contributed the following work for the publication:

- **Statistical analysis**
  - Data collection and preparation (WHO mortality database)
  - Statistical analysis from idea, design, and execution, accompanied by discussion on methodology with Nora Fenske, Felix Heinzl, and Christian Heumann
  - Conception and implementation of uncertainty assessment methods in statistical software *R*, including risk model derivation adapting methods from the statistical software *Epicure*
  - Conception and preparation of figures and tables
- **Writing**
  - Conception and writing of the manuscript
  - Literature screening
  - Review of the manuscript (together with all other authors)

Notes

A corresponding manuscript version of the presented arXiv publication was submitted to the *Health Physics* Journal on December 10^{th}, 2024. The manuscript was accepted for publication on March 10^{th}, 2025, following a single round of revision. At the time of writing this thesis, the manuscript was undergoing typesetting for publication. The final accepted version differs from the arXiv preprint in a more detailed discussion of smoking interaction and other contextual aspects. However, no additional analyses were conducted beyond those presented in the arXiv preprint.

Methods to derive uncertainty intervals for lifetime risks for lung cancer related to occupational radon exposure

Sommer M[(a)], Fenske N[(a)], Heumann C[(b)], Scholz-Kreisel P[(a)], Heinzl F[(a)]

Affiliations:

[(a)]Federal Office for Radiation Protection
Ingolstädter Landstrasse 1
85764 Oberschleissheim Neuherberg
Germany.

[(b)]Department of Statistics
LMU Munich
Ludwigstrasse 33
80539 Munich
Germany.

Abstract

Introduction

Lifetime risks are a useful tool in quantifying health risks related to radiation exposure and play an important role in the radiation detriment and – in the case of radon – for radon dose conversion. This study considers the lifetime risk of dying from lung cancer related to occupational radon exposure. For this purpose, in addition to other risk measures, the lifetime excess absolute risk (LEAR), is mainly examined. Uncertainty intervals for such lifetime risk estimates are only hardly presented in the literature.

Objectives

The objective of this article is to derive and discuss uncertainty intervals for lifetime risk estimates for lung cancer related to occupational radon exposure.

Methods

Based on previous work, uncertainties of two main components of lifetime risk calculations are modelled: uncertainties of risk model parameter estimates describing the excess relative risk for lung cancer and of baseline mortality rates. Approximate normality assumption (ANA) methods derived from likelihood theory and Bayesian techniques are employed to quantify uncertainty in risk model parameters. The derived methods are applied to risk models from the German "Wismut" uranium miners cohort study (full Wismut cohort with follow-up 2018 and 1960+ sub-cohort with miners first hired in 1960 or later). Mortality rate uncertainty is assessed based on information from the WHO mortality database. All uncertainty assessment methods are realized with Monte Carlo simulations. Resulting uncertainty intervals for different lifetime risk measures are compared.

Results

Uncertainty from risk model parameters imposes the largest uncertainty on lifetime risks but baseline lung cancer mortality rate uncertainty is also substantial. Using the ANA method accounting for uncertainty in risk model parameter estimates, the LEAR in % for the 1960+ sub-cohort risk model was 6.70 with a 95% uncertainty interval of [3.26; 12.28] for the exposure scenario of 2 Working level Months from age 18-64 years, compared to the full cohort risk model with a LEAR in % of 3.43 and narrower 95% uncertainty interval [2.06; 4.84]. ANA methods and Bayesian techniques with a non-informative prior yield similar results. There are only minor differences across different lifetime risk measures.

Conclusion

Based on the present results, risk model parameter uncertainty accounts for a substantial and sufficient share of lifetime risk uncertainty for radon protection. ANA methods are the most practicable and should be employed in the majority of cases. The explicit choice of lifetime risk measures is negligible. The derived uncertainty intervals are comparable to the range of lifetime risk estimates from uranium miners studies in the literature. These findings should be accounted for when developing radiation protection policies which are based on lifetime risks.

Keywords: radon, lung cancer, epidemiology, uncertainty, risk analysis

1 Introduction

Lifetime risks describe the probability of developing or dying from a specific disease (here: lung cancer death related to radon exposure) in the course of one's lifetime and play an important role in the epidemiological approach for radon dose conversion [1–3] and radiation detriment [4]. Valid lifetime risk estimates are crucial for effective radiation protection strategies. A lifetime risk estimate depends on several components, each imposing possible errors or uncertainties on the result. Lifetime lung cancer risk estimates related to radon exposure depend on (a) the exposure scenario, (b) baseline mortality rates for all causes of death and lung cancer, and (c) complex risk models describing the shape of the exposure-response relationship between radon exposure and lung cancer mortality. For occupational radon exposure, these risk models are derived from uranium miners cohorts. We focus on the latter two components (b) and (c) in the upcoming analysis, as own previous work [5] demonstrated their major influence on lifetime risk estimates.

Exposure to radon and radon progeny is a recognized leading cause of lung cancer. This association has been confirmed in uranium miners and residential radon studies [6–8]. Both uranium miners and residential radon studies have demonstrated a linear relationship between radon exposure and lung cancer risk, which is in case of uranium miners studies additionally influenced by factors like age, time since exposure, and exposure rate. The intricate nature of these models can make comparisons across different cohorts challenging. Lifetime risk estimates offer a valuable tool for comparison and interpretation of risk models and enable clearer public risk communication. However, current literature often lacks uncertainty intervals for lifetime risk estimates. Lifetime Excess Absolute Risk (LEAR) estimates derived from various international miners studies range from 2.5×10^{-4} to 9.2×10^{-4} per working level month (WLM) as reported by the large pooled uranium miners study PUMA [9]. The present study employs advanced statistical methods to quantify lifetime risk uncertainty with 95% uncertainty intervals.

Uncertainty intervals together with point estimates provide a more complete and more nuanced picture, allowing for informed decision-making, meaningful comparisons, and transparent communication. Uncertainty assessment for lifetime risks is a complex endeavor because final lifetime risk estimates are composite quantities depending on multiple, independently derived results.

The literature addressing lifetime risk estimation uncertainty for lung cancer related to radon exposure based on uranium miners cohorts is limited and generally does not prioritize uncertainty quantification [10, 11]. Existing studies typically employ Monte Carlo simulation techniques, incorporating various distributional assumptions for calculation components. For example, [10] investigated the LEAR and assumed a multivariate normal distribution for risk model parameters, while in the EPA Report [11] additionally a complex distribution for average residential radon exposure is assumed. A comparison of uncertainties across different lifetime risk measures could not be found in the literature. Uncertainties in risk measure estimates similar to lifetime lung cancer risks due to radon exposure, like "attributable cases", are better understood: In the BEIR VI report [6], Monte Carlo simulations are used to comprehensively quantify uncertainties for "attributable cases", similar to methods for lifetime lung cancer risks in [10].

Several software tools have been developed for calculating lifetime cancer risks and associated uncertainties. These tools, however, primarily rely on risk models derived from the Atomic Bomb Survivors Life-Span Study (LSS) [12], which involves acute external exposure to different radiation types, fundamentally different from the chronic internal exposure to radon progeny in occupational uranium miners studies. Notable among these tools are "CONFIDENCE" [13], "RadRAT" [14], and "LARisk" [15]. "CONFIDENCE" is a European software designed for cancer risk assessment post-radiation exposure from nuclear accidents. "RadRAT", a free tool based on the BEIR VII report [16], estimates lifetime cancer risks for the US population based on a user-specific exposure scenario. "LARisk" extends "RadRAT" by adding flexibility, such as modified baseline incidence rates, to tailor risk calculations for specific populations. While "CONFIDENCE" and "RadRAT" rely on Monte Carlo simulations and sampling from probability distributions for uncertainty assessment, "LARisk" employs parametric

bootstrap methods.

Despite these advanced tools, there is a notable gap in the literature regarding the uncertainty quantification of lifetime risks for lung cancer specifically related to occupational radon exposure. Addressing this, our study places special emphasis on refining the understanding of these uncertainties, utilizing risk models derived from uranium miners cohorts. We specifically focus on the LEAR measure while also examining alternative excess lifetime risk measures: Risk of Exposure Induced Death (REID), Excess Lifetime Risk (ELR), [17, 18] and Radiation-Attributed Decrease of Survival (RADS) [19]. We elaborate on sources of uncertainty for lifetime risks, discuss existing techniques, and introduce advanced methods to quantify these uncertainties by calculating 95% uncertainty intervals.

To derive such intervals, both frequentist methods derived from likelihood theory and Bayesian techniques, chosen for their flexibility, are employed to quantify uncertainty in risk model parameter estimates. These methods are applied to risk models derived from the German Wismut uranium miners cohort study as a practical example. Mortality rate uncertainty is assessed based on information from the WHO mortality database [20]. All uncertainty assessment methods are realized through Monte Carlo simulations.

By systematically analyzing and advancing the methodologies for quantifying uncertainties in lifetime risk estimates, this study aims to contribute to a more stable basis for radon protection strategies and provide a more comprehensive assessment of lifetime risks, especially for lung cancer related to occupational radon exposure.

2 Methods

2.1 Lifetime risk definition and computation

For a lifetime risk measure of choice, we employ the Lifetime Excess Absolute Risk (LEAR). This measure is often used [10, 18, 21–23] and is defined as

$$LEAR_E = LR_E - LR_0 = \int_0^\infty \left(r_E(t) - r_0(t)\right) S(t)\, dt = \int_0^\infty r_0(t) ERR(t;\Theta) S(t)\, dt. \tag{1}$$

The lifetime risk of dying from a specific disease (here: lung cancer) under exposure (here: radon and radon progeny) is $LR_E = \int_0^\infty r_E(t) S(t)\, dt$ and $LR_0 = \int_0^\infty r_0(t) S(t)\, dt$ is the corresponding baseline lifetime risk without exposure. $r_0(t)$ is the baseline lung cancer mortality rate and $r_E(t)$ is the lung cancer mortality rate under exposure at age t. $S(t) = \mathbb{P}(T \geq t)$ is the survival function and describes the probability to attain age t with $T \geq 0$ the unknown random retention time until death. The survival function is modeled as $S(t) = e^{-\int_0^t q_0(u)\, du}$ with baseline mortality rates $q_0(u)$ at age u for overall death (all-cause mortality rates). $ERR(t;\Theta)$ specifies the excess relative risk at age t with unknown parameter set Θ. Overall, we assume the following risk projection model:

$$r_E(t) = r_0(t)\left(1 + ERR(t;\Theta)\right). \tag{2}$$

The exact structure and complexity of the $ERR(t) := ERR(t;\Theta)$ term depends, in addition to age t, on the chosen risk model with parameters Θ and its included effect-modifying variables. The $LEAR$ from equation (1) is estimated and finally calculated with the approximation

$$LEAR \approx \sum_{t=0}^{t_{max}} r_0(t) ERR(t;\hat{\Theta}) \tilde{S}(t). \tag{3}$$

For lifetime risk calculations, parameter estimates $\hat{\Theta}$ are plugged into the corresponding risk model structure. $\tilde{S}(t) = e^{-\sum_{u=0}^{t-1} q_0(u)}$ approximates the true survival function $S(t)$ and is based on the Nelson-Aalen estimator of the cumulative hazard rate [24]. The maximum age t_{max} was set to $t_{max} = 94$ for

comparability with previous studies on lifetime risks [22, 23].

A lifetime risk estimate further depends on the chosen risk model shaping $ERR(t;\Theta)$, the mortality rates $r_0(t), q_0(t)$ for all ages $0 \leq t \leq t_{max}$ and the assumed radon exposure in WLM for all ages $0 \leq t \leq t_{max}$ (exposure scenario). In line with all considered risk models, the latency time L in risk models, i.e. the minimal time between age at exposure and age at lung cancer risk amplification, was chosen as $L = 5$ years.

Here, a generic lifetime risk estimate for a given risk model without uncertainty quantification is always calculated with an exposure scenario of 2 WLM from age 18-64 years (94 WLM total cumulative exposure over lifetime) to represent an occupational scenario, in line with the literature [10, 23, 25] and fixed mortality rates $r_0^{(ICRP)}(t), q_0^{(ICRP)}(t)$ for all ages $0 \leq t \leq 94$ from the Euro-American-Asian mixed reference population as presented in ICRP publication 103 [2]. Such a lifetime risk estimate does not reflect uncertainties and is referred to as "reference estimate (ICRP 103)" or simply "ref. estimate" in the following. Further, for enhanced readability, lifetime excess risk estimates such as LEAR are presented as percentages (LEAR in %, i.e. LEAR $\times 100$).

2.2 Data and risk models

To estimate the risk models associated with the German uranium miners cohort, this analysis employs cohort data, including cumulative radon exposure, age, and other variables of individual miners. This cohort data provides the basis for modeling and assessing the developed parametric (continuous) and categorical risk models, particularly for the quantification of uncertainties. All considered risk models include unknown parameters (indicated by Greek letters) which are estimated using Maximum-Likelihood methods. Access to the German uranium miners cohort data allows for re-fitting the subsequent described risk models and thereby for an uncertainty assessment of the resulting lifetime risks.

The following parametric (continuous) risk models are considered:

$$ERR(t;\beta_1,\beta_2,\ldots,\beta_6,\alpha,\varepsilon) = \sum_{j=1}^{6} er_j\beta_j W(t)\exp\left\{\alpha\left(AME(t)-30\right)\right) + \varepsilon\left(TME(t)-20\right)\right\}, \quad (4)$$

$$ERR(t;\beta,\alpha,\varepsilon) = \beta W(t)\exp\left\{\alpha\left(AME(t)-30\right)\right) + \varepsilon\left(TME(t)-20\right)\right\}, \quad (5)$$

$$ERR(t;\beta) = \beta W(t), \quad (6)$$

with cumulative radon exposure $W(t)$ at age t in WLM and continuous effect-modifying variables age at median exposure $AME(t)$ at age t in years, time since median exposure $TME(t)$ at age t in years, and binary variables er_j for $j = 1,\ldots,6$ for six categories of exposure rate at age t in units of working level (WL). Further, categorical BEIR VI exposure-age-concentration models (cf. [6]) are considered:

$$ERR(t;\theta^{(1)},\phi_{age},\gamma_{rate},\beta) = \beta\left(\theta_{5-14}W_{5-14} + \theta_{15-24}W_{15-24} + \theta_{25-34}W_{25-34} + \theta_{35+}W_{35+}\right)\phi_{age}\gamma_{rate}, \quad (7)$$

$$ERR(t;\theta^{(2)},\phi_{age},\gamma_{rate},\beta) = \beta\left(\theta_{5-14}W_{5-14} + \theta_{15-24}W_{15-24} + \theta_{25+}W_{25+}\right)\phi_{age}\gamma_{rate}, \quad (8)$$

with $\theta^{(1)} = (\theta_{5-14},\theta_{15-24},\theta_{25-34},\theta_{35+})$, $\theta^{(2)} = (\theta_{5-14},\theta_{15-24},\theta_{25+})$, and where W_{5-14}, W_{15-24}, W_{25-34}, W_{25+}, W_{35+} is the cumulative radon exposure in WLM in windows 5-14, 15-24, 25-34, 25+ or 35+ years ago and ϕ_{age} and γ_z are factors for attained age in years and exposure rate in WL, respectively.

All presented risk models are derived from the German Wismut cohort of uranium miners with follow-up 2018 and have been initially introduced in [23]. These models are used in this study as an application example of the subsequent introduced methods to quantify risk model parameter uncertainty. The models (5) "Parametric 1960+ sub-cohort", (6) "Simple linear 1960+ sub-cohort", and (8) "BEIR VI 1960+ sub-cohort" are derived from the Wismut sub-cohort with miners hired in 1960 or later (1960+ sub-cohort) and the models "Parametric full cohort" (4) and "BEIR VI full cohort" (7) are derived

from the corresponding full Wismut cohort. The derived parameter estimates are shown partly in the Supplement or can be inspected in the source paper [23]. The simple linear model (6) is included in this analysis for comparability. All other models were chosen because they showed the best fits for the corresponding cohort. The chosen risk models (categorical / BEIR VI structure, parametric / continuous with effect modifying variables, and simple linear risk model) offer a diverse range of risk models. Here, the terms "categorical" and "parametric / continuous" refer to the categorical or continuous nature of the effect-modifying variables.

All considered risk model parameters are estimated with maximum likelihood (ML) methods based on internal Poisson regression applied to grouped cohort data. The corresponding Likelihood function is based on the assumption that the number of lung cancer deaths C_i in cell i with $i = 1, \ldots, n$ are Poisson-distributed via

$$C_i \sim Poi\left(PY_i e^{\delta_1 + \sum_{k=2}^{K} \delta_k \mathbb{1}_{\{k\}}(x_i)} \left(1 + ERR_i\left(\Theta\right)\right)\right) \tag{9}$$

with offset for person-years at risk PY_i, excess relative risk $ERR_i\left(\Theta\right)$ and unknown parameter vector Θ. The specific shape of $ERR_i\left(\Theta\right)$ depends on the prescribed risk model structure. The baseline risk predictor $\eta_i = \delta_1 + \sum_{k=2}^{K} \delta_k \mathbb{1}_{\{k\}}(x_i)$ describes the stratified baseline with K levels, where x_i is a categorical variable with K levels. Each level represents a unique combination of conditions or classifications that are relevant variables in assessing the baseline risk. Here, the levels correspond to different groups categorized by age, calendar year, and duration of employment. Setting $\Delta = (\delta_1, \delta_2, \ldots, \delta_K)$, the likelihood model consists of the parameters $\Omega = (\Delta, \Theta)$.

2.3 Uncertainty assessment

2.3.1 Uncertainty intervals for lifetime risks

Uncertainties for a parameter of interest are quantified by deriving 95% uncertainty intervals, which is a range of values that is calculated to cover the true unknown parameter value with 95% certainty. It consists of a lower and an upper bound, enclosed in parentheses. The precise interpretation of the uncertainty interval depends on the underlying statistical inference system (frequentist or Bayesian). Lifetime risks are composite quantities depending on multiple, independently derived results. Hence, we rely on sampling techniques to derive lifetime risk uncertainty intervals.

Here, uncertainties are determined by quantifying the variability in statistical estimates that results from drawing a sample from the entire population (sampling uncertainty). Risk model parameter uncertainties and mortality rate uncertainties are considered here. Depending on the investigated lifetime risk calculation component, previously fixed values for calculation components are replaced by random variables. The uncertainty quantification is carried out with Monte Carlo simulations. Here, we focus on the excess lifetime risk measure LEAR. N = 100,000 samples from the underlying assumed probability distribution are drawn independently and a LEAR is calculated for each sample resulting in N independent LEAR estimate samples. The two-sided 95% uncertainty interval is the span of observed LEAR samples by disregarding the 2.5% lowest and 2.5% highest samples. All upcoming methods use this approach to derive uncertainty intervals unless explicitly stated otherwise, but differ in the calculation component analyzed and the assumed probability distribution. Corresponding probability density functions for the LEAR distribution are derived from the histogram of LEAR samples with a kernel density estimate. Note that for lifetime risks, we additionally present the relative span of the uncertainty interval in brackets, calculated as the interval span divided by the reference estimate (relative uncertainty span). This enables easier comparison across various estimates irrespective of their absolute values.

2.3.2 Mortality rates

Uncertainties in the mortality rates $r_0(t), q_0(t)$ are assessed by assuming gamma distributions for all ages t,

$$r_0(t) \sim G\left(a_t^{(r_0)}, b_t^{(r_0)}\right), \tag{10}$$

$$q_0(t) \sim G\left(a_t^{(q_0)}, b_t^{(q_0)}\right). \tag{11}$$

with age-dependent shape parameters $a_t^{(r_0)}, a_t^{(q_0)}$ and rate parameter $b_t^{(r_0)}, b_t^{(q_0)}$ (SC Table 7). The parameter estimates $a_t^{(r_0)}, b_t^{(r_0)}, a_t^{(q_0)}, b_t^{(r_0)}$ are derived from data from the WHO Mortality Database [20] with maximum-likelihood (ML) methods. Observations from all available countries from Europe, America, and Asia for females and males from the years 2001, 2006, 2011, 2016, and 2021 are used. The derivation of probability distributions for mortality rates in (10) and (11) from WHO data is independent of the ICRP Euro-American-Asian reference mortality rates $r_0^(ICRP))(t)$ and $q_0^(ICRP))(t)$. However, the geographical alignment of the chosen WHO data with the ICRP mortality rates ensures the appropriateness of the data for estimating mortality rate variability. An observation used for fitting models (10) and (11) is characterized as the mortality rate $\frac{d}{n}$ where d are the number of lung cancer deaths for r_0 or all-cause deaths for q_0 and n is the mid-year population size. Each observation is uniquely defined by a specific country (out of 153 countries), sex, and calendar year. Only observations with a positive number of individuals at risk n and a positive number of cases d were considered. To obtain uncertainty intervals for lifetime risks, independent samples from the above described gamma distributions (10) and (11) are drawn (Monte Carlo simulation), analogously to drawing samples in the ANA approach for risk model parameters.

2.3.3 Risk models - ANA approach

The idea behind the Approximate normality assumption (ANA) approach is the following: Risk model parameter estimates $\hat{\Theta}_0$ are obtained by fitting the $ERR(t;\Theta)$ model to miners cohort data with ML methods assuming Poisson-distributed numbers of lung cancer cases (9). The ML method provides statistically efficient estimates, meaning they tend to be close to the true values on average given a sufficiently large sample size. The estimated parameters are subject to sampling uncertainty. By statistical theory, under mild regularity conditions met in our case [26], the parameter estimator $\hat{\Theta}$ in a given risk model is asymptotically (for an infinitely large cohort size) normally distributed with expectation equal to the unknown true parameter value Θ and covariance matrix equal to the inverse Fisher information, see [27, Equation (5.14)] or [28, Theorem 9.7]. The true parameter Θ is approximated with the cohort-specific maximum likelihood estimate (MLE) $\hat{\Theta}_0$. The inverse Fisher information can be approximated by an estimate $\hat{\Sigma}_0$ of the parameter covariance matrix.

The ANA approach follows the frequentist inference where the true risk model parameter Θ is treated as a fixed but unknown value. The parameter estimator $\hat{\Theta}$ is considered as a random variable subject to variability depending on the specific sample used in the estimation process. The estimate $\hat{\Theta}_0$ is a realization of $\hat{\Theta}$ by applying specific sample data. Following this framework, risk model parameter uncertainty is quantified by assuming a multivariate-normal distribution on the parameter estimator $\hat{\Theta}$,

$$\hat{\Theta} \sim \mathcal{N}\left(\hat{\Theta}_0, \hat{\Sigma}_0\right) \tag{12}$$

with cohort-specific ML estimate $\hat{\Theta}_0$ and covariance matrix estimate $\hat{\Sigma}_0$. By generating a large number of samples from this approximate distribution, and calculating the corresponding lifetime risks for each sample, the distribution of lifetime risk estimates reflects the inherited parameter sampling uncertainty. This approach is called the "Approximate normality assumption" (ANA) approach. In this study, we employ the *Epicure* software [29] to obtain parameter estimates $\hat{\Theta}_0$ and their associated covariance matrix estimate $\hat{\Sigma}_0$. Note that this method implicitly incorporates knowledge from the estimation of baseline parameters Δ, as the covariance estimate $\hat{\Sigma}_0$ is adjusted accordingly [29]. Importantly,

after this theoretical introduction, the manuscript simplifies notation by referring to estimates using $\hat{\Theta}$ without further distinguishing the estimator notation. Note that the ANA approach requires access to the ML estimate $\hat{\Theta}_0$ and covariance matrix estimate $\hat{\Sigma}_0$., but no access to underlying cohort data since a re-estimation of parameters is not necessary.

2.3.4 Risk models - Bayesian approach

In contrast to frequentist inference underlying the above ANA approach, in the Bayesian approach (Bayesian inference) the unknown parameter Θ is interpreted as a random variable itself. To apply Bayesian statistics to account for prior information about the risk model parameters we assume the generic Bayesian framework

$$P(\Omega|X) = \frac{P(\Omega)\, L(X)}{\int_\Omega L(X|\Omega)\, P(\Omega)\; d\Omega} \propto P(\Omega)\, L(X), \tag{13}$$

where $P(\Omega|X)$ is the posterior probability density function of observing the parameter Ω given cohort data X. $P(\Omega)$ is the prior probability density for Ω and $L(X) = L(X|\Omega)$ is the likelihood function. Here $\Omega = (\Delta, \Theta)$, compare (9). Using concepts from [30] allows to derive the marginal posterior distribution $P(\Theta|X)$ for risk model parameters Θ of interest analytically. This requires assuming independence between prior distributions for Δ and Θ and a non-informative prior for Δ. The resulting marginal posterior given cohort data X reads

$$P(\Theta|X) = \frac{P(\Theta)\left[\prod_{i=1}^{n}\left(1+ERR_i(\Theta)\right)^{C_i}\right]\left[\sum_{i|x_i=1} PY_i\left(1+ERR_i(\Theta)\right)\right]^{-S_1}}{M\prod_{k=2}^{K}\left[\sum_{i|x_i=k} PY_i\left(1+ERR_i(\Theta)\right)\right]^{S_k}} \tag{14}$$

with lung cancer cases in strata k, $S_k = \sum_{i|x_i=k} C_i$ for $k = 1, \ldots, K$ and normalizing constant M. Parameter estimats are derived as the values that maximize the posterior distribution (mode), denoted as $Mod(P(\Theta|X)) = \hat{\Theta}$, analogously to the ANA approach. Note that the Bayesian approach requires a re-estimation of parameters and therefore access to the original cohort data in contrast to the ANA approach.

This approach is applied to the 1960+ sub-cohort models (6) and (5). Identical model structures were used in [25], which we employ as prior information. Due to increasing computational complexity, it was not feasible to apply this approach to full cohort risk models (4), (7) and the sub-cohort model (8), which involve larger cohort data size and/or more parameters. Non-informative, uniform prior distributions for Θ are applied to obtain the true marginal likelihood. Otherwise, the prior information about β in the simple linear risk model (6) is modelled with a gamma distribution $\beta \sim G\left(a, \frac{a-1}{\hat{\beta}_{CZ+F}}\right)$ with $\hat{\beta}_{CZ+F} = 0.016$ from [25]. The prior information about β, α and ε for model (5) is modelled as $\beta \sim G\left(a, \frac{a-1}{\hat{\beta}'_{CZ+F}}\right)$, and normal distributions $\alpha \sim \mathcal{N}\left(\hat{\alpha}_{CZ+F}, \sigma^2\right)$, $\varepsilon \sim \mathcal{N}\left(\hat{\varepsilon}_{CZ+F}, \sigma^2\right)$ with $\hat{\beta}'_{CZ+F} = 0.042$, $\hat{\alpha}_{CZ+F} = -0.06539$, $\hat{\varepsilon}_{CZ+F} = -0.07985$ from [25]. Adjustments to the certainty of the prior information are achieved by modifying the gamma shape parameter a for η and the standard deviation σ for α and ε. . By construction, the modes of the marginal prior distributions align with the corresponding parameter estimate from [25]. All three components are assumed to be independent in the prior, i.e. $P(\Theta) = P(\beta) \cdot P(\alpha) \cdot P(\varepsilon)$. Importantly, estimates from [25] are not assumed as true "prior" knowledge, but illustrate integrating diverse cohort information using Bayesian methods (see Discussion).

For the simple linear model with (6), Rejection Sampling [27] was applied to obtain N = 100,000 samples of the posterior distribution of β with uniform proposal distribution $\mathcal{U}(0, 0.04)$. For the more complex risk model (5), Markov Chain Monte Carlo (MCMC) techniques via the Metropolis-Hastings algorithm were applied [31]. The approximate multivariate normal distribution (12)) was chosen as the proposal distribution. The log acceptance ratio for a proposal sample for $\Theta \sim P(\Theta|X)$ was calculated

as the difference of the log marginal posterior evaluated at the proposal sample and the current sample. The initial proposal sample for Θ was chosen in proximity of the cohort-specific ML estimate $\hat{\Theta}$. N = 100,000 samples of the posterior distribution are used for uncertainty assessment after generating 110,000 samples and discarding the first 10,000 samples to account for a burn-in period. Overall, the resulting MCMC sample paths of risk model parameters indicate rapid convergence to stationarity, likely due to an effective proposal distribution. Here, the presented 95% LEAR uncertainty intervals are derived by choosing the narrowest interval that covers 95% of the derived LEAR samples, which we refer to as the Highest Posterior Density Interval (HPDI).

2.3.5 Joint effect of risk model and mortality rate uncertainty

The joint effect of risk model parameter estimate uncertainty and mortality rate uncertainty on LEAR estimates is assessed by simultaneously sampling from gamma distributions for the mortality rates $r_0(t)$ for all ages t according to (10), and from multivariate normal distributions for the risk model parameter estimator $\hat{\Theta}$ according to the ANA approach (12), independently. Note that $q_0(t)$ variability is here not accounted for as initial analysis showed a negligible impact (see Results). Analogous to the general Monte Carlo simulation approach, N = 100,000 LEAR samples are calculated from N = 100,000 sets of sampled values for $r_0(t)$ for all ages t and $\hat{\Theta}$. All computations were carried out with the statistical software *R* [32].

2.4 Sensitivity analysis

The Supplemental Section A details uncertainties for other lifetime risk measures besides LEAR. Likewise, an explorative uncertainty assessment derived from a simple interpretation of lifetime risks based on the Kaplan-Meier estimator for survival curves [33] is explored (Suppl. Section B).

Sensitivity analyses (Suppl. Sections C to E) explore the impact of assuming different probability distributions on lifetime risk uncertainties. Additional insights on risk model parameter uncertainty is shown in Suppl. Section C.1 and C.3. Furthermore, the Bayesian approach for risk model parameter uncertainty quantification is applied to the simple linear risk model (6) with log-normal priors for β (Suppl. Section C.2). Analyses for the specific influence of all-cause mortality rate uncertainties are conducted (Suppl. Section D.1). An alternative Bayesian approach to assess mortality rate uncertainty employing the WHO data is found in the Suppl. Section D.2. Log-normal distributed mortality rates (Suppl. Section D.3) and sex-specific uncertainties regarding mortality rate and risk model effects are investigated (Suppl. Section E). Exposure scenario uncertainty is briefly investigated in the Suppl. Section F.

3 Results

3.1 Effect of mortality rates

Introductory analyses revealed that all-cause mortality rates $q_0(t)$ impose considerably less uncertainty on the LEAR than lung cancer rates $r_0(t)$ for all risk models (Suppl. Section D.1). The empirical distribution of LEAR samples for gamma-distributed $q_0(t)$ is considerably narrower compared to the empirical distribution for gamma-distributed $r_0(t)$, which is also reflected in the 95% uncertainty intervals. The relative uncertainty span of 95% uncertainty intervals is very similar across all considered risk models with roughly 0.10 for uncertainties in all-cause rates $q_0(t)$ and roughly 0.50 for uncertainties in lung cancer rates $r_0(t)$ and joint uncertainties $r_0(t)$, $q_0(t)$, (Suppl. Table 10). Hence, all-cause mortality rate uncertainty can be reasonably neglected when assessing overall mortality rate uncertainty, as addressed in the subsequent analyses.

3.2 Effect of risk model parameter uncertainty

LEAR estimates derived from full cohort risk models are notably lower than estimates derived with 1960+ sub-cohort models [9]. This discrepancy is particularly pronounced for the Wismut cohort

and primarily comes from the significantly lower estimates for Excess Relative Risk per 100 WLM (ERR/100 WLM) observed in the full cohort [23]. The variation between these ERR/100 WLM estimates is similarly reflected in the LEAR calculations.

3.2.1 Approximate normality assumption (ANA) approach

Table 1 shows the resulting 95% uncertainty intervals. For risk models fit on the full cohort the resulting intervals are comparable although the model structures differ considerably: The relative uncertainty span is 0.81 and 1.03 for the parametric (4) and the BEIR VI risk model (7), respectively. For the 1960+ sub-cohort models, however, the results vary relatively widely. Especially risk model (8) implies very wide LEAR uncertainty intervals with a relative uncertainty span of 6.27 and a notable portion of implausible negative LEAR samples. The model (5) implies considerably less uncertainty compared to the model (8) with a relative uncertainty span of 1.34, although both models are derived from the 1960+ sub-cohort. Visually (Figure 1), the empirical distribution of LEAR samples resembles approximately a normal distribution for risk model parameter estimates derived from the full cohort (models (4) and (7)). Conversely, the empirical distribution of LEAR samples with parameter estimates derived from the 1960+ sub-cohort inherit considerably heavier tails and a slight right skewness. The 1960+ sub-cohort is smaller and comparably young with less person-years at risk and less lung cancer deaths. This results in higher statistical uncertainty which is reflected in wider LEAR uncertainty intervals.

Note that, for the simple linear risk model (6) we obtain analytically, without sampling, a normal distribution

$$LEAR \sim \mathcal{N}\left(0.0571, 1.65 \times 10^{-4}\right)$$

with corresponding 95% uncertainty interval [3.18; 8.22] and relative uncertainty span of 0.88 for LEAR in %. By definition, this uncertainty intervals is proportional to the 95% confidence intervals [0.75; 1.93] for $\hat{\beta}_0 \times 100 = 1.34$ from [23] by a factor of 4.27 here. The underlying theory is explained in Suppl. Section C.1.

3.2.2 Bayesian approach

Computational limitations restricted the applicability of this approach to models (5) and (6). For the simple linear model (6), analogous to the ANA approach, LEAR uncertainty is directly proportional to β uncertainty. The posterior mode of $P(\beta|X)$ with 95% uncertainty intervals (HPDIs) for varying certainty in the prior information is shown in Table 3 with corresponding plots in Figure 3. The resulting HPDI with a uniform prior are comparable to the conventional 95% confidence interval for the estimate $\hat{\beta}$. However, the lower bound of the HPDI is notably higher than that of the classical confidence interval for $\hat{\beta}$. Further, the relative uncertainty span of the uncertainty interval decreases with increasing certainty in the prior information (increasing a) from 0.94 for $a = 2$ up to 0.48 for $a = 50$.

The resulting 95% HPDIs for the more complex model (5) are shown in Table 2 for the special choice of a standard deviation $\sigma = 0.02$ in the prior distributions for α and ε (Suppl. Section C.3 for more choices for σ and histograms of parameter samples). The corresponding distribution of LEAR samples is shown in Figure 2 (Plot a). As expected, increasing the prior certainty (increasing shape parameter a) shrinks the uncertainty interval and moves the reference estimate (ICRP 103) of LEAR in % from 6.74 (95% HPDI [2.96; 11.09]) without prior influence towards the prior LEAR in % estimate of 4.30 derived with the Joint Czech+French risk model. For example, $a = 50$ results in a LEAR in % of 4.99 and a 95% HPDI of [3.14; 7.26]. A very similar effect is observed for decreasing the standard deviation σ for a fixed shape parameter $a = 10$ (Figure 2 Plot b).

3.3 Joint effect of mortality rate and risk model parameter uncertainty

The empirical distribution of resulting LEAR samples, along with the corresponding 95% uncertainty intervals, varies depending on the underlying risk model and its parameters, especially for the 1960+

sub-cohort models (Figure 1, Table 1), last column). Risk model complexity and cohort size directly influence LEAR uncertainty intervals, as seen in the separate analyses. In contrast, the 95% uncertainty intervals from uncertain $r_0(t)$ are overall narrower compared to those from uncertain risk model parameters and consistent across all risk models with a relative uncertainty span of roughly 0.5. The joint effect of uncertain risk model parameters and uncertain lung cancer mortality rates is with a relative uncertainty span of roughly 1 almost similar to the effect with only uncertain risk model parameters. Only the 95% uncertainty interval [-9:91; 23.17] of the joint effect with relative uncertainty span of 5.76 for the BEIR VI 1960+ sub-cohort model (8) remains implausible, although slightly narrower. Overall, accounting for lung cancer mortality rate uncertainty in addition to risk model parameter uncertainty has low impact on the overall LEAR uncertainty interval.

4 Discussion

This work provides a considerable methodological contribution in radiation protection research by successfully deriving uncertainty intervals for radon-induced lifetime lung cancer risk estimates. These intervals are grounded in a sound statistical framework, shifting the approach from solely assessing single lifetime risk estimates to quantifying the uncertainties around these estimates. For a comprehensive assessment of lifetime risks, it is advisable to consider both the point estimate and the uncertainty intervals. From this perspective, we investigate two key contributors to uncertainties: baseline mortality rates and risk models. We introduce advanced methods for quantifying these uncertainties, facilitating their application in radiation-related research questions. Our results confirm the BEIR VII report finding that risk model uncertainty is a major driver of overall lifetime risk uncertainty [16]. Accounting for risk model parameter uncertainty in risk models from the Wismut cohort study as a practical example yields plausible lifetime risk uncertainty intervals that encompass the range of reported lifetime risk estimates from miners studies in the literature, as summarized in [9, Table 4].

This study specifically addresses quantifying uncertainties in lifetime lung cancer risks associated with protracted occupational radon exposure. Existing tools like "CONFIDENCE", "RadRAT", and "LARisk", predominantly employ risk models derived from the Atomic Bomb Survivors Life-Span Study and focus on acute radiation exposure [12]. The latter two build on methods from the BEIR VII report [16] to quantify lifetime cancer risk uncertainties. Those methods consider sampling variability in risk model parameters similar to our ANA approach, uncertainties in the risk transfer between populations, and uncertainties in the dose and dose-rate effectiveness factor (DDREF) using the delta method [34, 35]. However, subjective variance inputs are needed for risk transfer and DDREF uncertainty assessment, which our study avoids. Results from the BEIR VII report differ from the results here due to different study populations and exposure metrics, but the span of uncertainty intervals are of comparable magnitude.

Moreover, in the context of occupational radon exposure, the present study adds to methods used in the BEIR VI report [6], the EPA report [11] and [10], all of which use sampling techniques similar to the ANA approach here to address risk model parameter uncertainty. Although [10] does not provide direct lifetime risk uncertainty intervals, they can be derived from the results therein and align well with our findings. Overall, this adds credibility to both approaches. However, the methodology to derive uncertainty intervals has not been extensively introduced, discussed, and compared with other approaches so far, as was done in the present study.

4.1 Sources of lifetime risk uncertainty

Following [17], three types of uncertainties arise in lifetime risk calculations: sampling uncertainty, uncertainty in choosing and deriving a suitable model structure (model uncertainty), and unspecified uncertainties like data errors and validity of assumptions, that cannot be formally specified with probability distributions. Quantifying uncertainties beyond sampling uncertainty is challenging, as acknowledged elsewhere [6, 36]. This analysis focuses on quantifiable sampling uncertainty. For a

comprehensive overview of uncertainties, decisions, and potential errors associated with lifetime risk calculations see [6, Table 3-13].

The risk model defining $ERR(t;\Theta)$ is a crucial component of LEAR calculations with inherent uncertainties, arising from factors such as disease classification, statistical power limitations, potential confounding, and particularly from exposure assessment – a major challenge in radiation research and risk model derivation [37]. Potential measurement errors, especially from early years of uranium mining are subject of ongoing research, e.g. exploring their effects within the Wismut cohort [38,39]. Assessing uncertainties in risk model derivation is beyond the scope of this study.

Different risk model structures (categorical or parametric) fitted to the same cohort data result in comparable lifetime risk estimates [9]. The non-parametric reference mortality rates $r_0^{(ICRP)}(t), q_0^{(ICRP)}(t)$ and the corresponding survival function $S(t)$ avoid parameter uncertainty and leverage available population data. The discretization of lifetime risks from a theoretical integral to a calculable sum is mandated by data availability. In the scope of generic lifetime risk calculation, this all suggests low model uncertainty or limited model flexibility, allowing us to concentrate on quantifiable sampling uncertainty.

Preliminary sensitivity analyses indicate that many factors (e.g. the choice of the lifetime risk measure, latency time L or the maximum age t_{max}) have only limited impact on lifetime risk variability [5]. Likewise, variability in the annual radon exposure is only briefly investigated (Suppl. Section F) since the exposure scenario is fixed for most lifetime risk applications, especially for the important dose conversion considerations. Thus, the present study focuses on the most influential components: sampling uncertainty in risk model parameters Θ and baseline mortality rates $r_0(t), q_0(t)$.

4.2 Risk model parameter uncertainty

4.2.1 Approximate normality assumption (ANA) approach

The ANA approach approximates the true underlying likelihood function for estimating risk model parameters using a normal distribution and follows the frequentist approach. The covariance matrix estimate $\hat{\Sigma}_0$ describes the amount of sampling uncertainty, which decreases as cohort size increases, resulting in narrower uncertainty intervals for lifetime risks. This explains why lifetime risk estimates with risk model parameters derived from the smaller, younger 1960+ sub-cohort have wider uncertainty intervals compared to those derived from the Wismut full cohort. This is particularly evident for models with BEIR VI structure [6], with dedicated parameters for miners data at higher age ranges.

The ANA method requires only parameter estimates and their covariance matrix to derive uncertainty intervals via Monte Carlo simulations. This makes the ANA approach practical and efficient, especially when complete access to cohort data is not available. While not entirely new, the idea of approximating the underlying likelihood function is rooted in earlier work [40] later coined to the term "Approximate Bayesian Computation (ABC)" [41, 42]. A similar method for uncertainty quantification of lifetime thyroid cancer risk related to radiation exposure was used in [43].

4.2.2 Bayesian approach

In contrast to the frequentist method, Bayesian statistics incorporates prior knowledge or beliefs about model parameters through probability distributions, providing an alternative perspective on uncertainty.

Since the statistical software *Epicure* [29] does not support Bayesian methods, we implemented a solution in *R* [32]. Although *R* can be computationally slower than *Epicure*, which is specifically optimized for fitting $ERR(t;\Theta)$ risk model structures, individual *R* solutions allow greater control over cohort data and model fitting. We calculate the marginal posterior distribution of risk model parameters, inspired by [30]. Computing the full posterior is computationally expensive due to numerous baseline

stratification parameters, but focusing on the marginal posterior simplifies this by reducing the parameter set to just the risk model parameters. Compared to [30], this technique is here extended to handle more complex risk models and protracted low exposure scenarios. Sampling from the true marginal posterior yields more nuanced uncertainty intervals that are not reliant on approximating asymptotic behavior as in the ANA approach.

A key strength of the Bayesian approach is the ability to integrate prior knowledge – e.g. the results from previous miners studies – through the selection of prior distributions. However, selecting these priors involves subjective judgment [44]. Decisions on prior distributions, in particular the degree of influence on the likelihood, have to be thoroughly considered, compare [45] . Non-informative priors, like uniform distributions, have minimal influence on the posterior and lead to uncertainty intervals similar to the ANA approach, especially for large cohorts, while informative priors enable a more adaptive integration of diverse cohort data. Note that labeling estimates from the Joint Czech+French cohort as "prior knowledge" is a structured test of the methodology's adaptability and effectiveness of combining different cohort information rather than a strict integration of prior results. Users can tailor the approach to their needs, but selecting appropriate priors is a separate consideration beyond this discussion.

Although Bayesian methods offer flexibility and deeper insights, they require full access to cohort data and significant computational resources, especially for complex models with many parameters. While sampling methods like MCMC are efficient in this case due to high acceptance rates by choosing the approximate (asymptotic) normal distribution as a proposal density, the computational challenge lies in calculating the marginal posterior distribution itself.

4.3 Mortality rate uncertainty

Mortality rates also introduce notable uncertainty to lifetime risk estimates. Unlike for risk model parameter estimates, which are derived through a rigorous statistical framework (likelihood theory), the ICRP mixed Euro-American-Asian reference mortality rates $r_0^{(ICRP)}(t), q_0^{(ICRP)}(t)$ are presented as plain numbers sourced from a database. These mortality rates do not result from a statistical estimation process, requiring careful consideration when imposing probability distributions. We assessed this uncertainty by applying gamma distributions to baseline mortality rates $r_0(t)$ and $q_0(t)$ for all ages t incorporating observed variability in mortality rates across countries in Europe, America, and Asia from WHO data [20], which aligns geographically with ICRP reference rates. The gamma distribution was finally chosen as it fits the observed rates for numerous age groups well. This allowed us to quantify how mortality rate uncertainty influences lifetime risk estimates. In the described method, each rate derived from WHO data is assigned equal weight. Consequently, observations from smaller countries are given the same weight as those from larger countries. The focus is on estimating the variability of mortality rates themselves, irrespective of the population size. Alternatively, a population-weighted approach is applied in Suppl. Section D.2.

Our analysis confirmed that uncertainties in all-cause mortality rates have negligible impact [5], while lung cancer mortality rate uncertainties resulted in uncertainty intervals similar to those from full cohort risk model parameter uncertainty.

The derivation of parameter estimates in (10) and (11) from WHO data is independent from ICRP reference rates $r_0^{(ICRP)}(t)$ and $q_0^{(ICRP)}(t)$. Using a centered distribution with the expected value (mean) set equal to the ICRP rates had low effect on lifetime risk estimates and according uncertainties (Suppl. Section D.1.2), so we retained the un-centered distribution for Monte Carlo simulations to avoid constraining parameter estimation.

Here, lung cancer mortality rates introduce uncertainty comparable to that of full cohort risk model parameters for the Wismut cohort study. However, including both sources of uncertainty has little effect on the uncertainty intervals compared to just considering risk model parameters. Therefore,

focusing solely on risk model parameter uncertainty is sufficient. Although unintuitive, this effect can be explained by acknowledging the product structure of $ERR(t;\Theta)$ and lung cancer rates r_0(t) in the LEAR calculation. The variance of products of (independent) random variables is not necessarily larger than the variances of single factors [46].

4.4 Interpretation of uncertainty intervals

Uncertainty intervals capture the variability in lifetime risk estimates. For risk model effects, uncertainty intervals derived with ANA methods reflect sampling variation in estimated risk model parameters and may be referred to as (approximate) Wald-type confidence intervals. Bayesian credible intervals, such as Highest Posterior Density Intervals (HPDIs), represent the probability (e.g., 95%) that the true value lies within the interval, incorporating prior beliefs in risk model parameters.

While both methods provide uncertainty intervals, their interpretations differ. ANA confidence intervals are less interpretable than Bayesian credible intervals. However, this theoretical distinction is practically less relevant for purposes in radiation protection research. In particular, credible intervals with non-informative priors are often similar to confidence intervals derived with the ANA approach.

Mortality rate uncertainty intervals are more difficult to interpret due to their dependence on external data and chosen distributions. They reflect sampling variability by accounting for observed mortality rate variation and can be considered as subjective confidence intervals, similar to [16]. They provide a valuable quantitative sense on mortality rate variability.

The derived uncertainty intervals for lifetime risks like the LEAR reflect the expectable range of potential values that arise from the inherent variability in each calculation component. In particular, as lifetime risks are not directly estimated from data with sampling uncertainty, the intervals should not be interpreted as classical confidence intervals.

4.5 Comparison with lifetime risk variation in the literature

The uncertainty in risk model parameters significantly contributes to the overall uncertainty in lifetime risk estimates. Our analysis using the ANA approach applied to risk models from the Wismut cohort study reveals uncertainty intervals that align well with the literature: in the context of the PUMA study [9], LEAR values from various studies were recalculated and summarized. Thereby, a range for the LEAR per WLM of 2.50×10^{-4} to 9.22×10^{-4} was reported across all published risk models of uranium miners studies that include time- and age-related effect modifiers. This range translates to an equivalent range for the LEAR in % of 2.35 to 8.65. The 95% uncertainty intervals derived in this study for the parametric 1960+ sub-cohort models, particularly [3.26; 12.28] for the best-fit model (5) and [3.19; 8:22] for the simple linear model (6), correspond well to the range of point estimates reported by the PUMA study group. To convert the reported LEAR per WLM values to the total LEAR, each value was multiplied by 94 (total cumulative exposure in WLM). The derived intervals for the full Wismut cohort exhibit a weaker alignment with this range: [2.06;4.84] for the parametric model (4) and [1.27;4.30] for the categorical model (7). However, the 1960+ sub-cohort Wismut models are preferred to full Wismut cohort models in order to estimate lung cancer risks at low protracted exposures due to high quality exposure assessment [23].

Heterogeneity in radiation risk estimates between studies may explain differences in the LEAR and can likely be attributed to diverse factors such as structural differences in cumulative exposure range, duration of employment, and methods in mortality tracking and data analysis [9].

While uncertainty intervals depend on the chosen confidence level (here 95%), the close alignment of our derived intervals with literature values supports the reliability and appropriateness of our approach. This is especially remarkable as our results are solely derived from the Wismut miner cohort data as a practical example. The consistency across recognized miner studies confirms the reliability of the

ANA methodology in assessing uncertainties in lifetime lung cancer risks from radon exposure. Further follow-up years for miners cohorts will refine our understanding of risk models and lifetime risks for radon-induced lung cancer and associated uncertainties.

4.6 Strengths and weaknesses

Our work benefits from the strengths of the German uranium miners cohort (Wismut cohort), the largest single cohort of uranium miners worldwide representing roughly half of all miners in the pooled PUMA cohort [47]. This large cohort (cf. [48]) allows us to achieve reliable estimates for risk model effects on lifetime risk uncertainties.

Furthermore, the present study pioneers the application of the comprehensive WHO mortality database [20] to assess mortality rate uncertainties in radon-induced lung cancer lifetime risks. These innovative approaches, along with the implementation of advanced Bayesian techniques, expand the methodological toolbox for uncertainty assessment in this field. To facilitate the application of the Bayesian technique, we developed a *R* procedure for data grouping and model fitting, overcoming the limitations of existing software for this specific analysis. Transparency in reporting, with detailed descriptions of methods, statistical analysis, and results, facilitates replicability.

Both methods for assessing risk model uncertainties are reliable due to statistically grounded assumptions and show broad applicability. The ANA approach requires minimal assumptions, making it versatile. While the Bayesian approach with the analytical computed marginal Posterior distribution offers stronger rigor, it has specific data needs (Poisson-distributed numbers of lung cancer deaths). However, its concept of marginal posterior distributions likely extends beyond lifetime risk assessments. These techniques, given appropriate data, can be applied in radiation epidemiology to analyze various quantitative figures derived from likelihood functions, encompassing different exposures, health outcomes, and risk models.

However, limitations are acknowledged. The uncertainty intervals depend on the baseline mortality rates applied, the choice of risk model and the data used to estimate the risk models. The Bayesian approach, while statistically rigorous and contributing to the reliability of results, was here limited in applicability to models with few parameters due to computational constraints. However, generally, better computing power allows for the analysis of more complex models. This study prioritizes the development of methodology for uncertainty assessment. In particular, lifetime risk calculation inherits methodological limitations of risk model estimation, such as the incorporation of detailed smoking behaviour. Data for radon effects on females are sparse. Based on findings from residential radon studies in [49] we decided to assume the same $ERR(t;\Theta)$ for females and males. Finally, the analysis does not account for uncertainties arising from transferring risk estimates from miners cohorts to the general population (here: multiplicative risk transfer [7, 50]. Aligning mortality rates with the specific characteristics of the cohort data, such as using national mortality rates relevant to the cohort's origin, can help partially mitigate the risk transfer issue. The overall composite nature of a lifetime risk estimate depending on multiple independently conducted analyses, limits an all-encompassing uncertainty assessment.

5 Conclusion

Uncertainty quantification is crucial for a comprehensive understanding of lifetime risk estimates. This study demonstrates that uncertainty from risk model parameter estimates explains a substantial fraction of overall lifetime risk uncertainty. Two advanced methods to derive uncertainty intervals are developed and applied. The simple ANA approach proves to be a suitable and reliable uncertainty assessment technique for most cases. The more flexible Bayesian approach offers a more nuanced view of uncertainty. However, the approach is computationally more demanding and requires full access to grouped cohort data, limiting its wider applicability. From a practical perspective, additionally accounting for uncertainties in mortality rates is less critical. The explicit choice of lifetime risk measures is negligible for uncertainty assessment. The uncertainty intervals derived in this study correspond to the range of LEAR values from different miners studies in the literature, thus uncertainties derived by both methods are mutually confirmed. The introduced methods allow for a more complete comparison of lifetime risk estimates across uranium miners studies. These findings should be accounted for when developing radiation protection policies which are related to lifetime risks.

Conflicts of interest and sources of funding:

The authors have no relevant financial or non-financial interests to disclose.

6 Tables

Risk model	Equation	LEAR in %	Effect of risk model	Effect of $r_0(t)$	Joint effect
Parametric full cohort	(4)	3.43	[2.06; 4.81] (0.80)	[2.57; 4.17] (0.47)	[1.88; 4.99] (0.91)
Parametric 1960+ sub-cohort	(5)	6.70	[3.26; 12.28] (1.34)	[4.96; 8.11] (0.47)	[3.00; 11.98] (1.34)
Simple linear 1960+ sub-cohort	(6)	5.71	[3.19; 8.22] (0.88)	[4.02; 6.66] (0.46)	[2.77; 8.14] (0.94)
BEIR VI full cohort	(7)	2.95	[1.27; 4.31] (1.03)	[2.18; 3.47] (0.44)	[1.15; 4.28] (1.06)
BEIR VI 1960+ sub-cohort	(8)	5.74	[−10.55; 25.42] (6.27)	[4.29; 7.36] (0.53)	[−9.91; 23.17] (5.76)

Table 1: Results from ANA approach. LEAR in % estimates with corresponding 95% uncertainty intervals (relative uncertainty span in brackets) for uncertain risk model parameters, lung cancer mortality rates $r_0(t)$ or both independently, in correspondence to Figure 1 Lung cancer rates $r_0(t)$ are sampled from a Gamma distribution according to Suppl. Table 7. Reference estimates for LEAR in % are calculated with ICRP Euro-American-Asian mixed reference mortality rates [2] and an exposure scenario of 2 WLM from age 18-64 years.

Prior information	$LEAR$ in %	Relative uncertainty span
Uniform Prior	6.74 [2.96; 11.09]	1.20
$a = 2$	5.56 [2.76; 8.98]	1.12
$a = 5$	5.41 [2.82; 8.45]	1.04
$a = 10$	5.27 [2.89; 8.15]	1.00
$a = 20$	5.13 [2.99; 7.58]	0.89
$a = 50$	4.99 [3.14; 7.26]	0.83

Table 2: Results from Bayesian approach. LEAR in % estimate with 95% highest posterior density interval (HPDI) and relative uncertainty span for uncertain risk model parameters for risk model (5) derived from sampling from the posterior distribution $P(\Theta|X)$. The prior distribution $P(\Theta) = P(\beta)P(\alpha)P(\varepsilon)$ for gamma-distributed β for varying shape parameter a and normally distributed α, ε with standard deviation $\sigma = 0.02$ in correspondence to Figure 2. The LEAR in % calculated with risk model parameters from the Joint Czech + French cohort [25] is 4.30.

Prior information	$\hat{\beta} \times 100$	$LEAR$ in %	Relative uncertainty span
Likelihood with Wald-type CI	1.34 [0.71; 1.97]	5.72 [3.03; 8.41]	0.94
Uniform Prior	1.34 [0.79; 2.08]	5.72 [3.37; 8.90]	0.96
$a = 2$	1.35 [0.81; 2.07]	5.77 [3.44; 8.84]	0.94
$a = 5$	1.38 [0.87; 2.06]	5.90 [3.72; 8.82]	0.86
$a = 10$	1.42 [0.94; 2.02]	6.06 [4.00; 8.64]	0.76
$a = 20$	1.46 [1.03; 1.99]	6.25 [4.41; 8.48]	0.65
$a = 50$	1.52 [1.18; 1.91]	6.50 [5.05; 8.17]	0.48

Table 3: Parameter estimate $\hat{\beta} = Mod\,(P(\beta|X))$ of posterior distribution $P(\beta|X)$ with LEAR calculated with the risk model (6) and corresponding 95% highest posterior density interval (HPDI) and relative uncertainty spans for varying prior parameter settings. The gamma-distributed prior $P(\beta)$ is centered at the corresponding parameter estimate from [25] for different values of prior gamma shape parameters a in correspondence to Figure 1. Wald-type confidence intervals (CI) are also shown for comparison and are calculated as $\hat{\beta} \pm 1.96 \times 0.003005$, where 0.003005 represents the parameter standard error as stated in [23].

7 Figures

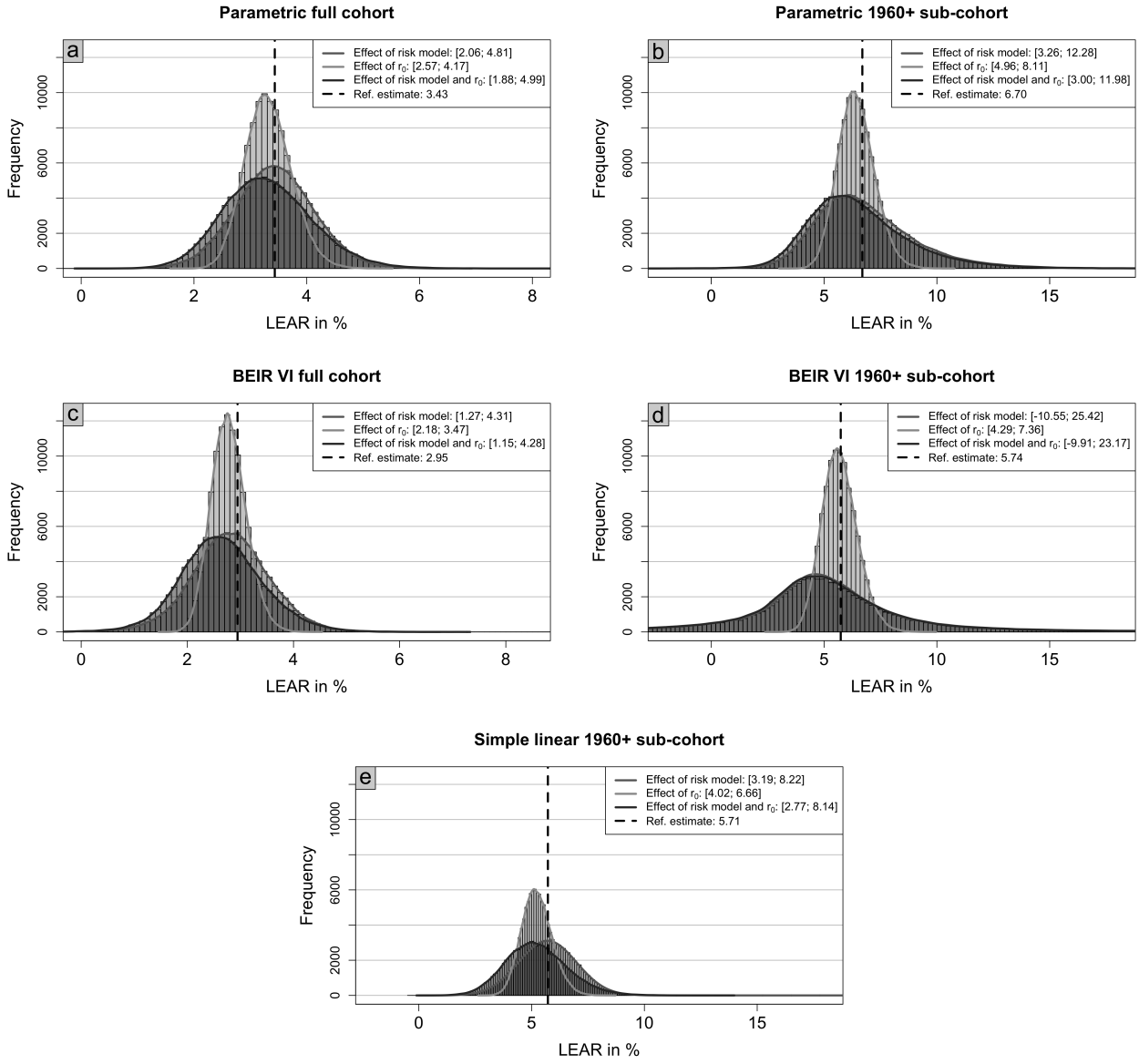

Figure 1: Results from ANA approach. Histograms of 100,000 resulting LEAR samples with kernel density (solid lines) for different risk models (Plot title a-e) and varying uncertain components in correspondence to Table 1. Risk model parameters (Effect of risk model) are assumed to follow a multivariate normal distribution (ANA approach). Lung cancer mortality rates $r_0(t)$ (Effect of r_0) are assumed to follow a gamma distribution with parameters as in Suppl. Table 7. The joint effect (Effect of risk model and r_0) results from independent sampling from both corresponding probability distributions. 95% uncertainty interval are presented in the legend.

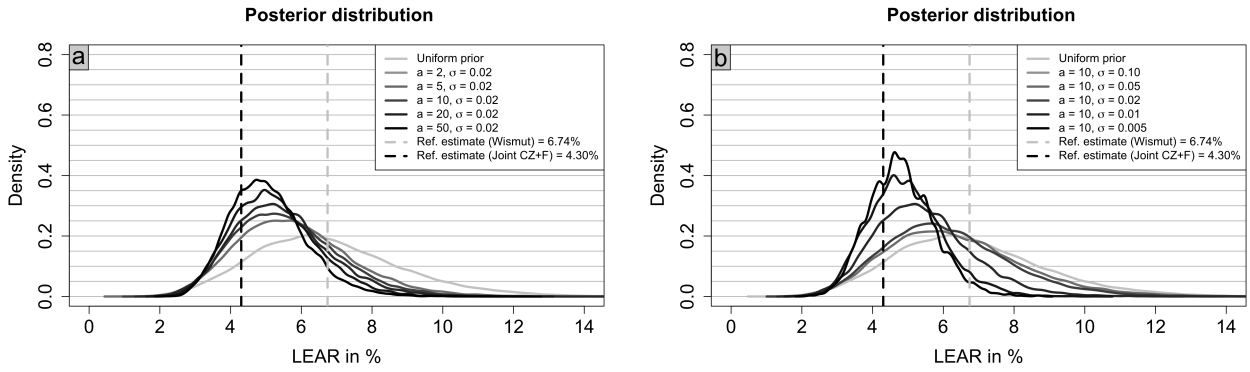

Figure 2: Results from Bayesian approach. Kernel density estimate of LEAR posterior distribution with uncertain risk model parameters $\Theta = (\beta, \alpha, \varepsilon)$ (model (5)) derived from sampling from the posterior distribution $P(\Theta|X)$ with prior $P(\Theta) = P(\beta)P(\alpha)P(\varepsilon)$ for gamma distributed β and normally distributed α, ε centered at the corresponding parameter estimate from [25] for different shape parameters a and standard deviations σ in correspondence to Table 2. The plots illustrate the effect of increasing prior certainty in parameter β (Plot a) and in parameters α, ε (Plot b). Vertical dashed lines indicate the reference estimate (ICRP 103) with the risk model fit on the Wismut or the Joint CZ+F cohort, respectively.

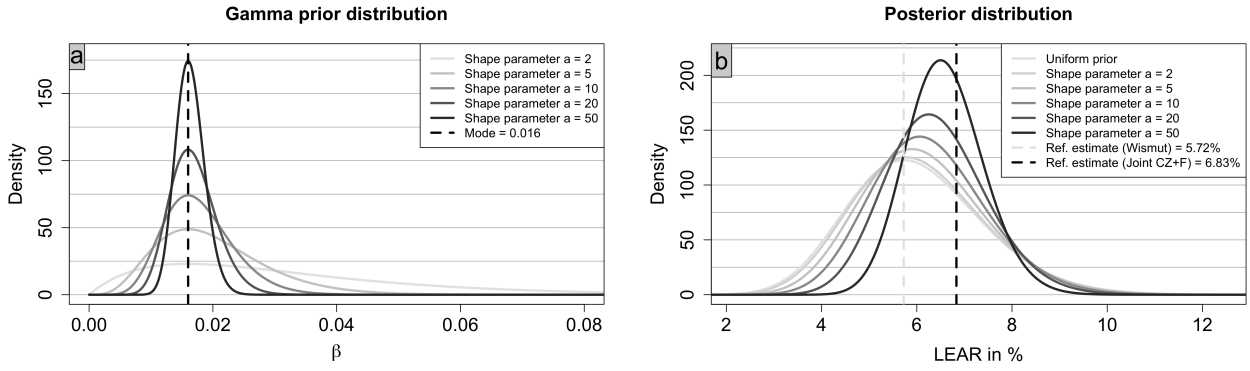

Figure 3: Gamma-distributed prior $P(\beta)$ centered at the parameter estimate from [25] for different shape parameters a and of corresponding posterior distributions LEAR for the simple linear 1960+ sub-cohort risk model (6) in correspondence to Table 3. The vertical dashed lines represent the β estimate from [25] and the correspondingly derived reference LEAR estimate.

References

[1] International Commission on Radiological Protection (ICRP). Protection against radon-222 at home and at work. *ICRP Publication 65, Annals of the ICRP*, 1993.

[2] International Commission on Radiological Protection (ICRP). The 2007 recommendations of the International Commission on Radiological Protection. *ICRP Publication 103, Annals of the ICRP*, 2007.

[3] International Commission on Radiological Protection (ICRP). Lung cancer risk from radon and progeny and statement on radon. *ICRP Publication 115, Annals of the ICRP*, 2010.

[4] International Commission on Radiological Protection (ICRP). Radiation detriment calculation methodology. *ICRP Publication 152, Annals of the ICRP*, 2022.

[5] M Sommer, F Heinzl, P Scholz-Kreisel, D Wollschläger, C Heumannn, and N Fenske. Lifetime risks for lung cancer due to occupational radon exposure: a systematic analysis of estimation components. Manuscript under review, February 2024.

[6] National Research Council. *Health Effects of Exposure to Radon: BEIR VI.* The National Academies Press, Washington, DC, 1999.

[7] United Nations: Scientific Committee on the Effects of Atomic Radiation. *UNSCEAR 2019 Report, Annex B, Lung cancer from exposure to radon.* United Nations Scientific Committee on the Effects of Atomic Radiation (UNSCEAR) Reports. United Nations, New York, NY, April 2021.

[8] M Kreuzer, C Sobotzki, M Schnelzer, and N Fenske. Factors modifying the radon-related lung cancer risk at low exposures and exposure rates among German uranium miners. *Radiation Research*, 189(2):165, December 2018.

[9] M Kreuzer, M Sommer, V Deffner, S Bertke, PA Demers, K Kelly-Reif, D Laurier, E Rage, DB Richardson, JM Samet, MK Schubauer-Berigan, L Tomasek, C Wiggins, LB Zablotska, and N Fenske. Lifetime excess absolute risk for lung cancer due to exposure to radon: results of the pooled uranium miners cohort study PUMA. *Radiation and Environmental Biophysics*, January 2024.

[10] L Tomasek. Lung cancer lifetime risks in cohort studies of uranium miners. *Radiation Protection Dosimetry*, 191(2):171–175, October 2020.

[11] DJ Pawel and Puskin JS. *EPA Assessment of Risks from Radon in Homes.* U.S. Environmental Protection Agency, Washington, DC, 2003.

[12] DL Preston, E Ron, S Tokuoka, S Funamoto, N Nishi, M Soda, K Mabuchi, and K Kodama. Solid cancer incidence in atomic bomb survivors: 1958-1998. *Radiation Research*, 168(1):1–64, July 2007.

[13] L Walsh, A Ulanowski, JC Kaiser, C Woda, and W Raskob. A new European cancer risk assessment tool for application after nuclear accidents. *Radioprotection*, 55:S95–S99, 2020.

[14] A Berrington de Gonzalez, A Iulian Apostoaei, LHS Veiga, P Rajaraman, B A Thomas, F Owen Hoffman, E Gilbert, and C Land. RadRAT: a radiation risk assessment tool for lifetime cancer risk projection. *Journal of Radiological Protection*, 32(3):205–222, September 2012.

[15] J Lee, YM Kim, Y Park, E Jang, J Yoo, S Seo, E S Cha, and WJ Lee. LARisk: An R package for lifetime attributable risk from radiation exposure. *medRxiv*, 2022.

[16] National Research Council, Division on Earth and Life Studies, Board on Radiation Effects Research, and Committee to Assess Health Risks from Exposure to Low Levels of Ionizing Radiation. *Health risks from exposure to low levels of ionizing radiation: BEIR VII Phase 2*. National Academies Press, Washington, DC, March 2006.

[17] D Thomas, S Darby, F Fagnani, P Hubert, M Vaeth, and K Weiss. Definition and estimation of lifetime detriment from radiation exposures. *Health Physics*, 63(3):259–272, September 1992.

[18] AM Kellerer, EA Nekolla, and L Walsh. On the conversion of solid cancer excess relative risk into lifetime attributable risk. *Radiation and Environmental Biophysics*, 40:249–57, January 2001.

[19] A Ulanowski, JC Kaiser, U Schneider, and L Walsh. On prognostic estimates of radiation risk in medicine and radiation protection. *Radiation and Environmental Biophysics*, 58(3):305–319, August 2019.

[20] WHO Mortality Database. `https://www.who.int/data/data-collection-tools/who-mortality-database`, 2022. Accessed: 2022-02-05.

[21] M Vaeth and DA Pierce. Calculating excess lifetime risk in relative risk models. *Environmental Health Perspectives*, 87:83–94, July 1990.

[22] L Tomasek, A Rogel, D Laurier, and M Tirmarche. Dose conversion of radon exposure according to new epidemiological findings. *Radiation Protection Dosimetry*, 130(1):98–100, April 2008.

[23] M Kreuzer, V Deffner, M Sommer, and N Fenske. Updated risk models for lung cancer due to radon exposure in the German Wismut cohort of uranium miners, 1946–2018. *Radiation and Environmental Biophysics*, September 2023.

[24] W Nelson. Theory and applications of hazard plotting for censored failure data. *Technometrics*, 14(4):945–966, 1972.

[25] L Tomasek, A Rogel, M Tirmarche, N Mitton, and D Laurier. Lung cancer in French and Czech uranium miners: Radon-associated risk at low exposure rates and modifying effects of time since exposure and age at exposure. *Radiation Research*, 169(2):125–137, February 2008.

[26] T Amemiya. *Advanced Econometrics*. Harvard University Press, London, England, July 1985.

[27] L Held and DS Bove. *Likelihood and Bayesian inference*. Statistics for Biology and Health. Springer, Berlin, Germany, 2nd edition, April 2021.

[28] Y Pawitan. *In All Likelihood : Statistical Modelling and Inference Using Likelihood*. Oxford University Press, London, England, January 2013.

[29] DL Preston, JH Lubin, DA Pierce, and M McConney. *Epicure Users Guide*. Hirosoft International Corporation, Seattle, WA, 1993.

[30] M Higueras and A Howes. Poisson excess relative risk models: New implementations and software. *SORT (Statistics and Operations Research Transactions)*, 42:237–252, December 2018.

[31] C Robert and G Casella. *Monte Carlo Statistical Methods*. Springer Texts in Statistics. Springer, New York, NY, 2nd edition, July 2005.

[32] R Core Team. *R: A Language and Environment for Statistical Computing*. R Foundation for Statistical Computing, Vienna, Austria, 2024.

[33] EL Kaplan and P Meier. Nonparametric estimation from incomplete observations. *Journal of the American Statistical Association*, 53(282):457–481, 1958.

[34] JL Doob. The limiting distributions of certain statistics. *The Annals of Mathematical Statistics*, 6(3):160–169, September 1935.

[35] JM Ver Hoef. Who invented the delta method? *The American Statistician*, 66(2):124–127, May 2012.

[36] S Hoffmann, F Schönbrodt, R Elsas, R Wilson, U Strasser, and AL Boulesteix. The multiplicity of analysis strategies jeopardizes replicability: lessons learned across disciplines. *Royal Society Open Science*, 8(4):201925, 2021.

[37] United Nations Scientific Committee on the Effects of Atomic Radiation. *UNSCEAR 2012 Report, Annex B, Uncertainties in risk estimates for radiation-induced cancer*. United Nations, December 2015.

[38] H Küchenhoff, V Deffner, M Aßenmacher, H Neppl, C Kaiser, and D Güthlin. Ermittlung der Unsicherheiten der Strahlenexpositionsabschätzung in der Wismut-Kohorte - Teil I - Vorhaben 3616S12223 [Determination of uncertainties of radiation exposure assessment in the Wismut cohort part I Project 3616S12223]. Technical Report http://nbn-resolving.de/urn:nbn:de:0221-2018080615802, Bundesamt für Strahlenschutz [Federal Office for Radiation Protection], 2018.

[39] N Ellenbach, R Rehms, and S Hoffmann. Ermittlung der Unsicherheiten der Strahlenexpositionsabschätzung in der Wismut-Kohorte - Teil II - Vorhaben 3618S12223 [Determination of uncertainties of radiation exposure assessment in the Wismut cohort part II - Project 3618S12223]. Technical Report http://nbn-resolving.de/urn:nbn:de:0221-2023071238488, Bundesamt für Strahlenschutz [Federal Office for Radiation Protection], 2023.

[40] DB Rubin. Bayesianly Justifiable and Relevant Frequency Calculations for the Applied Statistician. *The Annals of Statistics*, 12(4):1151 – 1172, 1984.

[41] MA Beaumont, W Zhang, and DJ Balding. Approximate bayesian computation in population genetics. *Genetics*, 162(4):2025–2035, December 2002.

[42] SA Sisson, Y Fan, and MA Beaumont. *Handbook of approximate Bayesian computation*. Chapman and Hall/CRC, September 2018.

[43] X Xue and RE Shore. Assessing excess lifetime risk for disease after radiation exposure. *Health Physics*, 80(5):462–469, May 2001.

[44] M Goldstein. Subjective Bayesian analysis: Principles and practice. *Bayesian Analysis*, 1(3):403–420, September 2006.

[45] S Greenland. Bayesian perspectives for epidemiological research: I. Foundations and basic methods. *International Journal of Epidemiology*, 35(3):765–775, June 2006.

[46] LA Goodman. On the exact variance of products. *Journal of the American Statistical Association*, 55(292):708–713, 1960.

[47] E Rage, DB Richardson, PA Demers, M Do, N Fenske, M Kreuzer, J Samet, C Wiggins, MK Schubauer-Berigan, K Kelly-Reif, L Tomasek, LB Zablotska, and D Laurier. PUMA - pooled uranium miners analysis: cohort profile. *Occupational and Environmental Medicine*, 77(3):194–200, March 2020.

[48] M Kreuzer, M Schnelzer, A Tschense, L Walsh, and B Grosche. Cohort Profile: The German uranium miners cohort study (Wismut cohort), 1946–2003. *International Journal of Epidemiology*, 39(4):980–987, June 2009.

[49] S Darby, D Hill, A Auvinen, J Barros-Dios, H Baysson, F Bochicchio, H Deo, R Falk, F Forastiere, M Hakama, I Heid, L Kreienbrock, M Kreuzer, F Lagarde, I Mäkeläinen, C Muirhead, W Oberaigner, G Pershagen, A Ruano-Ravina, and R Doll. Radon in homes and risk of lung cancer: Collaborative analysis of individual data from 13 european case-control studies. *BMJ: British medical journal*, 330:223, February 2005.

[50] A Ulanowski, E Shemiakina, and D Güthlin. ProZES: the methodology and software tool for assessment of assigned share of radiation in probability of cancer occurrence. *Radiation and Environmental Biophysics*, 2020.

[51] United Nations Scientific Committee on the Effects of Atomic Radiation (UNSCEAR). *Sources and effects of ionizing radiation: UNSCEAR 1994 report to the general assembly, with scientific annexes*. United Nations, New York, NY, December 1994.

[52] MP Little, DG Hoel, J Molitor, JD Boice, R Wakeford, and CR Muirhead. New models for evaluation of radiation-induced lifetime cancer risk and its uncertainty employed in the UNSCEAR 2006 report. *Radiation Research*, 169(6):660–676, June 2008.

[53] N Hunter, CR Muirhead, F Bochicchio, and RGE Haylock. Calculation of lifetime lung cancer risks associated with radon exposure, based on various models and exposure scenarios. *Journal of Radiological Protection*, 35(3):539–555, June 2015.

[54] AWS Henyoh, O Laurent, C Mandin, and E Clero. Radon exposure and potential health effects other than lung cancer: a systematic review and meta-analysis. *Front. Public Health*, 12, September 2024.

[55] United Nations Scientific Committee on the Effects of Atomic Radiation (UNSCEAR). *Sources and effects of ionizing radiation: Sources and effects of ionizing radiation report to the general assembly with scientific annexes v.1*. Stationery Office Books, Norwich, England, September 2000.

[56] M Greenwood. *A Report on the Natural Duration of Cancer*. Reports on public health and medical subjects. H.M. Stationery Office, 1926.

[57] WJ Hall and JA Wellner. Confidence bands for a survival curve from censored data. *Biometrika*, 67(1):133–143, 1980.

[58] VN Nair. Confidence bands for survival functions with censored data: A comparative study. *Technometrics*, 26(3):265–275, 1984.

[59] JP Klein and ML Moeschberger. *Survival analysis*. Statistics for Biology and Health. Springer, New York, NY, 2nd edition, March 2005.

[60] R Strobl. *km.ci: Confidence Intervals for the Kaplan-Meier Estimator*, 2022. R package version 0.5-6.

[61] S Zhizhilashvili, I Mchedlishvili, N Jankarashvili, R Camacho, and N Mebonia. Effect of age at diagnosis on the prognosis of gastric cancer patients: A population-based study in Georgia. *Cureus*, 16(6):e62154, June 2024.

[62] S Jablon. Atomic bomb radiation dose estimation at ABCC. *Atomic Bomb Casualty Commission Report ABCC TR/23-71*, 1971.

[63] L Hafner and L Walsh. Valid versus invalid radiation cancer risk assessment methods illustrated using Swiss population data. *Journal of Radiological Protection*, 41(4):1228–1242, November 2021.

Supplementary information

In this Supplement, additional information, alternative modeling approaches, and derivations of quantities from the main manuscript are presented regarding uncertainties in the lifetime risk for lung cancer related to occupational radon exposure. In particular, the basic methodology is identical to the main paper approach. For a comprehensive overview of the conducted analyses, see Supplementary Table 1.

Component	Methods	Sensitivities	Section
Mortality rates	Non-weighted regression	Gamma distribution	Main paper, Suppl. D.1
		Log-normal distribution	Suppl. D.3
		Sex-specific	Suppl. E.1
	Weighted Poisson regression (Bayesian)	Varying prior certainty	Suppl. D.2
Risk model parameters	ANA	-	Main paper, Suppl. C.1
	Bayesian	Varying prior certainty	Main paper, Suppl. C.2, Suppl. C.3
		Sex-specific	Suppl. E.2
Exposure scenario	Log-normal annual exposure	Exposure variability	Suppl. F
Other lifetime risk measures	ANA	-	Suppl. A
	Bayesian	Varying prior certainty	
	Kaplan-Meier	Windows of cumulative exposure	Suppl. B

Supplementary Table 1: Overview of lifetime risk uncertainty assessment by investigated component, methods, conducted sensitivity analyses, and where it is to find in the documents.

Overview

In Suppl. Section A, we derive uncertainty intervals for other lifetime risk measures (ELR, $REID$, and $RADS$) using ANA and Bayesian techniques. Across all measures, the relative uncertainty spans are comparable. Therefore, for practical purposes, relying on the $LEAR$ measure is sufficient. $RADS$ estimates are notably larger compared to the other measures.

We also present an exploratory Kaplan-Meier survival curve analysis [33], stratified by cumulative exposure in categories (Suppl. Section B, Suppl. Fig. 3). This approach relies on hardly any assumptions, using only miners cohort data, yields plausible uncertainty intervals and is useful for visual risk assessments.

Suppl. Section C shows additional insights for risk model parameter uncertainty. Particularly, the Bayesian approach for risk model parameter uncertainty for the simple risk model (24) showed only slight differences between log-normal and gamma priors for β (Suppl. Section C.2).

Suppl. Section D further explores mortality rate uncertainties: An alternative Bayesian approach using Poisson-distributed numbers of lung cancer deaths for population-weighted mortality rate uncertainty (Suppl. Section D.2) provided minimal new insights, as the extensive WHO data results in a highly peaked Likelihood function indicating low uncertainty in the parameter estimates and consequently overruled the prior's influence. In Suppl. Section D.3, we compare log-normal and gamma distributions for mortality rates, showing similar uncertainty intervals but with slightly larger upper bounds for log-normal distributions. Both distributions fit the WHO data comparably well. This indicates that accounting for mortality rate uncertainty in lifetime risks involves a degree of subjectivity, influenced by the researcher's methodological decisions and the need for careful interpretation of resulting uncertainty intervals.

For sex-specific lifetime risks with mortality rates derived from sex-specific WHO data (Suppl. Section E.1), estimates for males are roughly twice those of females due to overall higher male baseline all-cause and lung cancer mortality, though the relative uncertainty span remains similar. Lifetime

risk estimates calculated with mortality rates from females must be interpreted cautiously, as the underlying excess relative risk term is based on male miners cohorts. Sex-specific $LEAR$ estimates using sex-specific ICRP reference rates (Suppl. Section E.2) accounting for risk model parameter uncertainty for the parametric 1960+ sub-cohort risk model (21) with the Bayesian approach further confirm this pattern, with male $LEAR$ values being twice as high, while the relative uncertainty remains similar.

Finally, Monte Carlo simulations accounting for uncertainties in radon exposure scenarios (Suppl. Section F) showed that lifetime risks become approximately normally distributed across all risk models and lifetime risk measures under low exposure uncertainty, with prescribed annual exposure variability strongly affecting results but maintaining consistent relative uncertainty intervals.

A Comparison and results for other lifetime risk measures

Besides the $LEAR$, further (excess) lifetime risk measures are used in the literature. Here, we compare the $LEAR$ to three additional lifetime risk measures: the Risk of Exposure Induced Death ($REID$) (first introduced in [51] and employed in [52, 53]), the Excess Lifetime Risk (ELR) [21] and the Radiation Attributable Decrease of Survival ($RADS$) [19]. All considered excess lifetime risk definitions emerge from the difference between a risk under exposure and a risk in the absence of exposure. Except for $RADS$, the lifetime risk is the sum of annual lung cancer risks weighted by a certain survival probability, see e.g. [17]. Note that $RADS$ is special as it is the only measure that describes no risk per se but rather a relative change in the survival function. In particular, it is the only measure calculated without all-cause mortality rates. However, we will see that all four quantities are connected. Before comparing uncertainty intervals, we introduce the additional lifetime risk measures shortly.

A.1 Definition

The central difference of the additionally considered lifetime risk measures compared to $LEAR$ is the explicit accounting for radon exposure in the survival function $S(t)$. Survival under exposure shall be denoted by $S_E(t)$ and baseline survival by $S_0(t)$, It holds,

$$REID = \int_0^\infty r_E(t) S_E(t)\, dt - \int_0^\infty r_0(t) S_E(t)\, dt = \int_0^\infty r_0(t) ERR(t) S_E(t)\, dt, \tag{15}$$

$$ELR = \int_0^\infty r_E(t) S_E(t)\, dt - \int_0^\infty r_0(t) S_0(t)\, dt, \tag{16}$$

$$RADS = \lim_{t\to\infty} \frac{S_0(t) - S_E(t)}{S_0(t)} = 1 - \lim_{t\to\infty} \frac{S_E(t)}{S_0(t)}. \tag{17}$$

To calculate these additional lifetime risks, assumptions on the survival function affected by radon are necessary. Analogously to $S_0(t) = e^{-\int_0^t q_0(u)\, du} \approx \tilde{S}_0(t) = e^{-\sum_{u=0}^{t-1} q_0(u)}$, we set

$$S_E(t) = e^{-\int_0^t q_E(u)\, du} \approx \tilde{S}_E(t) = e^{-\sum_{u=0}^{t-1} q_E(u)},$$

where $q_E(u)$ describes the all-cause mortality rate at age u under exposure. Since there is currently no reliable evidence that radon can cause diseases other than lung cancer, we assume that radon exposure influences solely the lung cancer risk [54]. Hence $q_E(u) = q_0(u) + r_0(u)ERR(u)$ for all ages u and

$$S_E(t) = S_0(t) e^{-\int_0^t r_0(u) ERR(u)\, du} \approx \tilde{S}_E(t) = \tilde{S}_0(t) e^{-\sum_{u=0}^{t-1} r_0(u) ERR(u)}. \tag{18}$$

Employing the same approach as for the $LEAR$, the final approximations for all considered lifetime

risk measures read

$$
\begin{aligned}
LEAR &\approx \sum_{t\geq 0} r_0(t) ERR(t) \tilde{S}_0(t), \\
REID &\approx \sum_{t\geq 0} r_0(t) ERR(t) \tilde{S}_E(t), \\
ELR &\approx \sum_{t\geq 0} r_0(t)(1+ERR(t)) \tilde{S}_E(t) - r_0(t)\tilde{S}_0(t), \\
RADS &\approx 1 - e^{-\sum_{t\geq 0} r_0(u) ERR(u)}.
\end{aligned}
$$

Without assuming a protective effect of radon exposure [2,55], it holds $r_E(t) \geq r_0(t)$ and $S_E(t) \leq S_0(t)$ for all ages $t \geq 0$. Therewith one can easily deduce (proof in [5]),

$$ELR \leq REID \leq LEAR. \tag{19}$$

The inequality (19) is universal and holds for all choices and combinations of calculation components. For realistic excess absolute risks $r_0(t)ERR(t)$ (e.g. for moderate exposures observed in mines and reasonable lung cancer mortality rates) one can further deduce

$$ELR \leq REID \leq LEAR \leq RADS. \tag{20}$$

The relationship (20) is observed for the majority of reasonable exposure scenarios. However, technically $LEAR$ can exceed $RADS$, which is naturally bounded by one.

A.2 Uncertainty assessment

In the following, we employ the Bayesian approach and the approximate normality assumption (ANA) approach to assess risk model parameter effects in lifetime risk uncertainties across different previously introduced lifetime risk measures. We expand results from the main manuscript and give further insights. As in the main manuscript, a generic lifetime risk estimate without any uncertainty quantification is called "Reference estimate (ICRP 103)" or simply "ref. estimate". In addition to the 95% uncertainty intervals we often present the span of uncertainty intervals relative to the reference estimate (relative uncertainty span).

A.2.1 Bayesian approach for risk model parameter effects

For this Bayesian risk model parameter uncertainty assessment, we consider the parametric 1960+ sub-cohort risk model from [23],

$$ERR(t;\beta,\alpha,\varepsilon) = \beta W(t) \exp\{\alpha(AME(t)-30) + \varepsilon(TME(t)-20)\} \tag{21}$$

with parameter set $\Theta = (\beta, \alpha, \varepsilon)$ and estimates $\hat{\beta} = 0.0466$, $\hat{\alpha} = -0.0301$, and $\hat{\varepsilon} = -0.0755$. The prior assumptions are analogous to those described in the Methods section of the main paper. Note that we do not investigate the simple linear risk model here, as it provides a poorer fit to the miner data.

Supplementary Figure 1 shows sample distributions across different lifetime risk measures obtained by drawing risk model parameter samples from the posterior distribution $P(\Theta|X) \propto P(\Theta)L(X|\Theta)$ for varying prior certainty. The reference estimate with corresponding 95% highest density posterior intervals (HPDI) is shown in Suppl. Table 2. The results are overall very similar and only $RADS$ estimates are considerably larger. However, the relative uncertainty spans are similar across all lifetime risk measures. As expected, the reference estimates shift towards the lifetime risk estimates calculated using point estimates of the risk model parameters derived from the Joint Czech-French cohort. This behavior reinforces the reliability of the Bayesian methods employed in this analysis. For comparison, the ELR, $REID$, $LEAR$, and $RADS$ in % calculated with risk model parameters (21) derived from this cohort are 4.04, 4.20, 4.30, and 5.62, respectively.

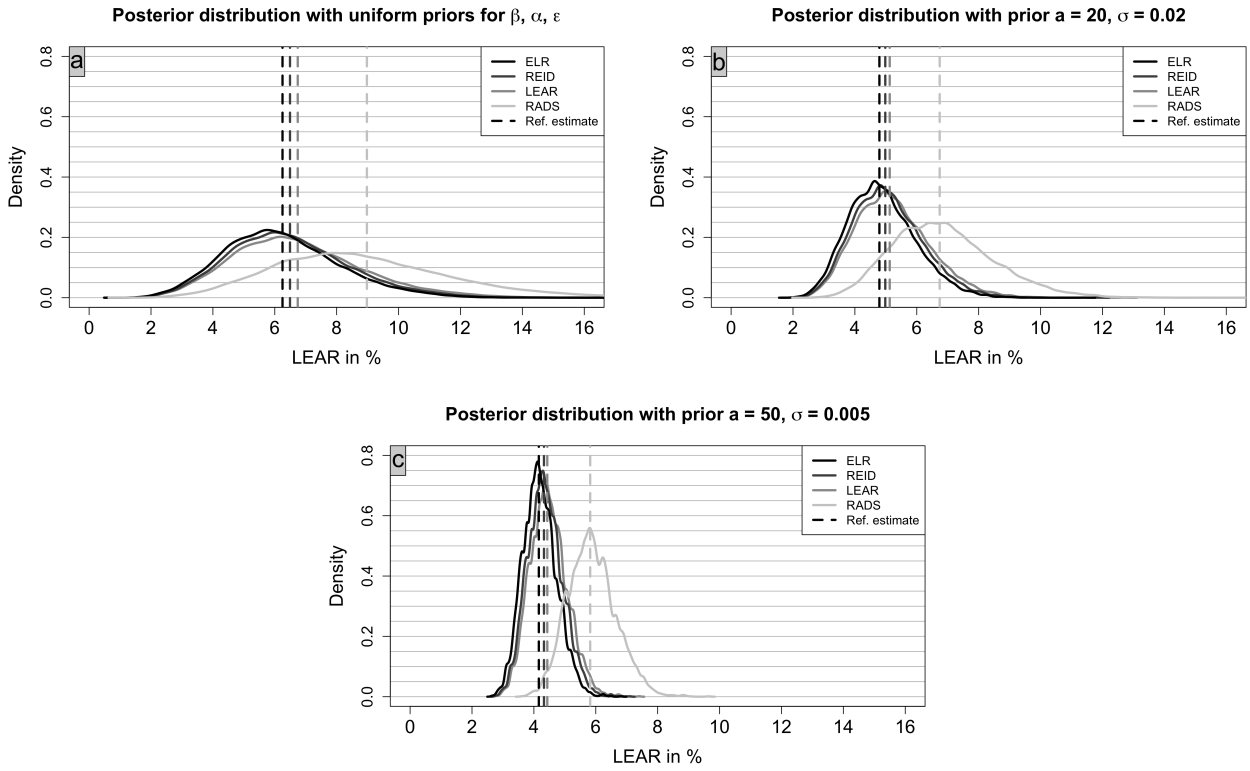

Supplementary Figure 1: Distribution of excess lifetime risk measures ELR, $REID$, $LEAR$ and $RADS$ with risk model (21) and parameter samples drawn from the posterior distribution with prior $P(\Theta) = P(\beta)P(\alpha)P(\varepsilon)$ for different combinations of gamma-distributed marginal prior for β and normally distributed marginal priors for α and ε for different shape parameters a and standard deviations σ in correspondence to Suppl. Table 2. The reference estimate (ICRP 103) corresponds to the excess lifetime risk measures evaluated at the mode $\hat{\Theta}$.

Prior information	ELR in %	$REID$ in %	$LEAR$ in %	$RADS$ in %
Uniform prior	6.25 [2.80; 10.04] (1.16)	6.49 [2.89; 10.40] (1.16)	6.74 [2.96; 11.09] (1.21)	8.98 [3.57; 14.56] (1.23)
$a = 20, \sigma = 0.02$	4.79 [2.83; 7.00] (0.87)	4.98 [2.94; 7.26] (0.87)	5.13 [2.99; 7.58] (0.89)	6.74 [3.98; 10.22] (0.93)
$a = 50, \sigma = 0.005$	4.33 [3.16; 5.27] (0.49)	4.43 [3.32; 5.53] (0.50)	4.43 [3.34; 5.66] (0.52)	5.82 [4.40; 7.40] (0.52)

Supplementary Table 2: Excess lifetime risk measures evaluated at the mode $\hat{\Theta}$ of risk model parameters and their 95% highest posterior density interval (HPDI) (relative uncertainty span in brackets) with prior $P(\Theta) = P(\beta)P(\alpha)P(\varepsilon)$ for different values of prior gamma shape parameters a and standard deviations σ in correspondence to Suppl. Figure 1.

Note that lifetime risks evaluated at the mode $\hat{\Theta}$ of the risk model parameter distribution (reference estimate) do sometimes not align with the sample distribution mode in Suppl. Figure 1. This discrepancy arises because a lifetime risk evaluated at a specific parameter estimate $\hat{\Theta}$ is essentially a non-linear parameter transformation of $\hat{\Theta}$. This affects the distribution characteristics. Here, the exponential nature of the employed risk model structure shifts the distribution mode slightly leftward depending on the magnitude of σ.[1] A comparable effect is observed in the upcoming analysis with the ANA approach.

A.2.2 Approximate normality assumption (ANA) approach

Analyses with the ANA approach showed that the resulting differences in lifetime risk measures are comparably low for all considered risk models (Suppl. Figure 2, Suppl. Table 3). Again, only *RADS* estimates are considerably larger, which is also reflected in the wider uncertainty intervals. However, the relative uncertainty span is similar across all considered lifetime risk measures.

The BEIR VI 1960+ sub-cohort risk model exhibits excessive parameter uncertainty. This is reflected in a high proportion of implausible (negative) *LEAR* samples, likely due to the inherent uncertainty in parameters for greater ages fit on a young cohort. This holds across all considered lifetime risk measures. However, the exponential nature of *RADS* amplifies negative parameter samples, resulting in a considerably wider lower uncertainty bound compared to other lifetime risk measures. Overall, the excessive uncertainty in BEIR VI 1960+ sub-cohort risk model parameters makes corresponding uncertainty quantification currently impractical. With additional follow-up data, the uncertainty in risk model parameters, especially at higher ages, will decrease, leading to more reliable estimates for the 1960+ sub-cohort.

Risk model	*ELR* in %	*REID* in %	*LEAR* in %	*RADS* in %
Parametric full cohort	3.24 [1.96; 4.51] (0.79)	3.37 [2.04; 4.69] (0.79)	3.43 [2.06; 4.81] (0.80)	4.62 [2.83; 6.55] (0.81)
BEIR VI full cohort	2.80 [1.22; 4.06] (1.01)	2.89 [1.26; 4.20] (1.02)	2.95 [1.27; 4.31] (1.03)	4.74 [2.10; 7.11] (1.06)
Parametric 1960+ sub-cohort	6.21 [3.08; 11.04] (1.28)	6.45 [3.20; 11.44] (1.28)	6.70 [3.26; 12.28] (1.35)	8.88 [4.41; 17.10] (1.43)
BEIR VI 1960+ sub-cohort	5.34 [−10.90; 20.77] (5.93)	5.56 [−11.26; 21.31] (5.86)	5.74 [−10.55; 25.42] (6.27)	7.07 [−18.86; 40.96] (8.46)
Simple linear 1960+ sub-cohort	5.35 [3.03; 7.60] (0.85)	5.52 [3.12; 7.84] (0.86)	5.72 [3.19; 8.26] (0.89)	9.98 [5.69; 14.09] (0.84)

Supplementary Table 3: Excess lifetime risks (reference estimates) with 95% uncertainty interval (relative uncertainty span in brackets) from the 100,000 risk model parameter estimates drawn from a multivariate normal distribution (ANA approach) for different lifetime risk measures and risk models in correspondence to Suppl. Figure 2.

In summary, the uncertainty intervals for the measures *ELR*, *REID*, and *LEAR* are similar for both the ANA and the Bayesian approach. Notable differences between measures *ELR*, *REID*, and *LEAR* are expected to occur only at higher exposures as they primarily differ in how they model the survival function, using either $S_0(t)$ or $S_E(t)$. However, low exposure scenarios are particularly prevalent today and therefore play a major role in radiation protection purposes. Therewith, regarding uncertainties, no clear difference or benefit between the three lifetime risk measures is observed. *RADS* being generally larger results in likewise shifted uncertainty intervals. The relative uncertainty span is similar across all lifetime risk measures. The BEIR VI 1960+ sub-cohort model results in peculiar uncertainty intervals and should, to date, be employed with care for uncertainty assessment.

[1] For example, the mode of $\exp\{Y\}$ for a normal distribution $Y \sim \mathcal{N}(\mu, \sigma^2)$ is $\exp\{\mu - \sigma^2\}$ instead of $\exp\{\mu\}$.

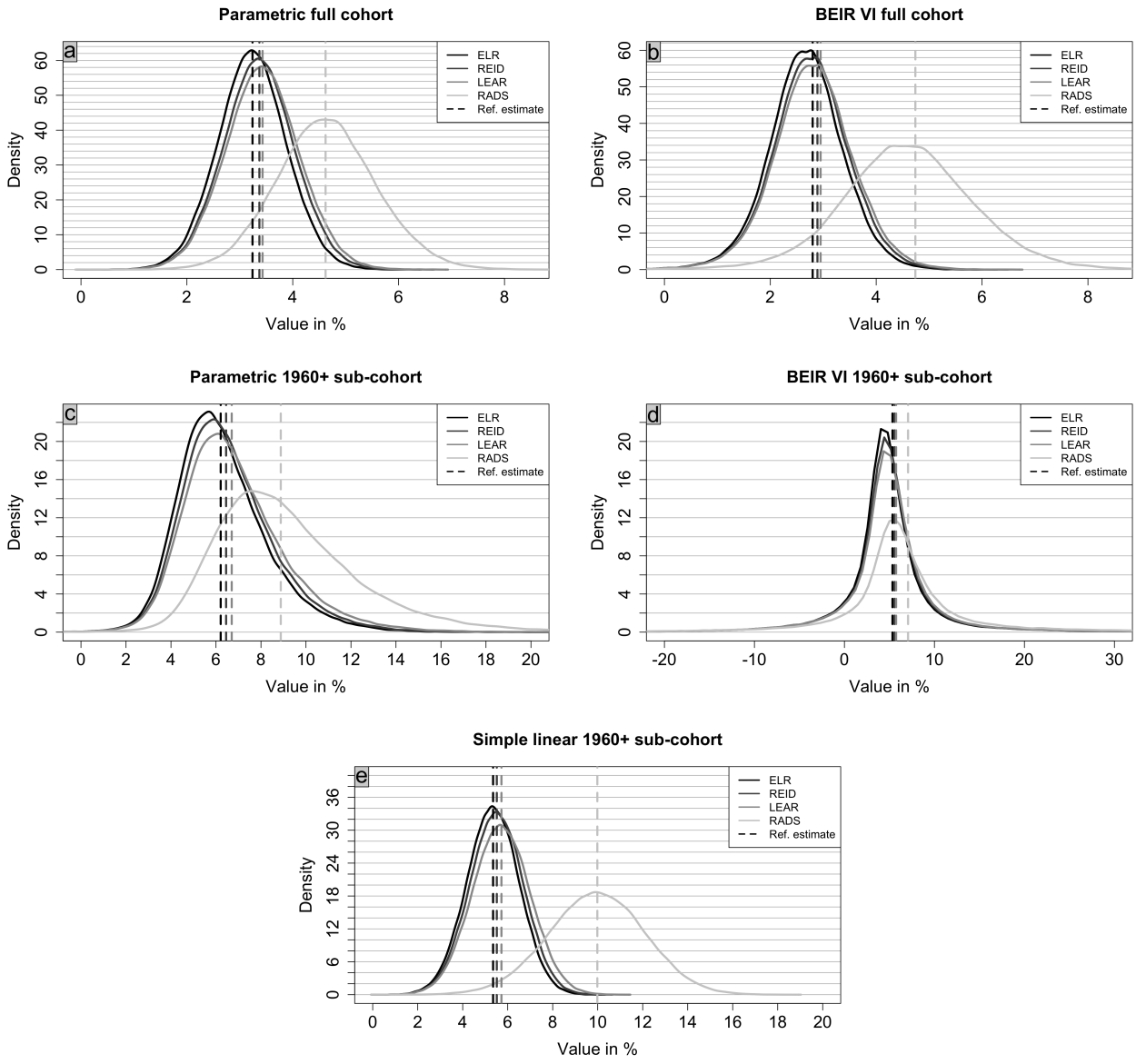

Supplementary Figure 2: Density from the histogram of 100, 000 excess lifetime risk estimates calculated with risk model parameter estimates drawn from a multivariate normal distribution (ANA approach) for different lifetime risk measures and risk models in correspondence to Suppl. Table 3.

B Explorative uncertainty assessment: Kaplan-Meier lung cancer survival curves

We present a simple, explorative approach to deducing uncertainty intervals for lifetime risks. This approach requires minimal assumptions and is in particular independent of the typical (excess) lifetime risk structure incorporating ERR risk models. Further, it only employs knowledge from miner cohorts and does not rely on external inputs like mortality rates or exposure scenarios.

B.1 Introduction and definition

Excess lifetime risks employed in the literature are the difference between a risk under exposure and a risk in the absence of exposure. In particular, for the $LEAR$ this relationship is expressed as $LEAR = LR_E - LR_0$ (see Methods section in the main manuscript for comparison). By interpreting $1 - LR_E$ and $1 - LR_0$ as (unknown) lifetime lung cancer survival probabilities, the excess lifetime risk can also be understood as a difference in survival probabilities, i.e.,

$$LEAR = LR_E - LR_0 = (1 - LR_0) - (1 - LR_E) =: S_0 - S_E. \tag{22}$$

We present a simple approach to calculate estimates for lung cancer survival curves S_0 and S_E for different radon exposures with uncertainty intervals.

Kaplan-Meier survival curves are such simple non-parametric estimates for survival probabilities in time-to-event analyses [33]. Using Kaplan-Meier survival curves to estimate the difference in lung cancer survival $S_0 - S_E$ has little in common with the original definition of $LEAR$. While a $LEAR$ can be calculated for any explicit exposure scenario, the Kaplan-Meier survival curves rely on more rough windows of cumulative exposure. The resulting lifetime risk estimates are referred to as (naive) $LEAR$ estimates for simplicity. Here, Kaplan-Meier lung cancer survival functions are calculated for miners at Wismut with follow-up 1946-2018 stratified by certain exposure windows. The time axis is age t in years whereas the event is lung cancer death. Due to the large number of miners in the Wismut cohort, we can calculate reliable Kaplan-Meier estimates $\hat{S}(t)$ for $S(t)$ for different radon exposures. Radon exposure is categorized into seven groups ("No exposure", 0-10, 10-50, 50-100, 100-500, 500-1000, and 1000+ WLM), and for each group, survival curves are calculated. For Kaplan-Meier survival estimates, it holds for the probability of not dying of lung cancer until age t,

$$\hat{S}(t) = \prod_{t_k \leq t} \left(1 - \frac{d_k}{n_k}\right)$$

with number of lung cancer deaths d_k and individuals at risk n_k at time point t_k.

Here, a confidence interval for $\hat{S}(t)$ is constructed with *Greenwood's formula* [56] via

$$\widehat{Var}\left(\hat{S}(t)\right) = \hat{S}(t)^2 \sum_{t_k \leq t} \frac{d_k}{n_k(n_k - d_k)} \tag{23}$$

and the asymptotically normal distribution of $\hat{S}(t)$ yields the symmetric point-wise confidence interval at level $1 - \alpha/2$,

$$\hat{S}(t) \pm z_{1-\alpha/2} \sqrt{\widehat{Var}\left(\hat{S}(t)\right)}.$$

Note that Greenwood's formula provides point-wise confidence intervals at each age t, suitable for our analysis. However, researchers seeking simultaneous confidence intervals across the entire survival curve might consider using Hall-Wellner confidence bands [57] or equal probability bands [58]. Detailed methodologies are available in [59, Chapter 4.4], with a practical implementation by the "km.ci" R package [60].

For each miner, we calculate the exact age at the end of follow-up (either 12/31/2018 or before, in case of death or loss-to-follow-up) in days in units of years: e.g. a person dying of lung cancer 10 days after its 85th birthday results in age at the end of follow-up of $85 + \frac{10}{365.25} = 85.03$. Every observed lung cancer death marks a time point t_k. Hence $d_k = 1$ in most cases. Rarely, multiple individuals died of lung cancer at the exact same age, resulting in $d_k > 1$.

B.2 Results

Lung cancer survival curves were constructed for individuals with different levels of cumulative radon exposure (Suppl. Figure 3). The three curves for no exposure, low exposure with at most 10 WLM, and slightly higher exposure with 10 to 50 WLM are close together and only the 50 to 100 WLM curve is notably below (left-hand side plot). Although the curve for 50-100 WLM is notably below the survival for unexposed individuals at practically all time points, the effect is not statistically significant as the point-wise 95% uncertainty interval for the unexposed overlaps with the point-estimate for the 50-100 WLM curve. Likewise, there are age sections where the 0-10 WLM and the 10-50 WLM curves show a slightly higher survival probability than the "No exposure" curve. However, incorporating uncertainty intervals, this effect is not statistically significant. Note that the uncertainty bands for positive exposure groups in the low exposure plot are not shown for readability. The right-hand side plot shows survival curves for considerably higher exposures. There, the survival probabilities are all statistically significantly different at the 95% confidence level. However, at the age of 95, the uncertainties increase resulting in overlap for the category $500 - 1000$ WLM and > 1000 WLM.

To calculate lifetime risks from these survival curves according to (22), setting a maximum age t is necessary. Here, we refer to the calculated lifetime excess risk as $LEAR$ for simplicity. Here, the naive $LEAR$ estimate is the vertical distance between a survival curve for a certain exposure and the "No exposure" survival curve at $t = 85$ (Suppl. Table 4), i.e.

$$LEAR = S_0(85) - S_E(85).$$

The naive $LEAR$ confidence interval bounds are constructed by comparing the "No exposure" curve S_0 with the corresponding exposed survival curve S_E. The lower bound is the difference between the lower bound of the "No exposure" curve and the upper bound of the exposed survival curve. The upper bound is the difference between the upper bound of the "No exposure" curve and the lower bound of the exposed survival curve. $LEAR$ increases for higher exposure with large uncertainties at lower exposure. In particular, the $LEAR$ for exposures below 100 WLM is not statistically significantly different from zero. For higher exposures, the confidence intervals get narrower relative to the reference estimate (relative uncertainty span). Note that in the German uranium miners cohort, the majority were smokers. This results in a presumably lower baseline survival probability compared to a general unexposed population.

This simple and naive approach to deriving uncertainty intervals for lifetime risks yields plausible results. Note that Log-Rank tests (compare [61]) confirmed that most survival curves in Suppl. Figure 3 are statistically significantly different from the "No exposure" curve at the 95% confidence level, i.e. p-values below 0.05. Only the "(0,10) WLM" and "[10,50) WLM" curves are not statistically significantly different from the "No exposure" curve with a p-value of 0.7 and 0.4, respectively.

Although the obtained intervals are rough, plotting the survival curves serves particularly well for an interpretable visual risk assessment to grasp the impact of radon exposure on lung cancer survival. Further, this approach can easily be applied to other endpoints than radon-induced lung cancer.

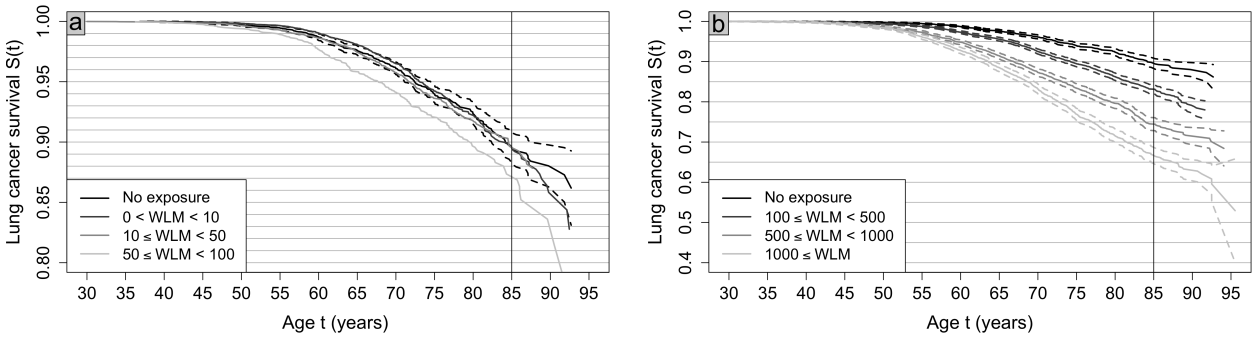

Supplementary Figure 3: Kaplan-Meier lung cancer survival curve estimates for miners from the Wismut cohort for different windows of total cumulative exposure in WLM. The corresponding dashed lines represent the point-wise upper and lower bound of the 95% uncertainty interval. A vertical line at age 85 indicates the cut-point for lifetime risk calculations. The left-hand side plot shows lung cancer survival curve estimates for lower exposures, whereas the right-hand side plot shows lung cancer survival curve estimates for higher exposures.

WLM interval	Cohort size	$\hat{S}_E(85)$ in %	$\widehat{LR}_E(85)$ in %	$LEAR$ in %
No exposure	8,213 (50.15%)	89.55 [88.28; 90.84]	10.45 [9.16; 11.72]	-
$(0, 10)$	16,544 (30.31%)	89.52 [88.28; 90.78]	10.48 [9.22; 11.72]	0.03 [−2.50; 2.56]
$[10, 50)$	11,185 (39.16%)	89.47 [88.12; 90.81]	10.53 [9.19; 11.88]	0.09 [−2.54; 2.71]
$[50, 100)$	3,314 (57.51%)	86.86 [84.67; 89.05]	13.14 [10.95; 15.33]	2.69 [−0.78; 6.17]
$[100, 500)$	8,979 (72.81%)	83.12 [81.97; 84.27]	16.88 [15.73; 18.03]	6.43 [4.01; 8.87]
$[500, 1000)$	6,039 (80.54%)	74.42 [72.81; 76.04]	25.58 [23.94; 27.19]	15.13 [12.22; 18.03]
$[1000, \infty)$	4,698 (85.89%)	66.58 [64.55; 68.61]	33.42 [31.39; 35.45]	22.97 [19.67; 26.29]

Supplementary Table 4: Values for Kaplan-Meier lung cancer survival estimates $\hat{S}_E(85)$, $\widehat{LR}_E(85) = 1 - \hat{S}_E(85)$ and $LEAR$ as $\widehat{LR}_E(85)$ minus the baseline $S_0(85)$ for different windows of total cumulative exposures in WLM with corresponding 95% uncertainty interval in correspondence to Suppl. Figure 3. For reference, the corresponding cohort size is shown, with the fraction of individuals deceased before age 85 in brackets.

C Risk model parameter uncertainty

This supplementary analysis on risk model parameter uncertainty presents the ANA approach for the simple linear risk model and extends the Bayesian approach for the parametric 1960+ sub-cohort model by incorporating a wider range of prior information combinations. Further, the Bayesian approach is applied to the simple linear risk model using gamma-distributed and log-normally distributed priors for β.

C.1 ANA approach for the simple linear 1960+ sub-cohort risk model - analytical solution

For the simple linear risk model,

$$ERR(t;\hat{\beta}) = \hat{\beta}W(t), \tag{24}$$

which is derived from the Wismut 1960+ sub-cohort, the ANA approach employs:

$$\hat{\beta} \sim \mathcal{N}\left(\hat{\beta}_0, \hat{\sigma}_0^2\right) \tag{25}$$

with $\hat{\beta}_0 = 0.0134$ and $\hat{\sigma}_0 = 0.003005$ as reported in [23]. Sampling from this distribution (25) is not necessary, as it holds

$$LEAR \approx \sum_{t\geq 0} r_0(t)ERR(t;\hat{\beta})\tilde{S}(t) = \hat{\beta}\sum_{t\geq 0} r_0(t)W(t)\tilde{S}(t) =: \hat{\beta}\cdot C, \tag{26}$$

with $C = \sum_{t\geq 0} r_0(t)W(t)e^{-\sum_{u=0}^{t-1} q_0(u)}$. Hence approximately, $LEAR \sim \mathcal{N}\left(\hat{\beta}_0 \cdot C, \hat{\sigma}_0^2 \cdot C^2\right)$ with confidence bands at level α,

$$\hat{\beta}_0 \cdot C \pm z_{1-\alpha/2} \cdot \hat{\sigma}_0 \cdot C, \tag{27}$$

where $z_{1-\alpha/2}$ is the standard-normal quantile at level $1-\alpha/2$. It holds $C = 4.27$ for ICRP reference mortality rates $r_0^{(ICRP)}(t), q_0^{(ICRP)}(t)$ for all ages t and an exposure scenario of 2 WLM from age 18-64 years. For this simple linear model, (27) yields the estimate 5.71 with 95% uncertainty interval ($\alpha = 0.05$), $[3.18; 8.22]$ for LEAR in %, as stated in the main manuscript.

C.2 Bayesian approach for the simple linear 1960+ sub-cohort risk model

Here, we investigate risk model parameter uncertainty and its influence on $LEAR$ estimates within the Bayesian framework for the simple linear risk model (24). The general methodology and notation are analogous to the main manuscript. To assess the influence of prior choices on the inference of β, we explore choosing a log-normal distribution as a prior in contrast to the gamma distribution in the main manuscript. To test this framework, again the "prior" information is the β estimate from [25] with $\hat{\beta}_{CZ+F} = 0.016$. The corresponding "prior" $LEAR$ in % estimate calculated with $\hat{\beta}_{CZ+F}$ is 6.83. We assume for the prior distribution $P(\beta)$ of the risk model parameter β,

$$\beta \sim \mathcal{LN}\left(\log\left(\hat{\beta}_{CZ+F}\right) + \sigma^2, \sigma^2\right) \tag{28}$$

such that again $Mod(\beta) = e^{\log\left(\hat{\beta}_{CZ+F}\right)+\sigma^2-\sigma^2} = \hat{\beta}_{CZ+F}$ to match the mode with the prior information. The variance is controlled via σ. Compared to a gamma distribution, this distribution is characterized by heavier right tails.

To be comparable with the assumed certainty with the gamma-distributed prior in the main manuscript, we assume an equal coefficient of variation between gamma- and log-normally distributed priors by prescribing $\sigma = \sqrt{\log\left(1+\frac{1}{a}\right)}$. This allows for comparison with the gamma prior while maintaining similar variation (Suppl. Table 5). The values $(2, 5, 10, 20, 50)$ for a translate to $(0.64, 0.43, 0.31, 0.22, 0.14)$ for σ. Log-normal priors lead to slightly narrower highest posterior density intervals (HPDIs) and a tendency toward larger values compared to gamma priors. This difference diminishes with increasing prior certainty (smaller σ).

Prior information	$\hat{\beta} = Mod(P(\beta\|X)) \times 100$	$LEAR$ in %
ML estimate with Wald-type CI	1.34 [0.71; 1.97]	5.72 [3.03; 8.41] (0.94)
Uniform prior	1.34 [0.79; 2.08]	5.72 [3.37; 8.90] (0.96)
Log-normal-distributed prior		
$\sigma = 0.64$	1.37 [0.85; 2.07]	5.85 [3.62; 8.81] (0.89)
$\sigma = 0.43$	1.40 [0.90; 2.05]	5.97 [3.85; 8.75] (0.82)
$\sigma = 0.31$	1.43 [0.97; 2.03]	6.11 [4.16; 8.66] (0.74)
$\sigma = 0.22$	1.47 [1.06; 1.99]	6.29 [4.54; 8.50] (0.63)
$\sigma = 0.14$	1.53 [1.20; 1.92]	6.52 [5.13; 8.19] (0.47)

Supplementary Table 5: Mode $\hat{\beta}$ of posterior distribution $P(\beta|X)$ with $LEAR$ calculated with the model (24) and their corresponding 95% highest posterior density interval (HPDI) (relative uncertainty span in brackets) for varying prior parameter settings. The log-normal-distributed prior $P(\beta)$ is centered at the corresponding parameter estimate from [25] for different values of prior standard deviation parameters σ. Wald-type confidence intervals (CI) are also shown for comparison and are calculated as $\hat{\beta} \pm 1.96 \times 0.003005$, where 0.003005 represents the parameter standard error as stated in [23].

C.3 Bayesian approach for the parametric 1960+ sub-cohort risk model - additional details

Here, supplemental results are shown for the Bayesian approach to quantify uncertainties for the parametric 1960+ sub-cohort risk model (5) from [23],

$$ERR(t; \beta, \alpha, \varepsilon) = \beta W(t) \exp\left\{\alpha \left(AME(t) - 30\right)) + \varepsilon \left(TME(t) - 20\right)\right\}.$$

The approach is completely analogous to the main manuscript. However, a more detailed view of results are shown with more choices for prior standard deviations σ. In particular, the derived risk model parameter estimates with 95% HPDI are shown (Suppl. Table 6 and Figure4).

Supplementary Figure 4 shows scatterplots for risk model parameters samples for varying prior parameter choices. The marginal probability densities are on the sides. To read Suppl. Figure 4, the first row shows the scattering of parameters for increasing certainty in the priors for β, α, ε. Varying gamma shape parameter a affects the β prior and varying σ affects both the priors for α and ε. The second row shows the effect of increased certainty in β without changing priors for α and ε. Analogously, the third row visualizes the effect of increased certainty in α and ε without affecting β. Similar to the simple linear risk model (24), we observe a concentration of samples for increased certainty in the prior information which likewise affects uncertainty intervals. Further, increasing certainty in one parameter barely affects the scattering for other parameters because the marginal prior distributions are mutually independent.

Prior information	$\hat{\beta} \times 100$	$\hat{\alpha} \times 100$	$\hat{\varepsilon} \times 100$	$LEAR$ in %
ML estimate with Wald-type CI	4.75 [1.60; 7.90]	−3.07 [−8.16; 2.01]	−7.63 [−11.80; −3.47]	6.74
Uniform prior	4.75 [2.13; 9.11]	−3.07 [−9.36; 1.26]	−7.63 [−12.89; −4.08]	6.74 [2.96; 11.09] (1.21)
Prior standard deviation $\sigma = 0.1$				
$a = 2$	4.75 [2.37; 8.55]	−3.25 [−9.05; 0.86]	−7.70 [−12.57; −4.42]	6.59 [2.96; 10.57] (1.15)
$a = 5$	4.61 [2.40; 7.59]	−3.17 [−8.83; 1.00]	−7.57 [−12.05; −4.40]	6.52 [2.91; 10.26] (1.13)
$a = 10$	4.49 [2.66; 6.88]	−3.08 [−8.66; 1.20]	−7.45 [−11.59; −4.29]	6.46 [2.83; 10.14] (1.13)
$a = 20$	4.38 [2.93; 6.18]	−3.01 [−8.58; 0.99]	−7.35 [−11.41; −4.60]	6.40 [3.04; 10.07] (1.10)
$a = 50$	4.29 [3.25; 5.45]	−2.95 [−8.57; 1.14]	−7.25 [−11.23; −4.65]	6.35 [2.95; 9.91] (1.10)
Prior standard deviation $\sigma = 0.05$				
$a = 2$	4.86 [2.41; 8.45]	−3.78 [−8.89; 0.07]	−7.96 [−12.16; −4.74]	6.32 [2.93; 10.19] (1.15)
$a = 5$	4.70 [2.55; 7.72]	−3.71 [−8.92; 0.01]	−7.82 [−11.79; −4.74]	6.22 [2.89; 9.89] (1.13)
$a = 10$	4.56 [2.79; 6.89]	−3.64 [−8.67; 0.30]	−7.70 [−11.51; −4.73]	6.12 [2.93; 9.66] (1.10)
$a = 20$	4.43 [2.92; 6.14]	−3.58 [−8.60; 0.37]	−7.58 [−11.32; −4.86]	6.04 [2.77; 9.23] (1.07)
$a = 50$	4.31 [3.28; 5.47]	−3.52 [−8.50; 0.51]	−7.48 [−10.96; −4.83]	5.96 [2.88; 9.20] (1.06)
Prior standard deviation $\sigma = 0.02$				
$a = 2$	4.97 [2.55; 8.23]	−5.17 [−8.37; −2.30]	−8.36 [−11.26; −5.91]	5.56 [2.76; 8.98] (1.12)
$a = 5$	4.80 [2.72; 7.53]	−5.16 [−8.41; −2.22]	−8.27 [−11.11; −5.90]	5.41 [2.82; 8.45] (1.04)
$a = 10$	4.64 [2.81; 6.92]	−5.15 [−8.31; −2.10]	−8.17 [−10.86; −5.81]	5.27 [2.89; 8.15] (1.00)
$a = 20$	4.49 [3.08; 6.21]	−5.16 [−8.27; −2.05]	−8.10 [−10.67; −5.79]	5.13 [2.99; 7.58] (0.90)
$a = 50$	4.34 [3.30; 5.50]	−5.16 [−8.39; −2.10]	−8.01 [−10.60; −5.82]	4.99 [3.14; 7.26] (0.83)
Prior standard deviation $\sigma = 0.01$				
$a = 2$	4.76 [2.67; 7.68]	−6.02 [−7.91; −4.23]	−8.24 [−10.08; −6.69]	5.00 [2.88; 8.13] (1.05)
$a = 5$	4.65 [2.76; 7.12]	−6.03 [−7.88; −4.22]	−8.21 [−10.06; −6.71]	4.90 [2.93; 7.53] (0.94)
$a = 10$	4.55 [2.90; 6.58]	−6.04 [−7.83; −4.21]	−8.17 [−9.85; −6.59]	4.79 [2.96; 7.03] (0.85)
$a = 20$	4.44 [3.05; 6.10]	−6.05 [−7.88; −4.28]	−8.14 [−9.77; −6.58]	4.68 [3.06; 6.63] (0.76)
$a = 50$	4.32 [3.32; 5.49]	−6.06 [−7.83; −4.15]	−8.11 [−9.78; −6.56]	4.57 [3.34; 6.17] (0.62)
Prior standard deviation $\sigma = 0.005$				
$a = 2$	4.59 [2.79; 7.35]	−6.40 [−7.36; −5.42]	−8.07 [−9.03; −7.12]	4.73 [2.74; 7.44] (0.99)
$a = 5$	4.52 [2.70; 6.76]	−6.39 [−7.36; −5.46]	−8.07 [−9.05; −7.19]	4.66 [2.85; 7.06] (0.90)
$a = 10$	4.45 [3.01; 6.41]	−6.39 [−7.34; −5.44]	−8.06 [−8.98; −7.17]	4.59 [3.07; 6.57] (0.76)
$a = 20$	4.38 [3.11; 5.99]	−6.40 [−7.35; −5.45]	−8.05 [−8.95; −7.11]	4.52 [3.17; 6.27] (0.69)
$a = 50$	4.30 [3.30; 5.39]	−6.40 [−7.39; −5.50]	−8.04 [−8.94; −7.12]	4.43 [3.34; 5.66] (0.52)

Supplementary Table 6: Components $\hat{\beta}, \hat{\alpha}, \hat{\varepsilon}$ of the mode vector $\hat{\Theta} = Mod(P(\Theta|X))$ of the posterior distribution $P(\Theta|X)$ with $LEAR$ evaluated at mode $\hat{\Theta}$ and the corresponding 95% highest posterior density interval (HPDI) (relative uncertainty span in brackets) for different values of prior gamma shape parameters a and prior standard deviation σ. The $LEAR$ in % with risk model parameter estimates derived from the Joint Czech+French cohort is 4.30. The Wald-type confidence intervals (CI) are calculated as $\hat{\theta} \pm 1.96 \times \hat{\sigma}_\theta$, where $\hat{\sigma}_\theta$ represents the parameter standard error from [23] for $\theta = \beta, \alpha, \varepsilon$, respectively.

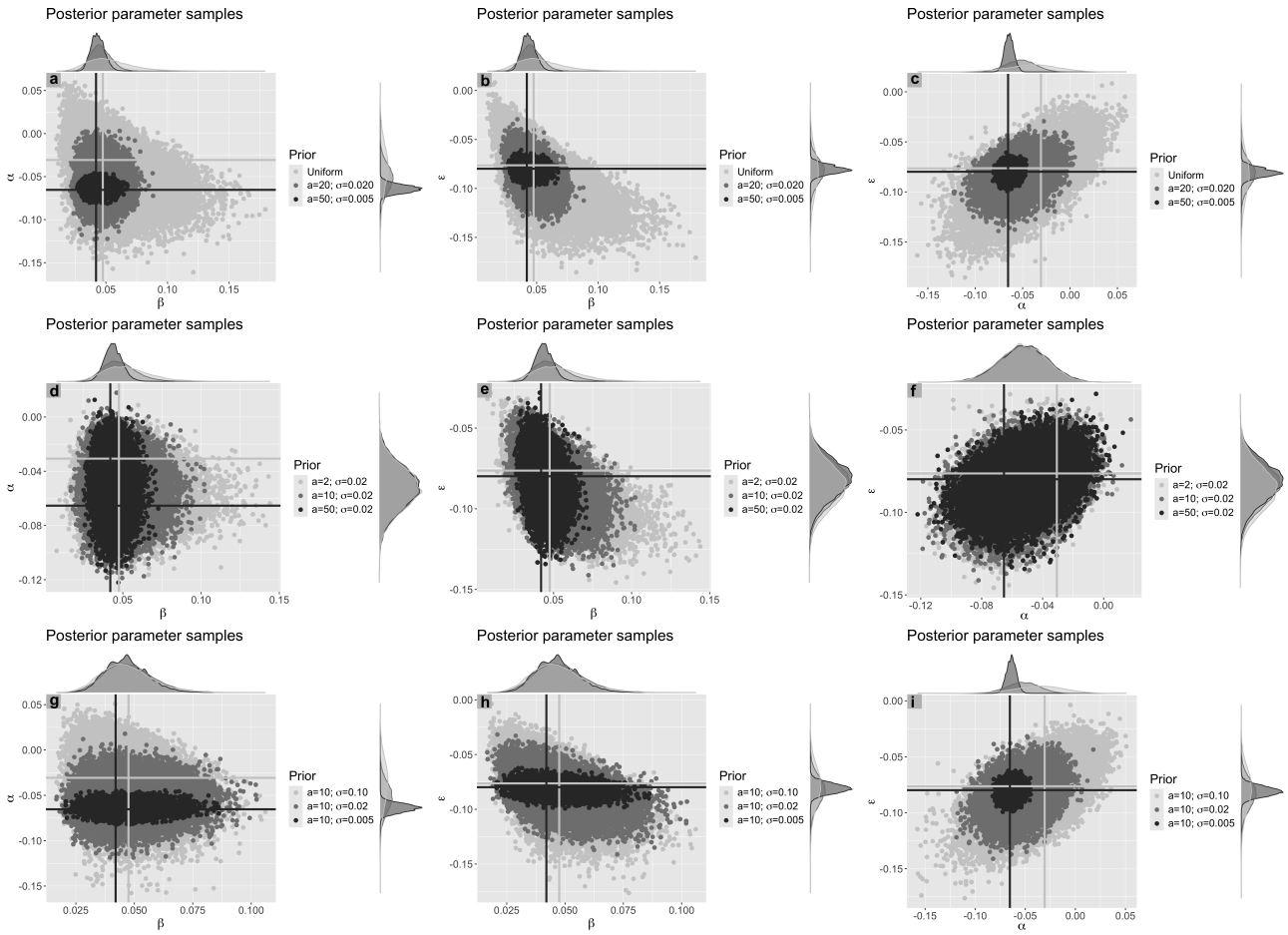

Supplementary Figure 4: Scatterplots of 100,000 parameter samples (β, α), (β, ε) and (α, ε) from posterior distribution $P(\Theta|X)$ using Bayesian inference methods with marginal probability density on the sides in correspondence to Table 6. The model parameters $\Theta = (\beta, \alpha, \varepsilon)$ (model (5) are estimated assuming prior distributions $P(\Theta) = P(\beta)P(\alpha)P(\varepsilon)$ for gamma-distributed β and normally distributed α, ε. The plots show the effect of increased certainty in all parameters $\beta, \alpha, \varepsilon$ (first row), only β (second row), and α, ε (last row). The intersection of horizontal and vertical lines indicates the optimal parameter values in the prior distribution (black) and the likelihood function (light grey).

D Mortality rate uncertainty

In this section, only mortality rates are assumed to be uncertain, analogously to the main manuscript (see uncertainty assessment in the Methods section). In particular, risk model parameters are fixed and do not influence uncertainty intervals.

D.1 Preliminaries

This section investigates the effect of all-cause mortality rate uncertainty and the impact of centering mortality rate distributions derived from sex-averaged WHO data around the ICRP reference value. Both effects will be found to be negligible for upcoming analyses.

D.1.1 Influence of all-cause mortality rates

Here, we compare the uncertainties in all-cause mortality rates $q_0(t)$ and lung cancer mortality rates $r_0(t)$ and their effect on the LEAR across various risk models.

As explained in the main manuscript, we assume a gamma distribution on both mortality rates for all ages t as in (10) and (11),

$$r_0(t) \sim G\left(a_t^{(r_0)}, b_t^{(r_0)}\right),$$
$$q_0(t) \sim G\left(a_t^{(q_0)}, b_t^{(q_0)}\right),$$

with age-dependent shape parameters $a_t^{(r_0)}, a_t^{(q_0)}$ and rate parameter $b_t^{(r_0)}, b_t^{(q_0)}$. The main manuscript outlines the model fitting on WHO data with resulting parameter estimates shown in Suppl. Table 7 and the corresponding derivation of LEAR uncertainty intervals.

The analysis reveals that all-cause mortality rates $q_0(t)$ impose considerably less uncertainty on the LEAR than lung cancer rates $r_0(t)$ for all risk models (Suppl. Figure 5). The empirical distribution of sampled LEAR estimates for gamma-distributed $q_0(t)$ is considerably narrower compared to the empirical distribution for gamma-distributed $r_0(t)$, which is also reflected in the 95% uncertainty intervals. The reference LEAR estimate is on the far right of the calculated uncertainty interval accounting for $q_0(t)$ uncertainty and even outside the interval for the BEIR VI 1960+ sub-cohort risk model. This is possible because reference estimates (ICRP 103) are calculated with ICRP reference mortality rates independent of WHO data. The combined effect of $r_0(t)$ with $q_0(t)$ is very similar to the effect when only $r_0(t)$ is considered. The relative uncertainty span is very similar across all considered risk models with roughly 0.45 for $r_0(t)$ uncertainties and joint uncertainties $r_0(t)$, $q_0(t)$, and roughly 0.10 for only uncertain $q_0(t)$.

D.1.2 Centered gamma distributed mortality rates

The derivation of gamma distribution parameters estimates in (10) and (11) from WHO data is independent of ICRP reference rates $r_0^{(ICRP)}(t)$ and $q_0^{(ICRP)}(t)$. In particular, the mean of the resulting gamma distributions does not match the ICRP reference rates. To address this, we investigated a centered gamma distribution with the expectation equal to the ICRP rate by setting

$$\hat{b}_t^{(r_0)} = \frac{\hat{a}_t^{(r_0)}}{r_0^{(ICRP)}(t)}$$

and

$$\hat{b}_t^{(q_0)} = \frac{\hat{a}_t^{(q_0)}}{q_0^{(ICRP)}(t)}$$

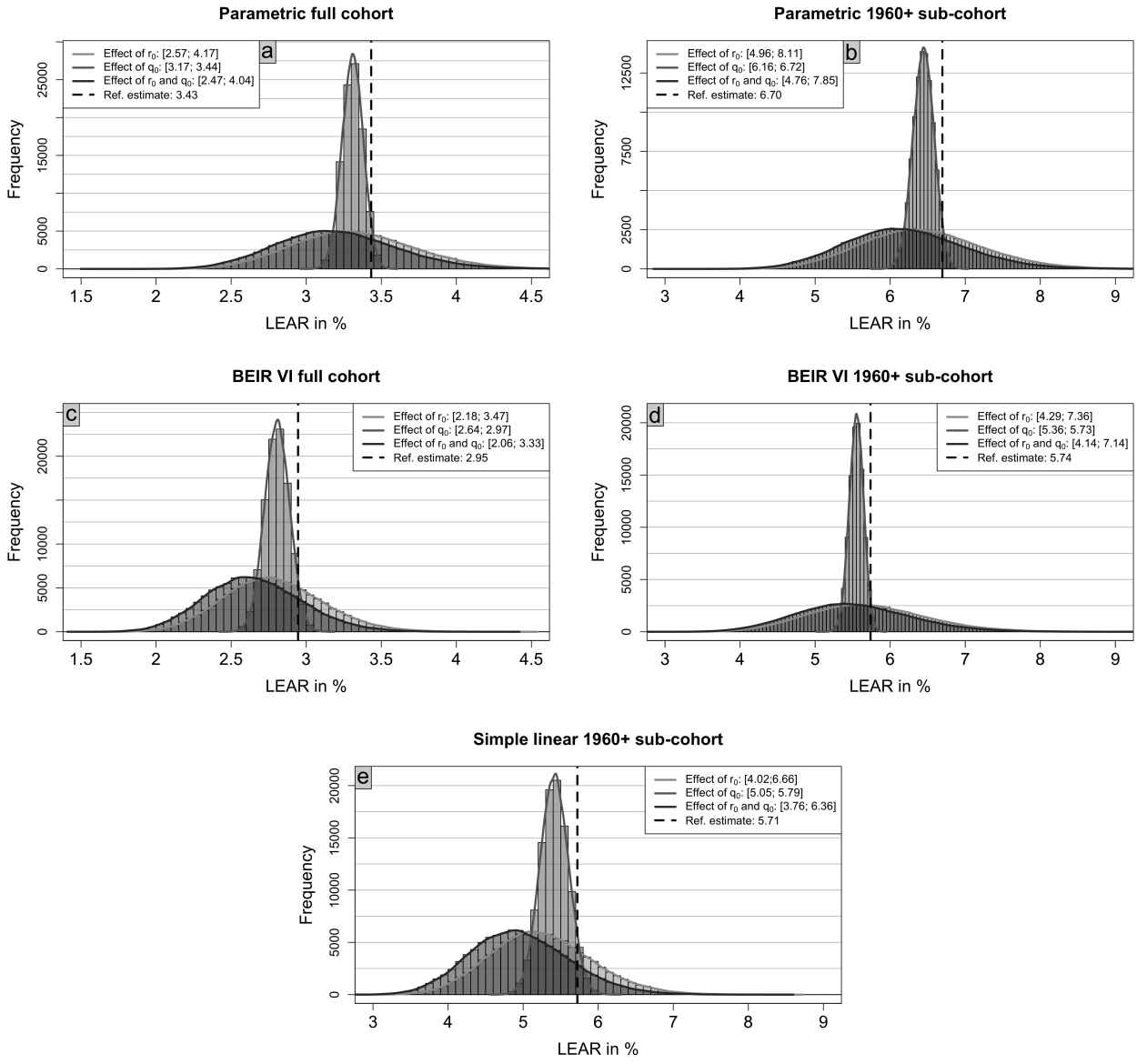

Supplementary Figure 5: Histogram of 100,000 resulting $LEAR$ estimates with kernel density (solid lines) for different risk models (plot title) and varying uncertainty in mortality rates (grayscale, different histograms per plot). Lung cancer mortality rates $r_0(t)$ (Effect of r_0) and all-cause mortality rates $q_0(t)$ (Effect of q_0) are assumed to follow gamma distributions with parameters as in Suppl. Table 7. The joint effect (Effect of r_0 and q_0) results from independent sampling from both corresponding probability distributions. 95% uncertainty intervals are presented in the legend.

	Lung cancer mortality				All-cause mortality			
Age t	$\hat{a}_t^{(r_0)}$	$\hat{b}_t^{(r_0)}$	$\frac{\hat{a}_t^{(r_0)}}{\hat{b}_t^{(r_0)}} \times 10^5$	$r_0^{(ICRP)}(t) \times 10^5$	$\hat{a}_t^{(q_0)}$	$\hat{b}_t^{(q_0)}$	$\frac{\hat{a}_t^{(q_0)}}{\hat{b}_t^{(q_0)}} \times 10^5$	$q_0^{(ICRP)}(t) \times 10^5$
$20-24$	0.97	244,677.63	0.40	0.14	2.33	3,952.30	58.95	51.48
$25-29$	1.30	219,930.33	0.59	0.32	2.26	3,255.88	69.41	58.12
$30-34$	2.56	248,034.10	1.03	0.98	2.30	2,568.26	89.55	76.26
$35-39$	2.34	100,097.58	2.34	2.64	2.38	1,867.51	127.44	104.91
$40-44$	2.03	30,061.06	6.75	6.99	2.56	1,278.99	200.16	160.86
$45-49$	1.79	10,422.60	17.17	14.86	2.80	878.12	318.86	238.39
$50-54$	1.83	4,940.48	37.04	29.98	2.99	592.00	505.07	363.15
$55-59$	1.66	2,448.62	67.79	56.76	3.29	424.11	775.74	589.27
$60-64$	1.74	1,595.66	109.05	107.21	3.60	302.02	1,191.97	1,044.14
$65-69$	1.69	1,078.86	156.65	174.41	4.13	222.12	1,859.36	1,717.99
$70-74$	1.70	830.72	204.64	240.85	5.05	170.36	2,964.31	2,855.71
$75-79$	1.69	690.09	244.90	284.17	5.88	121.95	4,821.65	4,618.33
$80-84$	1.70	627.56	270.89	304.90	9.65	117.77	8,193.94	7,807.24
$85-89$	1.47	594.61	247.22	274.92	6.85	48.92	14,002.45	11,369.96
$90-94$	1.68	714.17	235.24	233.50	29.31	127.69	22,954.03	20,897.22

Supplementary Table 7: Estimates $\hat{a}_t^{(r_0)}, \hat{a}_t^{(q_0)}$ and $\hat{b}_t^{(r_0)}, \hat{b}_t^{(q_0)}$ with corresponding fraction (mean of the distribution) for shape and rate parameter in the gamma distribution $\mathcal{G}\left(a_t^{(r_0)}, b_t^{(r_0)}\right)$ and $\mathcal{G}\left(a_t^{(q_0)}, b_t^{(q_0)}\right)$ based on observed lung cancer or all-cause mortality in the WHO data, respectively for different age groups with the corresponding ICRP mortality rates $r_0^{(ICRP)}(t)$, $q_0^{(ICRP)}(t)$.

for all ages t.[2] Preliminary analyses revealed that this adjustment yielded only minor differences and a negligible impact on lifetime risk estimates. For example, this can be inferred by comparing similar results for the values $r_0^{(ICRP)}(t)$, $\frac{\hat{a}_t^{(r_0)}}{\hat{b}_t^{(r_0)}}$ and $q_0^{(ICRP)}(t)$, $\frac{\hat{a}_t^{(q_0)}}{\hat{b}_t^{(q_0)}}$ for the important groups of older ages in Suppl. Table 7. Hence, we retained the un-centered gamma distributions for Monte Carlo simulations in the main paper to avoid constraining parameter estimation. The same applies to the log-normal distribution used in Section D.3. Note that this holds for sex-averaged mortality rates. For sex-specific mortality rates (Section E.1), larger discrepancies justify explicitly analyzing centered mortality rate uncertainties. Although centering may affect lifetime risk estimates, the relative uncertainty span is not notably affected.

D.2 Poisson distributed lung cancer deaths

We present an alternative, but similar approach, to assess mortality rate uncertainty on lifetime risks connecting ICRP reference mortality rates (Euro-American-Asian mixed population) with WHO mortality data (Countries from Europe, America, and Asia from the calendar years 2001, 2006, 2011, 2016, and 2021). Ultimately, this approach aims at a Bayesian assessment of mortality rate uncertainty:

Non-parametric Poisson regression on WHO lung cancer mortality data yields age-specific rates $r_0(t)$ for all ages t (Suppl. Table 8). Only observations with a positive number of cases and a positive number of individuals at risk were included. Focusing on lung cancer mortality (heavily influencing $LEAR$s), this approach is analogous to less influential all-cause mortality rates $q_0(t)$. Each data point (country, sex, and calendar year) comprises deceased and alive individuals (mid-year population), interpreted as cases and person-years for Poisson regression. Correlations between years and countries are neglected, assuming independence between observations for simplicity.[3]

[2] The expectation of a generic gamma distribution $G(a_t, b_t)$ is a_t/b_t.

[3] This is no major issue because the upcoming analyses reveal that also uncorrelated WHO data from a specific country and year yield narrow $LEAR$ uncertainty intervals.

D.2.1 Likelihood

We employ Poisson regression assuming the number of lung cancer deaths D_i for a certain age group (compare e.g. Suppl. Table 7) follows a Poisson distribution with $D_i \sim Poi(\lambda_i) = Poi(N_i e^{\theta})$ for WHO population data $X = \{N_i, d_i \mid i = 1, \ldots, M\}$. Here, θ is the unknown parameter, N_i are known person-years at risk, and d_i are observed lung cancer cases for M observations. Each observation i is uniquely defined by a specific country, sex, and calendar year.

Note that θ does not depend on the observations i. So, regardless of the country and year under consideration, the expected number of deaths depends only on the number of people in that group. Therefore, country- and calendar year-specific characteristics are only accounted for through the random fluctuation of the Poisson distribution. This approach is applied for every age group separately. Here we suppress the age dependency for simplicity, but later we write for the relevant parameter $\theta_t = \theta$. The probability of d_i deaths with N_i person-years at risk is:

$$\mathbb{P}\left(D_i = d_i | X, \theta\right) = \frac{\left(N_i e^{\theta}\right)^{d_i}}{d_i!} e^{-N_i e^{\theta}}. \tag{29}$$

The likelihood function $L(X|\theta)$ is then

$$L(X|\theta) = \prod_{i=1}^{M} \frac{\left(N_i e^{\theta}\right)^{d_i}}{d_i!} e^{-N_i e^{\theta}} \tag{30}$$

with log-likelihood $\ell\left(X|\theta\right)$,

$$\ell(X|\theta) = \sum_{i=1}^{M} d_i \left(\log\left(N_i\right) + \theta\right) - N_i e^{\theta} - \log\left(d_i!\right) \propto \sum_{i=1}^{M} d_i \left(\log\left(N_i\right) + \theta\right) - N_i e^{\theta}. \tag{31}$$

The simple structure yields the maximum likelihood estimate for θ:

$$\hat{\theta} = \log \frac{\sum_{i=1}^{M} d_i}{\sum_{i=1}^{M} N_i}. \tag{32}$$

This simplifies to $e^{\hat{\theta}} = \frac{d}{N}$ with $d = \sum_{i=1}^{M} d_i$ and $N = \sum_{i=1}^{M} N_i$ (estimates in Suppl. Table 8).

Notably, $e^{\hat{\theta}}$ can be interpreted as a population-weighted average of single mortality rates $\frac{d_i}{N_i}$ with weights $w_i = \frac{N_i}{N}$ and $N = \sum_{i=1}^{M} N_i$ due to the Poisson likelihood. The weights w_i correspond to the relative size of each population at risk N_i compared to the total population N. Each $\frac{d_i}{N_i}$ is equivalent to the maximum likelihood estimate for the probability of a single binomial experiment with known population N_i and observed successes d_i. Larger populations contribute more to the parameter estimation. This is a key difference to the other approach, utilizing a Gamma or Log-normal distribution, where observed mortality rates are all equally weighted for parameter estimation. In the above Poisson Regression, each observation is represented by the tupel (N_i, d_i), whereas in the applied Gamma (or Log-normal) regression, it is defined by the ratio d_i/N_i. In the latter approach, the specific information regarding the individual counts d_i,N_i is not accounted for.

The most suitable approach will depend on the assumptions made about the variance of the observations. If larger populations are assumed to lead to more precise estimates, the Poisson approach may be preferable. Alternatively, if all observations are considered equal, gamma regression could be a more appropriate choice.

D.2.2 Bayesian posterior

After setting up the Likelihood structure, we add the prior information for the Bayesian inference: A normal prior $\mathcal{N}(\mu_t, \sigma_t^2)$ is assumed for $\theta = \theta_t$ with $\mu_t = \log(r_0^{(ICRP)}(t))$ incorporating ICRP reference

Age	Observations	$N \times 10^{-6}$	d	$\frac{d}{N} \times 10^6$
Europe, America and Asia; 2001, 2006, 2011, 2016 and 2021				
$20-24$	118	195.89	326	1.66
$25-29$	210	265.12	777	2.93
$30-34$	259	285.62	2,073	7.26
$35-39$	313	300.78	6,261	20.82
$40-44$	352	302.67	18,933	62.55
$45-49$	378	293.17	46,568	158.84
$50-54$	380	274.87	93,770	341.14
$55-59$	383	245.26	155,584	634.37
$60-64$	384	213.69	220,337	1,031.10
$65-69$	384	184.51	278,720	1,510.60
$70-74$	386	154.22	313,580	2,033.39
$75-79$	388	126.34	312,099	2,470.33
$80-84$	372	86.59	238,244	2,751.36
$85-89$	365	61.16	134,348	2,196.53
$90-94$	167	8.99	21,826	2,428.93
Europe, America and Asia; 2016				
$20-24$	36	56.38	125	2.22
$25-29$	60	72.29	261	3.61
$30-34$	73	75.88	545	7.18
$35-39$	88	77.21	1,274	16.50
$40-44$	100	76.85	3,141	40.87
$45-49$	107	76.36	7,391	96.80
$50-54$	108	71.80	16,868	234.92
$55-59$	109	64.94	32,291	497.29
$60-64$	109	56.95	50,737	890.96
$65-69$	109	51.64	68,089	1,318.62
$70-74$	110	37.99	67,823	1,785.49
$75-79$	111	32.71	68,777	2,102.52
$80-84$	103	22.83	57,269	2,508.08
$85-89$	104	15.10	37,619	2,491.16
$90-94$	62	4.06	10,072	2,481.31
Germany; 2016				
$20-24$	2	4.58	3	0.65
$25-29$	2	5.38	8	1.49
$30-34$	2	5.19	26	5.01
$35-39$	2	5.01	60	11.99
$40-44$	2	4.91	208	42.40
$45-49$	2	6.39	755	118.12
$50-54$	2	6.97	2,143	307.48
$55-59$	2	6.13	4,037	658.47
$60-64$	2	5.24	5,833	1,112.81
$65-69$	2	4.45	6,832	1,536.11
$70-74$	2	3.81	7,223	1,894.77
$75-79$	2	4.31	8,535	1,980.40
$80-84$	2	2.61	5,564	2,132.05
$85-89$	2	1.49	3,415	2,288.84
$90-94$	2	0.60	995	1,659.25

Supplementary Table 8: Sex-averaged lung cancer mortality rate estimates $e^{\hat{\theta}} = \frac{d}{N}$ for all age groups derived from WHO data with total observed deaths $d > 0$ and individuals at risk $N > 0$.

lung cancer rates. Varying σ_t^2 controls the prior influence (visualized in Suppl. Figure 6 for ages 55-59 and different subsets of the WHO data). The likelihood dominates and differences between WHO rates and ICRP rates are minor, resulting in near-normal posteriors with minimal uncertainty (confirmed by Kolmogorov-Smirnov tests).

For the calculation of corresponding $LEAR$s, the simple linear risk model $ERR(t;\hat{\beta}) = \hat{\beta}W(t)$ with $\hat{\beta} = 0.0134$ is used. While decreasing the WHO data influence increases the impact of the prior distribution, the effect on $LEAR$ uncertainty remains negligible (Suppl. Table 9) with relative uncertainty spans of order 10^{-3}. Increasing prior certainty narrows uncertainty intervals and shifts the mode towards the $LEAR$ calculated with ICRP rates (Suppl. Figure 7). The dominance of WHO data raises questions about the overall benefit of this approach.

In conclusion, the integration of a population-weighted Poisson approach with the comprehensive WHO dataset results in mortality rate estimates with little uncertainty. Likewise, employing a Bayesian approach with arbitrary prior encoding beliefs from other sources (i.e. ICRP reference rates) offers minimal new insights. The extensive dataset provided by the WHO considerably diminishes the influence of prior assumptions on the analytical outcomes. Only when using unrealistically low prior variances or substantially reducing the WHO data does any impact of the prior become noticeable. However, the scientific value of such an approach for understanding mortality rate uncertainties is limited. Instead, it is evident that the combination of the WHO database and the population-weighted Poisson method yields low uncertainties, and the WHO rates align well with ICRP reference rates.

Prior	$LEAR$ in % (95% HPDI)		
σ_t	Full	Full 2016	Germany 2016
Uniform prior	5.1218 [5.1182; 5.1254]	4.5565 [4.5500; 4.5629]	4.6553 [4.6351; 4.6743]
0.050	5.1226 [5.1190; 5.1261]	4.5647 [4.5581; 4.5710]	4.7274 [4.7083; 4.7463]
0.010	5.1402 [5.1369; 5.1437]	4.7126 [4.7068; 4.7186]	5.2523 [5.2392; 5.2654]
0.005	5.1900 [5.1869; 5.1932]	4.9800 [4.9748; 4.9849]	5.5342 [5.5258; 5.5425]
0.002	5.3885 [5.3860; 5.3909]	5.4482 [5.4450; 5.4514]	5.6856 [5.6818; 5.6893]

Supplementary Table 9: $LEAR$ evaluated at the mode of the posterior distribution with 95% highest posterior density interval (HPDI) (relative uncertainty spans of order 10^{-3}) for the simple linear risk model $ERR(t;\beta) = \beta W(t)$ with $\beta = 0.0134$. The prior is modelled as $\log r_0(t) \sim \mathcal{N}\left(\mu_t, \sigma_t^2\right)$ and $\mu_t = \log\left(r_0^{(ICRP)}(t)\right)$. The $LEAR$ in % with ICRP reference rates is 5.7222. "Full" corresponds to WHO data from countries in Europe, America, and Asia from the calendar years 2001, 2006, 2011, 2016, and 2021.

D.3 Log-normal distributed mortality rates

Here, we compare utilizing a log-normal distribution for fitting sex-averaged mortality rates from WHO data, instead of a gamma distribution as in the main manuscript. Specifically, we model the mortality rates for all ages t as follows:

$$r_0(t) \sim \mathcal{LN}\left(\mu_t^{(r_0)}, \left(\sigma_t^{(r_0)}\right)^2\right), \tag{33}$$

$$q_0(t) \sim \mathcal{LN}\left(\mu_t^{(q_0)}, \left(\sigma_t^{(q_0)}\right)^2\right). \tag{34}$$

with age-dependent log-mean parameter $\mu_t^{(r_0)}, \mu_t^{(q_0)}$ and log-standard deviation parameter $\sigma_t^{(r_0)}, \sigma_t^{(q_0)}$. The parameters are fit on data from the WHO Mortality Database [20] with maximum-likelihood (ML)

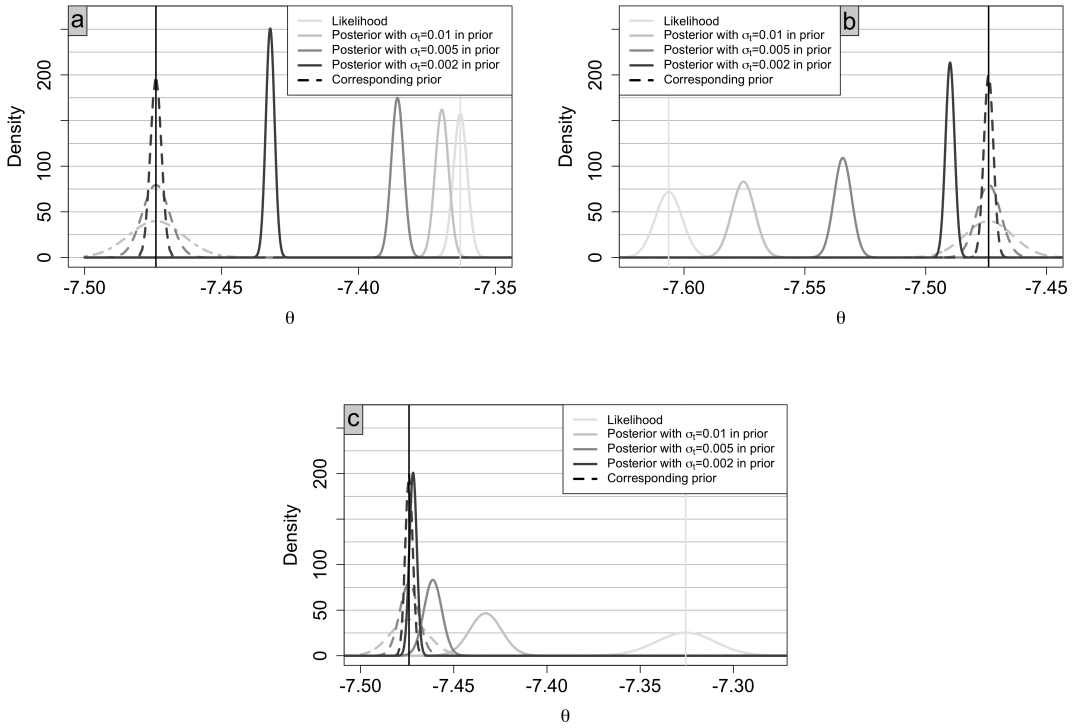

Supplementary Figure 6: Distribution of θ_t for $55 \leq t \leq 59$ for varying prior standard deviation σ_t. The first plot shows results using WHO data from all countries in Europe, America, and Asia with available data from 2001, 2006, 2011, 2016, and 2021. The second plot is reduced to data from 2016 and the last plot only employs German rates from 2016. The vertical solid black (light gray) line represents the prior (likelihood) mode.

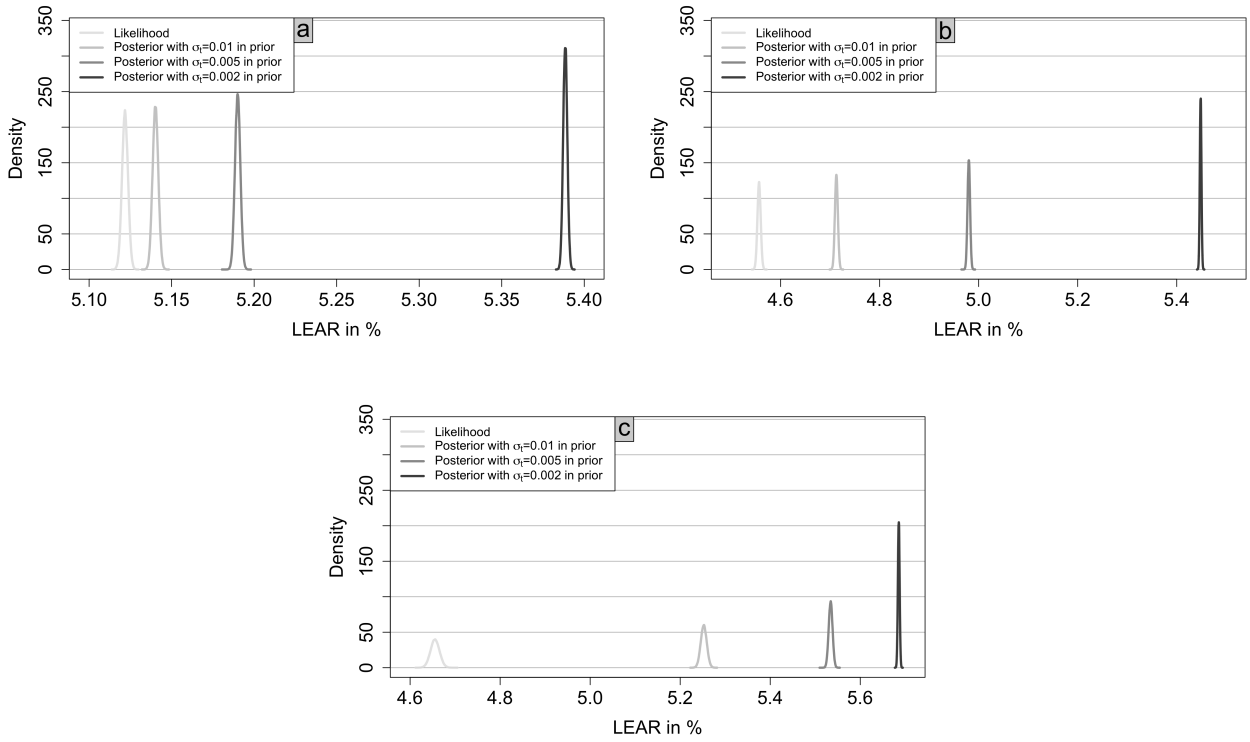

Supplementary Figure 7: Posterior distribution of $LEAR$ in % for uncertain lung cancer mortality rates and varying prior standard deviation σ_t (Bayesian framework). The first plot shows results using WHO data from all countries in Europe, America, and Asia with available data from 2001, 2006, 2011, 2016, and 2021. The second plot is reduced to data from 2016 and the last plot only employs German rates from 2016.

methods, just as for the gamma distribution in the main manuscript.

Both gamma and log-normal distributions fit the WHO data comparably well (Suppl. Figures 8 and 9). Resulting 95% uncertainty intervals are similar (Suppl. Table 10), with log-normal distributions yielding slightly wider intervals (Suppl. Figure 10). This is because log-normal distributions inherit heavier tails (direct comparison in Suppl. Figure 11). The lower bounds are very similar but the upper bounds are larger for log-normal mortality rates. All-cause mortality rates have minimal impact on $LEAR$ uncertainty, regardless of the chosen distribution, especially compared to lung cancer rates.

Acknowledging the impact of the chosen distribution on uncertainty intervals highlights the need for cautious interpretation. Sampling results and the data source (here: WHO mortality database) influence the intervals. Therefore, the overall tendency of interval span provides more valuable information than precise interval bounds. The computed intervals offer a quantitative sense of how mortality rate variability can influence lifetime risk estimates.

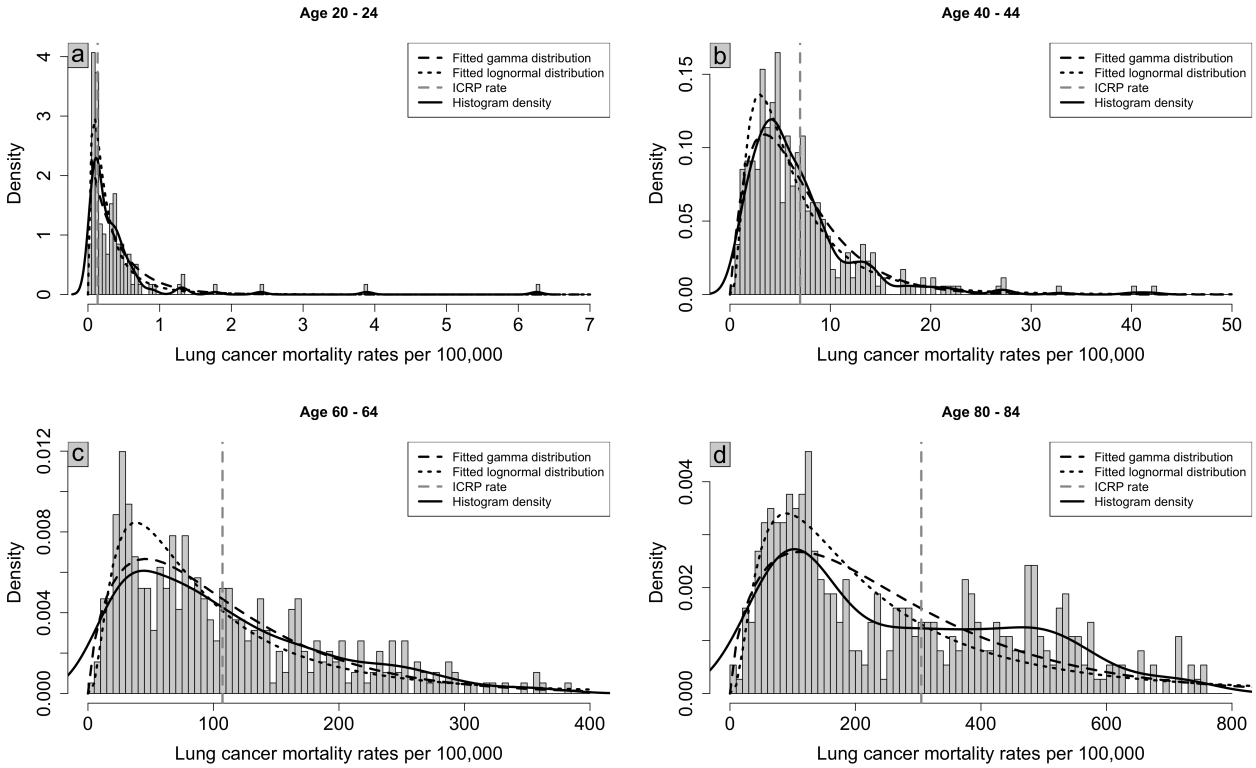

Supplementary Figure 8: Histogram of lung cancer mortality rates for the ages $20-24, 40-44, 60-64$ and $80-84$ derived from WHO data. For comparison, the reference lung cancer mortality rates from the ICRP Euro-American-Asian mixed population are shown with a vertical dashed line. The dashed (dotted) curve shows the density for a gamma (log-normal) distribution fitted to the histogram data.

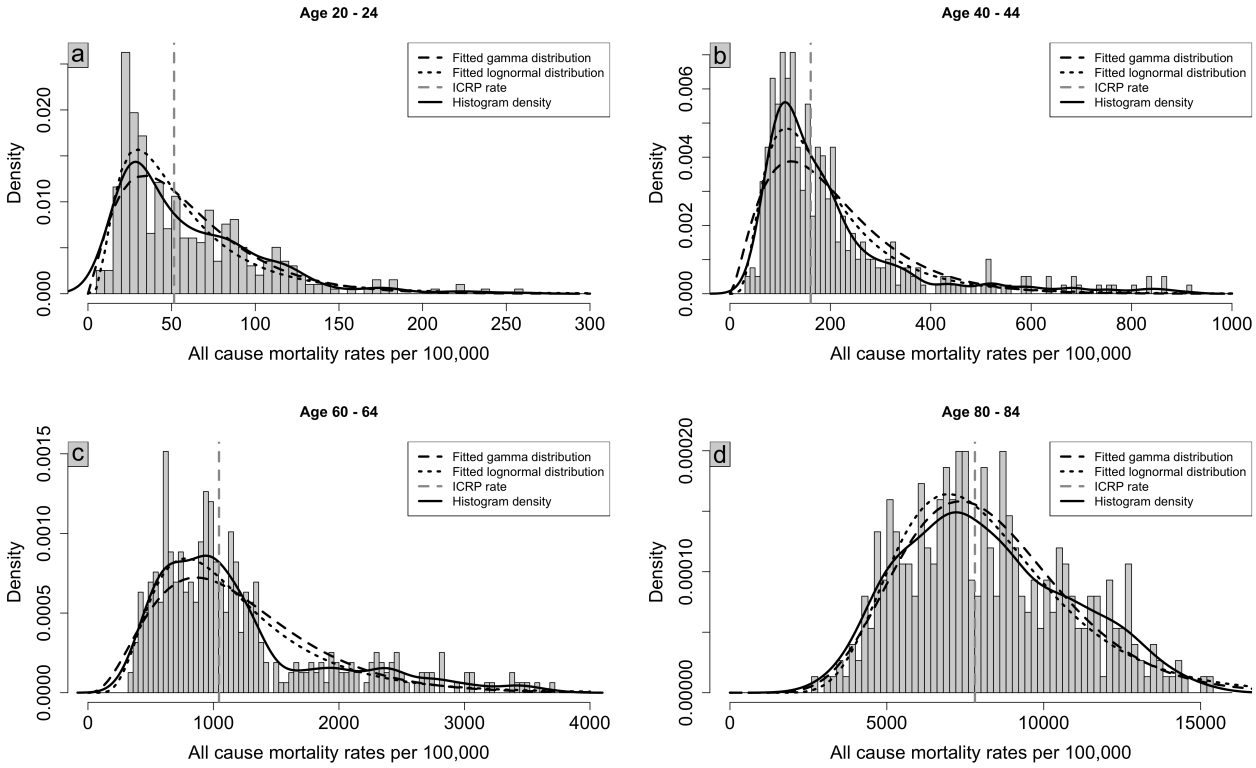

Supplementary Figure 9: Histogram of all-cause mortality rates for the ages $20-24, 40-44, 60-64$ and $80-84$ derived from WHO data. For comparison, the reference all-cause mortality rates from the ICRP Euro-American-Asian mixed population are shown with a vertical dashed line. The dashed (dotted) curve shows the density for a gamma (log-normal) distribution fitted to the histogram data.

Risk model	LEAR in %	Distribution	Effect of r_0	Effect of q_0	Effect of r_0 and q_0
Parametric full cohort	3.43	Gamma	[2.57; 4.17] (0.47)	[3.17; 3.44] (0.08)	[2.47; 4.04] (0.46)
		Log-normal	[2.53; 4.85] (0.68)	[3.16; 3.46] (0.09)	[2.44; 4.70] (0.66)
BEIR VI full cohort	2.95	Gamma	[2.18; 3.47] (0.44)	[2.64; 2.97] (0.11)	[2.06; 3.33] (0.43)
		Log-normal	[2.14; 4.02] (0.64)	[2.63; 2.98] (0.12)	[2.04; 3.86] (0.62)
Parametric 1960+ sub-cohort	6.70	Gamma	[4.96; 8.11] (0.47)	[6.16; 6.72] (0.08)	[4.76; 7.85] (0.46)
		Log-normal	[4.88; 9.45] (0.68)	[6.15; 6.74] (0.09)	[4.69; 9.15] (0.67)
BEIR VI 1960+ sub-cohort	5.74	Gamma	[4.29; 7.36] (0.53)	[5.36; 5.73] (0.06)	[4.14; 7.14] (0.52)
		Log-normal	[4.20; 8.58] (0.76)	[5.35; 5.75] (0.07)	[4.06; 8.36] (0.75)
Simple linear 1960+ sub-cohort	5.72	Gamma	[4.02; 6.66] (0.46)	[5.05; 5.79] (0.13)	[3.76; 6.36] (0.45)
		Log-normal	[3.94; 7.81] (0.68)	[5.02; 5.81] (0.14)	[3.70; 7.47] (0.66)

Supplementary Table 10: Reference $LEAR$ estimates in % with 95% uncertainty interval (relative uncertainty span in brackets) derived from $100,000$ sampled values for different risk models and distributional assumptions on the mortality rates $r_0(t), q_0(t)$ for all ages t derived from WHO data.

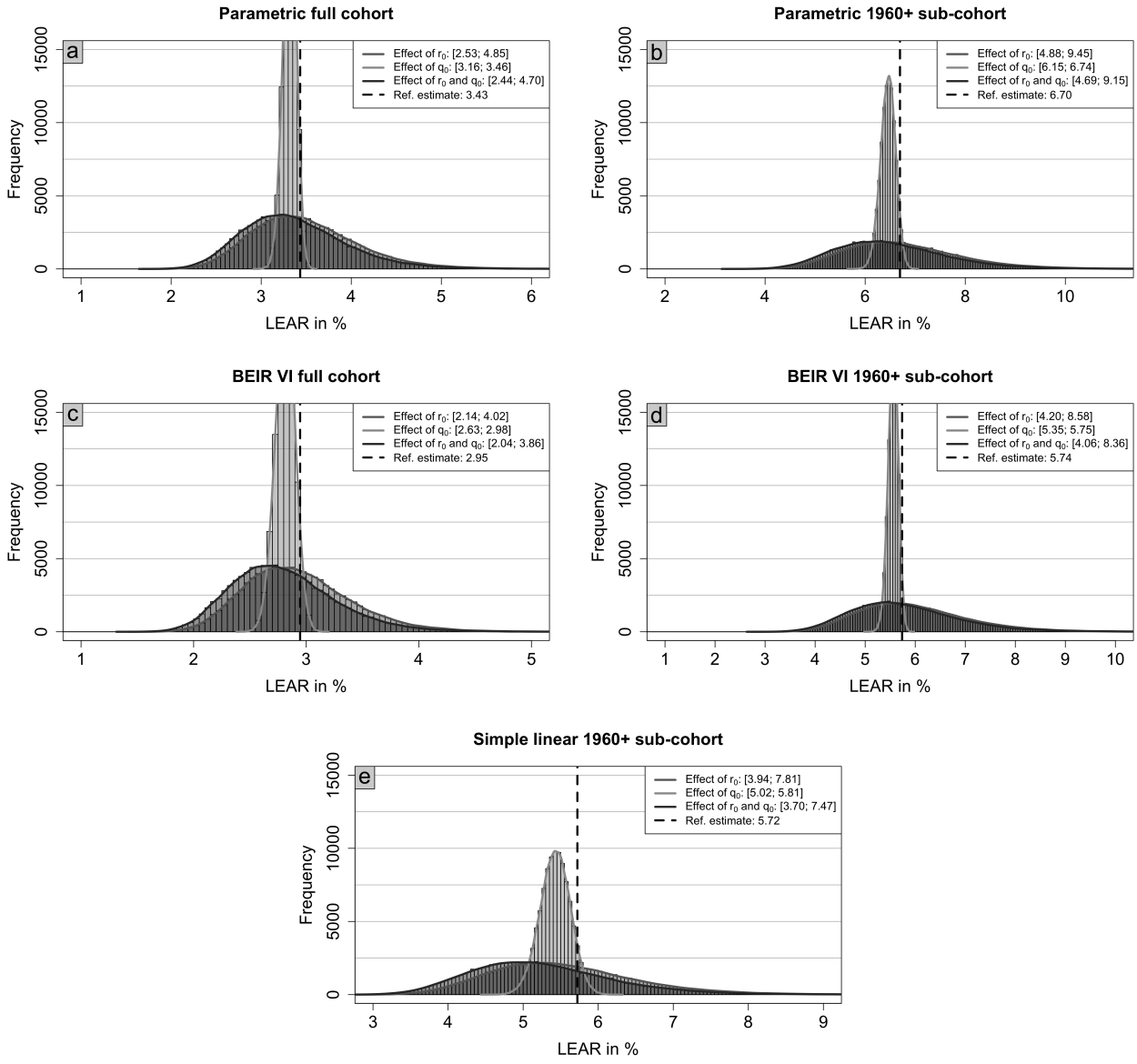

Supplementary Figure 10: Histogram of the 100,000 sampled $LEAR$ estimates with kernel density estimate (solid lines) for different risk models and varying uncertainty in mortality rates by grayscale. Lung cancer mortality rates $r_0(t)$ and all-cause mortality rates $q_0(t)$ are assumed to follow a log-normal distribution with parameter estimates derived from WHO data. The joint effect results from independent sampling from both corresponding probability distributions. The 95% uncertainty interval is presented in the legend.

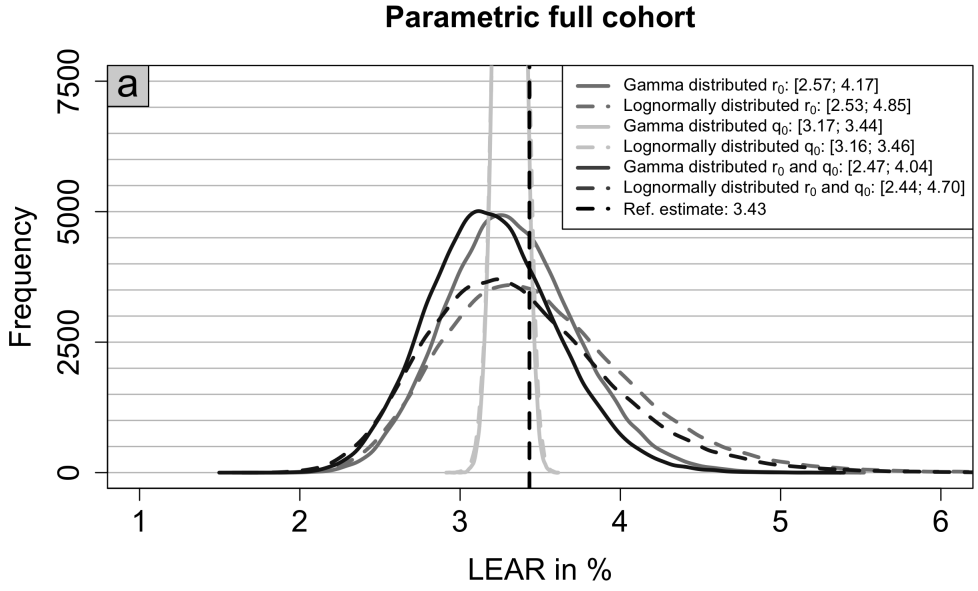

Supplementary Figure 11: Comparison of densities based on the distribution of $100,000$ sampled $LEAR$ estimates for the parametric full cohort risk model and varying uncertainty in mortality rates derived from WHO data by grayscale. The solid (dashed) lines show the distribution for gamma (log-normally) distributed baseline mortality rates (lung cancer $r_0(t)$, all-cause $q_0(t)$ or both). The joint effect results from independent sampling from both corresponding probability distributions. The 95% uncertainty intervals are presented in the legend. The dashed vertical line indicates the reference LEAR in % estimate.

E Sex-specific uncertainty

This section examines sex-specific $LEAR$ uncertainties by quantifying female- and male-specific mortality rate uncertainties and their impact on $LEAR$ estimates. Further, risk model parameter uncertainties are quantified with the Bayesian approach for sex-specific ICRP reference mortality rates.

E.1 Mortality rate uncertainty

Sex-specific uncertainty in mortality rates $r_0(t), q_0(t)$ and its impact on $LEAR$ are examined by deriving gamma distributions fit to sex-specific mortality rates from WHO data. Risk model parameters are fixed and not uncertain here.

Sex-specific mortality rates from the WHO data (Suppl. Figures 12 and 13) show higher mortality for males across all ages compared to females. Both gamma and log-normal distributions fit the data comparably well. We decided to use the gamma distribution for sex-specific mortality rate uncertainty in LEAR estimates (Suppl. Figure 14) to be comparable to the main paper approach.

The heavy differences in mortality rates result in almost non-overlapping histograms between female- and male-specific $LEAR$ estimates. WHO data reveals lower female all-cause and lung cancer mortality rates compared to ICRP reference rates, resulting in $LEAR$ estimates skewed leftward for females (Suppl. Figure 14). This left-skewing is even more pronounced for male all-cause mortality, though male lung cancer rates align with the male ICRP reference rates.

In contrast to the sex-averaged case, here large discrepancies between sample histogram means and ICRP rates motivate analysis of centered[4] mortality rates (Suppl. Figure 15). However, centering minimally affects relative uncertainty spans. In particular, low all-cause rate variation results in a negligible variation of $LEAR$ estimates. Notably, male-specific uncertainty remains slightly larger than female-specific uncertainty. The relative uncertainty span is similar for lung cancer rates between sexes, but about twice as large for male all-cause rates. Overall, the combined effect of both mortality rate uncertainties remains comparable between females and males.

This analysis showed that male-specific ICRP reference rates align better with observed male rates from WHO data compared to corresponding female rates. The derived uncertainty intervals suggest statistically significant differences in sex-specific $LEAR$ estimates. However, the overall relative uncertainty spans of $LEAR$ (incorporating lung cancer and all-cause mortality rates) remains comparable for both sexes. Notably, female-specific estimates have limited interpretability due to risk transfer issues since our risk models from [23] are derived entirely from male miners cohort data.

[4]The centering is carried out by setting the mean of the gamma-distributed mortality rate equal to the corresponding ICRP reference rate (compare Suppl. Section D.1.2).

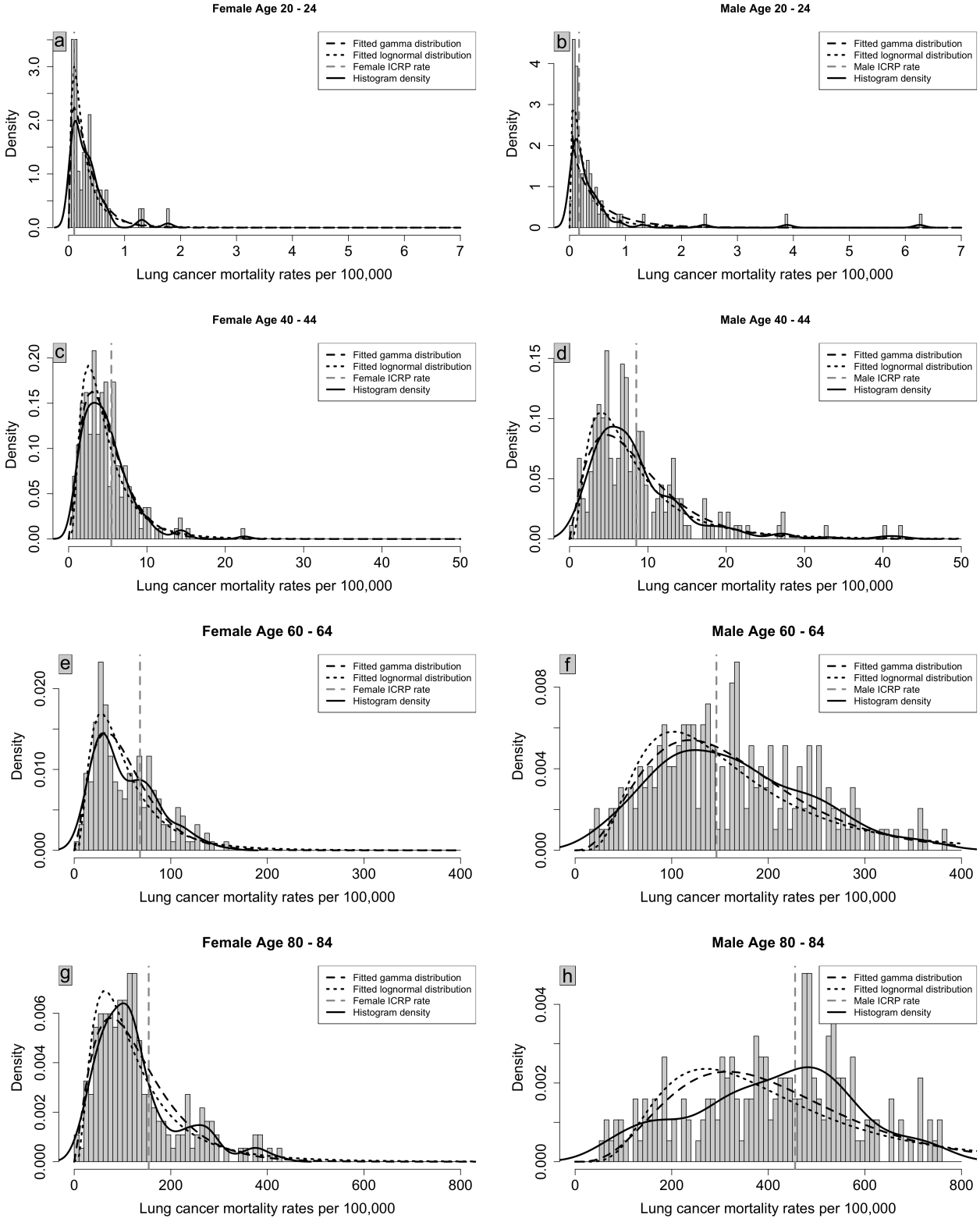

Supplementary Figure 12: Histogram of male and female lung cancer mortality rates for the ages $20-24, 40-44, 60-64$ and $80-84$ derived from WHO data. Every histogram is equipped with a corresponding kernel density estimate. For comparison, the male and female lung cancer mortality rates from the ICRP Euro-American-Asian mixed population are shown with a dashed vertical line. The dashed (dotted) curve shows the density for a gamma (log-normal) distribution fitted to the histogram data.

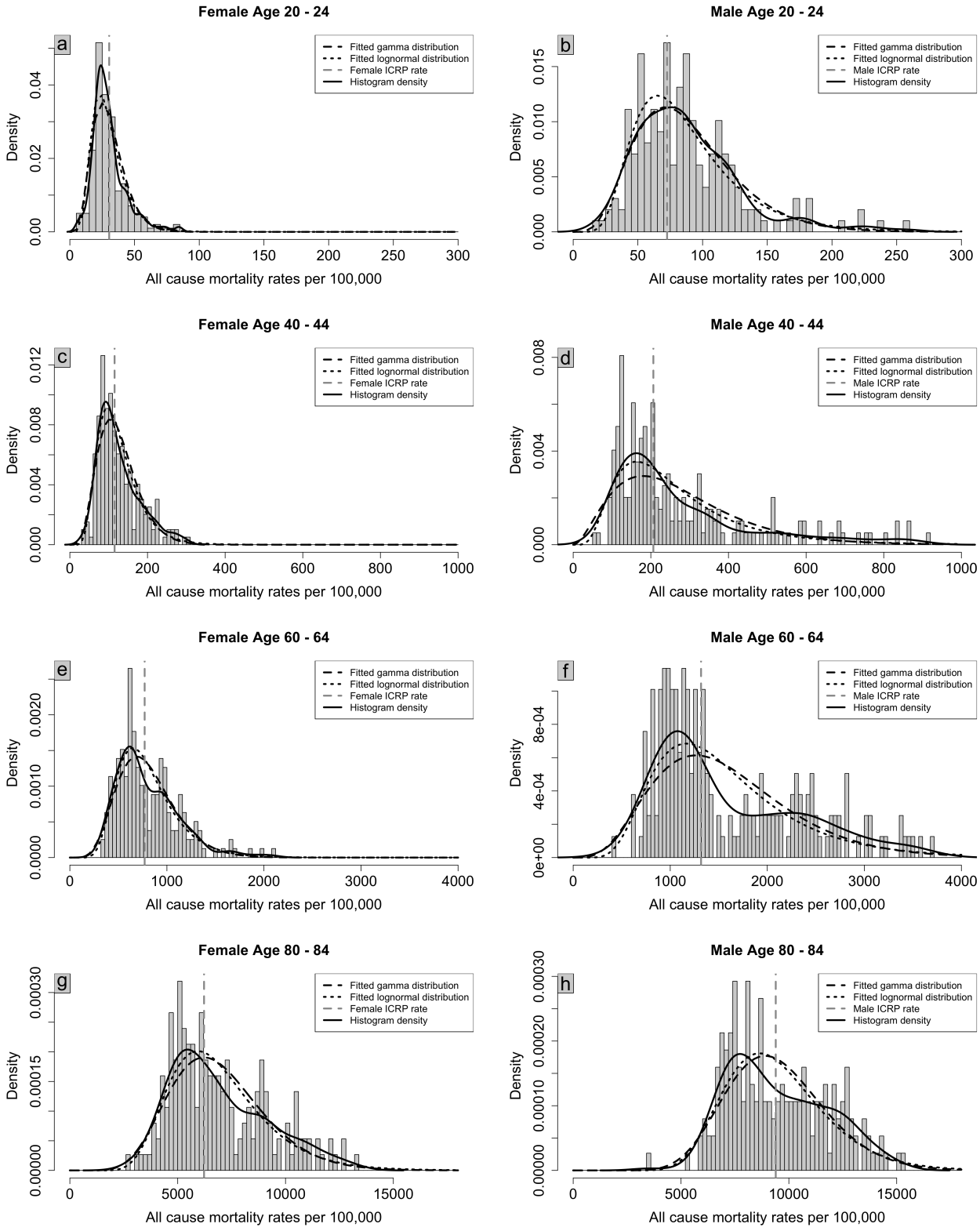

Supplementary Figure 13: Histogram of male and female all-cause mortality rates for the ages $20-24, 40-44, 60-64$ and $80-84$ derived from WHO data. Every histogram is equipped with a corresponding kernel density estimate. For comparison, the male and female all-cause mortality rates from the ICRP Euro-American-Asian mixed population are shown with a dashed vertical line. The dashed (dotted) curve shows the density for a gamma (log-normal) distribution fitted to the histogram data.

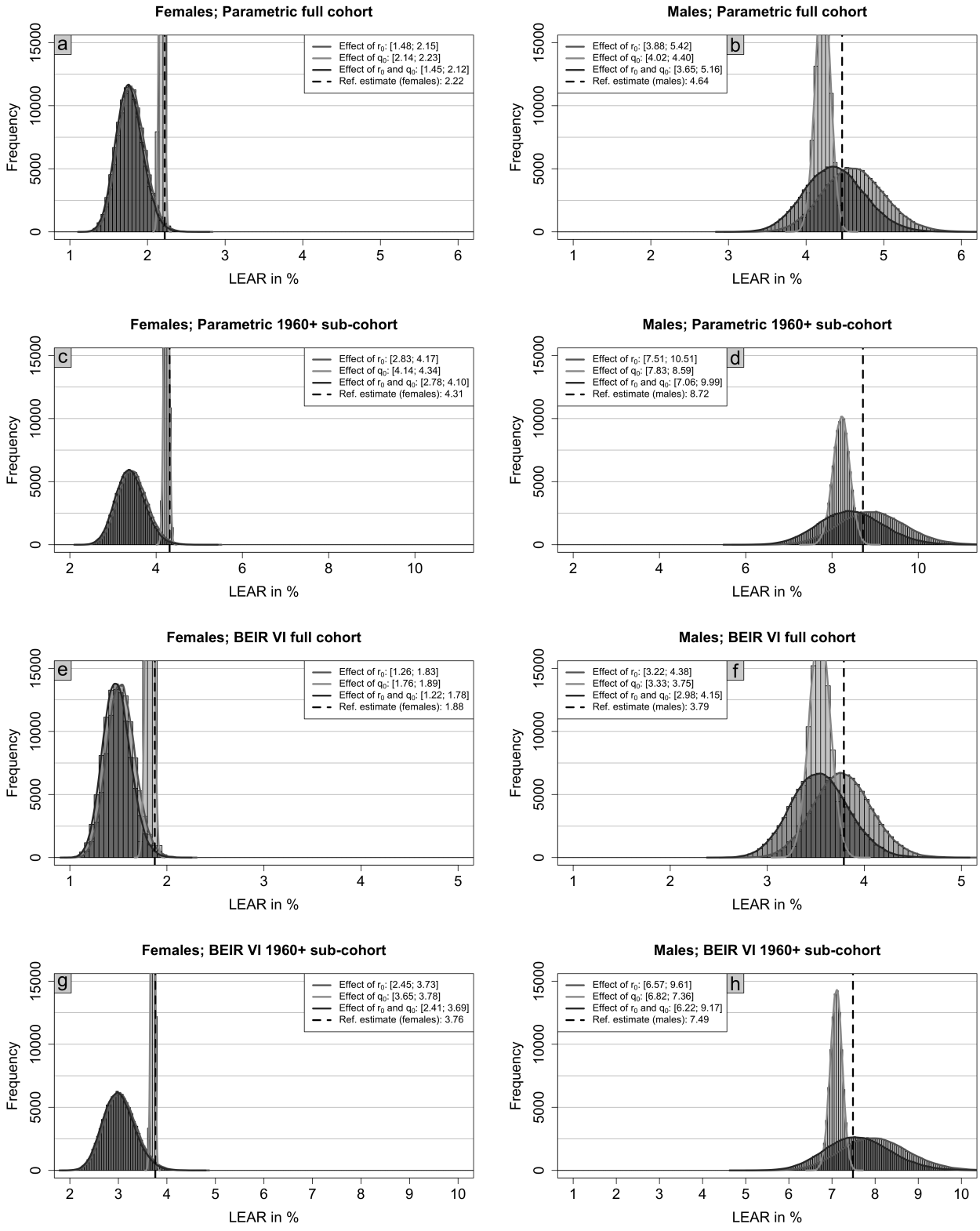

Supplementary Figure 14: Histogram of the 100,000 sampled $LEAR$ estimates with kernel density estimate (solid lines) for four risk models and varying uncertainty in sex-specific mortality rates by grayscale. Lung cancer mortality rates $r_0(t)$ and all-cause mortality rates $q_0(t)$ are assumed to follow a gamma distribution with parameter estimates derived from the histograms from Suppl. Figure 12 and Suppl. Figure 13, respectively. The joint effect results from independent sampling from both corresponding probability distributions. The 95% uncertainty interval is presented in the legend.

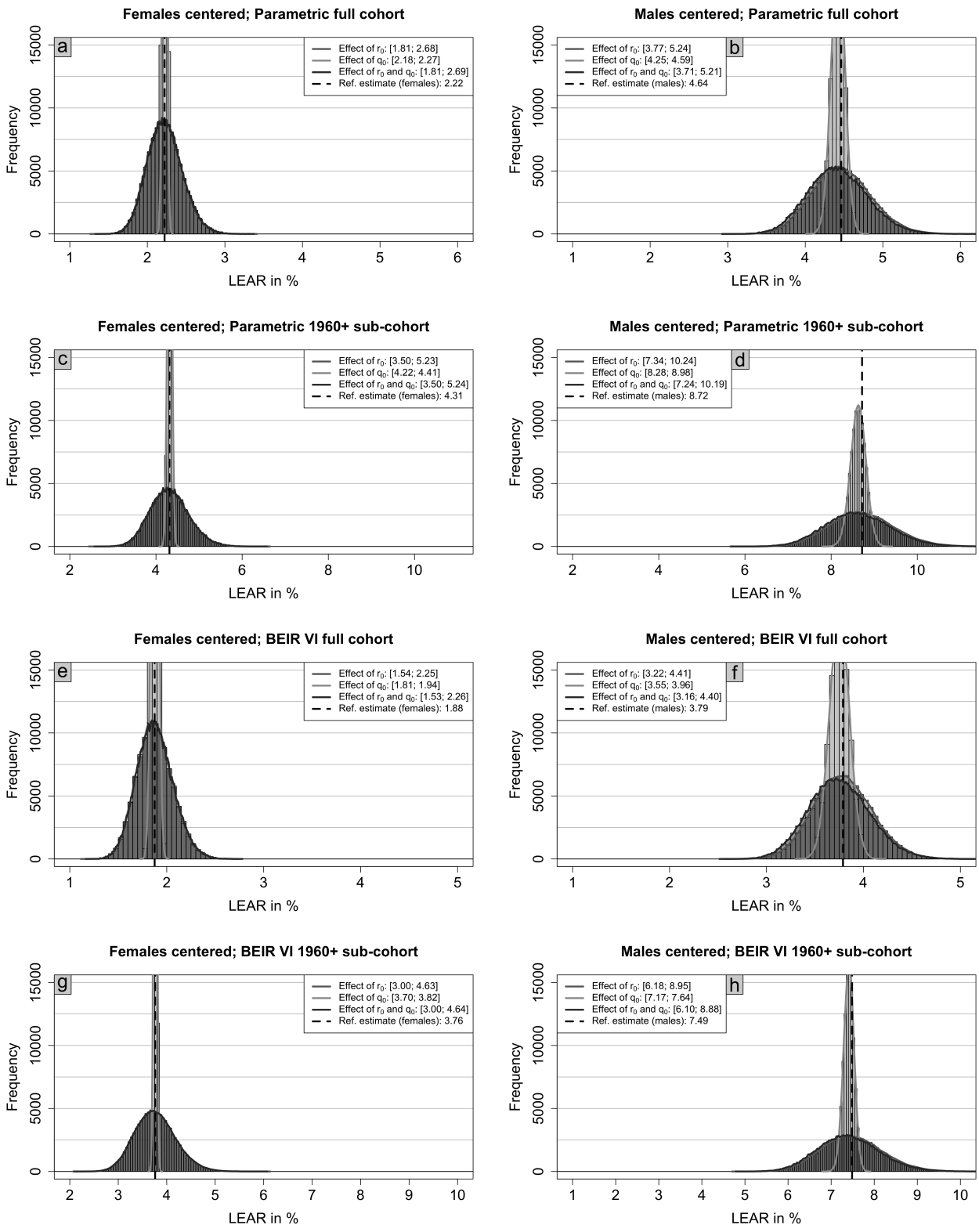

Supplementary Figure 15: Histogram of the 100,000 sampled $LEAR$ estimates with kernel density estimate (solid lines) for four risk models and varying uncertainty in sex-specific mortality rates by grayscale. Lung cancer mortality rates $r_0(t)$ and all-cause mortality rates $q_0(t)$ are assumed to follow a gamma distribution with parameter estimates derived from the histograms from Suppl. Figure 12 and Suppl. Figure 13 centered such that the mean is equal to the corresponding ICRP reference rate, respectively. The joint effect results from independent sampling from both corresponding probability distributions. The 95% uncertainty interval is presented in the legend.

E.2 Risk model parameter uncertainty for sex-specific ICRP reference mortality rates

ICRP reference mortality rates are sex-averaged (mean of male and female specific rates). We calculate male- and female-specific $LEAR$ estimates using the sex-specific mortality rates (Suppl. Figure 16). Notably, male reference lung cancer rates are notably higher at older ages (important for $LEAR$). We explore how these differences in mortality rates impact $LEAR$ using the Bayesian approach for the simple linear 1960+ sub-cohort risk model and the parametric 1960+ sub-cohort model, but without introducing randomness on mortality rates themselves. Note that we do not apply the ANA approach here because as other results here have shown, it yields results very similar to those of the Bayesian approach with a uniform prior.

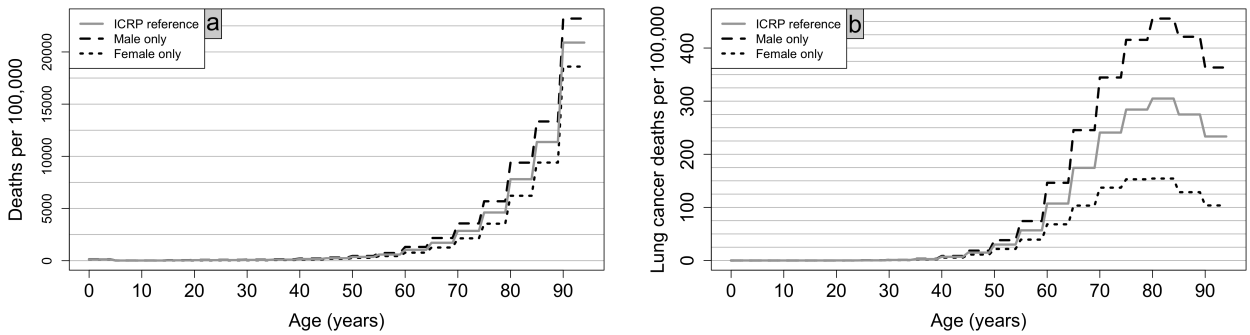

Supplementary Figure 16: Deaths and lung cancer deaths per 100,000 persons by age (i.e. $q_0(t) \times 10^5, r_0(t) \times 10^5$ for all t) in the ICRP reference population [2] and specifically for males and females only.

E.2.1 Simple linear 1960+ sub-cohort risk model

For the simple linear risk model structure $ERR(t;\beta) = \beta W(t)$, sampling is not necessary to assess differences in sex-specific risk model parameter uncertainties. It holds as in equation (26),

$$LEAR \approx \sum_{t\geq 0} r_0(t) ERR(t;\beta)\tilde{S}(t) = \beta \sum_{t\geq 0} r_0(t) W(t) e^{-\sum_{u=0}^{t-1} q_0(u)} = \beta \cdot C, \tag{35}$$

with $C = \sum_{t\geq 0} r_0(t) W(t) e^{-\sum_{u=0}^{t-1} q_0(u)}$. ICRP reference sex-mixed mortality rates and an exposure of 2 WLM from 18 to 64 years yields $C = 4.27$. Sex-specific mortality rates give different values for C with $C_M = 5.49$ and $C_F = 2.67$ for the male- and female-specific ICRP mortality rates, respectively. Results for $LEAR$ with the linear risk model are translated to a male or female ICRP reference population by multiplying the results with $C_M/C = 1.29$ or $C_F/C = 0.62$ for males or females, respectively. Hence, male-specific lifetime risk estimates are roughly twice as high as female-specific lifetime risk estimates due to higher male baseline mortality rates. This directly translates to sex-specific uncertainty intervals incorporating uncertain risk model parameters. However, by definition, the span of uncertainty intervals relative to the reference estimate (ICRP 103) remains identical between female- and male-specific $LEAR$ uncertainty intervals. Note that this result does not depend on the specific parameter estimate $\hat{\beta}$.

E.2.2 Parametric 1960+ sub-cohort risk model

For the parametric 1960+ sub-cohort risk model Markov Chain Monte Carlo (MCMC) methods are applied to obtain $N = 100,000$ samples from the posterior distribution $P(\Theta|X)$ analogously to the main paper approach. The overall higher baseline mortality for men directly shows in the $LEAR$ estimates and corresponding 95% HPDIs (Suppl. Table 11, Suppl. Figure 17). At very high prior

certainty ($a = 50, \sigma = 0.005$) the 95% HPDIs do not intersect, indicating a statistically significant difference between female- and male-specific $LEAR$ estimates. However, it depends on subjective reasoning on the prior information. Further, as seen for the simple linear risk model, the relative uncertainty span is very similar between female- and male-specific $LEAR$ uncertainty intervals.

Prior information	Male $LEAR$ in %	Female $LEAR$ in %
Uniform prior	8.78 [3.79; 14.40] (1.21)	4.34 [1.92; 7.09] (1.19)
$a = 20, \sigma = 0.02$	6.67 [3.89; 9.87] (0.90)	3.33 [1.99; 4.91] (0.88)
$a = 50, \sigma = 0.005$	5.76 [4.41; 7.42] (0.52)	2.89 [2.19; 3.69] (0.52)

Supplementary Table 11: Sex-specific $LEAR$ estimate with 95% highest posterior density interval (HPDI) (relative uncertainty span in brackets) for underlying Bayesian random risk model parameters $\Theta = (\beta, \alpha, \varepsilon)$ with posterior distribution $P(\Theta|X)$ for different values of prior gamma shape parameters a and standard deviation σ. The male and female $LEAR$ in % with the risk model derived from the Joint Czech+French cohort (prior information) is 5.59 and 2.81, respectively.

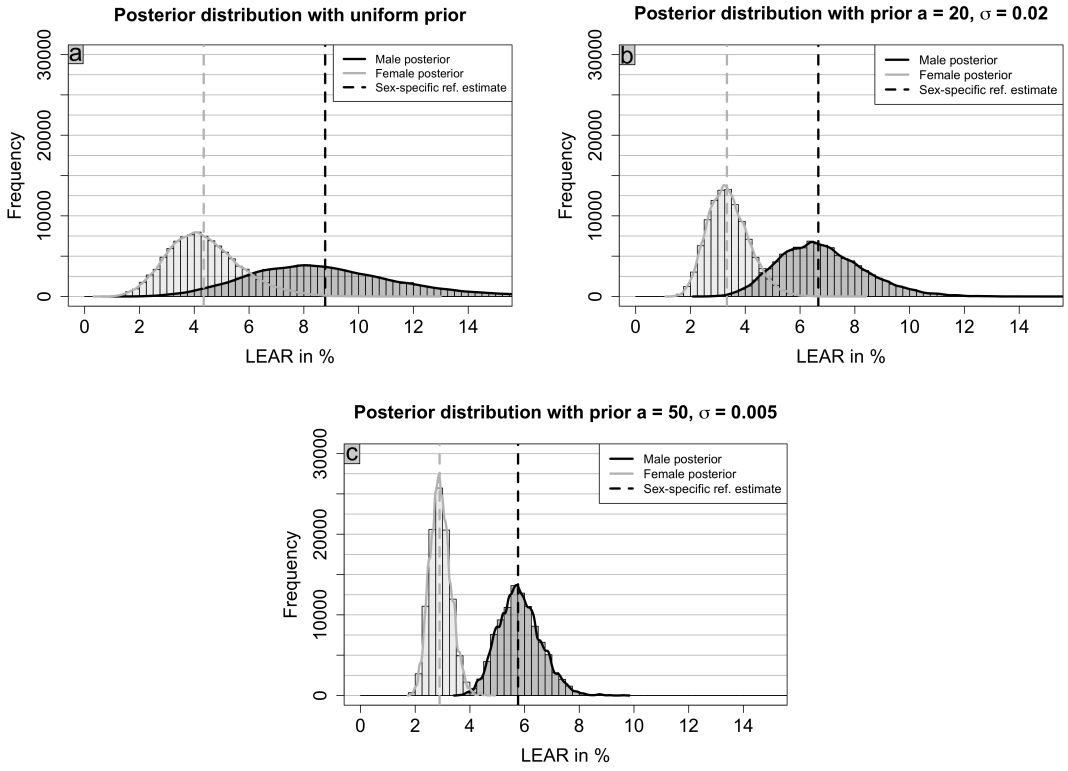

Supplementary Figure 17: Distributions of $LEAR$ estimates using ICRP reference male and female mortality rates, respectively calculated from 100,000 risk model parameter estimates drawn from the posterior distribution. The risk model parameter prior $P(\Theta) = P(\beta)P(\alpha)P(\varepsilon)$ is varied for different combinations of gamma-distributed β and normally distributed α, ε for different shape parameters a and standard deviations σ.

Overall, our analysis revealed that $LEAR$ estimates differ roughly by a factor of two between female- and male-specific mortality rates. However, the relative uncertainty span remained comparable across sexes. Acknowledging that current lifetime risk calculations in the literature employ sex-mixed reference mortality rates, shows that mortality rate uncertainty should not be underestimated. Although there was no clear difference in sex-specific (relative) uncertainty, supporting the assessment of sex-mixed mortality rate uncertainties, the inherent uncertainty associated with risk transfer uncertainty between excess relative risk terms and female-specific mortality rates remains.

F Radon exposure uncertainty

Although lifetime risks like $LEAR$ related to radon exposure are often used with a fixed exposure scenario (e.g. for dose conversion purposes 2 WLM from age 18-64 years), we briefly explore how exposure uncertainty may affect lifetime risk estimates. This exploration aims to provide a more comprehensive assessment of how variability in calculation components impacts lifetime risk variability. A typical situation with exposure uncertainty arises for compensation claims, where an individual lifetime risk is estimated based on given exposure data. However, for compensation claims for radiation-induced cancer, the specialized software "ProZES" [50] is recommended and typically applied in Germany.

Inspired by results from [62] that errors in the Japanese atomic bomb dosimetry are approximately log-normally distributed, we assume a log-normally distributed yearly exposure in WLM to explore its impact on lifetime risk estimates for different lifetime risk measures and different risk models. Note that also normal distributions are viable options [13, 63]. However, this is rather an explorative approach and results are interpreted with care.

The reference case is the exposure scenario of 2 WLM from age 18-64 years. Let $w(t)$ be the exposure in WLM at age t and $W(t) = \sum_{u=0}^{t} w(u)$ be the corresponding cumulative exposure in WLM at age t. We assume for every age t,

$$w(t) \sim \mathcal{LN}\left(\log(2) - \frac{\sigma^2}{2}, \sigma^2\right) \tag{36}$$

to guarantee that the mean of the distribution is at 2 WLM. The standard deviation σ governs the uncertainty and 95% uncertainty intervals are obtained as the span of observed estimates via simulations by calculating 10,000 estimates and discarding the 500 (2.5%) highest and lowest values (Suppl. Table 12). For each lifetime risk estimate, $w(t)$ is sampled from the log-normal distribution (36) for all ages $18 \leq t \leq 64$.

Risk model	ELR in %	$REID$ in %	$LEAR$ in %	$RADS$ in %
Exposure variability $\sigma = 1$				
Parametric full cohort	3.24 [2.24; 4.78] (0.78)	3.37 [2.33; 4.97] (0.78)	3.43 [2.36; 5.11] (0.80)	4.65 [3.21; 6.88] (0.79)
Parametric 1960+ sub-cohort	6.21 [4.08; 9.94] (0.94)	6.45 [4.24; 10.32] (0.94)	6.70 [4.34; 10.98] (0.99)	8.94 [5.82; 14.39] (0.96)
BEIR VI full cohort	2.80 [1.95; 4.06] (0.75)	2.89 [2.02; 4.20] (0.75)	2.95 [2.04; 4.31] (0.77)	4.85 [3.39; 7.02] (0.75)
BEIR VI 1960+ sub-cohort	5.34 [3.70; 7.70] (0.75)	5.56 [3.86; 8.03] (0.75)	5.74 [3.94; 8.40] (0.78)	7.11 [4.95; 10.24] (0.74)
Simple linear 1960+ sub-cohort	5.35 [3.75; 7.74] (0.75)	5.52 [3.87; 7.98] (0.74)	5.72 [3.97; 8.43] (0.78)	9.98 [7.04; 14.33] (0.73)
Exposure variability $\sigma = 0.5$				
Parametric full cohort	[2.77; 3.78] (0.31)	[2.88; 3.93] (0.31)	[2.92; 4.02] (0.32)	[3.98; 5.43] (0.31)
Parametric 1960+ sub-cohort	[5.17; 7.45] (0.37)	[5.38; 7.74] (0.37)	[5.54; 8.10] (0.38)	[7.42; 10.77] (0.37)
BEIR VI full cohort	[2.41; 3.24] (0.30)	[2.49; 3.35] (0.30)	[2.53; 3.42] (0.30)	[4.18; 5.62] (0.30)
BEIR VI 1960+ sub-cohort	[4.58; 6.20] (0.30)	[4.77; 6.46] (0.30)	[4.90; 6.69] (0.31)	[6.12; 8.24] (0.30)
Simple linear 1960+ sub-cohort	[4.61; 6.18] (0.29)	[4.75; 6.37] (0.29)	[4.91; 6.65] (0.30)	[8.63; 11.49] (0.29)
Exposure variability $\sigma = 0.1$				
Parametric full cohort	[3.15; 3.34] (0.06)	[3.27; 3.47] (0.06)	[3.33; 3.54] (0.06)	[4.52; 4.79] (0.06)
Parametric 1960+ sub-cohort	[6.00; 6.43] (0.07)	[6.23; 6.68] (0.07)	[6.46; 6.94] (0.07)	[8.63; 9.26] (0.07)
BEIR VI full cohort	[2.72; 2.88] (0.06)	[2.81; 2.97] (0.06)	[2.86; 3.03] (0.06)	[4.72; 4.99] (0.06)
BEIR VI 1960+ sub-cohort	[5.19; 5.49] (0.06)	[5.41; 5.72] (0.06)	[5.57; 5.91] (0.06)	[6.92; 7.32] (0.06)
Simple linear 1960+ sub-cohort	[5.21; 5.50] (0.05)	[5.37; 5.67] (0.05)	[5.56; 5.89] (0.06)	[9.72; 10.25] (0.05)

Supplementary Table 12: Lifetime risk estimates with 95% uncertainty intervals (relative uncertainty span in brackets) derived from 10,000 sampled estimates for log-normally distributed yearly exposure in WLM (assumption (36)), with corresponding reference estimates for different risk models, lifetime measures, and exposure variability σ. Reference estimates are only stated for $\sigma = 1$ as they do not change with varying σ.

Similar to previous findings, differences between lifetime risk measures are minimal with only $RADS$ being considerably larger. Relative uncertainty interval spans are comparable across all lifetime risk measures and risk models, except for the parametric 1960+ sub-cohort model (wider intervals). Exposure-affected effect-modifying variables do not impose additional uncertainty (compare simple

linear model to others, Suppl. Figure 18b). As expected, smaller σ leads to narrower and more symmetrical intervals due to less influence from right-skewed random exposure. This effect is stronger, the larger σ. For small σ, the probability mass of log-normal random variables is very centered with less heavy tails. The span of lifetime risk uncertainty intervals decreases proportionally with decreasing σ.

Lower exposure uncertainty (smaller σ) leads all lifetime risk measures (e.g., LEAR, Suppl. Figure 18a) to resemble a normal distribution, regardless of the chosen risk model. This is because the assumed log-normal distribution approximates normality for smaller σ, which translates to the lifetime risk measures. After all, sums of independent normally distributed random variables are again normally distributed. Notably, this applies even to complex risk models with non-linear exposure-risk relations.

Note that the observed magnitude of uncertainty does not translate to the $LEAR$ per WLM, defined as the $LEAR$ divided by total cumulative exposure accrued over the entire exposure scenario in WLM. The quantity $LEAR$ per WLM is hardly affected by varying radon exposure [5]. In conclusion, account-

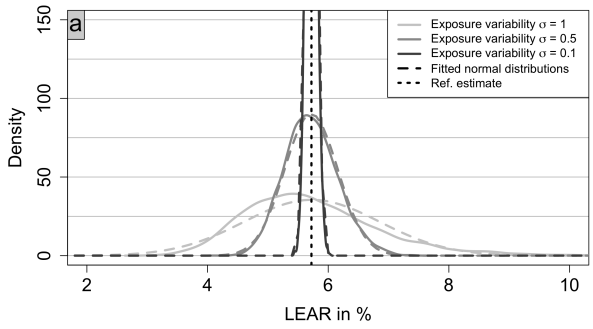

(a) $LEAR$ densities for the simple linear risk model $ERR(t;\beta) = \beta W(t)$ with $\beta = 0.0134$ and different σ values. A normal distribution fitted on the $10,000$ $LEAR$ samples is shown for comparison (dashed lines).

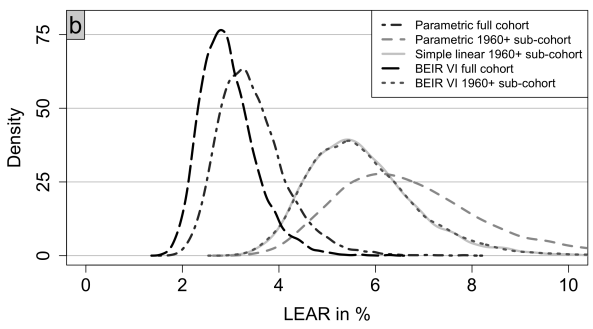

(b) $LEAR$ densities for different risk models and fixed log-normal standard deviation $\sigma = 1$.

Supplementary Figure 18: Density of $LEAR$ estimates based on the distribution of $10,000$ sampled values with random annual exposure in WLM from age 18-64 years (assumption (36)) for varying σ and different risk models.

ing for uncertainties in annual radon exposure (on a simple scale) results in an approximately normally distributed lifetime risk, regardless of the chosen lifetime risk measure or risk model. However, this approach requires knowledge or assumptions on exposure errors directly influencing uncertainty intervals. While this analysis can be extended to more complex exposure scenarios, it is beyond the scope here as exposure uncertainty assessment is not a core focus for lifetime risk calculations. Nevertheless, accurate exposure assessment and uncertainty quantification remain crucial for uranium miners cohorts and risk model derivation [38, 39].